

C#1

SEP 6 1973  
SEP 21 1973  
1974

AGARD-R-601

AGARD-R-601

SEP 14 1988

# AGARD

ADVISORY GROUP FOR AEROSPACE RESEARCH & DEVELOPMENT

7 RUE ANCELLE 92200 NEUILLY SUR SEINE FRANCE

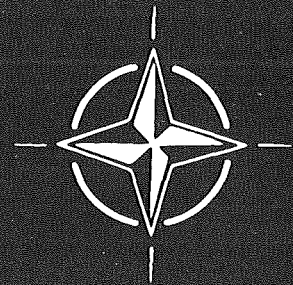
AGARD REPORT No. 601

on

## Problems in Wind Tunnel Testing Techniques

Property of U. S. Air Force  
F40600-74-C-0001

NORTH ATLANTIC TREATY ORGANIZATION



DISTRIBUTION AND AVAILABILITY  
ON BACK COVER

Property of U. S. Air Force  
AEDC LIBRARY  
F40600-74-C-0001

ey 1

NORTH ATLANTIC TREATY ORGANIZATION  
ADVISORY GROUP FOR AEROSPACE RESEARCH AND DEVELOPMENT  
(ORGANISATION DU TRAITE DE L'ATLANTIQUE NORD)

AGARD Report No.601

PROBLEMS IN WIND TUNNEL TESTING TECHNIQUES

---

2 " " " " " *Lisbrun*

This Report is sponsored by the Fluid Dynamics Panel of AGARD as a complementary paper to AGARD Advisory Report AR 60 of the Large Wind Tunnels Working Group.

The AGARD Fluid Dynamics Panel wishes to thank Professor P.E.Colin, Mr. M. de Maistre, Mr R.A.Hills, Mr J.P.Hartzuiker, Mr J.Y.G.Evans, Dr R.Göthert, and Professor D.Küchemann for their contribution in editing papers included in this Report.

## THE MISSION OF AGARD

The mission of AGARD is to bring together the leading personalities of the NATO nations in the fields of science and technology relating to aerospace for the following purposes:

- Exchanging of scientific and technical information;
- Continuously stimulating advances in the aerospace sciences relevant to strengthening the common defence posture;
- Improving the co-operation among member nations in aerospace research and development;
- Providing scientific and technical advice and assistance to the North Atlantic Military Committee in the field of aerospace research and development;
- Rendering scientific and technical assistance, as requested, to other NATO bodies and to member nations in connection with research and development problems in the aerospace field;
- Providing assistance to member nations for the purpose of increasing their scientific and technical potential;
- Recommending effective ways for the member nations to use their research and development capabilities for the common benefit of the NATO community.

The highest authority within AGARD is the National Delegates Board consisting of officially appointed senior representatives from each member nation. The mission of AGARD is carried out through the Panels which are composed of experts appointed by the National Delegates, the Consultant and Exchange Program and the Aerospace Applications Studies Program. The results of AGARD work are reported to the member nations and the NATO Authorities through the AGARD series of publications of which this is one.

Participation in AGARD activities is by invitation only and is normally limited to citizens of the NATO nations.

The material in this publication has been reproduced directly from copy supplied by AGARD or the author.

Published April 1973

533.6.071

*Printed by Technical Editing and Reproduction Ltd  
Harford House, 7-9 Charlotte St. London. W1P 1HD*

## PREFACE

The Large Wind Tunnels Working Group (LaWs) of the Fluid Dynamics Panel of AGARD has been helped considerably in its deliberations by a large number of non-member scientists and engineers from the participating countries, who investigated particular problems, provided specially-written papers, or took part in the discussions. This help was very much appreciated by the members of the Group, and the information contained in the LaWs Papers, in particular, has proved to be very valuable. However, the number of LaWs Papers is so large (over 130) that it was not possible to publish them all or to include them in full in the Report of the Group (AGARD Advisory Report 60 entitled "The Need for Large Wind Tunnels in Europe"). On the other hand, some of the LaWs Papers present substantial surveys of particular fields and others describe possible options for future wind tunnels in detail. These papers supplement the Report of the Group in essential respects. The Group decided, therefore, to publish a selection of the LaWs Papers in AGARD Reports, so that they are generally available and can be read in conjunction with the Report of the Group.

As a result, four AGARD Reports are being published, collecting a number of papers together on subjects related to the design and operation of low-speed and transonic wind tunnels, with particular reference to possible future large wind tunnels in Europe. There are thus three further Reports in addition to the present Report. Their contents are listed in Appendix I at the end of this Report.

Wherever appropriate, the individual papers have been edited by a member of the LaWs Working Group. On behalf of the members of the LaWs Group, the undersigned wishes to thank all those who helped the Group and especially the authors of the papers published here.

D.Küchemann  
Chairman, LaWs Working Group

November 1972

## CONTENTS

	Page
PREFACE	iii
	Reference
REVIEW OF SOME PROBLEMS RELATED TO THE DESIGN AND OPERATION OF LOW SPEED WIND TUNNELS FOR V/STOL TESTING by M. Carbonaro	1
SURVEY OF METHODS FOR CORRECTING WALL CONSTRAINTS IN TRANSONIC WIND TUNNELS by J.Ch. Vayssaire	2
INTERFERENCE EFFECTS OF MODEL SUPPORT SYSTEMS by E.C. Carter	3
MINIMUM REQUIRED MEASURING TIMES TO PERFORM INSTATIONARY MEASUREMENTS IN TRANSONIC WIND TUNNELS by J.W.G. van Nunen, G. Coupry and H. Försching	4
SOME CONSIDERATIONS OF TESTS UNDER DYNAMIC CONDITIONS IN LOW-SPEED WIND TUNNELS by D.N. Foster	5
USE OF MODEL ENGINES (V/S/CTOL) by E. Melzer and R. Wulf	6
WIND TUNNEL REQUIREMENTS FOR HELICOPTERS by I.A. Simons and H. Derschmidt	7
ACOUSTIC CONSIDERATIONS FOR NOISE EXPERIMENTS AT MODEL SCALE IN SUBSONIC WIND TUNNELS by T.A. Holbeche and J. Williams	8
APPENDIX I – Details of other documents complementary to Advisory Report 60	

REVIEW OF SOME PROBLEMS RELATED TO THE DESIGN AND OPERATION OF  
LOW SPEED WIND TUNNELS FOR V/STOL TESTING

Mario Carbonaro  
Assistant  
von Karman Institute for Fluid Dynamics  
72, Chaussée de Waterloo  
1640 Rhode-Saint-Genèse  
Belgique

SUMMARY

A review is made of a number of operational problems associated with the wind tunnel testing of V/STOL aircraft including helicopters. The following topics are discussed in the study :

- Wall constraints
- Use of ventilated walls
- Testing for ground effect
- Flow disturbances in the tunnel circuit

LIST OF SYMBOLS

a	slot width
A	aspect ratio
b	wing span or rotor diameter
B	test section width
c	wing chord
C	wind tunnel cross sectional area
$C_L$	lift coefficient
$C_D$	drag coefficient
$C_M$	pitching moment coefficient
d	jet nozzle diameter
$D_i$	induced drag
h	model height above floor
H	test section height
K	parameter defining slot geometry of porous walls
l	slot spacing
L	lift
n	coordinate normal to wind tunnel walls
P	slot parameter
q	measured dynamic pressure
$q_c$	corrected dynamic pressure - average at wing location
$q_t$	corrected dynamic pressure - average at tail location
S	wing or rotor disk area
t	test section wall thickness
$T_e$	temperature at the exit of a jet engine
$V_0$	free stream velocity
$V_j$	jet velocity
x	longitudinal coordinate
$x_f$	wake impingement distance
y	spanwise coordinate
$\alpha$	angle of attack
$\Delta\alpha$	average incidence correction at the wing
$\Delta\alpha_j$	interference angle at zero lift
$\Delta i_t$	additional incidence correction at the tail
$\Delta i_w$	variation in incidence correction across wing span
$\Delta q$	variation in dynamic pressure across wing span
$\delta$	lift interference factor
$\phi$	perturbation potential
$\Lambda$	wing sweep angle

x momentum wake angle  
 $x_e$  effective wake angle

## 1. INTRODUCTION

Based on the present state of the art in four important aspects of low speed wind tunnel operation for V/STOL testing, the report aims at providing information pertinent to the design of large low speed tunnels.

The topics considered in the study are :

- Wind tunnel wall constraints and the limitation they may impose on the test conditions (model size relative to tunnel size, tunnel speed)
- Potential of ventilated test sections for the reduction of boundary induced corrections
- Requirements for proper simulation of ground effects
- Effects of flow disturbances originating at the model and propagating around the tunnel circuit

## 2. WIND TUNNEL WALL CONSTRAINTS

### 2.1 Introduction

For tests of CTOL aircraft well established methods exist for applying wall corrections. Ref.1 gives an extensive bibliography of the published work on this subject up to 1966. An example of a method for applying blockage, lift and moment corrections to wind tunnel measurements is reported in the more recent Refs 2 and 3.

When conducting and interpreting wind tunnel tests of V/STOL aircraft and helicopters, the three following problems arise in connection with the existence either of downward directed jets or of non-horizontal wakes originating from the lifting elements :

- a) The methods used in calculating the wall corrections for tests of CTOL aircraft employ schemes based on undeflected wakes, i.e., on horizontally trailing vortex filaments. However, as the overall lift on the model increases, the wakes are progressively deflected downward thus departing from their mathematical representation and therefore leading to an error which increases with the overall lift. Because wall corrections are thus inevitably approximate it is necessary to set an upper limit on them, depending on the accuracy called for in the final evaluation of the data. This was recognized in the pioneering work conducted at R.A.E. some fifteen years ago. Thus Anscombe and Williams (Ref.4) suggested that the mean incidence corrections on the wing,  $\Delta\alpha$ , should not exceed  $2^\circ$  for a sufficiently accurate prediction of corrections based on simple wing theory assuming undeflected wakes. This criterion, mentioned again by Butler and Williams in Ref.5, has become since a generally accepted limit. However, the magnitude of the limit depends on the method used for correcting the data, and thus a larger value than  $2^\circ$  might be acceptable, if the method were based on a better approximation of the lifting scheme than the classical one assuming undeflected wakes as used for CTOL aircraft.
- For tests of V/STOL aircraft, Heyson has suggested more elaborate schemes of wall corrections as indicated in the next paragraph. He has also suggested limits to the maximum acceptable corrections (Ref.6). They have been determined partly from experience and partly arbitrarily. In fact, to determine such limiting criteria, there is a need for systematic tests to be performed on identical models in wind tunnels of different sizes and/or for flight data to be compared with results on models of identical configuration.
- b) The lifting schemes based on the superposition of horseshoe vortices with horizontal trailing filaments are not acceptable for V/STOL aircraft and helicopters where a proper mathematical model describing the flow field induced by a highly loaded wing (e.g., a jet flap), a rotor or a lifting jet, is needed. Some mathematical schemes have been proposed by Heyson for a rotor wake, represented as a skewed elliptical cylinder of distributed vorticity (Refs 7, 8, 9) or as a line of doublets (Refs 7, 10) together with the suggestion (Ref.11) that such "elementary wakes" may be combined to represent any lifting system, wing or rotor. Heyson's schemes, however, employ rectilinear wakes which may not be truly representative of a lifting jet deflected by the cross flow. Heyson and various other researchers have worked on a scheme employing curved wakes, in which doublets are distributed on a suitable, often empirically determined, curved path for the deflected jet. However, such methods have been hampered by excessive computing complexity and are not at the present time capable of providing tables or charts of corrections.
- c) For high wake deflections or jet directions approaching the vertical, and for small distances of the model from the wind tunnel floor, flow reversal in the test section may occur. This phenomenon, known as flow breakdown, starts on the wind tunnel floor and is accompanied by the formation of a reversed flow bubble; flow direction may thereby be significantly affected in the vicinity of the model, and the validity of the tests becomes questionable. This situation, reported first by Rae (Ref.12) really sets a limit either on the minimum test speed or on the maximum ratio of model to test section dimension. The problem has also been investigated in Refs 13 to 17 and a discussion on the subject has recently been presented by Owen (Ref.18).

### 2.2 Methods for dealing with wall effects

A survey has been made of the different methods proposed for dealing with wall effects in tests of complete aircraft. They fall into two different types of approach. In the

first one, test results are corrected by means of formulae based on theoretical estimates of boundary effects; in the second one, tests are made in special test sections which do not impose constraints on the flow so that there is no need for corrections. However, it is important to note that in both cases a mathematical model is required for the far velocity field induced by the aircraft to be tested in order to calculate, at the wind tunnel wall location, the velocities induced by the aircraft in free air. This mathematical model must represent the lifting devices (wing, rotor or jet) sufficiently well to enable the induced velocities far from the model to be satisfactorily predicted.

The first approach groups the following methods :

- (i) The image method : Wind tunnel walls are simulated by infinite series of images of the mathematical model simulating the aircraft. The sum of the velocities induced by all the images of the model is the boundary interference velocity. This method is mainly applicable to wind tunnels of rectangular cross section, though it has been used for circular or elliptical test sections, either open or closed, but not in the case of slotted walls. This is the classical method described in most published reports, e.g., Refs 1, 3, 7, 10.
- (ii) The wall perturbation potential method : It is based on the numerical solution of the Laplace equation for the wall perturbation potential. The numerical solution is obtained for a certain boundary condition to be satisfied by the sum of the wall and model perturbation potentials. This boundary condition is applied at the test section boundaries, which may therefore have any shape and be of any type, open, closed or slotted. A method of this kind is illustrated in Ref.19.
- (iii) The vortex lattice method : This method, due to Joppa (Ref.20) is applicable to closed test sections of any shape; it uses a double lattice of vortices lying on the wind tunnel walls, parallel and perpendicular to the free stream velocity, forming a pattern of rectangular cells. The boundary condition of no flow through the walls, applied at the center of each cell, gives a linear relationship between the vorticities associated with the cells. The resulting system of equations can be solved for the wall distributed vorticity. Of course, in each of these equations, will also appear the contribution from the mathematical model describing the actual physical model located in the test section. Once the wall distributed vorticity which simulates the presence of the wall is found, the wall induced velocities anywhere in the test section can be directly evaluated.

The second approach consists of :

- (i) Employing a very large test section compared to the model. The question of how large the test section must be is answered by evaluating the wall induced velocities by one of the methods described above and checking if the resulting correction can be neglected.
- (ii) Employing a slotted wall test section, where the type of slot is chosen so as to minimize the wall interference. It is undoubtedly true that with slotted walls a decrease in wall interference can be obtained, but a practical test section design for zero interference on both lift and pitching moment has not really been demonstrated yet.
- (iii) Having a special test section with porous walls surrounded by several plenum chambers. During the test the static pressures on the wind tunnel walls are monitored and compared with the pressures that should exist in free air far from the model, and which can be predicted by the mathematical model simulating the aircraft. Then by suitable adjustment of the pressures in the plenum chambers, the wind tunnel wall static pressure is modified till it coincides with the static pressure existing in free air at the location of the wind tunnel boundaries. This approach has been proposed by Kroeger and Martin (Ref.21) and investigated at Northrop (Ref.22).

Some of these procedures may be applied iteratively to take into account the influence of the wind tunnel walls on the mathematical model describing the aircraft.

As already stressed, an important decision to be taken is the choice of the mathematical model describing the far field of the aircraft. For CTOL aircraft, doublets, sources and sinks are used for blockage corrections (Refs 2 and 23), and a superposition of horseshoe vortices for lift corrections. The only existing schemes for V/STOL and helicopters, which yield directly applicable correction charts appear to be those proposed by Heyson. They refer to downward deflected straight wakes on which vertically and horizontally oriented doublets or vortex rings are distributed. The vertical and horizontal interference velocities, and hence, the lift and moment corrections as well as the wake blockage correction are thereby obtained. The blockage due to the model volume and any separated flow regions should of course also be accounted for, as in the case of CTOL models (Refs 2 and 3).

### 2.3 Flow breakdown

When the high energy wake from a V/STOL lifting system impinges on the wind tunnel floor, flow reversal can occur on it due to : (a) floor boundary layer separation before the impingement point caused by the wall static pressure rise upstream of the impingement point, and (b) equilibrium of momenta at the impingement point which always requires the existence of some reverse flow on the wind tunnel floor. By employing a moving ground, cause (a) can be eliminated, therefore delaying flow breakdown but not eliminating it because cause (b) does not depend on the existence of a boundary layer on the wind tunnel floor.

#### 2.3.1 Criteria for occurrence

Flow breakdown has been studied by various investigators who deduced the testing limit at which it occurred. This limit can be expressed in terms of any one of the following parameters (Fig.1) :

$$C_{Lhb} = \frac{L}{\frac{1}{2} \rho V^2 \cdot h \cdot b}$$



$$\frac{C_L}{A} = \frac{h}{b} C_{Lhb}$$

$$\frac{V_0}{V_j} \frac{h}{d}$$

$$\frac{h \tan \chi}{b} = \frac{x_f}{b}$$

a) South's criterion : In Ref.14 experimentally determined flow breakdown limits for jet flap wings, defined as corresponding to incipient separation on the wind tunnel floor, are expressed by :

$$C_{Lhb} \leq 3.0 \quad \text{for } \frac{D_i}{L} \leq 0$$

$$C_{Lhb} \leq \frac{3}{\sqrt{1 + 4\left(\frac{D_i}{L}\right)^2}} \quad \text{for } \frac{D_i}{L} \geq 0$$

b) South's correlation of Rae's data : According to Ref.14, results obtained by Rae for rotors at  $D_i/L$  close to zero indicate that flow breakdown occurs at values of  $C_{Lhb}$  between 2 and 4.

c) Tyler and Williamson limit : Experimental results for vertical jets, reported in Refs 15 and 16 yield the following limit at which stagnation of the main flow first occurs on the wind tunnel floor :

$$\frac{V_0}{V_j} \frac{h}{d} \geq 1.6$$

Tilting the jets slightly modifies the value of the numerical constant. Thus for a forward or rearward inclination of  $20^\circ$  the constant respectively becomes 1.55 and 1.67 instead of 1.6.

d) Heyson's correlation : Various limits of flow breakdown, experimentally determined by Rae (Ref.12) on rotors, by Heyson (Ref.24) on a jet flap and by Grunwald (Ref.25) on a tilt wing were correlated by Heyson (Ref.26) in terms of minimum allowable value for  $x_f/b$ , for various wind tunnel width to height ratios, as follows :

$$\begin{aligned} x_f/b &\geq 1.25 && \text{for } B/H = 3 \quad \text{to } 4/3 \\ x_f/b &\geq 1.75 && B/H = 1 \\ x_f/b &\geq 1.25 && B/H = 2.3 \\ x_f/b &\geq 1.5 && B/H = 1/2 \end{aligned}$$

Here  $x_f = h \tan \chi$  is calculated using for  $\chi$  the momentum wake skew angle as determined in Ref.27 and not the effective (vorticity) wake skew angle.

e) Heyson's theoretical analysis : In Ref.28, the potential flow in a test section containing a rotor is graphically pictured by a numerical technique in which the rotor wake is represented by a skewed circular cylinder of distributed vorticity and the walls by the rotor wake images. The flow on the wind tunnel floor is found to be never reversed for  $\chi > 70^\circ$  and always reversed for  $\chi < 30^\circ$ . However, from the charts presented, no quantitative conclusion can be drawn of the effect of angle of attack, model vertical location, rotor load distribution and relative size on the value of  $\chi$  at which reversal occurs. These effects appear to be small from such an analysis and the limiting value for  $\chi$  to be around  $50^\circ$ .

f) Owen's correlation of Vogler's data : In Ref.29, Owen examined data on ground effect measurements by Vogler (Ref.30), obtained from models with various jet configurations. Using a formula due to Hurns and Akers (Ref.31), he suggested a limit based on the assumption that flow breakdown occurs when the jet path, calculated in the absence of the floor, intersects the floor at an angle of  $60^\circ$ .

These limits can be plotted in terms of  $h/b$  or  $h/d$  versus  $V_0/V_j$  (Fig.2a), or in terms of  $C_L/A$  versus  $b/B$  (Fig.2b). In the second case, the shape of the test section and the vertical location of the model must be specified. Fig.2b applies to a wind tunnel having a width to height ratio of 4:3 and a model centered ( $h/H = 1/2$ ) in the test section.

One set of curves may be obtained from the other using the following relationships :

$$\frac{C_L}{A} = \frac{1}{b^2} \frac{\pi}{4} b^2 \rho \frac{V_j^2}{2} = \frac{\pi}{2} \left(\frac{V_j}{V_0}\right)^2$$

and

$$\frac{b}{B} = \frac{1}{h/b} \frac{h}{H} \frac{H}{B}$$

therefore, for the case considered :

$$\frac{b}{B} = \frac{1}{2} \frac{3}{4} \frac{1}{h/b}$$

It should be noted that acceptable test conditions lie above the limit curves of Fig.2a and below the limit curves of Fig.2b. The different ranges for which the various curves are valid should also be noted, some applying to high and others to low disk loading systems. Furthermore, when we consider that Owen's limit has been experimentally obtained for high disk loading systems (vertical jets), while that of South for low disk loading systems (jet flaps) we may infer that the disagreement between South's and Owen's limits in the high disk loading range may be partly due to extrapolation of the former beyond the range of experimental conditions used. The discrepancy between the Tyler-Williamson curve and the other curves on Fig.2b is due to the same cause, because of the unrealistic dimensions implied for the jet nozzle diameter.

Because Heyson's limit seems to follow the trend indicated by experiments in both high and low disk loading ranges, it has been retained in the present analysis.

A further comment should be made about the discrepancy between Tyler and Williamson's and Owen's limit. The first one refers to the condition of incipient separation on the wind tunnel floor, while Owen's has been deduced from measurements on models. The difference between the two limits probably means that there is a range of speeds for which separation occurs on the wind tunnel floor without affecting the flow at the model location. Further research relating the extent of flow breakdown to its effect on model measurements is needed. In this context, recent data at R.A.E. reported by Owen (Ref.18) appear to indicate that the true limit for flow breakdown is about 20% more severe than that suggested by the formula derived from the measurements of Vogler (Refs 29 and 30). Furthermore, as mentioned in Ref.18, Tyler and Williamson conclude that interference effects start to appear at speeds about 0.8 times lower than the incipient separation speed predicted by the formula  $V_0 h / V_j d = 1.6$ . Thus the Tyler and Williamson limit would become

$$\frac{V_0 h}{V_j d} \geq 1.28$$

This limit has also been plotted in Figs 2a and 2b.

### 2.3.2 Testing limitation due to flow breakdown

The testing limit imposed by flow breakdown can be quite severe. However, the limitations arising from wall corrections may become more restrictive in some cases as discussed later.

To illustrate this, three model configurations will be considered :

(i) Testing of a jet lift engine : The limit of Tyler and Williamson in its corrected form is taken as

$$\frac{V_0 h}{V_j d} \geq 1.28$$

and can be directly expressed in terms of the total lift of the jet engine

$$L_j = \frac{\pi}{4} d^2 V_j^2 \rho$$

giving

$$h V_0 \geq 1.28 \sqrt{\frac{4 L_j}{\pi \rho}}$$

Assuming a jet exit temperature of about 700°K this reduces to

$$h V_0 \geq 6.37 \sqrt{L_j}$$

Thus, if a real lift engine having  $L_j = 1600$  Kg (similar to the Rolls Royce RB 162 for the Mirage III-V) is to be tested, the condition for no flow breakdown would be

$$h V_0 \geq 255 \frac{m}{s}$$

Therefore if tests were to be carried out at a minimum speed of 25 m/s, the position of the model above the wind tunnel floor should be about 10 meters at least.

The limit has also been plotted in Fig.3a for two hypothetical lift engines having the following characteristics :

$d = 0.4$ m	$d = 0.5$ m
$T_e = 700^\circ\text{K}$	$T_e = 700^\circ\text{K}$
$V_j = 450$ m/s	$V_j = 450$ m/s
$L_j = 1305$ Kg	$L_j = 2040$ Kg

Two additional cases of engines with  $L_j = 100 \text{ Kg}$  and  $L_j = 500 \text{ Kg}$  are considered. These values are too low to correspond to full scale lift engines.

Limits have also been plotted in Fig.3b where the maximum lift of the vertical jet engine which can be tested without flow breakdown is indicated for a model located at mid-height of test sections having the following typical dimensions : 18m x 13.5m and 25m x 18.75m.

(ii) Testing of a jet flap wing : An example is given in Fig.2b showing that the testing of a jet flap wing having an aspect ratio of 6 and centered in a test section having a width to height ratio of 4:3 is limited to a lift coefficient of 13.2 or 9.0 when the wingspan is equal to 1/2 or 3/4 of the wind tunnel width.

(iii) Testing of a lift fan : If tests of a lift fan of diameter  $d$  and having an ejection velocity  $V_j$  are to be made at test speeds down to one tenth of  $V_j$ , then the minimum model height above the wind tunnel must be 12.8 times the fan diameter.

#### 2.4 The method of Heyson for calculating wall interference

In the last decade, Heyson has worked extensively on the problem of V/STOL wind tunnel wall corrections using the image method. During this time his theory has undergone various modifications so that in any application it is important to specify the method employed. The various modifications differ by :

- a) The choice of the mathematical model for simulating the lifting elements :
- (i) a skewed cylinder with distributed vorticity, i.e., ring vortices lying in planes inclined with respect to the undisturbed velocity  $V_0$  by the angle of attack  $\alpha$  of the rotor. In each of these planes there may be a single vortex ring or several to simulate different radial loading conditions of the rotor blades.
  - (ii) a line of doublets directed downward (for lift) and forward (for drag) or rearward (for thrust, i.e., negative induced drag). This model alone is of course only valid for aircraft or rotor models which are vanishingly small with respect to the test section size.
  - (iii) superposition of some of the preceding schemes for representing rotors or wings of finite size with arbitrary planform and loading.

b) The choice of the wake inclination with respect to the vertical ( $\chi$ ). Ref.27 presents a nomographic solution of the momentum equation which, once the flight velocity  $V_0$  and the induced drag to lift ratio  $D_i/L$  are known, allows the determination of  $\chi$ . This value has been used in Refs.7, 10 and 32. In Ref.24, it is observed that due to the rolling up of the edges of the wake caused by the cross wind, the edges of the wake in which vorticity is concentrated are penetrating in the cross flow only about half as far as the central part of the wake. This suggested to Heyson the use of an "effective" wake skew angle  $\chi_e$ , larger than  $\chi$ , and given by

$$\frac{\pi}{2} - \chi_e = \frac{1}{2} \left( \frac{\pi}{2} - \chi \right)$$

where the approximate figure of 1/2 on the right hand side is not too different from the factor  $4/\pi^2$  obtained from a theoretical treatment (Ref.33) of the vortex sheet deformation, behind an elliptically loaded wing.

But because the proposed relation yields an uncorrect value of  $\chi_e = \frac{\pi}{4}$  instead of 0 when  $\chi = 0$ , the expression for  $\chi_e$  has recently been modified (Ref.6) to

$$\tan\left(\frac{\pi}{2} - \chi_e\right) = \frac{4}{\pi^2} \tan\left(\frac{\pi}{2} - \chi\right).$$

A discussion on the choice of  $\chi_e$  is also reported in Ref.6.

#### 2.5 Acceptable limits to wall corrections

The testing limits for V/STOL models correspond not only to the onset of flow breakdown, but also to some maximum acceptable value for the flow angularity and dynamic pressure corrections at the wing and tail location, and to some maximum acceptable value for the non-uniformity of the corrections over the wing span.

The problem of determining the maximum acceptable values for those parameters has not yet been resolved. As a preliminary approach, Heyson has suggested (Ref.6) the following three sets of limits, corresponding respectively to maximum acceptable corrections, to moderate corrections and to the case when no corrections need to be applied to the test results :

parameter	maximum acceptable corrections	moderate corrections	no corrections
$\Delta\alpha$	$\pm 5^\circ$	$\pm 5^\circ$	$\pm 1/2^\circ$
$q_c/q$	$1 \pm 10\%$	$1 \pm 10\%$	$1 \pm 5\%$
$\Delta i_t$	$\pm 5^\circ$	$\pm 2^\circ$	$\pm 1/2^\circ$
$q_t/q_c$	$1 \pm 10\%$	$1 \pm 5\%$	$1 \pm 5\%$
$\Delta i_w$	$\pm 2^\circ$	$\pm 1/2^\circ$	$\pm 1/2^\circ$
$\frac{d(\Delta i_w)}{d(y/b)}$	$\pm 5^\circ/\text{semi-span}$	$\pm 1^\circ/\text{semi-span}$	$\pm 1^\circ/\text{semi-span}$
$\Delta q/q_c$	$\pm 10\%$	$\pm 5\%$	$\pm 5\%$

No other criterion was found in the literature besides, of course, the well known limit of  $\Delta\alpha < 2^\circ$  for CTOL when  $\Delta\alpha$  is calculated with the conventional theory assuming an undeflected wake (Refs. 4 and 5).

## 2.6 Application of Heyson's theory to the determination of testing limits in a V/STOL wind tunnel

The criteria presented in the preceding paragraph have been used for the determination of testing limitations in low speed wind tunnels having a closed test section. The limitation due to flow breakdown has been added, using Heyson's criterion indicated in paragraph 2.3.1, i.e.,  $x_f/b \geq 1.25$ .

The theory of Heyson used in the present analysis refers to the method of superposition of several identical lines of doublets and allows the representation of a uniformly loaded swept or unswept wing. The wake skew angle used was that given by :

$$\tan\left(\frac{\pi}{2} - \chi_e\right) = \frac{4}{\pi^2} \tan\left(\frac{\pi}{2} - \chi\right)$$

Heyson's results for this scheme are presented in graphical form in Ref. 6 as functions of the following parameters :

wind tunnel shape	$\gamma = B/H$
wing span to tunnel width ratio	$\sigma = b/B$
wing sweep angle	$\Lambda$
wing angle of attack	$\alpha$
induced drag to lift ratio	$D_i/L$

and for an aircraft model having a standardized tail located at the same height as the wing and at a distance behind it equal to 3/4 of the wing span.

The results presented in Ref. 6 have therefore been cross plotted to obtain Figs 4 to 7 which present for a wind tunnel having a width to height ratio of 4:3 as proposed in Ref. 34, the maximum acceptable  $C_L/A$  as a function of the wing span to wind tunnel width ratio. This has been done for normal mounting of the model at the center of the test section and for semi-span mounting on the wind tunnel floor which is equivalent to normal mounting in a 4:6 test section.

Of course it is necessary to specify the value of  $D_i/L$ . Two cases have therefore been considered : the first one suggested by Heyson is  $D_i/L = 0$  (Figs 4 and 5) corresponding to a powered test in which the forward thrust is equal to the drag of the model; the second one (Figs. 6 and 7) is the case of an unpowered wing, with mechanical high lift devices only, for which a one to one relationship exists between  $C_L/A$  and  $D_i/L$ . This relationship is deduced in Ref. 6 and leads to the result already obtained by McCormick (Ref. 35) that the maximum value of  $C_L$  cannot exceed  $1.21A$ , taking into account the deflection of the wake.

The effect of sweep angle is also considered in Figs 5 and 7 and is seen to lower the testing limits.

The limit curve of  $\Delta\alpha < 2^\circ$  is also indicated in Figs 5 and 7,  $\Delta\alpha$  being calculated in this case from the conventional theory of undeflected wakes :

$$\Delta\alpha = \delta \frac{S}{C} C_L = \delta \frac{S}{C} \frac{C_L}{A} \frac{b^2}{S} = \delta \left(\frac{b}{B}\right)^2 \frac{B}{H} \frac{C_L}{A}$$

$$\delta = \delta_{\chi=90^\circ}$$

It is important to note that the available calculations in Ref. 6 give, for a wind tunnel having a 4:3 width to height ratio, only three points per curve corresponding to values of  $b/B$  of 0.25, 0.5 and 0.75. Although this is hardly sufficient to realistically define the curves shown in Figs 4 to 7, they are indicative of test limitations.

An alternative way of presenting the same results is shown in Fig. 8, obtained from Heyson during the visit made by the author to the Langley Research Center. It is related to the testing limits in the American full scale wind tunnel proposal having a 40m x 60m test section, and has been obtained from the graphs of Ref. 6 for moderate corrections by the use of the relationship

$$\frac{L}{b^2} = \frac{1}{2} \rho v_0^2 \frac{C_L}{A}$$

The curves show the limit for performing powered tests at  $D_i/L = 0$  and with a constant lift equal to the weight of the aircraft. Because of this condition, the curves are velocity dependent, the tests at lower velocities being carried out at higher angles of attack. Also shown on the figure are the operating points of some CTOL and STOL aircraft and helicopters, for full scale tests.

The testing limits shown in Figs 4 to 7 have been obtained for wings only, according to the available correction charts of Ref. 6 which also presents similar data for rotors, but only for wind tunnels having a width to height ratio of 3:2. However, comparison of the limits for wings and rotors in 3:2 test sections as reported in Ref. 6 does not show large differences. Therefore, as done by Heyson in Fig. 8, the same limits for rotors as for wings could be considered for the purpose of the present discussion.

Inspection of Figs 4 to 7 shows, for instance, that the testing limits for an unpowered unswept wing having an aspect ratio of 6 and employing mechanical high lift devices only are expressed by the following tables :

Normal mounting at the center of a 4:3 test section		
	moderate corrections	maximum corrections
$b/B = 1/2$	$C_L < 5.2$	$C_L < 7.2$
$b/B = 3/4$	$C_L < 0.81$	$C_L < 3.84$

The limit  $C_L < 0.81$  is clearly insufficient; it corresponds to the condition

$$d\Delta i_w / d(\frac{Y}{b}) < 1^\circ / \text{semispan},$$

and so is related to the spanwise variation of induced interference velocity.

Semispan mounting on the floor of a 4:3 test section		
	moderate corrections	maximum corrections
$\frac{b}{2H} = 1/3$	$C_L < 7.2$	$C_L < 7.2$
$\frac{b}{2H} = 1/2$	$C_L < 4.32$	$C_L < 6.9$
$\frac{b}{2H} = 2/3$	$C_L < 2.24$	$C_L < 5.16$

The first two cases considered here correspond to wings having the same physical scales as those considered in the case of normal mounting at the center of a 4:3 test section. The testing range is therefore extended to cover all the values of  $C_L$  obtainable with pure mechanical systems. The third case corresponds to a wing having  $b/B = 1$  and cannot for obvious reasons be tested with a normal mounting.

The same considerations applied to a jet flapped unswept wing having the same aspect ratio of 6 and tested at zero values of  $D_i/L$  lead to the following tables :

Normal mounting at the center of a 4:3 test section		
	moderate corrections	maximum corrections
$b/B = 1/2$	$C_L < 6.3$	$C_L = 14.1$
$b/B = 3/4$	$C_L < 0.81$	$C_L < 4.14$

Semispan mounting on the floor of a 4:3 test section		
	moderate corrections	maximum corrections
$\frac{b}{2H} = 1/3$	$C_L < 15$	$C_L < 20.4$
$\frac{b}{2H} = 1/2$	$C_L < 4.86$	$C_L < 11.0$
$\frac{b}{2H} = 2/3$	$C_L < 2.4$	$C_L < 5.82$

It can therefore be concluded that testing an unpowered wing of aspect ratio 6, having a maximum theoretical lift coefficient of 7.36 (Ref.35) and actually attaining  $C_{Lmax}$  values around 4.0 is possible for normally mounted models spanning half the tunnel width and for semispan floor mounted models having a semispan of half the tunnel height. Due to the higher lift coefficients attainable, the testing of a jet flap wing is more severely restricted.

It is very important to fix realistic values for the maximum corrections that can be accepted whilst retaining confidence in the corrected values. Thus the two proposed limits differ widely in the case of normal mounting for  $b/B = 3/4$ , which is one often encountered in practice. Further studies are required on this particular aspect. Furthermore, it has been observed, during the cross plotting which led to Figs 4 to 7 that flow breakdown effectively limits the testing range only for models which are small compared with the test section, i.e., for span to width ratios below about  $1/4$ . For models of larger dimensions, the wall corrections become unacceptably large before flow breakdown begins.

However, this conclusion is valid only for the cases to which Figs 4 to 7 refer, i.e., for powered or unpowered wings and as a first approximation for rotors. It does not apply for single or multiple vertical lifting jets issuing from a wing or from a complete model, in which there is not only a wake originating at the wing but also a jet much closer to the vertical, issuing from the lift engine. The limits so far described apply only to the part of the lift given by the wing  $L_w$ , expressed in terms of the coefficient  $C_{L_w}/A$ . A second limit arising from flow breakdown caused by the vertical jet can be considered by introducing a lift coefficient for the jet

$$\frac{C_{L_j}}{A} = \left( \frac{C_L}{A} \right)_{\text{total}} - \frac{C_{L_w}}{A}$$

where

$$\frac{C_{L_j}}{A} = \frac{\frac{\pi}{4} d^2 \rho V_j^2}{\frac{1}{2} \rho V_0^2 S} \frac{1}{\frac{b^2}{S}} = \frac{\pi}{2} \left( \frac{V_j}{V_0} \frac{d}{b} \right)^2$$

If we use Tyler and Williamson's corrected criterion for flow breakdown caused by vertical jets (see paragraph 2.3.1), which requires that

$$\frac{V_0}{V_j} \frac{h}{d} \geq 1.28$$

we obtain, for a model centered in a 4:3 test section :

$$\frac{V_0}{V_j} \frac{h}{d} = \frac{V_0}{V_j} \frac{h}{H} \frac{H}{B} \frac{1}{\frac{b}{B} \frac{d}{b}} \geq 1.28$$

that is

$$\frac{V_0}{V_j} \frac{b}{d} \geq 3.41 \frac{b}{B}$$

and therefore

$$\frac{C_{L_j}}{A} \leq \frac{\pi}{2} \frac{1}{(3.41 \frac{b}{B})^2}$$

providing a limit which is independent of the jet nozzle diameter  $d$ , and which coincides with the limit  $C_L/A = f(d/B)$  for an isolated jet. This limit is plotted in Fig.2b, but no conclusion can be drawn if the ratio of  $C_{L_w}$  to  $C_{L_j}$  during transition flight is not known. This depends on the variation  $\alpha_w = \alpha_w(V_0)$  during transition.

Furthermore, the approach neglects possible interactions between the two wakes, a situation for which no information seems available. It seems therefore that further studies of flow breakdown and of corrections are needed for V/STOL aircraft employing a highly loaded wing and additional lifting jets.

The limits of flow breakdown shown in Fig.2b can, depending on the proportion of lift provided by the wing and the jet, impose the most stringent limits on test conditions. Thus, for a V/STOL model having an unpowered wing of aspect ratio 6 and a lifting jet in the fuselage, the testing limits are the following for normal mounting at the center of a 4:3 test section :

	moderate corrections	maximum corrections
$b/B = 1/2$	$C_{L_w} < 5.2$	$C_{L_w} < 7.2$
	$C_{L_j} < 3.24$	$C_{L_j} < 3.24$
$b/B = 3/4$	$C_{L_w} < 0.81$	$C_{L_w} < 3.84$
	$C_{L_j} \quad 1.44$	$C_{L_j} \quad 1.44$

## 2.7 Test sections with open or open and closed boundaries

For tests of CTOL aircraft, an open or partly open test section may look attractive because of the reduction in blockage corrections compared with a closed test section and because of the greater accessibility to the model. However, the boundary condition  $\partial\phi/\partial x = 0$  on a free boundary does not recognize the existence of a mixing layer between the jet and the surrounding air. Furthermore, it is applied without taking into account the deformation of the free jet boundaries. It does not therefore appear to be very realistic and it is not clear what should be used instead.

The situation is even worse when tests of V/STOL aircraft are envisaged because of the existence of larger force coefficients and therefore of larger corrections. Also, the high energy wake associated with the lifting elements may impinge on the free lower boundary especially when these elements consist of high velocity vertical jets.

An open lower boundary would seem useful for eliminating the flow breakdown which would occur with a solid lower boundary but, as pointed out in Refs 7 and 36, other difficulties arise in this case. Either the deflected wake will impinge on the open lower boundary, distort it and thus invalidate correction calculations; or it will approach the solid lower surface of the diffuser following the test section, and under these conditions the effect of finite jet length (Ref.36) will become so large as to be no longer negligible.

For these reasons, it is felt that the use of an open lower boundary should not be recommended for V/STOL tests, until the effects of jet penetration in the lower boundary have been assessed.

On the other hand, a partly open wind tunnel with a solid lower boundary may look attractive for reducing corrections and for studies of ground effects. Thus, a test section having closed top and bottom walls and open sidewalls may, as pointed out many years ago by Theodorsen and Toussaint (Ref.3), yield zero lift interference for CTOL models centered in the test section. The suitability of partly open test sections for V/STOL tests has recently been discussed by Heyson (Ref.37) who calculated the correction factors for a test section having a solid lower wall only. Results indicate that by a suitable choice of width to height ratio  $B/H$ , zero vertical interference due to lift can be achieved. However, the appropriate value of  $B/H$  depends on the wake skew angle  $\chi$ . Thus for  $\chi = 90^\circ$  (horizontal wake such as for CTOL models) a test section closed at the bottom only with  $B/H = 2$  is required, while a test section having  $B/H = 4/3$  would be suitable for  $\chi = 66^\circ$  and a test section with  $B/H = 1/2$  for  $\chi$  around  $30^\circ$ .

Because of this, Heyson suggests the use of variable geometry wind tunnels in which  $B/H$  can be varied (Ref.37) according to the wake deflection angle obtained. This obviously leads to a complicated wind tunnel design but additional benefits include major improvements in uniformity of interference, pitching moment corrections, and minimum speed for recirculation free testing.

Another suggestion by Heyson (Ref.37) is to use the "variable model height" technique in a test section of fixed width to height ratio with a single lower solid wall. Again reduction of interference is obtained although it is less significant than in the case of variable  $B/H$ . It would seem desirable, however, to seek experimental verification of these concepts.

## 2.8 Comparison of Heyson's theoretical treatments with experiment

Several experimental investigations of the accuracy of Heyson's theory in predicting wall effects for V/STOL aircraft have been carried out and have resulted in the theory undergoing several modifications during the last decade.

Thus, in Ref.25, Grunwald applies Heyson's theory to a tilt wing model by using the momentum skew angle given by Ref.27 and by approximating the wing lifting scheme by linear doublet wakes. Differences between corrections obtained with one or three doublet wakes are seen to be negligible. The theory was found to be adequate for correcting lift and drag, but not pitching moment. However, pitching moment was adequately corrected for a model tail-off configuration thus indicating that the theory satisfactorily predicts interference velocities at the wing location but not at the tail location. This is due to an incorrectly predicted longitudinal variation of the vertical interference velocity arising from the linear assumption for the wake or from the choice of its skew angle  $\chi$ . This probably is also the reason for the disagreement between corrected data and flight data found in Ref.32.

Subsequently, Heyson in Ref.24 applies his theory to a jet flap model and concludes that (i) It is necessary to include the effects of finite model span, at least when the model span is greater than about one half the tunnel width and (ii) The substitution of the momentum wake skew angle  $\chi$  by an effective wake skew angle  $\chi_e$  improves the correlation. Furthermore, prediction of wall effects including effects on the tail is seen to be reasonable at moderate blowing coefficients ( $C_u < 5.0$ ) only.

An experimental programme is currently being conducted at Langley (Ref.38) in order to check the more elaborate form of Heyson's theory.

## 2.9 Other theories for wall corrections

The major criticism to be made of Heyson's theory probably concerns the assumption of a straight wake rather than a curved one. In fact, calculations have been made mainly by Heyson (Refs 26 and 38) and Lo (Ref.39) by distributing doublets on an empirically determined (Ref.40) curve representing the centerline of a jet deflected by a crossflow.

This approach neglects the effect of the walls on the wake path. Heyson's calculations (Ref.26) show that the replacement of a straight wake by a curved wake does not change the average vertical interference velocity, but shifts the vertical interference velocity profile downstream. This leads further support to the argument that a correct definition of the wake is necessary if corrections for pitching moment and tail forces are to be realistically assessed. Calculation of this type have been made for a few cases only and tables of a more general nature allowing a discussion of testing limits are not available. It is considered that the curved wake simulation for V/STOL aircraft is one of the most important problems at present.

Another method which looks promising is the vortex lattice method suggested by Joppa (Ref.20) for simulating wind tunnel walls. It is applicable to test sections of arbitrary cross section. The method could be applied taking into account the effect of the walls on the wake curvature. Again, further theoretical studies are needed on the subject.

### 3. VENTILATED WALLS

#### 3.1 Introduction

Ventilated walls, in the form of either slotted or perforated walls, were first used around the 50's in transonic wind tunnel for reducing the model blockage. Without such precautions, the model can cause choking of the wind tunnel flow at high transonic free stream Mach numbers, thereby invalidating test results (Ref.23). Ref.1 presents a good review of the work carried out up to 1966 on slotted or perforated walls for transonic testing, and a more recent survey which discusses methods for correcting CTOL test results for wall constraints in subsonic wind tunnels with slotted or perforated walls has been reported (Ref.41). In fact the methods for correcting results at low speeds are basically identical to those used at high subsonic speeds and can therefore be obtained from the literature available on the latter, if the compressibility parameter  $\beta$  is taken to be unity.

The use of slotted or perforated walls for low speed testing decreases the boundary interference. From the consideration that fully open and fully closed test sections yield corrections of opposite sign, it may be inferred that some combination of open and closed boundaries could yield zero corrections, or at least smaller corrections than for fully open or fully closed boundaries. This has been validated by several investigations carried out by comparing the results obtained on the same model in a closed test section, in a slotted test section of the same size, and in a closed test section of dimensions large enough to produce "interference free" data. A typical investigation of this kind (Ref.42), performed on a jet flap model having an aspect ratio of 4 and fitted with a horizontal tail, shows that the use of test section configurations with three or four slotted walls results in large reductions in the wall interference effects.

#### 3.2 The theoretical approach

For slotted or perforated walls, image methods are not directly applicable and thus the various theoretical approaches proposed are based on solutions for the wall perturbation potential. Such a solution requires (i) a mathematical model for predicting the farfield velocity induced by the aircraft to be tested so giving the model perturbation potential, and (ii) a boundary condition on the sum of the wall and model perturbation potentials which correctly simulates the slotted or porous boundaries. Except for a few cases (Refs 39, 43) only mathematical models typical of CTOL aircraft, i.e., using sources and sinks or doublets, for blockage corrections, and horizontally trailing horseshoe vortices or horizontal lines of downward directed doublets, for lift interference, have been employed in ventilated wall analysis. A recent example of this type of approach is given in Ref.19.

On the other hand, two approaches have been followed for the choice of the boundary condition. Either a non-homogeneous boundary condition has been used, i.e.:

$$\frac{\partial \phi}{\partial n} = 0 \text{ at the solid strips}$$

and

$$\frac{\partial \phi}{\partial n} = 0 \text{ at the slots,}$$

in which the viscous effects in the slots are neglected or a homogeneous boundary condition (Refs 44, 45 and 46) is derived which is valid when the slot width and spacing are small compared with the test section size:

$$\frac{\partial \phi}{\partial x} + K \frac{\partial^2 \phi}{\partial x \partial n} + \frac{1}{R} \frac{\partial \phi}{\partial n} = 0$$

where K is a geometrical parameter which is a function of slot width and spacing, and R a porosity coefficient related to the pressure drop across the test section boundaries. A discussion of the experimental methods for the determination of the porosity coefficient has been reported by Vaissaire (Ref.41). For the geometrical parameter K, the following expression is derived in Refs 44 and 45:



$$K = -\frac{\ell}{\pi} \ln \left| \sin\left(\frac{\pi a}{2\ell}\right) \right|$$

a and  $\ell$  being the slot width and spacing respectively. However, it is pointed out in Ref.47 that the use of the following alternative expression derived in Ref.48, yields a better correlation between theory and experiment :

$$K = -\frac{\ell}{2} \left(1 - \frac{a}{\ell}\right) \frac{\cos \pi \left(1 - \frac{a}{\ell}\right) - \cosh \frac{\pi t}{\ell}}{\sin \pi \left(1 - \frac{a}{\ell}\right)}$$

where t is the thickness of the wind tunnel wall. Whereas the first expression given for K is derived for flow through a thin slotted screen, the second is obtained by representing the slots in the tunnel wall by distributions of doublets whose strength is evaluated in terms of the slot width, thickness and spacing.

Results are often presented in terms of a non-dimensional slot parameter,  $P = 1/(1 + 2K/H)$  which is 0 for a completely closed test section and 1 for a completely open section.

An alternative approach is the one followed by Rushton (Ref.49) who developed an electrical analogue computer to study slotted wall interference effects. It consists of a rectangular array of resistors which form a model of a wing and of the tunnel cross section. The exact non-homogeneous boundary conditions are applied by insulating the solid portions of the wall ( $\partial\phi/\partial n = 0$ ) and grounding the slotted portions ( $\phi = \text{const.}$ ).

### 3.3 Theoretical results

As a first step in a theoretical study of the slotted wall interference for V/STOL aircraft, Refs 19 and 50 present a method to calculate the interference induced by walls with slots of uniform width for the case of a conventional lifting wing represented by a horizontal trailing horseshoe vortex of vanishingly small span. Results in terms of a lift interference factor  $\delta$  versus slot parameter P are in good agreement with the data obtained by Rushton with his network analyzer. Results indicate that it is possible to achieve zero lift interference factor  $\delta$  for a certain value of P on the top and bottom walls. This value is around 0.4 for a wind tunnel having a width to height ratio of 3:2 and is almost independent of the side wall value : for a side wall slot parameter variation from 1.0 to 0.05, the top and bottom slot parameter required for zero  $\delta$  varies only from 0.34 to 0.42.

Subsequently Lo (Ref.51) extended the previous calculations to take into account the effect of the deflection of the wake, by replacing the horseshoe vortex simulating a lightly loaded conventional wing by the mathematical model suggested by Heyson (Ref.7). This simulates the wake originating from a rotor at zero angle of attack by means of a skewed cylinder of vortex rings of constant strength lying in planes parallel to the rotor plane. Because Refs 19 and 50 indicate that the porosity of the side walls has a negligible effect, the calculations have been developed for solid side walls only. Results for equal porosities of the top and bottom walls indicate that the value of slot opening required in order to have zero vertical interference is a function of the wake angle which in turn depends (Ref.27) on the test velocity.

This dependence of the slots required on the test speed is of course an undesirable feature, and Lo has further extended his work (Ref.52) to the case when top and bottom walls have different porosities. The slots are again uniformly spaced and have a constant width, and the mathematical model again simulates a lifting rotor at zero angle of attack. The value of K appearing in the boundary condition is, as in previous work, given by the first expression above. Results (see Fig.2 of Ref.52) indicate that the curve of top porosity versus bottom porosity for zero vertical interference is dependent on the wake skew angle. However, it is also found that with a 3:2 test section, the curves of required top and bottom porosities for different wake angles cross each other around values of  $P_{\text{top}} = 0.27$  and  $P_{\text{bottom}} = 0.70$ , thereby indicating that for such values, almost zero vertical interference at the model location is obtained independently of the wake angle. This produces almost zero lift interference. The longitudinal distribution of lift interference varies somewhat, thereby indicating non-zero pitching moment correction. But the latter is much smaller than that obtained by Heyson in variable geometry wind tunnels for minimizing corrections (Ref.37).

A recent theoretical study at AEDC (Ref.39) makes use of the second expression for the coefficient K mentioned earlier as suggested by the experimental verification in Ref.47. Viscous effects in the slots are not taken into account. The slots again have a uniform width, though some previous results (Ref.51) indicate that zero upwash interference, not only at the model location but along the wind tunnel longitudinal axis, can be obtained with shaped slots having a width varying with longitudinal distance. However, the main effort has not been directed toward the analysis of slots of non-uniform width but rather toward a more detailed representation of the wake. This has been simulated by a distribution of doublets either on a straight inclined line or on the curved line given by the empirical relation of Margasson (Ref.40) and representing the centerline of a jet deflected by a cross flow. Thus the effects of wake curvature as well as wake deflection can be accounted for.

Unpublished results (Ref.39) of the calculations, run with straight and curved wakes show that substantially different results are obtained for the top and bottom slot configuration required for zero lift interference. Considering uniform slots, it is also shown that the conditions of zero lift and pitching moment corrections are obtained for different amounts of porosity.

### 3.4 Experimental studies

Ref.47 describes the experimental work of Binion intended to check the theoretical results of Lo (Refs 19, 50, 51 and 52). A model consisting of a rectangular wing, a tail and a fuselage with a vertical lifting jet has been tested in a low speed wind tunnel having a 3:2 width to height ratio, solid side walls and various combinations of slotted top and bottom walls; the ratio of model span to tunnel width was  $b/B = 2/3$ . The results were compared with interference free data, obtained by testing the same model in a much larger test section ( $b/B = 0.05$ ). Different shapes of slot, including the use of varying width in the longitudinal direction, as shown in Fig.9, were investigated. The incidence correction was expressed in the form

$$\Delta\alpha = \delta \frac{S}{C} C_L + \Delta\alpha_j$$

where it was necessary to introduce the additional term  $\Delta\alpha_j$ , the interference angle, at zero lift.

For slots of uniform width it was found that the theory reported in Ref.19 assuming an undeflected wake, agreed with experiments carried out with the lifting jet not operating (CTOL) but that a more recent analysis assuming a deflected wake (Ref.39) predicted rather lower values of slot parameters for zero lift interference with lifting jet operating, than those found by experiment.

However, experimental results show that for slots of uniform width, the top and bottom wall porosity (ratio of open to total area of the test section boundaries) required for zero lift interference factor  $\delta$ , varies from 4% to 16% when the velocity ratio  $V_j/V_0$  varies from 0 to 4.5. But the value of porosity which gives zero  $\delta$  does not in general give zero  $\Delta\alpha_j$ ; for instance, a porosity of 22% is required for zero  $\Delta\alpha_j$  at  $V_j/V_0 = 4.5$ . In fact,  $\Delta\alpha_j$  and  $\delta$  are simultaneously zero only when  $V_j/V_0 = 2.7$ , the porosity being then 10%.

Furthermore, if the porosity is chosen to maintain  $\delta = 0$ , the measured pitching moment coefficient is seen not to coincide with the interference free data thereby indicating that for uniform slots, the conditions of zero lift and pitching moment interference cannot be realized simultaneously. Comparison of results for uniform slot width and lifting jet inoperative (CTOL regime) indicate that better agreement with theory is obtained if the value of K in the boundary condition is determined from the second equation for K mentioned in a previous chapter and which takes into account the thickness of the walls.

The slot configuration of the side walls was also found by experiment to have a negligible effect on the lift interference factor  $\delta$ .

The results for non-uniform slot width are summarized in Fig.10 taken from Ref.47. It is seen that, for the configurations examined consisting of the same porosity on the top and bottom walls and solid side walls, the value of the top and bottom porosity required for zero  $\delta$  or  $\Delta\alpha_j$  is a function of the velocity ratio  $V_j/V_0$ . Furthermore, the porosity required for zero  $\delta$  is different from the porosity required for zero  $\Delta\alpha_j$ , except at a well defined value of the velocity ratio  $V_j/V_0$ . Although in general, pitching moment and lift corrections were not zero simultaneously, for some particular shapes of slots (types D and E of Ref.47) this condition was satisfied for the CTOL case ( $V_j/V_0 = 0$ ). It is concluded in Ref.47 that to obtain zero correction for lift and pitching moment, other ways of slotting the walls should be investigated. Possibilities include the use of different porosities on the top and bottom walls, as recommended by Lo in his theoretical work of Ref.52, or the use of wall porosity which varies not only in the longitudinal but also in the transverse direction.

The research programme has recently been continued along these two directions by Binion at AEDC (Ref.53) and preliminary results appear to indicate that it is possible, by imposing both longitudinal and transverse variation of wall porosity, to obtain zero lift and pitching moment interference at more than one specified velocity ratio. It must be observed however, that the aircraft model used in the research had a lifting jet at the center of the fuselage, and that any resulting optimum zero interference test section may be valid only for similar configurations and not for instance, for jet flap wings. In fact the results discussed in Ref.53 show that a large porosity is required for the test section floor at the approximate location of jet impingement on the ground. It is possible therefore that a model with a different distribution of lifting jets will require a different distribution of porosity on the test section floor.

### 3.5 Conclusions

From the theoretical and experimental data examined, the following conclusions can be drawn :

- 1) Slotting the wind tunnel side walls has negligible effect in the case of a 3:2 test section.
- 2) For CTOL aircraft, zero lift and pitching moment corrections are not obtained simultaneously for the same wall porosity when employing uniform width slots.
- 3) For CTOL aircraft, zero lift and pitching moment corrections can be obtained simultaneously by the use of shaped slots.
- 4) For V/STOL aircraft, zero interference for lift can be obtained independently of the wake skew angle when employing slots of uniform width with a slot parameter of 0.27 on the top wall and of 0.7 on the bottom wall.

- 5) Preliminary results suggest that zero correction for lift and pitching moment in the case of V/STOL aircraft can be obtained by the use of shaped slots non-uniformly distributed in the transverse direction; investigation of this possibility is continuing at AEDC at the present time.
- 6) Further work is needed to determine the extent to which the design of a test section for zero interference is dependent on model configuration.

#### 4. GROUND EFFECT TESTING

##### 4.1 Introduction

Ground effect data on CTOL aircraft is usually obtained by mounting the model close to a plate or a board representing the ground; such a board can be the tunnel floor or it can be slightly displaced with respect to the tunnel floor or placed at mid-height of the test section with a mirror-image of the model fixed underneath it. The geometrical parameter characterizing the measured ground effect data is the ratio  $h/c$  or  $h/b$  of the height of the model expressed in terms of the wing chord or span. However, the motion of the air flow relative to the ground in the wind tunnel test causes a boundary layer to form on the ground board, while in actual flight this boundary layer does not exist.

Different tunnel testing procedures can be envisaged to determine the effect of ground proximity for V/STOL aircraft :

- use of a special test rig which correctly simulates the flight situation, i.e. a fixed ground board with a moving model. This method allows data to be taken in hover or for low forward speeds, but rather large and complex facilities are needed in the latter case,
- use of the normal and simple technique of the fixed ground board in the wind tunnel. The results for the effect of the board boundary layer displacement thickness must be corrected,
- use of suitable means for removing the boundary layer on the simulated ground. This can be done by boundary layer suction and/or the use of a moving ground belt. Energizing the boundary layer by blowing can also be considered.

##### 4.2 Ground effect test rigs

Outdoor ground effect test rigs would provide, in the absence of natural winds, the most reliable way of obtaining ground effect data at hover or at low forward speeds, because of the strict similarity of conditions during testing and actual flight. Although the existence of uncontrollable natural winds suggests the use of indoor facilities, in this case the test room must be sufficiently large for spurious recirculation effects induced by the room walls to be avoided. The investments involved and the difficulties associated with making measurements on a moving model while maintaining the testing configuration constant during a run do not make the method a practicable one.

##### 4.3 Wind tunnel tests with a fixed ground board

In such tests there is always an advantage in trying to reduce the ground board boundary layer. This is the reason for using a short ground board located some distance above the tunnel floor. But this type of ground board divides the test section into two air passages and it is necessary to determine the true free stream dynamic pressure at the model location by means of suitable calibration procedures (Ref.54). This difficulty is removed if the set up in the test section is symmetrical, i.e. if the ground board is mounted at mid height in the test section with the model to be tested above it and a dummy image of the model below. However, this mounting effectively halves the usable test section and approximately halves the model dimensions while requiring the construction of two models. In any case, with either of these two mountings, a boundary layer will develop between the air stream and the ground board; its effect on measurements made on CTOL aircraft configurations has recently been investigated by East (Ref.54). His experimental results show that the measured values of  $C_L$ ,  $C_D$ ,  $C_M$  depend on  $\delta^*/h$  which is the ratio of the ground board boundary layer displacement thickness to the model height above it. The relations are reasonably linear and their slope increases with the model angle of attack. The overall effects can be significant. Thus for a CTOL model with a wing of aspect ratio 8, a model height to chord ratio  $h/c = 0.79$ , and with  $\delta^*/h = 0.05$ , the increase in lift due to ground effect and the apparent error in lift coefficient are respectively 5% and 2% of the free-air lift coefficient.

The procedure suggested in Ref.54 for correcting any measured aerodynamic coefficient  $C$  for the effect of ground board boundary layer is to use the following linearization :

$$C_{\text{corr.}} = C_{\text{meas.}} + \frac{\delta^*}{h} \frac{\partial C}{\partial (\delta^*/h)} + \frac{\partial \delta^*}{\partial x} \frac{\partial C}{\partial (\partial \delta^*/\partial x)}$$

where the gradients of  $C$  are determined by carrying out an additional test with another ground board configuration yielding a different value of  $\delta^*$ .

This method however, was devised for CTOL tests and does not seem to be directly applicable to V/STOL tests for which the interaction between the deflected wake and the boundary layer on the floor must be taken into account. But if the boundary layer on the fixed ground board has not separated, so that incipient flow breakdown has not

occured, an approach similar to that of Ref.54 would also seem to be possible for V/STOL testing but would require that  $\delta^*$  on the ground board be measured for every model configuration. Validation of this statement needs further study.

#### 4.4 Use of a moving ground belt

The boundary layer which is developed on a fixed ground plate normally requires corrections to be applied to the measured quantities. If however, separation of this boundary layer occurs due to the pressure rise associated with a wake impinging on the ground, then the tests cannot be considered as representative anymore. It follows that if such separation is to be expected then the ground boundary layer must be removed.

In Refs 55 and 56, Turner discusses the use of a moving ground belt for this purpose. The system is preceded by a suction slot for removing any boundary layer up to the moving belt leading edge. Ground effect tests were made on double slotted flap, jet flap and tilt wing configurations above a fixed ground plane and above a moving ground belt; the  $C_L$  versus  $\alpha$  curves obtained in the two cases were seen to coincide at low values of  $C_L$  but to diverge beyond a certain value of  $C_L$ . A correlation was found between this value of  $C_L$  and the relative height  $h/b$  of the model, and is shown in Fig.10. For  $h/b > C_L/20$  the results obtained with a conventional ground board and with a moving belt coincide. For  $h/b < C_L/20$  they differ and a moving belt is required if the flow field existing between the aircraft and the ground is to be correctly reproduced.

In Ref.14, South suggests that Turner's results could be replotted (Fig.11) in terms of  $h/b$  versus  $C_L/A$ . In this diagram, straight lines from the origin correspond to a constant value of South's lift coefficient

$$C_{Lhb} = \frac{C_L/A}{h/b},$$

and Turner's criterion for the need of a ground belt reduces to  $C_{Lhb} > 3.3$ , a value not too different from South's criterion for flow breakdown ( $C_{Lhb} > 3.0$ ).

Subsequent studies were carried on at NRC (Ref.57) on a jet flap wing in ground effect, with a moving ground belt. Flow breakdown was detected by the appearance of a definite and sudden change in the slope of the lift curve. The breakdown lift coefficient varied linearly with the relative height  $h/c$ , and at zero D/L was given by  $C_L = 5.5 h/c$  corresponding to a value of  $C_{Lhb} = 5.5$ . This limit, also shown in Fig.10, indicates when flow breakdown will also occur in reality. Thus three regions can be distinguished in Fig.11 :

- (i)  $C_{Lhb} < 3.0$  or  $3.3$ . No boundary layer separation occurs on the wind tunnel fixed ground board, which may therefore be used.
- (ii)  $3.3 < C_{Lhb} < 5.5$ . Boundary layer separation occurs on the wind tunnel fixed ground board, but not in real flight. Use of a moving belt to eliminate the boundary layer on the floor of the tunnel is essential.
- (iii)  $C_{Lhb} > 5.5$ . Boundary layer separation occurs on the wind tunnel fixed ground board, and in real flight there is a region of flow on the ground beneath the aircraft where flow reversal occurs. The moving belt does not avoid the formation of a recirculation bubble underneath the model, but is still required to maintain similarity between the wind tunnel test and real flight.

#### 5. FLOW DISTURBANCES IN THE TUNNEL CIRCUIT

For a good simulation of real flight, the flow in the wind tunnel test section must be uniform. Flow may be non-uniform either in space (velocity gradients across or along the test section, swirl) or in time (low frequency flow oscillations, turbulence). Furthermore, non-uniformities may be due to the wind tunnel itself or to flow perturbations originating at the model. By very careful design of the wind tunnel diffuser, corner vanes and contraction, by the use of straightener vanes and screens, and probably with the aid of flow surveys conducted in a pilot tunnel of reduced scale, the flow non-uniformities due to the tunnel itself can be avoided or eliminated. It must be pointed out however, that this is frequently an empirical cut-and-try study, relying on ingenuity of the design engineer rather than on well established methods.

The situation is even worse for the flow perturbations originating at the model and travelling around the wind tunnel circuit. These perturbations may be the trailing vortex filaments of lifting systems, or regions of low velocity (wakes) associated with some large separated flow region, or velocity fluctuations connected with the unsteady character of separated flows. No general treatment of this problem has been found in the literature. Only a few examples are available on this subject, each one relating to a well defined configuration in a specified wind tunnel. Thus in the Ames 40' x 80' wind tunnel it was observed (Ref.58) that the model wake could be detected along the diffuser and up to but not beyond the fan section so that in this particular case, the problem was not important. On the other hand, there were cases of wind tunnels in which it was necessary to eliminate undesirable characteristics attributable to model perturbations. An example is the Langley 7' x 10', 300 mph V/STOL wind tunnel, in which boundary layer blowing on the diffuser walls was needed to cure local flow separation arising from this cause.

As the problem is closely dependent upon the tunnel configuration and the type of model tested, it does not seem possible to establish guide lines of general application. If, for a new tunnel, a small scale pilot tunnel is available, it would be worthwhile to conduct experiments in it which are specially designed to test the operation of the facility when

representative wakes are produced in the test section.

LIST OF REFERENCES

1. Garner, H.C., Rogers, E.W.E., Acum, W.E.A., Maskell, E.C. : "Subsonic wind tunnel wall corrections", AGARDograph 109, October 1966.
2. Vayssaire, J.C. : "Corrections de blocage dans les essais en soufflerie et effets des décollements", AGARD Meeting "The fluid dynamics of aircraft stalling", Lisbon, 26-28 April 1972.
3. Vayssaire, J.C. : "Nouvelle méthode de calcul de corrections des résultats d'essais en soufflerie basse-vitesse", articles published in "L'Aéronautique et l'Astronautique", N° 15 and 16, 1969.
4. Anson, A., Williams, J. : Some comments on high-lift testing in wind tunnels with particular reference to jet-blowing models", AGARD Report 63, August 1956.
5. Butler, S.F.J., Williams, J. : "Further comments on high-lift testing in wind tunnels with particular reference to jet blowing models", AGARD Report 304, March 1959.
6. Heyson, H.H. : "Rapid estimation of wind tunnel corrections with application to wind tunnel and model design", NASA TN-D-6416, September 1971.
7. Heyson, H.H. : "Jet boundary corrections for lifting rotors centered in rectangular wind tunnels", NASA TR R-71, 1960.
8. Heyson, H.H. : "Equations for the induced velocities near a lifting rotor with non-uniform azimuthwise vorticity distribution", NASA TN D-394, 1960.
9. Heyson, H.H. : "Induced flow near a helicopter rotor", Aircraft Engineering Vol. XXXI, N° 360, February 1959, pp 40-44.
10. Heyson, H.H. : "Linearized theory of wind tunnel jet boundary corrections and ground effect for V/STOL aircraft", NASA TR R-124, 1962.
11. Heyson, H.H. : "Use of superposition in digital computers to obtain wind tunnel interference factors for arbitrary configurations, with particular reference to V/STOL models", NASA TR R-302, February 1969.
12. Rae, W.H. : "Limits on minimum speed V/STOL wind tunnel tests", Journal of Aircraft, Vol. 4 N° 3, May-June 1967.
13. Lazzaroni, F.A., Carr, L.W. : "Problems associated with wind tunnel tests of high disk loading systems at low forward speeds", Aerodynamics of rotary wings and V/STOL aircraft. Vol. II. Wind tunnel testing new concepts in rotor control, Cornell Aeron. Lab. Inc., and U.S. Army Aviat. Mater. Lab., June 1969.
14. South, P. : "Measurements of flow breakdown in rectangular wind tunnel working sections", N.R.C., Aeron. Report LR-513, November 1968.
15. Tyler, R.A., Williamson, R.G. : "Observations of tunnel flow separation induced by an impinging jet", N.R.C. Aeron. Report LR-537, April 1970.
16. Tyler, R.A., Williamson, R.G. : "Tunnel flow breakdown from inclined jets", N.R.C. Aeron. Report LR-545, March 1971.
17. Tyler, R.A., Williamson, R.G. : "Experience with the N.R.C. 10 ft x 20 ft V/STOL propulsion tunnel. Some practical aspects of V/STOL engine model testing, N.R.C., Lab. Tech. Report LTR-GD-13, May 1972.
18. Owen, T.B. : "Limiting test conditions in wind tunnels used for V/STOL model testing", LaWS paper N°37, January 1972.
19. Lo, C.F. : "Method of calculating the wind tunnel interference for steady and oscillating wings in tunnels of arbitrary wall configuration", AEDC-TR-68-42, March 1968.
20. Joppa, R.G. : "A method of calculating wind tunnel interference factors for tunnels of arbitrary cross-section", NASA CR-845, July 1967.
21. Kroeger, R.A., Martin, W.A. : "The streamline matching technique for V/STOL wind tunnel wall corrections", AIAA Paper N°67-183, January 1967.
22. Hall, D.G., Gamage, R.W. : "Principles of reducing boundary interference at subsonic speeds using a forced draft, porous wall wind tunnel", Northrop Corp., Aircraft Division, NOR-70-96, April 1970.
23. Pindzola, M. : "Transonic wind tunnels", UTSI/VKI short course on "Transonic wind tunnel testing", von Karman Institute for Fluid Dynamics, January 1972.
24. Heyson, H.H., Grunwald, K.J. : "Wind tunnel boundary interference for V/STOL testing", conference on V/STOL and STOL aircraft, NASA SP-116, paper N°24, April 1966.
25. Grunwald, K.J. : "Experimental study of wind tunnel wall effects and wall corrections for a general research V/STOL tilt-wing model with flap", NASA TN D-2887, July 1965.
26. Heyson, H.H. : "Wind tunnel wall effects at extreme force coefficients", Ann. New York Acad. Sci., Vol 154, Art. 2, Nov. 22, 1968, pp. 1074-1093.
27. Heyson, H.H. : "Nomographic solution of the momentum equation for V/STOL aircraft", NASA TN D-814, April 1961.
28. Heyson, H.H. : "Theoretical study of conditions limiting V/STOL testing in wind tunnels with solid floor", NASA TN D-5819, 1970.

29. Owen, T.B. : "Wind tunnel and other facilities required for V/STOL model testing", RAE Tech. Memo Aero 1198, 1970.
30. Vogler, R.D. : "Ground effects on single and multiple jet STOL models at transition speeds over stationary and moving ground planes", NASA TN D-3213, 1966.
31. Hurns, A.G., Akers, G.A. : "Notes on the effect of a jet emerging from a surface in the presence of a main stream flow", Boulton Paul Aircraft Ltd., T.N. 5, 1955.
32. Cook, W.L., Hickley, D.H. : "Comparison of wind tunnel and flight-test aerodynamic data in the transition-flight speed range for five V/STOL aircrafts", conference on V/STOL and STOL aircraft, NASA SP-116, paper N°26, April 1966.
33. Coqne, C.D. : "A theoretical investigation of vortex-sheet deformation behind a highly loaded wing and its effect on lift", NASA TN D-657, April 1961.
34. Spence, A., Spee, B.M. : "European needs for low speed wind tunnels", LaWs paper N° 46B, June 1972.
35. McCormick, B.W. : "The limiting circulating lift of a wing of finite aspect ratio", J. Aerospace Sci., Vol.26, N°4, pp. 247-248, April 1959.
36. Katzoff, S., Gardner, C.S., Diesendruck, L. and Eisenstadt, B.J. : "Linear theory of boundary effects in open wind tunnels with finite jet lengths", NACA Rep. 976, 1950.
37. Heyson, H.H. : "Theoretical study of the use of variable geometry in the design of minimal correction V/STOL wind tunnels", NASA TR R-318, August 1969.
38. Heyson, H.H., Lazzeroni, F.A. : Personal communication, April 1972.
39. Lo, C.F. : "Corrections in slotted wall test sections accounting for the deflection and curvature of lifting jets", Personal communication, April 1972.
40. Margasson, R.J. : "The path of a jet directed at large angles to a subsonic free stream", NASA TN D-4919, November 1968.
41. Vayssaire, J.C. : "Survey of methods for correcting wall constraints", LaWs paper N° 85, May 1972.
42. Grunwald, K.J. : "Experimental investigation of the use of slotted test section walls to reduce wake interference for high-lift model testing", NASA TN D-6292, June 71.
43. Wright, R.H. : "Test sections for small theoretical wind tunnel boundary interference on V/STOL models", NASA TR R-286, August 1968.
44. Davis, D.D., Moore, D. : "Analytical study of blockage and lift interference corrections for slotted tunnels obtained by the substitution of an equivalent homogeneous boundary for the discrete slots, NACA RM L530E7b, 1953.
45. Baldwin, B.S., Turner, J.B., Knechtel, E.D. : "Wall interference in wind tunnels with slotted and porous boundaries at subsonic speeds", NACA TN 3176, May 1954.
46. Goodman, T.R. : "The porous wall wind tunnel - Part II - Interference effect on a cylindrical body in a two-dimensional tunnel at subsonic speed", Cornell Aeron. Lab. Rep. N°AD 594-A-3, 1950.
47. Binion, T.W. : "An investigation of several slotted wind tunnel wall configurations with a high disk loading V/STOL model", AEDC-TR-71-77, May 1971.
48. Chen, C.F., Mears, J.W. : "Experimental and theoretical study of mean boundary conditions at perforated and longitudinally slotted wind tunnel walls", AEDC-TR-57-20, December 1957.
49. Rushton, K.R. : "Studies of slotted wall interference using a electrical analogue, Part II. Particular examples of slotted wall tunnel interference, ARC R&M 3452, 1965.
50. Lo, C.F., Binion, T.W. : "A V/STOL wind tunnel wall interference study", Journal of Aircraft, Vol.7 N°1, Jan.-Feb. 1970.
51. Lo, C.F. : "Wind tunnel boundary interference on a V/STOL model", ATAA paper 70-575, May 1970.
52. Lo, C.F. : "Test section for a V/STOL wind tunnel", Journal of Aircraft, Vol.7 N°4, Jul.-Aug. 1970.
53. Binion, T.W. : Personal communications, April 1972.
54. East, L.F. : "The measurement of ground effect using a fixed ground board in a wind tunnel", ARC R&M 3689, 1972.
55. Turner, T.R. : "Endless-belt technique for ground simulations", Conference on V/STOL Aircraft, NASA SP-116, paper N°25, April 1966.
56. Turner, T.R. : "A moving belt ground plane for wind tunnel ground simulation and results for two jet flap configurations", NASA TN D-4228, November 1967.
57. Wickens, R., South, P., Rangl, R.S., Henshaw, D. : "Experimental developments related to V/STOL wind tunnel testing". NRC, unpublished paper.
58. Kelly, M. : Personal communications, April 1972.

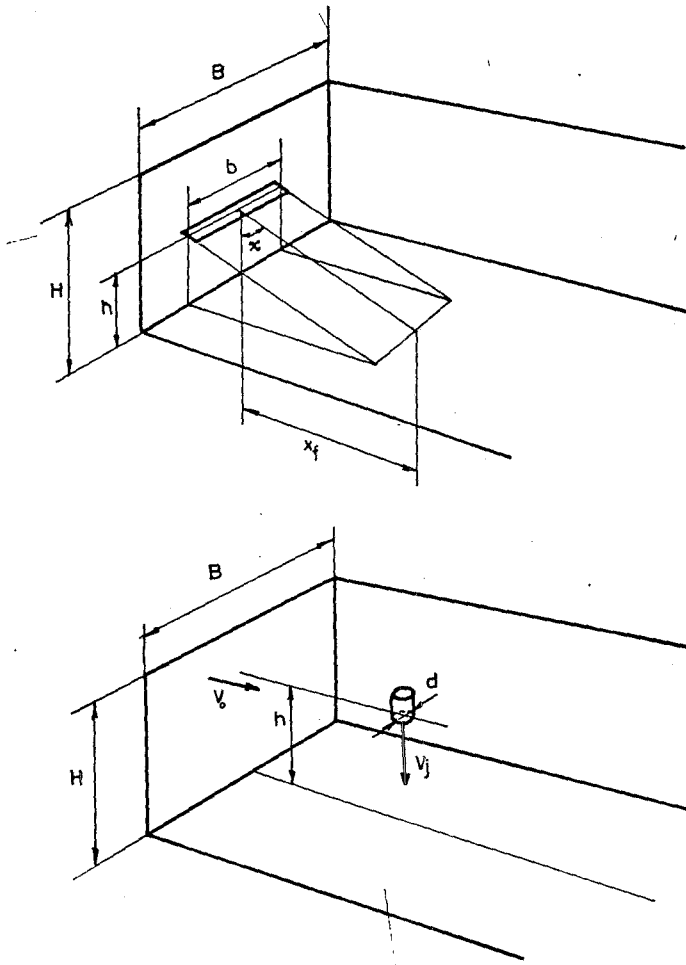


Fig. 1 Definition of symbols used in Section 2

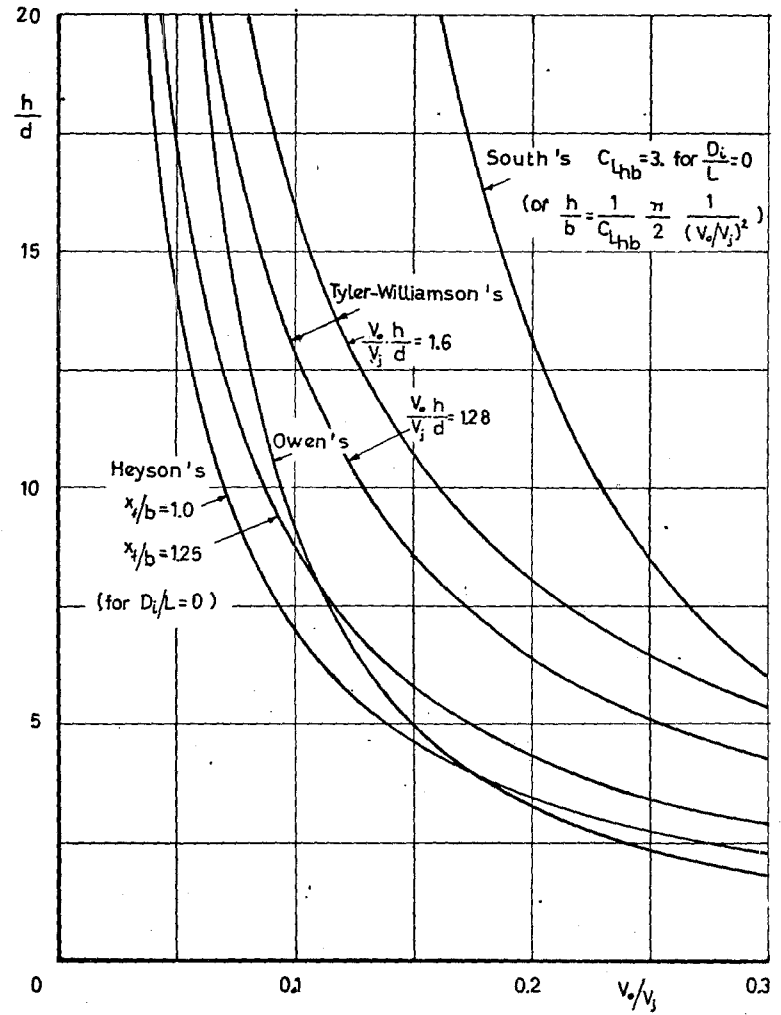


Fig. 2a Flow breakdown limits

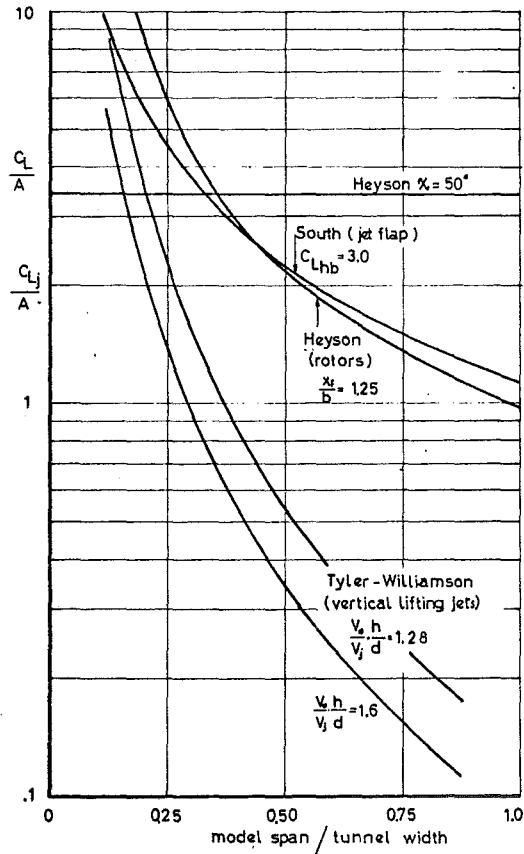
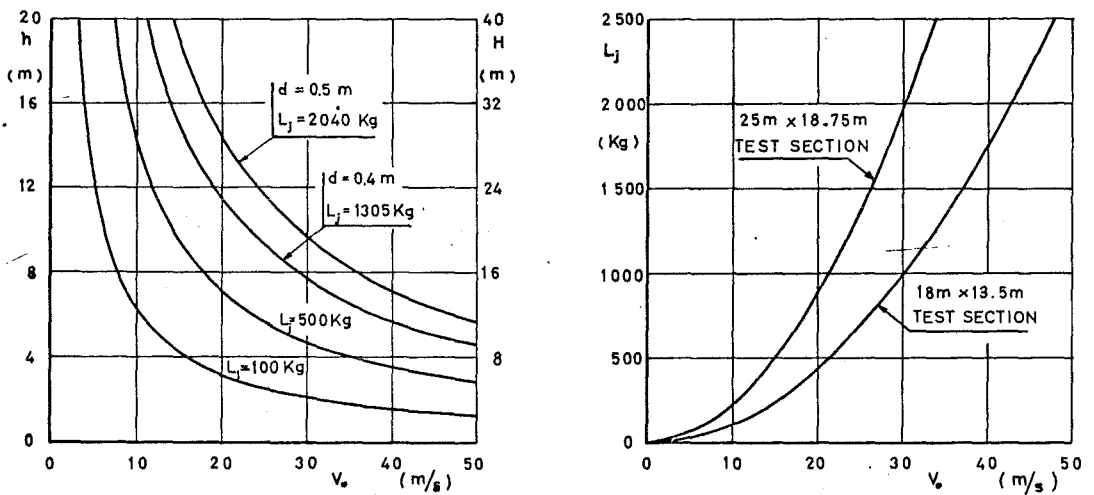


Fig.2b Flow breakdown limits for a model centered in a closed test section ( $B/H = 4/3$ ) and with  $D_i/L = 0$



a) minimum model height above floor for various values of jet lift

b) maximum lift achievable by jet engines in two different test sections

Fig.3 Testing limitations due to flow breakdown according to Tyler and Williamson for lifting jet engines centered in the wind tunnel test section



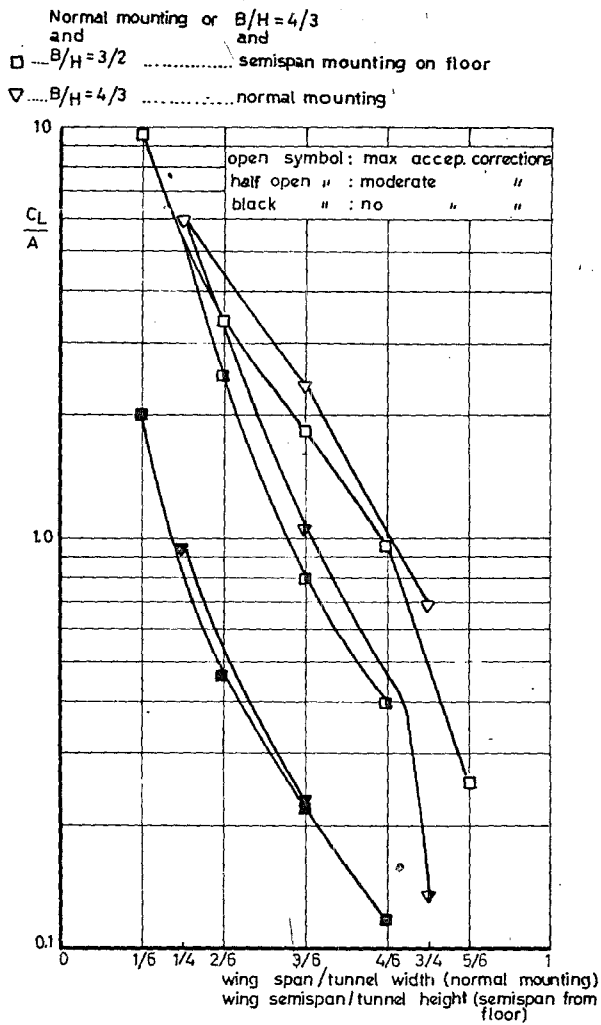


Fig.4 Testing limits for an unswept powered wing at  $Di/L = 0$  (Ref 6)

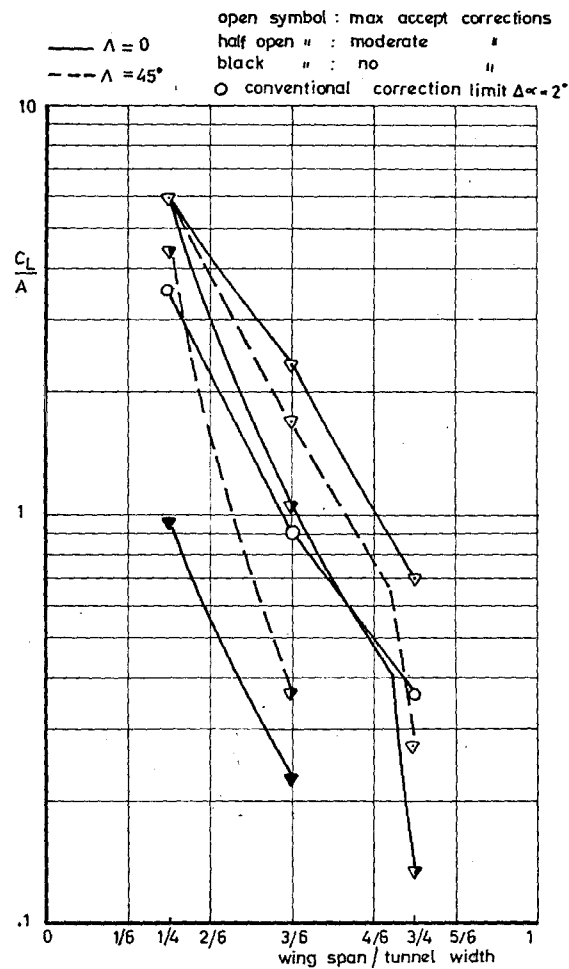


Fig.5 Effect of sweep angle on testing limits for a powered wing at  $Di/L = 0$  (Ref 6) and for normal mounting in a 4:3 test section

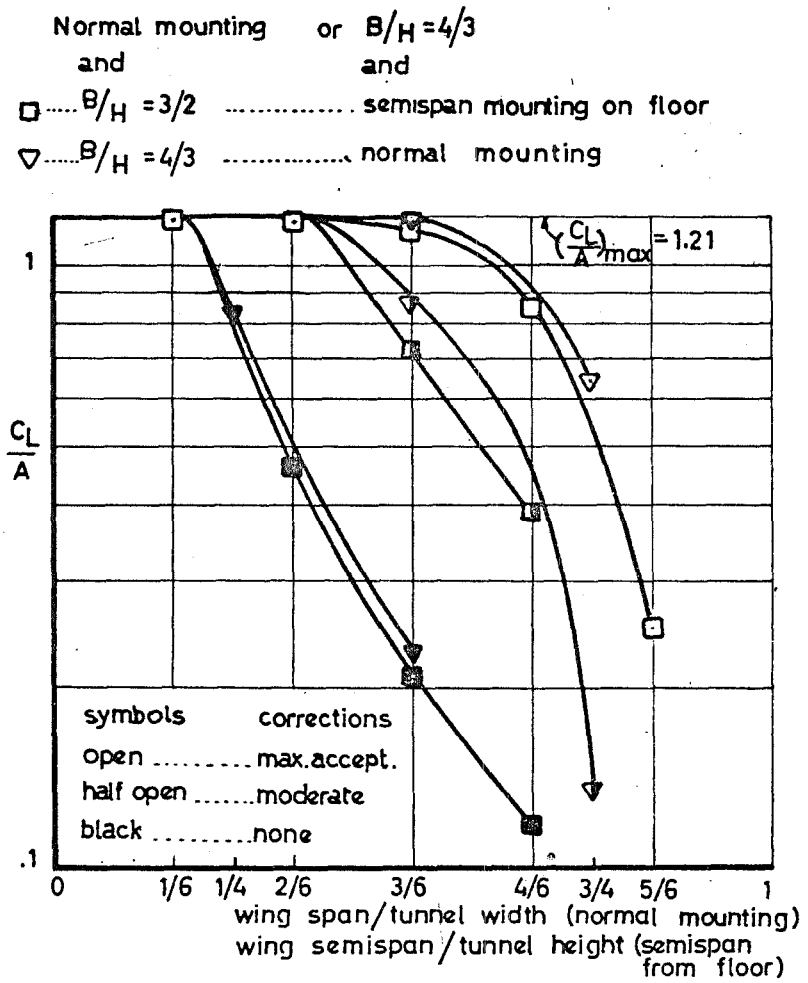


Fig.6 Testing limits for an unswept and unpowered wing

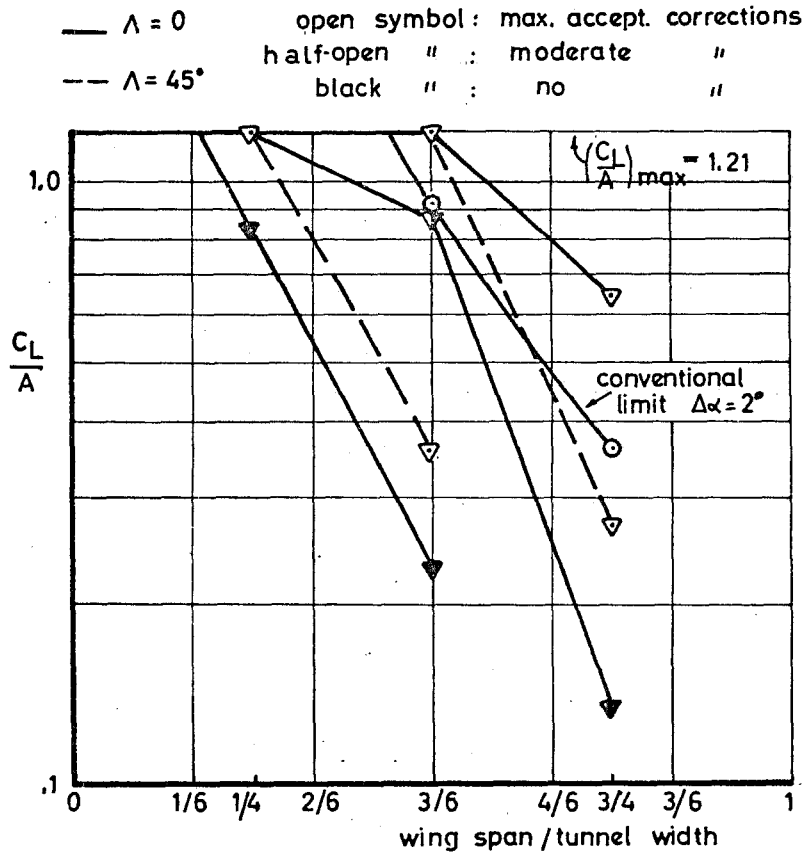


Fig.7 Effect of sweep angle on testing limits for an unpowered wing and for normal mounting in a 4:3 test section (Ref 16)

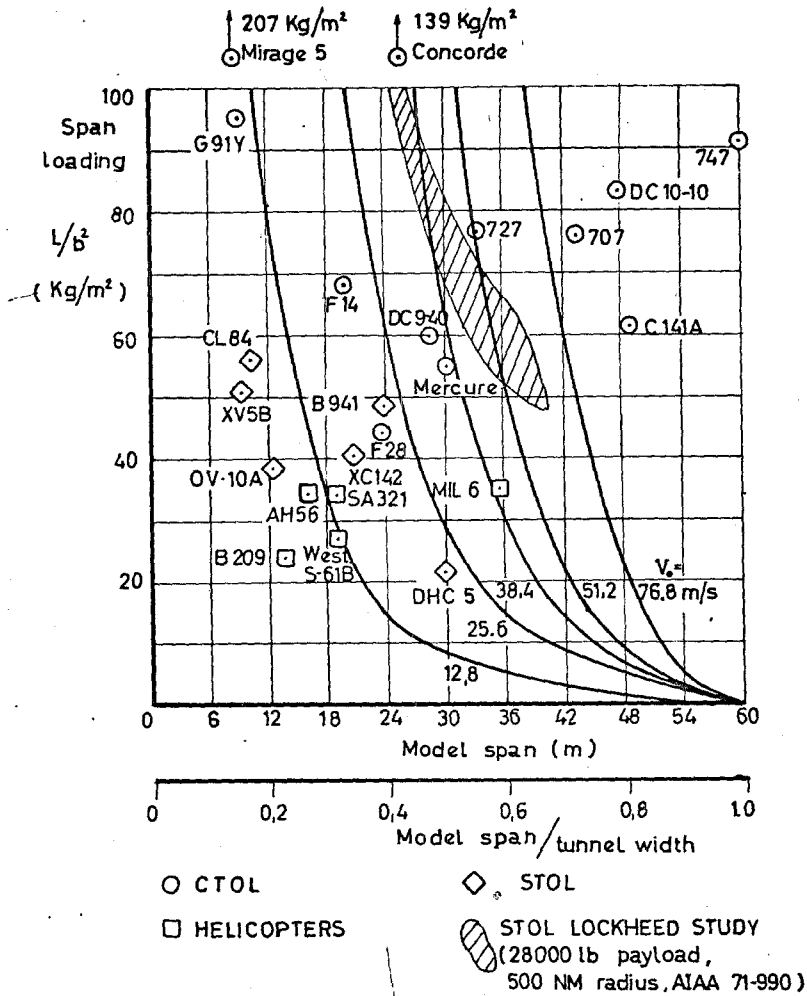


Fig.8 V/STOL and helicopter testing limits, with moderate corrections (Ref.38) for the American full-scale wind-tunnel proposal

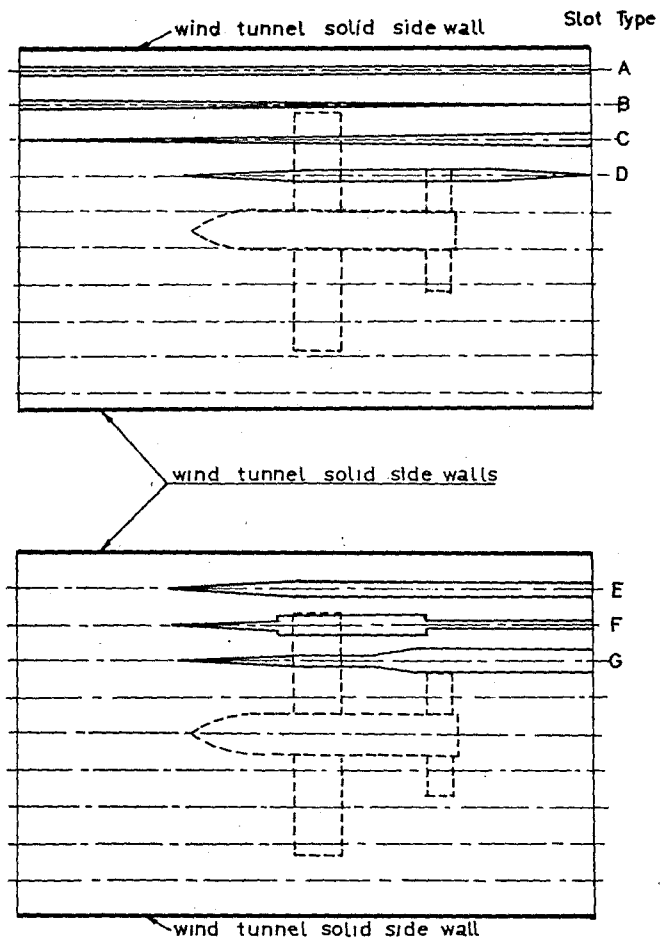


Fig.9 Shapes considered in Ref.47 for the top and bottom wall slots

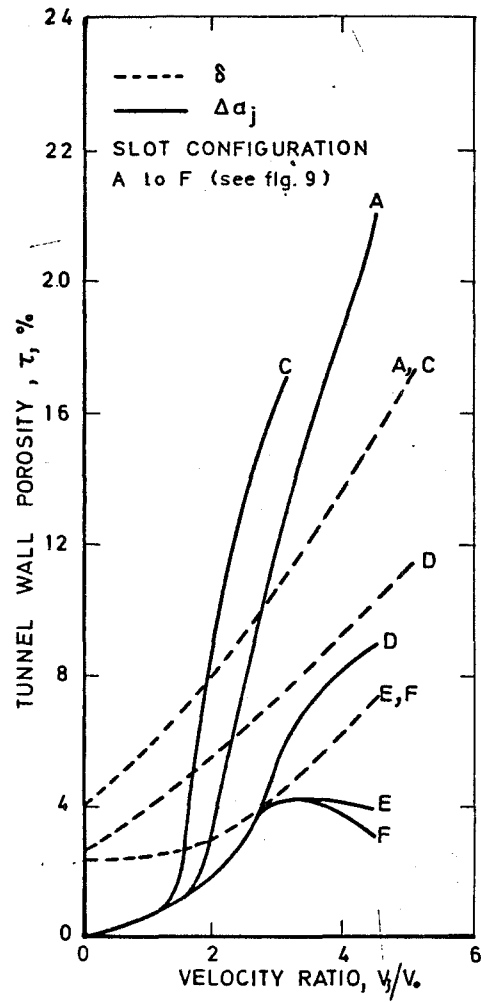


Fig.10 Porosity required for zero  $\sigma$  and  $\Delta\alpha_j$  (reproduced from Ref.47)

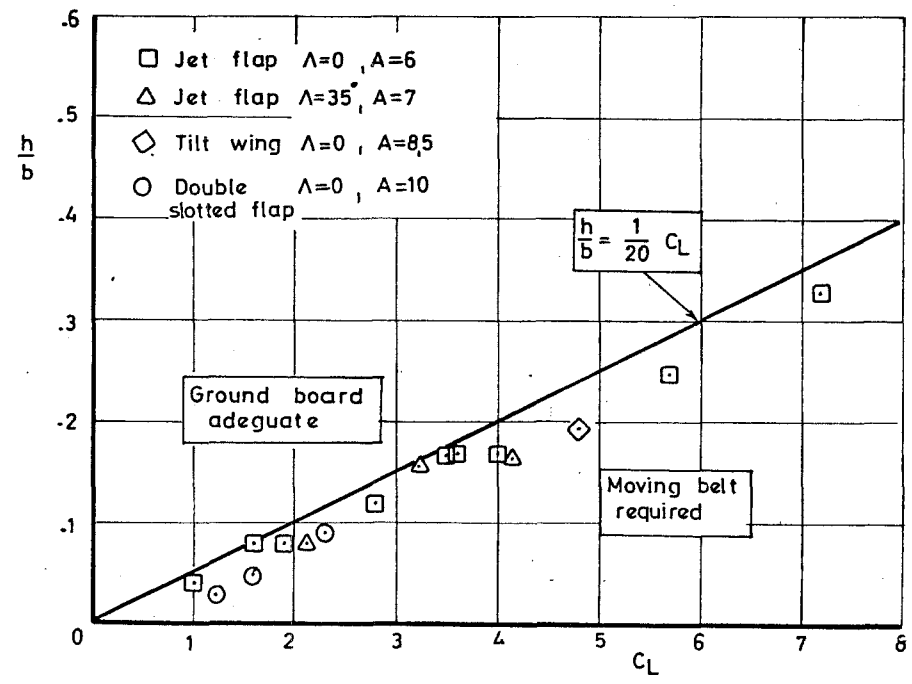


Fig.11 Conditions requiring a moving belt, according to Turner

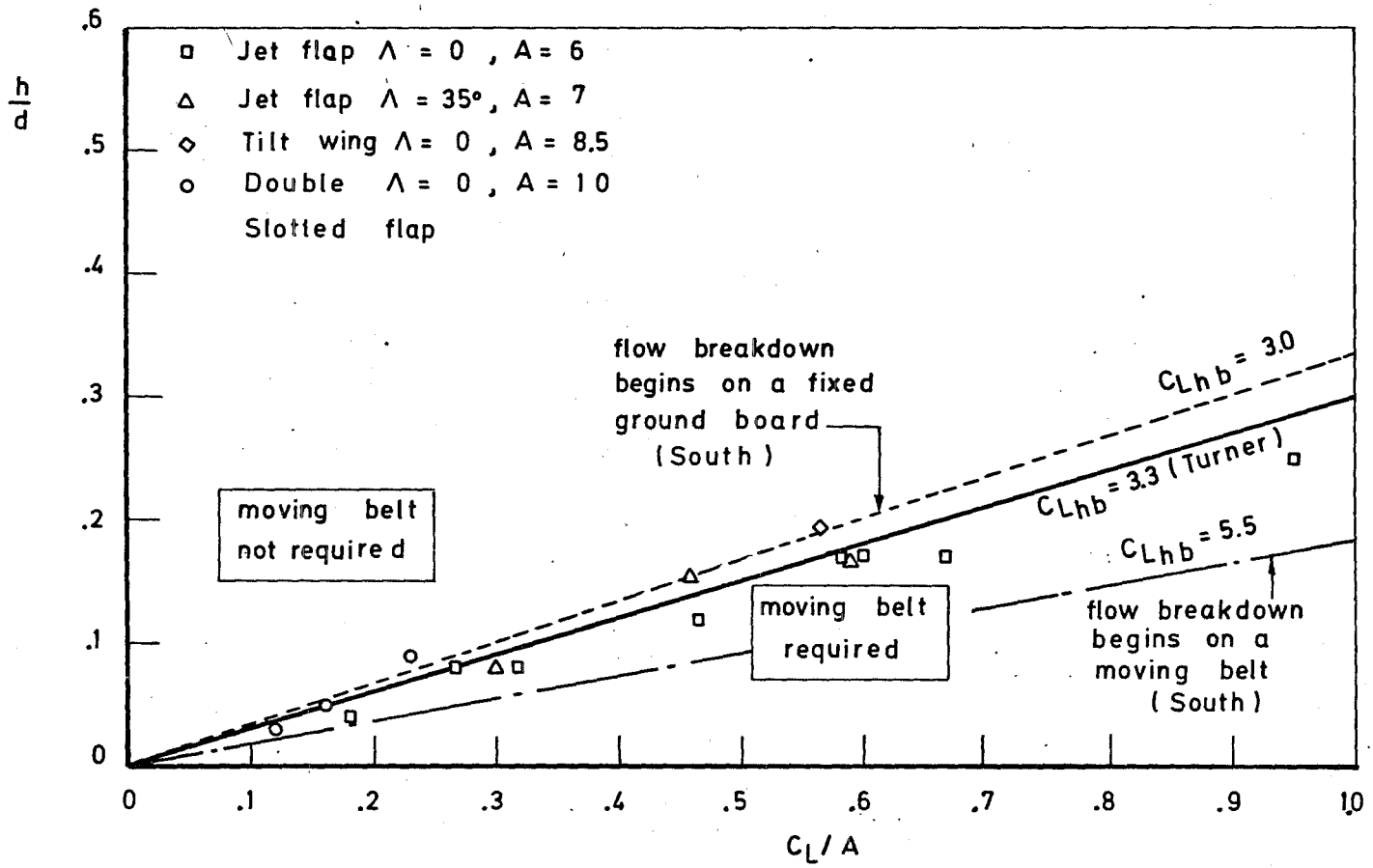


Fig.12 Conditions requiring a moving belt, according to South

# SURVEY OF METHODS FOR CORRECTING WALL CONSTRAINTS IN TRANSONIC WIND TUNNELS

by

Jean - Ch. Vayssaire

Aerodynamics Department  
Avions Marcel Dassault - Breguet Aviation  
92210 - Saint-Cloud  
France

## SUMMARY

Wider and wider use of ventilated walls in transonic wind tunnels has considerably complicated the problem of wall interference corrections.

Mathematical application of the studies available permits to obtain known results in extreme cases of zero permeability (solid walls) and infinite permeability (open jet).

Application of these studies to actual cases is difficult and it appears that the operational stage has been reached in only a very few cases. Several original solutions were proposed to overcome the difficulties.

The author of this paper makes a comparison of these solutions and high lights the precautionary measures to be taken during the experimental work.

Recent researches have shown that in relation to theoretical working sections of infinite length, the realistic working sections have a stronger influence. This influence can be theoretically explained but too few studies are conducted though several researches are in progress. Experimental evidence of this influence is even rarer.

This paper concludes with some suggestions for the future researches.

## RESUME

La généralisation des parois ventilées dans les souffleries transsoniques a compliqué notablement le problème des corrections de parois.

Des théories existent dont les développements mathématiques permettent de retrouver dans les cas limites de perméabilité nulle (veine guidée) et de perméabilité infinie (veine libre) des résultats connus.

Leur application à des cas réels est délicate et ne semble que rarement avoir atteint le stade opérationnel. De nombreuses solutions originales ont été proposées pour tenter de tourner les difficultés.

L'auteur les compare et met en lumière les précautions expérimentales qu'elles nécessitent.

Des travaux récents ont montré que, par rapport à une veine théorique infinie, les configurations réalistes ont des effets importants. Ces effets, accessibles à la théorie, sont encore trop peu étudiés bien que plusieurs travaux soient en cours. Les validations expérimentales en sont encore plus rares.

L'auteur termine par quelques recommandations pour des recherches futures.

## CONTENTS

### SYMBOLS

#### 1 - INTRODUCTION

#### PART I Theoretical approach

- 2 - REVIEWAL OF THEORIES
- 3 - CORRECTION TERMS
- 4 - CORRECTION FACTORS
- 5 - REMARKS AND CONCLUSIONS REGARDING CORRECTION FACTORS

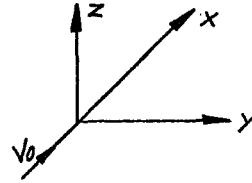
#### PART II Theory/experimental work correlation

- 6 - DEFINITION OF POROSITY PARAMETER (R)
- 7 - REMARKS ABOUT BLOCKAGE MEASUREMENTS - GENERALIZATION
- 8 - LENGTH RESTRICTION OF VENTILATED WALLS
- 9 - MODEL SIZE
- 10 - VARIABLE POROSITY CONCEPT
- 11 - GRADIENTS
- 12 - CONCLUDING REMARKS - SUGGESTIONS
- 13 - REFERENCES
- 14 - APPENDIX - Theoretical approach - Summary.  
Comments on wall constraint problems in transonic wind tunnels.

## SYMBOLS

$A_m$	Cross - sectional area of aerofoil (in z, x plane - Refer to Table II).
$B$	= $2b$ Width of tunnel working section.
$C$	Cross - sectional area of tunnel working section = $S_o$ with complete model in tunnel. < $S_o$ with half - model in tunnel (in some instances).
$C_D$	Drag coefficient
$C_{Dd}$	Separated flow component of $C_D$ .
$C_L$	Lift coefficient
$C_m$	Pitching moment coefficient
$C_f$	Force or moment coefficient
$D$	Equivalent circle diameter of fuselage maximum frontal area.
$F$	$\frac{K_1}{h}$ Non dimensional slot parameter
$H$	= $2h$ Height of tunnel working section Height of a rectangular tunnel Diameter of a circular tunnel.
$K_1$	$\frac{d}{\pi} \log_e \operatorname{cosec} \left( \frac{\pi}{2} \frac{a}{d} \right)$ Geometric slot parameter
$L$	Length of fuselage (refer to Table II)
$M$	Mach number
$P$	$\frac{1}{1 + \frac{K_1}{h}}$ Relative slot parameter
$Q$	$\frac{1}{1 + \frac{\beta}{R}}$ Relative porosity parameter
$R$	Porosity parameter
$S$	Reference area of the model
$S_e$	Area of horizontal stabilizer, including part in fuselage.
$S_o$	Geometric cross - sectional area of tunnel = $B \cdot H$ (rectangular working section) = $\pi C^2 H^2 / 4$ (circular working section)
$V_m$	Volume of model (refer to Table II)
$V_o$	Velocity of undisturbed stream
$a$	Width of slot (refer to Fig. 4)
$c$	Chord of aerofoil (refer to Table II - 2 dim.)
$c_b$	Wing tip chord (refer to Table II)
$c_o$	Wing chord along aircraft centerline (refer to Table II)
$c_r$	Reference chord (3 dim.)
$d$	Periodic spacing of slots (refer to Fig. 4)
$e_m$	Maximum thickness of aerofoil (refer to Table II)
$\bar{c}$	Mean aerodynamic chord
$l_e$	Refer to Table II
$l_G$	Refer to Table II
$q$	Kinetic pressure
$2s$	Wing span
$u$	Perturbation velocity in the axial direction

$v_n$	Velocity of the flow normal to the wall
$w$	Upwash velocity
$x, y, z$	Cartesian coordinates
$x_G$	Refer to Table II
$\Delta C_D$	Drag wall correction
$\Delta C_{Dg}$	Buoyancy correction imposed by velocity gradient within the empty working section
$\Delta C_{D1}$	Buoyancy correction imposed by velocity gradient due to solid blockage
$\Delta C_{D2}$	Buoyancy correction imposed by velocity gradient due to wake blockage
$\Delta C_L$	Lift wall correction
$\Delta C_m$	Pitching moment wall correction
$\Delta \alpha$	$= \frac{w}{V_0}$ Angle of attack wall correction
$\alpha$	Aerofoil angle of attack
$\beta$	$(1 - M_0^2)^{1/2}$ Compressibility factor
$\delta_0$	Lift interference parameter
$\delta_1$	Lift interference parameter associated with streamline curvature
$\epsilon$	$= \frac{u}{V_0}$ Blockage interference factor $\epsilon_1 + \epsilon_2 + \epsilon_3$
$\epsilon_1$	Solid blockage factor
$\epsilon_2$	Wake blockage factor
$\epsilon_3$	Stall blockage factor defined by $\epsilon_d$
$\lambda$	Aspect ratio
$\Omega$	Blockage factor ratio
$\rho$	Density of stream
$\sigma$	$2s/B =$ Wing span / Width of working section ratio
$\theta$	$= \frac{v_n}{V_0}$ Flow angle at the wall
$\varphi$	Perturbation velocity potential
$\varphi_i$	Interference velocity potential induced by walls
$\varphi_m$	Velocity potential of the model in free air
$\phi_\infty$	$= V_0 \cdot x + \varphi_m -$ Velocity potential in unconstrained flow
$\phi_{W.T}$	$= V_0 x + \varphi_m + \varphi_i = V_0 x + \varphi$ Velocity potential of the flow within the tunnel.



### Subscripts

a	denotes wing or aerofoil
c	corrected
e	denotes tail
f	denotes fuselage
G	denotes C.G.
M	denotes compressible flow
O	denotes incompressible flow or denotes "upstream" within the tunnel
p	denotes ventilated walls
u	uncorrected
$\infty$	denotes free air



## 1 - INTRODUCTION

1.1 - A survey of the methods used to correct the wind tunnel model results for wall effect cannot be restricted to the sole study of said walls.

It is true that interactions are produced by the presence of these walls which restrict the air flow within the test section. But if the walls act on the model the wall action is affected by the general arrangement of the wind tunnel.

The shape of the section or the length of the test section, for example, are important parameters.

Furthermore corrections are meaningful only when measurements are accurate thereby implying exact uncorrected results.

When considering only aerodynamic criteria, the following parameters must be positively known : reference kinetic pressure referred to as "upstream" pressure, distribution of velocities and static pressures, wind ascendance, etc.

Due allowance shall also be made for interactions caused by the supporting means, i.e. struts or stings. These interactions are either direct in relation to the model (by modifying, for example, its  $C_{m0}$  or the base pressures) or indirect due to the wall effect on the supporting means which acts, in turn, on the model.

1.2 - Therefore the working section is considered to be affected by all the elements placed upstream or downstream.

The working section is bordered by solid, ventilated, or open jet walls, surrounded by a plenum chamber. Upstream, the working section is bordered by the collector together with its settling chamber and downstream by the diffuser (Fig. 1). Consideration shall also be given to the working section inlet throat and the downstream throat, close to the diffuser, whose suction is either natural or controlled by moving flaps from the plenum chamber. When placed in certain positions, these flaps can interact on the boundary layers which develop on the walls thus causing velocity gradients.

Possibility of wall mobility (rather limited mobility) shall also be considered as well as an auxiliary suction from the plenum chamber.

Therefore the purpose of this paper is to investigate to what extent all the configurations are covered in recent papers relating to wall constraints. Some suggestions can thus be made as to the cases not previously covered.

1.3 - First a statement will be made of the theoretical principles of these corrections which appear to be definitely accepted following the issue of original or review papers from Garner, Acum, Rogers, Maskell (1) Pindzola (2,4), Lo (2,3) and Oliver (3).

The compressibility effect is introduced in the correction terms in conformance with Göthert's rule (5), stated as far back as 1940, and which is a development of Prandtl and Glauert's researches. This rule is applied through the factors  $\beta^{-\pi} = (1 - M_0^2)^{-\pi/2}$  where  $\pi$  is an integer.

Theories and rules are based upon linearized and effect superposition hypotheses which necessarily impose validity limits on the corrections.

1.4 - The conclusion of this introduction states a number of useful remarks regarding the ventilated wall sections which are the essential subject of this paper.

First it must be recalled that during the years 1932 to 1942, semi-closed wall test sections were made, for the theories showed that it was possible to neutralize or minimize their action under incompressible flow conditions and using a proper open jets / solid walls distribution.

From Prof. Toussaint's calculations and suggestions (6), two semi-closed (floor and roof) rectangular wind tunnels were built in this country. These are the tunnel n°.2 of the Institut Aérotechnique, at St. Cyr (width : 2,10 m (6.89 ft) ; height : 1,80 m (5.90 ft)) and the BREGUET tunnel, at Vélizy (width : 3,80 m (12.46 ft) ; height : 3,08 m (10.10 ft)). These tunnels are still being operated and the wall effect is negligible for usual low speed tests.

Prof. Toussaint's research work essentially dealt with corrections (at the level of the wing unit) depending on the coefficient of lift ( $C_L$ ) and emphasized the span influence. These researches should be associated with Wieselsberger's which dealt with the blockage caused by the volume of models installed in semi-closed rectangular sections. Wieselsberger extended the results of his research work to the compressible flow field (7).

The principal results obtained by Prof. Toussaint and Wieselsberger appear in Fig. 2 and 3.

Semi-closed walls are a particular case of longitudinally - slotted walls and are thus classified among the ventilated walls.

1.5 - Immediately after WWII and with the outbreak of high speed jet planes, multiple longitudinal slot walls were proposed for high subsonic tests in order to minimize the blockage caused by the volume of models and to suppress sonic blockage (8).

Then, a few years later, evidence was given of the following fact : it was possible, in low supersonic flow, to absorb the shock waves originating from the models thus preventing the wave reflection (9) when porous walls are used and when their porosity is made to match each Mach number value.

Perforated walls are the practical result of porous walls, provided that the holes are very close to one another and have a very small diameter in relation to the other sizes of the working section.

1.6 - Ventilated wall sections with longitudinal slots or perforations have then been more and more used for transonic flow tests. Now such sections are used for a very wide range of Mach numbers. Therefore it becomes necessary to apply corrections derived from theoretical works to tests and to prove validity of these corrections.

Wright (10) conducted the first detailed attempt of theoretical/experimental work correlation. Within the same scope Göthert (5) carried out a very comprehensive study.

Finally, in September 1970, a meeting was held in Florence (Italy) with Prof. Ferri as chairman. During this meeting a review was made of the experiments in progress in various countries, in order to make use of and develop wall constraints in ventilated wall sections (11).

This paper, of course, makes use of data already stated at the Florence meeting where, in particular, efforts were made to define the transonic in relation to the high subsonic or supersonic domain. Following this the National Aerospace Laboratory, N.L.R., of Amsterdam, suggested to assess the transonic domain as a Mach number between 0.9 and 1.3.

## 2 - REVIEWAL OF THEORIES

### 2.1 - Linearized potential flow

It appears that the theory of linearized potential flow relating to the concept of homogeneous porous boundary of infinite length is definitely accepted (12, 13).

$\Phi_{WT}$  represents the potential flow within the test section around the model :

$$\begin{aligned}\Phi_{WT} &= V_0 \cdot x + \varphi_m + \varphi_i \\ &= \Phi_\infty + \varphi_i \\ &= V_0 \cdot x + \varphi\end{aligned}$$

where :

$V_0 \cdot x$  is the steady potential flow of velocity  $V_0$  parallel to the X-axis

$\varphi_m$  is the potential of perturbation velocities representing the model.

$\Phi_\infty$  is the velocity potential around the model in free air

$\varphi_i$  is the additional interaction potential due to presence of walls

A theoretical approach is given in Appendix.

### 2.2 - Boundary conditions

Generally the boundary conditions along walls can be expressed as (14) :

$$\frac{\partial \varphi}{\partial x} + K_1 \frac{\partial}{\partial x} \left( \frac{\partial \varphi}{\partial n} \right) + \frac{1}{R} \frac{\partial \varphi}{\partial n} = 0$$

where :

$K_1$  defines the geometric parameter (Fig. 4) applicable to longitudinally-slotted walls (15, 12, 13, 14) :

$$K_1 = \frac{d}{\pi c} \log_e \left( \operatorname{cosec} \frac{\pi c}{2} \frac{\partial}{d} \right)$$

$R$  is the aerodynamic porosity parameter related to viscosity of the air flow which crosses the ventilated walls (15) :

$$R = \frac{\rho_0 V_0}{\Delta p} v_n = 2 \frac{\theta}{C_p},$$

with :

$$C_p = \frac{\Delta p}{q_0} \quad \text{and} \quad \theta = \frac{v_n}{V_0},$$

where  $\Delta p$  is the pressure difference between the section and the plenum chamber and  $v_n$  the perturbation velocity component normal to the wall.

No allowance is made for compressibility effect in  $K_1$  which corresponds to the definition of ideal slotted walls, i.e., walls through which viscosity effect is negligible. However under compressible flow conditions, porosity  $R$ , (porous wall Reynolds number) becomes  $R/\beta$ .

Now it is accepted that operation of longitudinally slotted walls (having necessarily a low permeability) defined by the sole parameter  $K_1$  is far from being realistic. Allowance shall also be made for the term  $\beta/R$  more specially used in the study of porous walls, and, in a wider sense, perforated walls.

### 2.3 - Remarks

The boundary conditions are expressed as follows :

for an open jet :

$$\frac{\partial \varphi}{\partial x} = 0$$

for solid walls :

$$\frac{\partial \varphi}{\partial n} = 0$$

for perforated walls :

$$\frac{\partial \varphi}{\partial x} + \frac{1}{R} \frac{\partial \varphi}{\partial n} = 0$$

## 3 - CORRECTION TERMS

### 3.1 - Definitions

Corrections terms are classified in two groups : blockage corrections and lift corrections.

Blockage corrections are defined by induced axial perturbation velocities :

$$u = \frac{\partial \varphi_1}{\partial x}$$

which modify the magnitude of upstream velocity ( $V_0$ ) at the level of the model.

Lift corrections are defined by induced perturbation velocities (upwash) :

$$w = \frac{\partial \varphi_2}{\partial z}$$

perpendicular to velocity  $V_0$  and which modify velocity direction, at the level of the model.

The logical sequence for utilization of correction terms (or correction program to be applied to uncorrected results) is shown in Table I ; this is supplemented by a few definitions of symbols in Table II.

### 3.2 - Blockage corrections

Let  $q_0$  be the upstream kinetic pressure and  $q_c$  the corrected kinetic pressure at the level of the model ; hence :

$$q_c = q_0 \left[ 1 + (2 - M_0^2) \epsilon_{MP} \right]$$

applying the relevant correction for Mach number :

$$\Delta M = M_0 (1 + 0,2 M_0^2) \epsilon_{MP}$$

For an unpowered model placed in the center of the working section :

$$\epsilon_{MP} = \epsilon_{1MP} + \epsilon_{2MP} + \epsilon_{3MP}$$

where :

$E_{1MP}$  is the blockage correction term due to model volume defined by potential  $\varphi_{m1}$  of a doublet :

$$E_{1MP} = \frac{1}{V_0} \cdot \frac{\partial \varphi_{i1}}{\partial x} = \frac{u_1}{V_0} = \Omega_1 \beta^{-3} E_1$$

$E_{2MP}$  is the blockage correction term due to model wake defined by potential  $\varphi_{m2}$  of a source (or a sink associated with said source and located far downstream) :

$$E_{2MP} = \frac{1}{V_0} \cdot \frac{\partial \varphi_{i2}}{\partial x} = \frac{u_2}{V_0} = \Omega_2 \beta^{-2} (1 + 0.4 M_0^2) E_2$$

$E_{3MP}$  is the blockage correction term due to stalling

$$E_{3MP} = \frac{u_3}{V_0} = \beta^{-3} E_3 = \beta^{-3} \frac{E_d}{2} \frac{S}{C} C_{Dd}$$

$E_{3MP}$  is not derived from a perturbation velocity potential, but forms a semi-empirical solution peculiar to wake problems associated with the "dead water" concept (16).

### 3.3 - Lift corrections

Lifting component or wing potential  $\varphi_{mz}$  is defined by one or several vortex (vortices) distributed spanwise.

Basic correction applies to the angle of attack of the model :

$$\Delta \alpha_0 = \frac{1}{V_0} \cdot \frac{\partial \varphi_{iz}}{\partial z} = \frac{w}{V_0}$$

with the coefficient :

$$\delta_0 = \frac{S_0}{S \cdot C_L} \left( \frac{w}{V_0} \right)_{x=0}$$

Evolution of  $w$  along the longitudinal direction of the working section emphasizes the streamline curvature, hence :

$$\delta_1 = \frac{\beta \cdot S_0 \cdot H}{S \cdot C_L} \left( \frac{1}{V_0} \cdot \frac{\partial w}{\partial x} \right)$$

Total correction for angle of attack considering an element located on the X-axis is expressed as follows :

$$\Delta \alpha = \left( \delta_0 + \delta_1 \frac{x}{\beta H} \right) \frac{S}{S_0} \cdot C_L$$

This yields the following drag corrections :

$$\Delta C_D \cong \Delta \alpha \cdot C_L \cong \Delta \alpha_0 \cdot C_L$$

and lift corrections :

$$\Delta C_L = - \delta_1 \frac{x}{\beta H} \cdot \frac{S}{S_0} \cdot C_L \cdot \left( \frac{dC_L}{d\alpha} \right)_{\alpha}$$

Providing  $x$  with values  $c/4$  (2 dim.) or  $\bar{r}_d/4$  (3 dim.) as defined in Table II we obtain the commonly used relationships. In most cases, in 3 dim., the correction  $\Delta C_L$  is transferred to the angle of attack (17).

The suggested corrections are shown in Table I.

It is true that angle of attack correction can also be integrally transferred to  $\Delta C_L$  correction, as is sometimes the case in 2 dim (18).

Pitching moment corrections should also be considered :

$$\Delta C_m = k \left( \delta_1 \frac{x}{\beta H} \right) \frac{S}{S_0} C_L \left( \frac{dC_L}{d\alpha} \right)$$

either applied to :

- the wing unit,  $\Delta C_{m\alpha}$ , with :

$$4x = c = \bar{l}_\alpha,$$

and

$$k = \frac{x}{\bar{l}_\alpha} = \frac{x_\alpha}{\bar{l}_\alpha} \approx \frac{1}{4}$$

- or the tail unit (horizontal stabilizer),  $\Delta C_{m_e}$ , with :

$$x = l_e$$

and

$$k = \frac{s_e}{s} \cdot \frac{l_e}{c_r} \cdot \frac{q_e}{q_c}$$

Of course,  $\Delta C_{m\alpha}$  and  $\Delta C_{m_e}$  are a function of wing and tail lift gradients  $(dC_L/d\alpha)_\alpha$  and  $(dC_L/d\alpha)_e$  respectively, but also of  $\delta_1(x) = \delta_{1\alpha}$  and  $\delta_1(x) = \delta_{1e}$  whose values are taken on x-axis preferred points, i.e. at three-quarter downstream of the leading edges of wing or tail mean aerodynamic chord.

Therefore it is necessary to know how  $\delta_1$  develops along the X-axis (streamwise).

### 3.4 - Important note

As a matter of fact, velocity  $W$  also develops spanwise and the resulting calculation - an example of which is given in Ref. 20 - permits to obtain roll corrections. This problem will not be further investigated. Now let us reconsider the factor  $\delta_1$  which defines the streamline curvature along the X-axis.

The factor  $\delta_1$  appears as a gradient.

Mention should also be made of gradients corresponding to blockage terms :

$$\frac{\partial \epsilon_{MP}}{\partial x} = \left( \frac{\partial \epsilon_{1MP}}{\partial x} \right)_{x=0} + \left( \frac{\partial \epsilon_{2MP}}{\partial x} \right)_{x=0}$$

The gradient due to wake blockage,  $\partial \epsilon_{2MP} / \partial x$ , proportional to solid blockage correction term, i.e. proportional to  $-\Omega_1 \epsilon_1$ , appears regardless of wall type : solid walls, ventilated walls, or open jet. However the gradient due to solid blockage, as defined by the factor  $\Omega_1' = \partial \Omega_1 / \partial (x/\beta H)$ , appears only for ventilated wall sections through which viscosity effect is felt.

Proportionally to these gradients, drag corrections appear, such as :  $\Delta C_{D2MP}$  and  $\Delta C_{D1MP}$

Calculation assumptions are so made that stall-induced blockage has no gradient (16).

Finally, the correction term  $\Delta C_{Dg}$  should be recalled : this term applies to the static pressure gradient which can be present in the empty section. In most cases, wind tunnels have zero gradient and  $\Delta C_{Dg} = 0$

## 4 - CORRECTION FACTORS

### 4.1 - Definitions of interferences

From the correction terms stated in the previous paragraph correction factors can be classified under two groups as follows :

- blockage correction factors :  $\Omega_1, \Omega_2, \epsilon_d, \Omega_1'$
- lift correction factors :  $\delta_0, \delta_1$

The six above-mentioned factors are dependent upon wind tunnel and model.

(\*) Factor  $\Omega_1$  is generally multiplied by a product  $K\mathcal{E}$  slightly lower than 1 ; this allows for model wing span and working section cross-sectional area (refer to Herriot : NACA Report 995 - 1950).

Product  $K\mathcal{E}$  is sometimes replaced by parameter  $T$  as defined for a given working section and depending upon the model wing span (19).

Interferences due to wind tunnel are as follows :

- working section geometrical shape (circular, elliptical, square, rectangular, octagonal, etc.)
- wall type (solid, semi-closed, ventilated, open jet)
- wall length ; this factor is particularly important when open jets or ventilated walls are concerned

Interferences due to model are as follows :

- model wing aspect ratio, as evidenced by 2 dim or 3 dim tests
- hence, wingspan
- model size, especially wing chord, area, volume.

As a matter of fact, one should bear in mind that correction terms are derived from linearized hypotheses which impose validity limits upon induced velocities  $u$  and  $u^*$ , thus upon limit size of models.

There are also model/wind tunnel interactions.

Among these, the following should be considered : upward movement of the model in relation to its central position within the test section or in the fore-and-aft direction, positions of wing and tail unit with respect to a developing permeability of the perforated wall (21), for example. So we are again faced with the former problem regarding the model position in an open jet in relation to the collector outlet and diffuser inlet.

Finally, when ventilated sections are concerned, mention should be made of a possible influence of an auxiliary suction from the plenum chamber upon correction factors.

#### 4.2 - Representation of correction factors

When longitudinally - slotted ventilated walls are concerned, correction factors are, in most cases, plotted against :

$$P = \frac{1}{1 + \frac{2K_1}{H}}$$

which is a geometrical parameter where  $P=0$  for solid walls ;  $P=1$  for an open jet and  $H$  is height of working section.

No allowance is made for compressibility effect in  $P$ . Besides it should be recalled that criterion  $\beta/R$  also applies to longitudinally - slotted ventilated walls.

By analogy with  $P$ , the following parameter is introduced :

$$Q = \frac{1}{1 + \frac{\beta}{R}}$$

so that :  $Q=0$  for the solid wall and  $Q=1$  for the open jet.

Representation of correction factors as a function of  $P$  and  $Q$  for slotted walls and as a function of the sole  $Q$  for perforated walls is particularly convenient for general theoretical analyses. This representation can also be conveniently used for ventilated wall sections with variable geometry, i.e. capable of operating from the solid wall to the semi-closed wall configuration (two high-permeability ventilated walls) or to the open jet configuration (four high-permeability ventilated walls).

#### 4.3 - Parameter for present definition of ventilated wall tunnels

In the present state of the art, variable-geometry wind tunnels are not commonly used or their operation is not yet optimized. In other words, wind tunnel geometry is "frozen" in three or four preferred positions (22).

In fact, most wind tunnels in use feature ventilated walls of fixed geometry.

There is a tendency to define each wind tunnel from its specific parameter  $\beta/R$ .

The same applies to longitudinally-slotted walls, as evidenced by the work carried out by the National Aerospace Laboratory, N.L.R. of Amsterdam (23).

However similar parameters can be used. So it is that Carter (21) of Aircraft Research Association (Bedford) returns to Küssner's or Göttert's definitions, using the parameter  $\beta K$  as follows :

$$\beta K = \frac{2\beta}{R}$$

Mackrodt (18) and Lorenz-Meyer (19) of AVA Göttingen (DFVLR) use the following factor :

$$\frac{1}{2} K\beta$$

plotted against Mach number (M). So through this agency, these authors can show evolution of factors  $\Omega_1, \Omega_2, \delta_0$ , and  $\delta_1$  of a transonic wind tunnel against Mach number (M).

In a paper from A.E.D.C. relating to porosity varying with fore-and-aft direction of the working section, i.e.  $R(x)$ , C.F.Lo (24) additionally introduces the following parameter :

$$T(x) = \frac{\beta}{R(x)}$$

## 5 - REMARKS AND CONCLUSIONS REGARDING CORRECTION FACTORS

5.1 - Let us reconsider the correction factors as a function of parameters  $P$  and  $Q$  mentioned in paragraph 4.2.

In ventilated wall sections, these factors should obligatorily lie between those associated with solid walls ( $P=Q=0$ ) and those associated with open jets ( $P=Q=1$ )

This is the case for  $\Omega_1, \delta_0$ , and  $(\delta_1)_{x=0}$ . Thus the factor  $\Omega_1$  lies between limit values shown in the table below :

Working section	Solid walls	Open jet - 2 dim	Open jet - 3 dim
$Q$	0	1	1
$\Omega_1$	1	-0,50	-0,25

Another example, 2 dim, can be suggested where these factors lie between limit values shown in the table below :

Working section	$Q$	$\Omega_1$	$\delta_0$	$(\delta_1)_{x=0}$
Solid walls-2 dim	0	1	0	$\pi/24$
Open jet - 2 dim	1	-0,50	-0,25	$-\pi/12$

Similarly, the factor  $\Omega_2$  is zero for  $Q=0$  and  $Q=1$ .  $\Omega_2$  develops up to a maximum value which nearly corresponds to  $\Omega_2=0$  (10, 2).

Nevertheless these concluding remarks are true only when applied to the theory of linearized potential flow. This gives rise to problems regarding model size in relation to test section size. Therefore there are also correction validity limits for angles of attack or, to a greater extent, for lift coefficients and test Mach numbers.

5.2 - Oppositely, the factor  $\Omega_2$  which defines wake blockage, is not affected by the above-mentioned remarks. When considering solid walls, with  $Q=0$ ,  $\Omega_2=1$ . For ideal-slotted walls, i.e. with no viscous effect and for an open jet with  $Q=1$ ,  $\Omega_2$  is zero.

But when viscous effect is not negligible, i.e. when  $0 < Q < 1$ ,  $\Omega_2$  is always negative, starting from zero for  $Q=1$ , but tending toward -1 when  $Q=0$ .

The above result is thus paradoxical since the specific parameter of solid walls is not obtained.

In fact this result is the consequence of the simplifying hypothesis concerning the boundary conditions which assume that ventilated walls have an infinite length.

A further problem is thus posed, which takes into account the finite length of the wall perforated part whose influence upon correction factors will be determined.

5.3 - It should be recalled that analyses should be continued in order to obtain full knowledge of the development of stall blockage factor within ventilated wall and open jet sections. However it is known that for wing aspect ratios between 1 and 10,  $\epsilon_d = 2.5$  for solid walls and  $\epsilon_d = 2$  for semi-closed walls. In 2dim  $\epsilon_d = 1$  within solid walls (16).

To summarize, it should be stated that use of correction factors requires assessment of validity limits for linearized hypotheses and definition of the influence of a finite length for open jets, or ventilated walls.

5.4 - For ventilated walls - slotted or perforated - the parameter R and, to a greater extent,  $\beta/R$ , are the criteria applicable to validity or influence domains that have just been stated. It is thus mandatory to know these parameters.

It should be recalled that each correction factor becomes zero when it is allocated a value of  $\beta/R$ . So in order to cancel a correction factor for any value of M, the parameter R must be strictly adapted to each value of  $\beta$  in accordance with the theory of porous walls (15). This is the approach to the problem of variable geometry wind tunnels, in the form R ( $\beta$ ).

For practical purposes, it can be contemplated, for example, to minimize blockage effect. Then Mach domains shall be investigated without involving considerable errors; in these Mach domains,  $\beta/R$  can be considered as a constant value applicable to fixed geometry wind tunnels. However lift corrections can exist for this value of  $\beta/R$ .

Besides, variations of factors  $\Omega(x)$  and  $\delta_f(x)$  in the fore-and-aft direction of the test section show the importance of gradients. We are again faced with the problems relating to developing effects of porosity R ( $x$ ) and variable permeability (22, 24).

It would also be possible to consider  $\delta_f(z)$  developments for instance, but this would lead to contemplation of theories other than those already mentioned and bring the subject to V/STOL aircraft.

5.5 - We consider that we have examined the present problems posed by experimental utilization of wall constraints, particularly in ventilated wall sections, from theoretical knowledge which is still far from being fully acquired.

Recent papers covering this subject fit within the framework of the research work just mentioned and considerable improvements have been made since the Florence meeting.

These papers largely contribute to the knowledge of all these domains. It is our intention to show this briefly in the following pages.

Of course the brief analysis of these papers is not intended to replace their thorough perusal.

## 6 - DEFINITION OF POROSITY PARAMETER R

For ventilated wall wind tunnels the basic problem consists in defining the porosity parameter R associated with the aerodynamic operation criterion  $\beta/R$  of the working section.

For this purpose there are three essentially experimental measuring methods, as follows :

- direct measurements,
- indirect measurement,
- comparison of measurements.

### 6.1 - Direct measurement

Direct measurement consists in the calibration of a sample consisting of a perforated flat panel.

A great number of sampling panels of different thickness and with straight or slanted holes and different geometrical permeabilities can be calibrated with a view to selecting walls for the wind tunnels to be built.

A wall element of a wind tunnel already in operation can also be calibrated.



6.1.1 - A.E.D.C. method

The wall sampling panel is used in place of one of the four solid walls of a wind tunnel specially designed for calibration purposes (4, 25). A secondary chamber is installed on the opposite side of the ventilated wall in relation to the main working section within which velocity ( $V_0$ ) and Mach number ( $M$ ) are made to vary. Owing to an auxiliary suction produced from the secondary chamber, a flow is induced across the wall to be calibrated. For a given Mach number the suction flow is made to vary. The following are then measured : pressure difference ( $\Delta p$ ) between primary air stream and chamber ; secondary flow / primary flow ratio ( $\theta$ ) of working section of velocity  $V_0$ .

For a well-defined sample and for each value of Mach number, the factor  $C_p = \Delta p / \rho V_0^2$  is plotted against the parameter  $\theta = \rho V_n / \rho V_0 \approx V_n / V_0$ . A check is then performed in a wind tunnel with four ventilated walls (25).

Several calibration reports so obtained were issued by the Arnold Engineering Development Center. Some references to these reports appear in G6thert's book (5).

From one of these studies (25), Lorenz-Meyer plotted the operating curve :

$$\frac{\beta}{R} = \frac{\beta^2}{2} \frac{\partial C_p}{\partial \theta} = f(M)$$

of G6ttingen transonic wind tunnel (19) \*.

- \* Square section wind tunnel (1 x 1 m<sup>2</sup> 10.76 sq ft) - 4 perforated ventilated walls - Geometrical permeability : 6% - holes slanted through 60°.

Then Lorenz-Meyer related the square test section with four ventilated walls to a circular test section of similar permeability.

It was later demonstrated by Lo and Oliver papers (3) that this relation was justified. Therefore for these two types of sections, the factors  $\Omega_1$  and  $\delta_0$  become zero for  $Q = 0.45$ , i.e.  $\beta/R = 1.22$ .

6.1.2 - Institut A6rotechnique (St-Cyr) method (22)

A sample of the perforated horizontal walls of the wind tunnel  $\Sigma 4$  at Saint-Cyr (\*\*\*) is placed in a duct (Fig. 5). Pressure drop  $\Delta p$  of this element was measured against velocity  $V_n$  :

$$\Delta p = K \frac{\rho}{2} V_n^2$$

Pressure difference  $\Delta p$  between the working section of wind tunnel  $\Sigma 4$  and the associated plenum chamber was then measured against velocity  $V_0$  in the test section :

$$\Delta p = p - p_c = K_p \frac{\rho_0}{2} V_0^2$$

Assuming equality of  $\Delta p$  yields :

$$\frac{V_0}{V_n} \approx \sqrt{\frac{K}{K_p}}$$

By definition :

$$R = \frac{\rho_0 V_0}{\Delta p} \cdot V_n,$$

hence :

$$R = \frac{\rho_0 V_0 V_n}{K \frac{\rho}{2} V_n^2} \approx \frac{2}{K} \frac{V_0}{V_n} = \frac{2}{\sqrt{K_p \cdot K}}$$

For maximum geometrical permeability of horizontal walls, i.e. 29%,  $R$  was found to be 5

- \*\* Square section wind tunnel (0.85 x 0.85 m<sup>2</sup> - 9.14 sq. ft) solid vertical walls - perforated horizontal walls - straight holes.

### 6.1.3 - Comments

The two following remarks should be made when using the method of sampling and calibration of a ventilated wall panel.

First the boundary layer which develops on the working section walls can be different from that existing on the sampling panel.

However, precautionary measures were taken at the A.E.D.C. which consisted in slanting the walls of the calibrating auxiliary wind tunnel so as to obtain a boundary layer with constant thickness. As a matter of fact, it is essential that the static pressure gradient along the ventilated wall is made negligible before it is crossed by a flow.

For each rate of flow, the wall slanting angle shall be corrected.

When assessing R experimentally, allowance shall also be made for influence of generating pressure change.

Besides, the difference in size (width, length) between the ventilated wall and the sampling panel can, during utilization, result in R values different from those obtained during calibration.

The method suggested by the Institut Aérotechnique of Saint-Cyr appears to be difficult to use when the sampling panel originates from a perforated wall having slanted holes. In addition the aerodynamic operation during the tests is quite different from that existing in the wind tunnel.

Finally, it appears that, when using the previously mentioned methods, it is unpracticable to calibrate a wall with developing permeability, this permeability resulting both from a graded geometry tunnel and certain types of variable geometry tunnels.

### 6.2 - Indirect measurement

The N.L.R. suggests a method of indirect measurement (two-dimensional) referred to as "drag-balance" (23). This method permits to assess the parameter  $\beta/R$  of the walls (longitudinally - slotted walls in the N.L.R. Pilot Tunnel)\* with an airfoil placed in the test section. This method takes into account the working section geometry, which leaves out of consideration most of the remarks of paragraph 6.1.3. However application of this method requires highly-skilled operators and very close and accurate measurements.

The "drag-balance" method is based on the following equation :

$$C_{Dp} + C_{Df} + \sum \Delta C_{Di} = \chi C_{Dw}$$

where :

$C_{Dp}$  is the profile drag coefficient, as obtained from pressure measurements on the model.

$C_{Df}$  is the skin friction drag coefficient, which is theoretically calculated from the pressure distributions.

$\chi C_{Dw}$  is the total drag coefficient, as measured by a wake rake placed in the airfoil wake and sufficiently far downstream of the airfoil so that the blockage correction factor  $\chi$  appears as being close to 1.

$\sum \Delta C_{Di}$  is the sum of all interactions due to wall effect.

Index  $u$  represents uncorrected values measured in the wind tunnel. With the airfoil set to an angle of attack  $\alpha$ , the lift coefficient  $C_{Lu}$  is calculated by integration of pressures and an induced angle  $\Delta\alpha$  due to walls appears.

Very small terms, obtained from calculations or substantiated by experience, shall be disregarded. Under these conditions the drag-balance equation becomes :

$$C_{Dwu} = C_{Dpu} + C_{Dfu} - \Delta C_{Dg} + C_{Lu} \Delta\alpha + \Delta C_{D1MP} + \Delta C_{D2MP}$$

It should be recalled that :

$\Delta C_{Dg}$  is the buoyancy drag associated with the static pressure gradient of the working section without model in it.

\* Rectangular section with solid vertical walls - height : 0.55 m (1.80 ft) - slotted horizontal walls - (permeability : 10 % on each horizontal wall) - width : 0.42 m (1.37 ft).

$\Delta C_{D1MP}$  is the buoyancy drag due to solid blockage gradient.

$\Delta C_{D2MP}$  is the buoyancy drag due to wake blockage gradient.

Hence :

$$\Sigma \Delta C_{D_i} = C_{LW} \Delta \alpha + \Delta C_{D1MP} + \Delta C_{D2MP} \quad (1)$$

and the equation becomes :

$$\Sigma \Delta C_{D_i} = C_{DHW} - (C_{DpW} + C_{DfW} - \Delta C_{Dg}) \quad (2)$$

From equation (1),  $\Sigma \Delta C_{D_i}$  can be calculated against  $\beta/R$ , for a given Mach number, a given angle of attack, hence a given lift coefficient, taking the value of K1 imposed by slotted wall geometry.

In equation (2),  $\Sigma \Delta C_{D_i}$  stems from values assessed experimentally.

Therefore by comparing the  $\Sigma \Delta C_{D_i}$  calculated values with experimental values, the  $\beta/R$  value corresponding to each Mach number and angle of attack can be obtained.

In the Pilot Tunnel,  $\beta/R$  was found to be equal to  $1.7 \pm 0.1$ , with several airfoils and angles of attack up to  $8^\circ$ . This value was regarded as constant over a Mach number ranging from 0.4 to critical Mach number.

### 6.3 - Comparison of measurements

The methods permitting to determine R by comparison of measurements are classified in two groups :

- a) - A model is placed in the test section which can be arranged in various configurations as follows :
  - solid wall section, ventilated wall section,
  - ventilated wall section, high-permeability ventilated wall section comparable to an open jet in this instance (four ventilated walls) or to a semi-closed wall section (two ventilated walls). This configuration is suitable to comparative tests at high Mach numbers.
- b) - Two or more models manufactured at various scales from the same model are used together with a ventilated wall section featuring a single configuration.

This test method leads to the use of various wall permeabilities to improve the accuracy of test results. This method is more open to criticism than the above-mentioned method in so far as Reynolds number effect is taken into account.

The models are first installed with an angle of attack corresponding to zero lift so as to eliminate deflection effect.

#### 6.3.1 - Same model placed within a section with two configurations

##### 6.3.1.1 - A.R.A. Method (21)

The method consisting in using the same model placed in a working section with two configurations was used by Carter in the 9 ft x 8 ft A.R.A. wind tunnel. First the ventilated wall section was used ; then all the wall holes were blanked to obtain a solid wall section. Carter compared the values of  $\Delta M_p$  measured in the ventilated wall section with the  $\Delta M$  values calculated and corrected (26) from the results measured in the solid wall section. Carter infers that the high-permeability ventilated wall section is free from blockage, contrary to all expectations. In fact, a geometric permeability of 22% could suggest that this section would act as an open jet with, in this case :

$$0.4 < \beta K < 0.8$$

$$\text{i.e. : } 5 < R < 2.5 \quad (*)$$

(\*) For reference, it should be stated that the General Dynamics High Speed Wind Tunnel has a square section (4 ft x 4 ft), four perforated walls providing 22% geometric permeability and is characterized by  $R = 5.5$  (refer to AIAA Paper 71-292).

But the permeability which gradually develops along the X-axis counteracts this effect. Therefore Carter infers that :

$$\beta K = 2,$$

$$\text{i.e. } R = 1.$$

However, at the level of wing unit, lift corrections are defined by a factor  $\delta_0$  equal to half the factor associated with an open jet. From Rogers' paper, it is inferred that  $\beta/R \cong 0.35$  (1). Thus  $\beta K = 0.7$  and  $R \cong 3$ .

#### 6.3.1.2 - NAR Corporation method (27)

Methodical research work was carried out in the North American Rockwell Corporation square section (7 ft x 7 ft) transonic wind tunnel. This work was intended to determine ventilated walls which did not cause interactions.

Two basic configurations were used : 1) solid walls ; 2) perforated walls with straight holes, providing 19.7% geometric permeability, and comparable to an open jet.

The results obtained with the same model and corrected accordingly permitted, by comparison, to determine perforated walls with moderate permeability (of the order of 6%) satisfying the desired needs.

Utilization of models provided with various blockage ratios substantiated these results.

All tests and test data are shown in figure 6. The graphs associated with the measurement methods are shown in figure 7.

Therefore it can be noted that a square section provided with four perforated walls having straight holes and 6% permeability permits to obtain results which need no correction. Since these tests, Lo and Oliver (3) have shown that, in this case, blockage correction factor  $\Omega_1$  and wall correction factor  $\delta_0$  are zero for the same value of Q, i.e. 0.45, as already stated in 6.1.1. Hence :

$$R^{-1} \cong 1.2$$

The same square section provided with vertical solid walls operates very similarly. Pindzola and Lo (2) infer that  $Q \cong 0.50$ , i.e.  $R \cong 1$ . In fact, in the latter case, wall constraints are low and cannot be observed in measurements.

It is encouraging to note that, considering the accuracy of these measurements, a relationship exists between theoretical and experimental works. It can also be seen that it is possible to experimentally admit sensibility ranges of  $\beta/R$  regardless of Mach number.

#### 6.3.2 - Models placed within a test section with various configurations

In the previous paragraph the examples shown referred to the tri-dimensional case. The method described below is that used in 2 dim by the O.N.E.R.A. (28).

Models having the same airfoil (NACA 0012 for example) but manufactured at various scales, are placed, with zero lift, in a test section comprising walls of various permeabilities to determine, for all test cases, the shock wave location by measuring the pressure distribution on the models. Shock location emerges as a very sensitive criterion which can be relied upon provided the tests are conducted at Reynolds numbers in excess of  $2 \cdot 10^6$  (28).

For a given wall permeability and for the same test Mach number (i.e. uncorrected Mach number) the same shock location can be obtained regardless of airfoil size. It is inferred that this permeability causes zero blockage.

The same shock location can be obtained on the various airfoils confronted with walls of various permeabilities, but at different Mach numbers. By difference, the correction  $\Delta MP$  can be inferred. Comparing correction  $\Delta MP$  with correction  $\Delta M$  as measured for the solid wall section shows a correction term less than 1 (refer to Fig. 8). Assuming that the perforated ventilated element has an infinite length and that wake blockage factor  $E_{2MP}$  is negligible, this term is thus related to solid blockage factor  $\Omega_{1MP}$ . From the theoretical curves giving  $\Omega_{1MP}$  versus Q (2, 4) or  $\beta/R$  (1), R value is thus assessed for each ventilated wall. Then  $\delta_0$  and  $\delta_1$  together with the associated corrections are inferred.

In reference 29 a thorough description of this method is given. Furthermore it is pointed out it should be ascertained that the value of  $R$  determined in this manner also applies to any type of airfoil.

This remark should be considered as a general rule.

## 7 - REMARKS ABOUT BLOCKAGE MEASUREMENTS - GENERALIZATION

As a supplement to the previous chapter, paragraphs 7.1 and 7.2 refer to the experimental methods used for determining Mach number variation  $\Delta M$  due to model blockage.

### 7.1 - Measurements from the model (21)

Static ports are provided on the wing trailing edge, since this region is considered as being representative of the measurements taken in the middle of the model, a complete aircraft model in this instance.

Measurements are taken of pressure coefficients  $C_p$  with respect to static pressure within the ventilated test section.

At the wing trailing edge, the coefficient  $C_p$  is very close to zero and hardly sensitive to the lift coefficient ( $C_L$ ) and Mach number, at zero lift.

Therefore any deviation of this pressure coefficient from the "corrected" coefficient in a solid wall section shows an improper static pressure as well as a blockage effect associated with a variation of Mach number  $\Delta M$ .

This method was used during the tests mentioned in paragraph 6.3.1.1. These tests showed that the A.R.A. ventilated test section was free from blockage when the model under consideration was that of a conventional transport airplane. These results were checked and substantiated with another model of the "canard" type.

### 7.2 - Measurements from the walls (17)

In this method the model is placed at the center of a solid wall section.

Pressure ports are provided in the region of the model on floor and roof walls.

Other things being equal, a pressure difference ( $\Delta p$ ) between the test section without model and the test section with model indicates an excess velocity on the wall due to blockage.

Linearized hypotheses show that excess velocity at the wall is directly proportional to excess velocity along the test section centerline (1,30). This relationship is hardly influenced by compressibility (30). Therefore blockage can be determined by using simple calculations.

This method is used by Taylor in the solid wall pressurized wind tunnel (8 ft x 8 ft) of the Royal Aircraft Establishment, Bedford (17). This method was previously mentioned by Gøthert for circular sections (30).

### 7.3 - Supplementary and general remarks

7.3.1 - Very often, test results obtained in a ventilated test section are compared with those obtained in a solid wall section. If blockage correction factors are applied to test results (drag coefficients for example), with zero lift, it is expected to find a corrected drag coefficient equal to the drag coefficient measured in the ventilated test section and to which the gradient corrections only would have been applied. This equality can occur over a rather wide range of Mach numbers or at a preferred Mach number as shown by the drag curves plotted against Mach number in reference 21 and Fig. 9. For these/this Mach number (s), roughly 0.7 in the present case, it can be said that blockage is zero in a ventilated test section.

From increasing angles of attack and, by comparison, lift / incidence curves corrected in a solid wall section and uncorrected in a ventilated test section, (as shown in Fig. 9), the corrections  $\Delta \alpha$  can be derived and the corresponding value of  $R$  can be calculated.

This method requires very accurate measurements.

7.3.2 - From reference 31 Taylor suggests a similar method to determine wall corrections in the pressurized slotted wall wind tunnel (8 ft x 6 ft)\* of the R.A.E., Farnborough (17).

\* Four slotted walls for 3 dim tests.  
Two slotted walls (reduced width) for 2 dim tests.

The slots are so arranged as to provide zero blockage over a wide range of Mach numbers. This was verified by pressure distribution on airfoils, at zero lift.

Then an angle of attack is given to symmetrical airfoils of same maximum frontal area, but with different chords, while providing the same Reynolds number.

Then plotting  $dC_m/dC_L$  curves against  $(c/H)$  and allowing  $c/H$  to approach zero (i.e. allowing  $H$  to approach infinity) corrections  $\Delta C_m$  and factor  $\delta_1$  can be derived. Using this method for  $dC_L/d\alpha$  curves, the factor  $\delta_0$  can be obtained,  $\delta_1$  being known. The Fig. 10 illustrates this method.

## 8 - LENGTH RESTRICTION OF VENTILATED WALLS

8.1 - In analyses regarding corrections it is assumed that the walls have an infinite length. This simplifying hypothesis is correct only for solid wall sections.

Influence of ventilated walls with a finite length upon correction factors was evidenced by Woods who showed that, with the same geometric permeability, the length variation is equivalent to a variation of porosity  $R$  (32).

This result, obtained in 2 dim, was subsequently worked up by Parkinson and Lim who suggested that factors  $\delta_0$  and  $\delta_1$  are much less affected than factors  $\Omega_1$  and  $\Omega_2$  (33).

As a matter of fact a recent paper from Veullot shows the influence of perforated wall length upon  $\Omega_1$  and  $\Omega_2$  (34). Furthermore this paper gives an answer to the paradoxical result mentioned in paragraph 5.2.

With ventilated walls of finite length, the factor  $\Omega_2$  approaches + 1 when permeability approaches zero.

8.2 - This theoretical analysis was experimentally evidenced by 2 dim tests conducted on N.A.C.A. 0012 airfoils, in the O.N.E.R.A. S3 wind tunnel, at Modane. This wind tunnel is provided with perforated horizontal walls (35). With 9% geometric permeability, no blockage was noted for a value of  $\beta/R = 0.7$  which corresponds to the length of the ventilated portion equal to 2.7 H, H being the test section height.

It should be recalled that, for an infinite length of the perforated element,  $\beta/R \leq 1.65$ ; this value allows for solid blockage and wake blockage.

8.3 - Still in 2 dim, Mokry performed a theoretical work which clarified the paradoxical result of paragraph 5.2 relating to the factor  $\Omega_2$ . Mokry analysis also started from the notion of perforated walls with a finite length.

In fact, this notion is also in close connection with the location of static pressure port referred to as "infinity upstream" pressure (36).

In the theory of infinite length walls it is assumed that this reference pressure is located at infinity upstream, i.e.  $x = -\infty$

Actually this reference pressure is located at a distance X equal to or greater than  $-1.5 H$  upstream of the model, on the X-axis on which correction factors become negligible.

So for very low permeabilities, i.e. for values of Q (or t depending on Mokry's symbols) less than 0.3, the factor  $\Omega_2$  slowly decreases toward  $x = -\infty$ . Consequently this factor shall be corrected in the region of the model, taking reference pressure location into account.

8.4 - Such a remark (which did not, however, result in detailed calculations as Mokry's) was already made, in the 3 dim case, by Lo in a paper issued by the Tennessee University in 1969. This remark is mentioned in reference 3.

More generally speaking, influence of ventilated walls with a finite length upon correction factors would be worth being extended to the 3 dim case.

Therefore it would be advisable to develop analyses such as Keller and Wright's. This analysis consists in separating the test section walls into rectangular elements, each element being represented by source distributions (or vortices) (20).

Application of this method is considered by Taylor, of the R. A. E. in reference 17.

## 9 - MODEL SIZE

9.1 - Large size models can nullify the validity of linearized hypotheses. In 3 dim case, a large model is meant to be a model whose wing span is equal to  $\sigma \cdot B$  with  $0.5 < \sigma < 0.7$  and models whose length  $L$  is of the order of  $\beta \cdot H$  (17).

The Langley Research Center, of the N. A. S. A., states that for wing aspect ratios  $\lambda$  of the order of 7,  $\sigma$  shall be less than 0.7, and 0.5 if aspect ratio is nearly 3 (37).\*

As a matter of fact, the parameter so evidenced is obtained in the ratio  $S/C$  which appears in the correction terms.  $S/C$  is equal or proportional to the product of both parameters  $\sigma \lambda a/H$  which shall obligatorily vary inversely.

The model scale which determines the model area  $S$  can be selected from the model maximum frontal area  $\Sigma$ , for the blockage ratio  $\Sigma/C$  is a specific blockage criterion, especially in the high subsonic domain.

These empirical relationships should be replaced by theoretical analyses which would provide calculated results thus permitting to determine dimensions of the models considering the desired lift coefficients and Mach numbers.

9.2 In 2 dim, a Mokry's analysis (38) seems to indicate a procedure consisting in the use of series from which solutions diverge or converge. The quantity  $\mathcal{L}/\beta H$  is taken as a perturbation parameter of these series.

An example using  $\mathcal{L}/\beta H = 0.314$  indicates that the solutions converge correctly. Mokry also infers that the solution stops converging if  $\mathcal{L}/\beta H$  approaches 1. Therefore there is an interdependence between the test Mach number and the ratio  $\mathcal{L}/H$ . So, for  $\mathcal{L}/H = 0.34$  and small angles of attack, limit Mach number is of the order of 0.94.

9.3 - Dutch and French experimental test results substantiate a possible limit to the validity of linearized hypotheses, as defined by  $\beta/R$  versus  $\mathcal{L}/H$ .

The N.L.R. gives the ratio  $\mathcal{L}/H = 0.34$  as an experimental limit. Below this value, the criterion  $\beta/R$  is always allocated the value 1.7. (23).

Above this value, for example for  $\mathcal{L}/H = 0.36$ , the value of  $\beta/R$  substantially varies with the angle of attack.

The results obtained from the O.N.E.R.A. S3 wind tunnel are in agreement with the N.L.R.'s concluding remarks (35).

With  $\mathcal{L}/H = 0.19$  and  $0.27$  for all test conditions, the value  $\beta/R = 0.7$  can be maintained. It should be recalled that this value corresponds to zero blockage obtained at zero lift, in accordance with the theory of perforated walls with finite length (32, 34). For this value of  $\beta/R$ , the lift corrections are given by the factors  $\mathcal{C}_0$  and  $\mathcal{C}_\gamma$  in agreement with the theory of perforated walls with infinite length. This seems to substantiate Parkinson and Lim's remarks previously stated in paragraph 8.1: the finite length of perforated walls essentially affects blockage correction factors.

But for  $\mathcal{L}/H = 0.38$ , lift corrections are characterized by  $\beta/R = 1.1$ , value which is not connected, at the present time, with any known criterion of zero blockage.

9.4 - Besides, the N.L.R. points out that the value  $\beta/R = 1.7$ , which characterizes the N.L.R. Pilot Tunnel for ratios  $\mathcal{L}/H < 0.34$ , was obtained before shocks appear. As suggested by the N.L.R., experimental work should be undertaken in order to find out variations of  $R$  or  $\beta/R$ , at supercritical Mach numbers. However it appears that the theoretical approach of this problem can be derived from Berndt's work (who suggests that the thickness ratio can then affect the porosity parameter  $R$  (39)). The notion of blockage ratio is thus replaced by that of model cross section thickness at which the sonic line appears.

Generally this cross-section is located upstream of the maximum frontal area of the model. But use of non-linearized equations for transonic flows would be out of the scope of this paper.

9.5 - Both test results and theoretical knowledge show the importance of this program of tests conducted on calibration models as suggested by the O.N.E.R.A. to assess experimentally the 3 dim validity limits. These test programs were extensively dealt with at the Florence meeting, then at Göttingen by Poisson-Quinton (40).

\* The Langley Research Center suggests, under supersonic conditions, the empirical relationship  $L = 0.6 H$  imposed for  $M_0 = 1.2$ , in order that a model with a length  $L$  is not disturbed by reflection of waves produced by the walls. This relationship appears to be rather close to the expression:  $L \approx H \sqrt{M_0^2 - 1}$  and to the above-mentioned expression relating to a subsonic flow.

It should be added that corrections prove satisfactory provided they are all used, as evidenced by Mackrodt (18) and in Ludwig's defined terms, specially those incorporating the coefficient  $C_{Du}$  (41). These terms supplement the compressibility factors  $\beta^{-n}$  mentioned in the introduction. Mackrodt's and A.V.A Göttingen test results are shown in Fig. 11.

9.6 - Most results which are satisfactorily corrected are those applicable to Mach numbers up to 0.86 - 0.9 and lift coefficients equal to or smaller than 0.7.

So it is for the model of a modern civil transport airplane whose blockage ratio is 0.74% (21). This model is also defined by the following ratios :

$$\sigma = \frac{\text{wing span}}{\text{test section width}} = \frac{2A}{B} = 0.57$$

$$\frac{\text{fuselage length}}{\text{test section height}} = \frac{L}{H} = 0.66$$

For a Mach number  $M = 0.86$ ,  $L/\beta H = 1.30$ . With the same geometric characteristics, but with a blockage ratio of 1%, a sudden drag increase appears at a Mach number of 0.65, and the tests with correction factors were conducted to only  $M \leq 0.7$  (21).

Further test results and limits are summarized in the table of figure 6.

Therefore it appears that a blockage ratio of 0.74% is an acceptable limit. In NASA TMX 1655 and 1656 papers, such concluding remarks appeared, regarding tests conducted on cylindrical bodies.

9.7 - Finally, Lorenz-Meyer's research works should also be mentioned. These works covered Mach numbers up to 1.2, with lift coefficients of the order of 0.4. These values would be worth being considered later (19).

## 10 - VARIABLE POROSITY CONCEPT

### 10.1 - Theoretical variations in subsonic flow

10.1.1 - The various correction factors become zero in the region of the model only for values of parameter  $\beta/R$  specific to these correction factors. This means that it is not possible to cancel out all corrections for a same value of  $\beta/R$ . Therefore a selection should be made and, as part of the studies carried out, it may be desirable to minimize a given correction over a rather wide operating range of the wind tunnel. Once this selection is made, the theory shows that the porosity parameter  $R$  will undergo a simple development, constant throughout the test section length, so this development can be adapted to the compressibility factor  $\beta = \sqrt{1 - M_0^2}$ , for each value of Mach number.

10.1.2 - Then, a more complex development of parameter  $R$  can be considered along the fore - and - aft direction of the test section.

This will be the case if it is envisaged to cancel out simultaneously the lift corrections in the region of the model and the corrections applicable to the pitching moment produced by the horizontal stabilizer, as evidenced by Lo's analysis, who defines a development of parameter  $R$  along the X-axis (24). Development of  $R(x)$  also alters the value of factor  $\Omega_\gamma$  which is calculated with  $R$  as a constant (24).

### 10.2 - Practical variations

The latter theoretical case was already evidenced and partly controlled during preliminary research tests conducted in the variable - geometry  $\Sigma 4$  wind tunnel of the Institut Aérotechnique of Saint-Cyr (22). Whereas the former case has not yet given rise to the issue of experimental work reports, so far as it is known.

The following brief report is limited to consideration of fore-and-aft graded development of geometric permeability along the X-axis with the sole intention of providing a steady and homogeneous air stream within the test section, at all Mach numbers.

This practical achievement is positively connected with correction problems through the use of gradients (21). This will normally remind us, in the next chapter, existence of these gradients and their surprising effects, as evidenced by Carter.



### 10.3 - Theoretical variations in supersonic flow

In supersonic flow the shock waves originating from the model impinge on the test section walls and are reflected therefrom. The greater the model length with respect to the test section size or the closer to 1 is the Mach number the stronger the influence of these reflected waves upon the model.

In other words, for each Mach number, there is a maximum interaction length which approaches zero when the Mach number  $M$  approaches 1.

This wave reflection is strictly local. Theoretically it was demonstrated that the use of porous walls tends to absorb the waves and prevent wave reflection, especially in the low supersonic domain. So it is when :

$$R = \sqrt{M_0^2 - 1}$$

This relationship was obtained by application of the linearized hypotheses for 2 dim. flow (9, 13).

Extension of this relationship to the 3 dim. case was discussed by the Cornell Aeronautical Laboratory during a meeting of the "Institute of the Aeronautical Sciences" held at Los Angeles in 1954 ; the subject covered was "Transonic testing techniques". Deviation of parameter  $R$  in relation to its theoretical value assessed for a given Mach number was examined. It appears that a rather wide operating range is available.

## 11 - GRADIENTS

### 11.1 - Preliminary remarks

Assuming that a velocity gradient initially exists in the empty test section (without model) it is always possible to allow for this gradient in test result corrections. Taylor's formula (A.R.C.R and M 1166), also used by Glauert, still holds for the compressible flow conditions. However at high Mach numbers, Taylor's formula can be improved by adding compressibility effect upon the virtual volume of the model, as suggested by Ludwig (41).

Anyhow it is preferable to cancel this gradient. Several possibilities are available to that effect : the walls can be tilted to various angles (29) ; wall liners can be placed within the test section (35) ; position of throat flaps near the diffuser can be varied (22) ; finally an auxiliary suction from the plenum chamber can be considered (28).

Generally all relevant papers emphasize knowledge of gradients. Therefore very close aerodynamic calibration measurements are required.

With reason, Taylor reminds that reference velocity measurements should be carried out with the greatest care (17).

Location of total pressure ports in the collector or settling chamber shall be clearly specified, as well as location of static pressure (reference) ports on the walls of the working section or plenum chamber. Furthermore air temperature shall be noted and relative humidity taken into account.

Of course, the static pressure (reference) ports referred to as "upstream infinity pressure" should not be affected by model induced interference, such as, for example, gradients produced by solid or wake blockage.

These instructions particularly apply to tests conducted on half - models facing a reflection plate. This can either be a panel placed in a circular section or one of the walls of a rectangular section. Wall effect corrections are known and validity of correction applicability need no longer be demonstrated, especially at low speed (42). Nevertheless such arrangements have their own characteristics which become more and more complex as the Mach number increases.

More particularly the reflection plate shall necessarily be solid.

Finally it should be recalled that use of variable stagnation pressures involves knowledge of the effects of these pressure variations upon boundary layers and consequently, upon the gradients.

### 11.2 - Solid blockage gradient due to viscous effect

In the A.R.A. wind tunnel with  $\beta K = 2$ , as stated in paragraph 6.3.1.1, a drag correction resulting from the solid blockage gradient due to viscous effect was first theoretically calculated (21).

But owing to the graded development of geometric permeability of test section walls and arrangement of the model in relation to the walls, it was noted that the gradient acted only upon the downstream half of the fuselage following pressure measurements taken on the model nose, center, and base.

Experimental correction is equal to half the theoretically calculated correction (Fig. 12 a).

This is a typical example of the precautionary steps to be taken for measurements and interpretation of corrections connected with graded permeabilities and relative position of the model along the X-axis.

### 11.3 - Wake blockage gradient

Again attention of the reader should be drawn to the extremely low development (refer to paragraph 8.3) of the factor  $\Omega_2$  against X to upstream infinity, for permeabilities of very small perforated walls. This development requires a double correction depending on static (reference) pressure port location (Fig. 12 b).

### 11.4 - Influence of struts and stings

Struts placed under a model require blockage corrections regarding the model. In certain cases struts can produce a curvature of the air stream which appears as a complementary induced angle.

Oppositely, a sting, due to its solid blockage, produces a gradient affecting the model. Corrections shall be applied accordingly (17).

## 12 - CONCLUDING REMARKS - SUGGESTIONS

### 12.1 - Concluding remarks

It should be granted that general theories regarding wall corrections are known and widely spread at the present time, thus becoming conventional.

However, and contrarily to general opinion, comprehensive theoretical knowledge has not yet been gained and gaps still exist. Considerable research work should be initiated or carried on, especially on ventilated walls.

Practical use of these corrections is still in the experimental stage. These corrections are not routinely used and a universal language common to all wind tunnel operators is not yet available.

However a commendable effort was made to this effect by the major European or American research laboratories, as stated in the previous chapters.

### 12.2 - Correction calculations are based upon two assumptions, as follows :

- Linearized potential theories,
- Boundary conditions applicable to infinite length walls.

The former assumption puts forward the problem of applicability domain for utilization of theories and requires additional theoretical approaches for model size and, consequently, for assessment of lift coefficients and limit Mach numbers.

Test programs of models at various scales will substantiate the limits so assessed.

The latter assumption puts forward the problem - except for solid walls - of finite length ventilated wall influence upon corrections.

The solution partly applied to the 2 dim case is only outlined for the 3 dim case.

Therefore it appears preferable to conduct tests in solid wall sections at as high a Mach number as practicable. Then from a given limit Mach number it appears desirable to make use of ventilated walls.

12.3 - For ventilated sections, it is taken for granted that porosity parameter R and associated criterion  $\beta/R$  are the basic aerodynamic grounds. This criterion is necessarily used for porous or perforated walls and shall also be applied to longitudinally - slotted walls.

However it would be encouraging to know the conditions from which the parameter R becomes of importance, in other words the slot length and depth from which viscosity is effective.

Therefore, although there is no basic difference between a semi-closed wall section and a slotted ventilated wall section, influence of parameter R is negligible in the former instance and may be very important in the latter instance.

In fact, it is essential to make use of ventilated walls as defined by their specific geometric permeability which satisfies the theoretical criteria for porous walls.

12.4 - It appears that it is not possible to assess porosity parameter  $R$  using analytical methods ; therefore this parameter will be assessed experimentally.

No universal method has been suggested to date. Each laboratory conducts its own approach depending on its specific needs and facilities.

It would be desirable to produce a type of catalog summarizing the geometric data of the walls, the suggested principles for measuring the parameter  $R$  and the obtained values of porosity parameter.

Allowance shall be made for influence stagnation pressure variations and of boundary layers upon value of parameter  $R$ . It appears that this influence is great in the transonic domain. As a matter of fact, a thick boundary layer developing on solid walls can contribute to reduce blockage interaction and even retard the Mach number at which sonic blockage occurs (43). The boundary layer can also increase the effective porosity  $R$  of ventilated walls (10). This is perceptible in  $M_0$  between 0.9 and 1.4 as shown in Fig. 13 (44).

12.5 - Knowledge of parameter  $R$  is often critical for graded permeability walls, produced to obtain an undisturbed air stream.

Besides, the theory emphasizes importance of parameter  $R$  development against  $\beta$  and  $X$ .

For such arrangements, knowledge of parameter  $R$  becomes difficult.

Theoretical analyses should endeavor to highlight magnitude of errors which can be made when a constant value of  $R$  is adopted for a wide range of Mach numbers, whereas parameter  $R$  should be adapted to each value of Mach number  $M$ .

12.6 - Adaptation of parameter  $R$  along the fore - and - aft direction of the test section still is a problem to be solved. Theoretical analyses show that it is essential to solve this problem if wall effects in the region of the model wing and horizontal stabilizer need be suppressed.

It is necessary to have a good knowledge of the corrections before suppressing or applying them. This remark leads to point out that no mention is made - or only a broad statement if any - in most of the relevant analyses, of pitching moment corrections applicable to a complete airplane model, i.e. a model comprising a horizontal stabilizer.

The major problem consists in calculating the factor  $\delta_1$ , known in  $X = 0$ , against  $X$  and for several values of the parameter  $R$ . Then the pitching moments will be accurately corrected.

It would be desirable, in the immediate future at least, to find experimental procedures for correcting pitching moments  $C_m$ . A number of tests should also be conducted to show the possibility of cancelling corrections in the region of the tail unit, while maintaining, if applicable, blockage and lift corrections in the region of the wing.

Theoretical analysis of development of factors  $C_{m0}$  and  $\alpha_0$  with Mach number, permeability or any other parameter shall also be considered. Experimentally this problem is far from being solved.

12.7 - Emphasis was placed on investigation for a wall geometry suited to cancel pitching moment corrections.

However it should be recalled that the various correction factors become zero for values of parameter  $\beta/R$  specific to these correction factors.

Therefore, considering both the magnitude of corrections in relation to one another and analysis and research work envisaged, it appears of prime importance to assess the parameters considered as prevailing ones and which need be cancelled. Choice of these parameters depends on operators of future wind tunnels and can lead to ventilated walls of varied geometries.

12.8 - In connection with the previous problems, it may also be good to know what are the advantages or disadvantages when using test sections with two or four ventilated walls, bearing in mind that permeability above and below the model is generally more efficient than permeabilities on walls arranged normal to the model wing span.

Pindzola and Lo (2), then Lo and Oliver (3) approached this problem by calculation of the reciprocal effects of permeability on vertical and horizontal walls of rectangular sections against the section width  $B$  to height  $H$  ratio.

For example, the theory shows that the factor  $\delta_o$  is not affected by permeability of vertical walls when the height - to - width ratio is equal to or less than 0.8. Moreover it appears that practice is less stringent than theory, as seen in paragraph 6.3.1.2.

Besides, Keller's and Wright's calculations suggest that vertical ventilated walls provide more steady spanwise upwash velocities than horizontal ventilated walls (20).

12.9 - In 12.5, mention was made of the necessity for an undisturbed air stream free from velocity gradient within the test section, which, sometimes, results in a thin boundary layer thus maintaining linearized porous operation of ventilated walls. (44)

To that effect, an auxiliary suction from the plenum chamber could be used.

This brief report purposely ends with this technical aspect which was virtually not dealt with.

Theoretical analyses from Woods (32) or Gøthert (5), for example, emphasize the influence of this suction upon correction factors or wall boundary layers. But no experimental results providing positive conclusions have been published of late years.

12.10 - Likewise, if we do not consider the corrections in connection with the use of special gases whose compressibility laws do not necessarily agree with Prandtl's, Glauert's, Gøthert's rules, it may be asked how the correction terms are affected by stagnation pressure change.

12.11 - Finally it should be recalled that the purely transonic domain has not yet been rigorously dealt with, whereas the supersonic domain has already been investigated, although partly. (9, 13, 5, 4).

$M = 1$  still remains the major unknown quantity.

As a matter of fact, linearized hypotheses introduced by Gøthert to lay down his rule (showing compressibility effect in correction terms) suggest that it is impossible to use the corrections in the forms proposed for Mach numbers close to 1.

However for test Mach numbers greater than 0.8 - 0.85, it may be necessary to use, in the proposed correction terms, the compressibility factor  $\beta_c$ , which is a function of the corrected Mach number  $M_c$ , provided that the value of  $\Delta M$  is lower by 3% or 4% than Mach number  $M_o$  (26).

Furthermore it should be noted (refer to paragraphs 10.1 and 10.3) that the theory, supported by experience, shows that, under supersonic conditions, the permeability should decrease with Mach number, whereas under subsonic conditions, the permeability should decrease when Mach number increases. In other words, the permeabilities meet each other in the region of Mach 1.

12.12 - Together with these problems of prime importance, there are secondary problems for which it is almost embarrassing to quote an example, considering their relative slight importance.

Are formulas used for calculations of airfoil cross-sectional areas  $A_m$ , model volumes  $V_m$ , and blockage accurate enough, in so far as fine correction terms, such as  $K_C$  or  $T$  are introduced? Eventually would it not be better to produce a universal formula instead of the proposed choice of formulas and try to standardize the relationships?

Obviously much work still remains to be done, as can be seen from the A.E.D.C. draft analyses, in broad domains and in detail as well. One example of these numerous outstanding tasks could consist in finding out a more precise definition of the influence of wingspan upon factors  $\delta_o$  and  $\delta_r$  in ventilated walls, as already attempted by Holder (45) who used conventional hypotheses, or Wright and Keller (20) through more realistic hypotheses.

Note : Influence of aeroelasticity of the model and supporting means, wind tunnel turbulence and noise are covered in other papers.

## 13 - REFERENCES

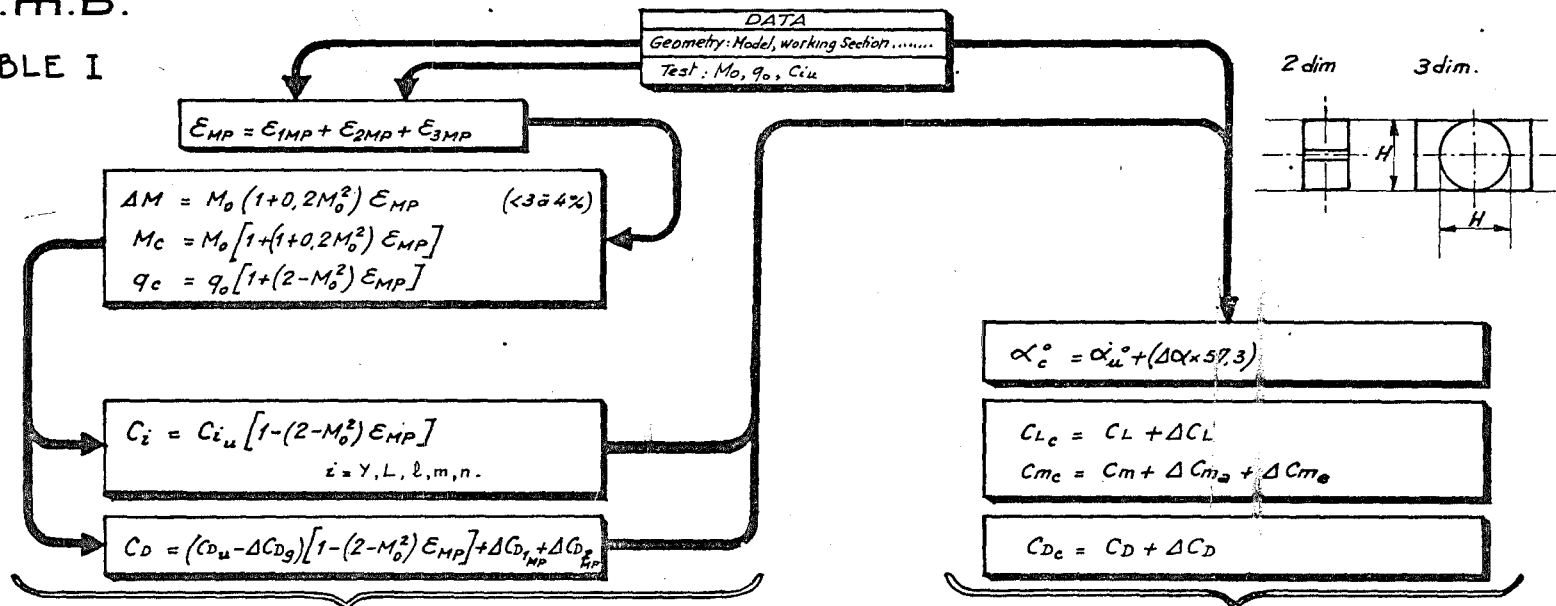
- 1 - H.C. Garner  
E.W.E. Rogers  
W.E.A. Acum  
E.C. Maskell  
Subsonic wind tunnel wall corrections.  
AGARD ograph - 109 - 1966.
- 2 - M. Pindzola  
C.F. Lo  
Boundary interference at subsonic speeds in wind tunnel with ventilated walls.  
A.E.D.C - T.R 69-47-1969.
- 3 - C.F. Lo  
R.H. Oliver  
Boundary interference in a rectangular wind tunnel with perforated walls.  
A.E.D.C - TR 70 - 67 - 1970.
- 4 - M. Pindzola  
Transonic wind - tunnels - Short course : Lecture series 42 -  
Transonic Aerodynamic Testing.  
Von Karman Institute for Fluid Dynamics, Brussels 1972.
- 5 - B. Göthert  
Transonic wind-tunnel testing - AGARD ograph 49 - 1961.
- 6 - A. Toussaint  
Experimental methods - Wind - Tunnels - Influence of the dimensions of the  
air stream. Aerodynamic Theory - Ed. W.F. Durand, Vol III, Div. I,  
Chapter III - J. Springer - Berlin 1935 - pp. 294 - 299.
- 7 - C. Wieselsberger  
Über den einfluss der windkanalbegrenzung auf den widerstand insbesondere  
im bereiche der kompressiblen strömung. Luftfahrtforschung - Vol 19 - 1942 -  
p. 124 -  
Traduction française G.R.A. n° 403 - Paris 1943.
- 8 - R.H. Wright  
V.G. Ward  
N.A.C.A. Transonic wind tunnel sections.  
N.A.C.A. Report 1231 - 1955.  
N.A.C.A. R.M. L 8 J 06 - 1948.
- 9 - T.R. Goodman  
The porous wall wind tunnel - Part III - The reflection and absorption of  
shock waves at supersonic speeds. Cornell Aeronautical Laboratory -  
Report n° AD 706 A1-- 1950.
- 10 - R.H. Wright  
The effectiveness of the transonic wind tunnel as a device for minimizing  
tunnel boundary interference for model tests at transonic speeds.  
AGARD Report 294 - 1959.
- 11 - R. Monti  
Wall corrections for airplanes with lift in transonic wind tunnel tests.  
Report of the AGARD Ad Hoc Committee on engine - airplane interference  
and wall corrections in transonic wind tunnel tests. AGARD - AR 36 - 71.
- 12 - D.D. Davis Jr.  
D. Moore  
Analytical study of blockage and lift interference corrections for slotted  
tunnels obtained by the substitution of an equivalent homogeneous boundary  
for discret slots. NACARM L 53 E 07 b - 1953.
- 13 - P.F. Maeder  
A.D. Wood  
Transonic wind tunnel test sections.  
ZAMP - Vol VII Fasc. 3 - 1956. pp. 177 - 212.
- 14 - B.S. Baldwin  
J.B. Turner  
E.D. Knechtel  
Wall interference in wind tunnels with slotted and porous boundaries at  
subsonic speeds.  
NACA TN 3176 - 1954.
- 15 - T.R. Goodman  
The porous wall wind tunnel - Part II - Interference effect on a cylindrical  
body in a two dimensional tunnel at subsonic speed - Cornell Aeronautical  
Laboratory - Rep. n° AD 594-A-3 - 1950.
- 16 - J.C. Vayssaire  
Corrections de blocage dans les essais en soufflerie - Effets des décollements.  
Fluid Dynamics of Aircraft stalling. Lisbon - A.G.A.R.D. C.P 102 - 1972.

- 17 - C.R. Taylor Tunnel wall interference at transonic and high - subsonic speeds - Procedures used to correct measurements in tunnels at R.A.E. Unpublished 1972.
- 18 - P.A. Mackrodt Windkanalkorrekturen bei messungen an zweidimensionalen profilen im transsonischen windkanal der Aerodynamischen Versuchsanstalt Göttingen. Z. Flugwiss - 19 (1971) pp. 449 - 454.
- 19 - W. Lorenz-Meyer Kanalkorrekturen für den transsonischen windkanal der Aerodynamischen Versuchsanstalt Göttingen bei messungen an dreidimensionalen modellen. Z. Flugwiss 19 - 1971 - pp. 454 - 461.
- 20 - J.D. Keller  
R.H. Wright A numerical method of calculating the boundary induced interference in slotted or perforated wind - tunnels of rectangular cross section - NASA TR R 379 - 1971.
- 21 - E.C. Carter Some measurements of porous tunnel wall interference in the A.R.A. 8 ft x 9 ft tunnel - Aircraft Research Association Report n° 19 - 1971.
- 22 - I.A.T.  
St.Cyr Etude en écoulement transsonique - Rapport 347/Sigma 4 - Institut Aérotechnique de Saint-Cyr 1972.
- 23 - M.E.E. Enthoven 2 dimensional wall - interference investigations at NLR. National Aerospace Laboratory. Internal note AC 71-029-1971.
- 24 - C.F. Lo Wind tunnel wall interference reduction by streamwise porosity distribution. A.I.A.A. Journal - Vol 10 n° 4 - April 1972 - p. 547.
- 25 - W.L. Chew Experimental and theoretical studies on three dimensional wave reflection in Transonic test sections - Part III : Characteristics of perforated test section walls with differential resistance to cross-flow. A.E.D.C. - TN 55 - 44 - 1956.
- 26 - J.Y.G. Evans Corrections to velocity for wall constraint in any 10 x 7 rectangular subsonic wind tunnel - A.R.C. R and M 2662 - 1949.
- 27 - J.R. Ongarato Subsonic wind-tunnel wall interference studies conducted in the NAR trisonic wind-tunnel. A.I.A.A. Paper 68-360. Journal of Aircraft - Mars - Avril 1969 pp. 144 - 149.
- 28 - J.P. Chevalier Preliminary results on wall interference - Analysis in the two - Dimensional transonic wind - tunnel R1 (ONERA - Chalais Meudon). - French Communication - Attachement I Florence 1970.
- 29 - M. Bazin  
R. Bernard-Quelle  
J. Ponteziere Critique des techniques d'essais de profils transsoniques - ONERA - 7e colloque d'aérodynamique appliquée - Modane - 1970.
- 30 - B. Göthert Wind tunnel corrections at high subsonic speeds particulary for an enclosed circular tunnel (Translation of D.V.L. F.B 1216 - 1940). N.A.C.A. T.M 1300 - 1952. Traduction Française - Ministère de l'armement - S.D.I 3803 - Paris 1946.
- 31 - M.C.P. Firmin  
T.A. Cook Detailed exploration of the compressible viscous flow over two - dimensional aerofoils at high Reynolds number - I.C.A.S. - Paper n° 68 - 09.
- 32 - L.C. Woods i) - On the theory of two dimensional wind tunnels with porous walls - Proc. Roy. Soc - Series A - Vol 233 - 1955 pp. 74 - 90.  
ii) - On the lifting aerofoil in a wind tunnel with porous walls - Proc. Roy. Soc. Series A - Vol 242 1957 pp. 341 - 354.
- 33 - G.V. Parkinson  
A.K. Lim On the use of slotted walls in two - dimensional testing of low - speed air-foils - I.C.A.S. - Paper n° 70 - 08.

- 34 - J.P. Veuillot Contribution à l'étude des corrections de blocage : influence de la longueur des parois perforées - Service Technique Aéronautique - Section "Etudes Générales" - Memo 72/1 - Paris - 1972.
- 35 - M. Bazin ONERA - Soufflerie S3 Modane - Essais en bidimensionnel - Résultats provisoires - 1971.
- 36 - M. Mokry A wake - blocage paradox in a perforated wall wind - tunnel - A.I.A.A. Journal - Vol 9 - n° 12 - 1971 - pp. 2462 - 2464.
- 37 - D.D. Baals  
G.M. Stokes A facility concept for high Reynolds number testing at transonic speeds - Facilities and techniques for Aerodynamic testing at transonic speeds and high Reynolds number - Göttingen - AGARD C.P. 83 - 1971.
- 38 - M. Mokry Higher - order theory of two - dimensional subsonic wall interference in a perforated wall wind tunnel. National Research Council of Canada - Aeronautical Report - LR - 553 - 1971.
- 39 - S.B. Berndt Theoretical aspects of the calibration of transonic test sections. The Aeronautical Research Institute of Sweden - FFA Report 74 - 1957.
- 40 - Ph. Poisson-Quinton Transcript of tape of round - table discussion - Facilities and techniques for aerodynamic testing at transonic speeds and high Reynolds number. Göttingen - AGARD C.P. 83 - 1971.
- 41 - H. Ludwieg Drag corrections in high - speed wind tunnels - (Translation of Deutsche Luftfahrtforschung F.B. 1955 - 1944). N.A.C.A. T.M. 1163 - 1947.
- 42 - J.C. Vayssaire Nouvelle méthode de calcul de corrections des résultats d'essais en soufflerie basse vitesse. L'Aéronautique et l'Astronautique n° 15 et 16 - Paris 1969.
- 43 - S.B. Berndt On the influence of wall boundary layers in closed transonic test section. The Aeronautical Research Institute of Sweden FFA Report 71 - 1954.
- 44 - J. Lukasiewicz Effects of boundary layer and geometry characteristics of perforated walls for transonic wind tunnels - Aerospace Eng. Vol 20 n° 4 - 1961.
- 45 - D.R. Holder Upwash interference on wings of finite span in a rectangular wind tunnel with closed side walls and porous slotted floor and roof. A.R.C. R and M 3395 - 1965.

A.M.D.

TABLE I



BLOCKAGE INTERFERENCE

Blockage interference corrections $E_{MP}$			
		2 Dim.	3 Dim.
S O L I D	$E_{1MP} = \Omega_1 E_{1M}$ ↓ $\Omega_1 \beta^{-3} E_1$	$E_1 = \frac{\pi \cdot A_m}{6 \cdot H^2}$	$\frac{k \cdot V_m}{C^{3/2}}$
	$E_{2MP} = \Omega_2 E_{2M}$ ↓ $\Omega_2 \frac{1 + 0.4 M_o^2}{\beta^2} E_2$	$E_2 = \frac{1}{4} \cdot \frac{E}{H} \cdot C_{D_u}$	$\frac{1}{4} \cdot \frac{S}{C} \cdot C_{D_u}$
W A K E	$E_{3MP} = E_{3M}$ ↓ $\beta^{-3} E_3$	$E_3$	$\frac{E_d}{2} \cdot \frac{S}{C} \cdot C_{D_d}$

Buoyancy corrections		
	2 Dim.	3 Dim.
$\Delta C_{D_g}$	$\frac{A_m \cdot dp}{C q_o \cdot dx}$	$\frac{V_m \cdot dp}{S q_o \cdot dx}$
$\Delta C_{D_{1MP}}$	$-\frac{2 A_m}{C} \cdot \frac{E_1}{\beta H} \cdot \Omega_1'$	$-\frac{2 V_m}{S} \cdot \frac{E_1}{\beta H} \cdot \Omega_1'$
$\Delta C_{D_{2MP}}$	$-\Omega_1 \frac{1 + 0.4 M_o^2}{\beta^3} \cdot E_1 \cdot C_{D_u}$	

LIFT INTERFERENCE

Lift interference corrections		
	2 Dim.	3 Dim.
$\Delta \alpha$	$\delta_o \frac{c}{H} \cdot C_L + \delta_1 \frac{c^2}{4 \beta H^2} \cdot C_L$	$\delta_o \frac{S}{S_o} \cdot C_L + \delta_1 \frac{E_s}{2 \beta H S_o} \cdot S \cdot C_L$
$\Delta C_D$	$\delta_o \frac{c}{H} \cdot C_L^2$	$\delta_o \frac{S}{S_o} \cdot C_L^2$
$-\Delta C_L$	$\frac{\pi}{2} \left( \frac{c}{\beta H} \right)^2 \delta_1 \cdot C_L$	0
$\Delta C_{m_a}$	$\frac{\pi}{8} \left( \frac{c}{\beta H} \right)^2 \delta_1 \cdot C_L$	$\frac{1}{4} \left[ \frac{\delta_1 E_s}{\beta H S_o} \cdot S \cdot C_L \right] \left( \frac{dC_L}{d\alpha} \right)$
$\Delta C_{m_e}$	0	$\left[ \frac{\delta_1 E_s}{S \cdot C_u} \right] \left[ \frac{E_s}{\beta H} \delta_1 \frac{S}{S_o} \cdot C_L \right] \times \frac{q_e}{q_c} \left( \frac{dC_L}{d\alpha} \right)$



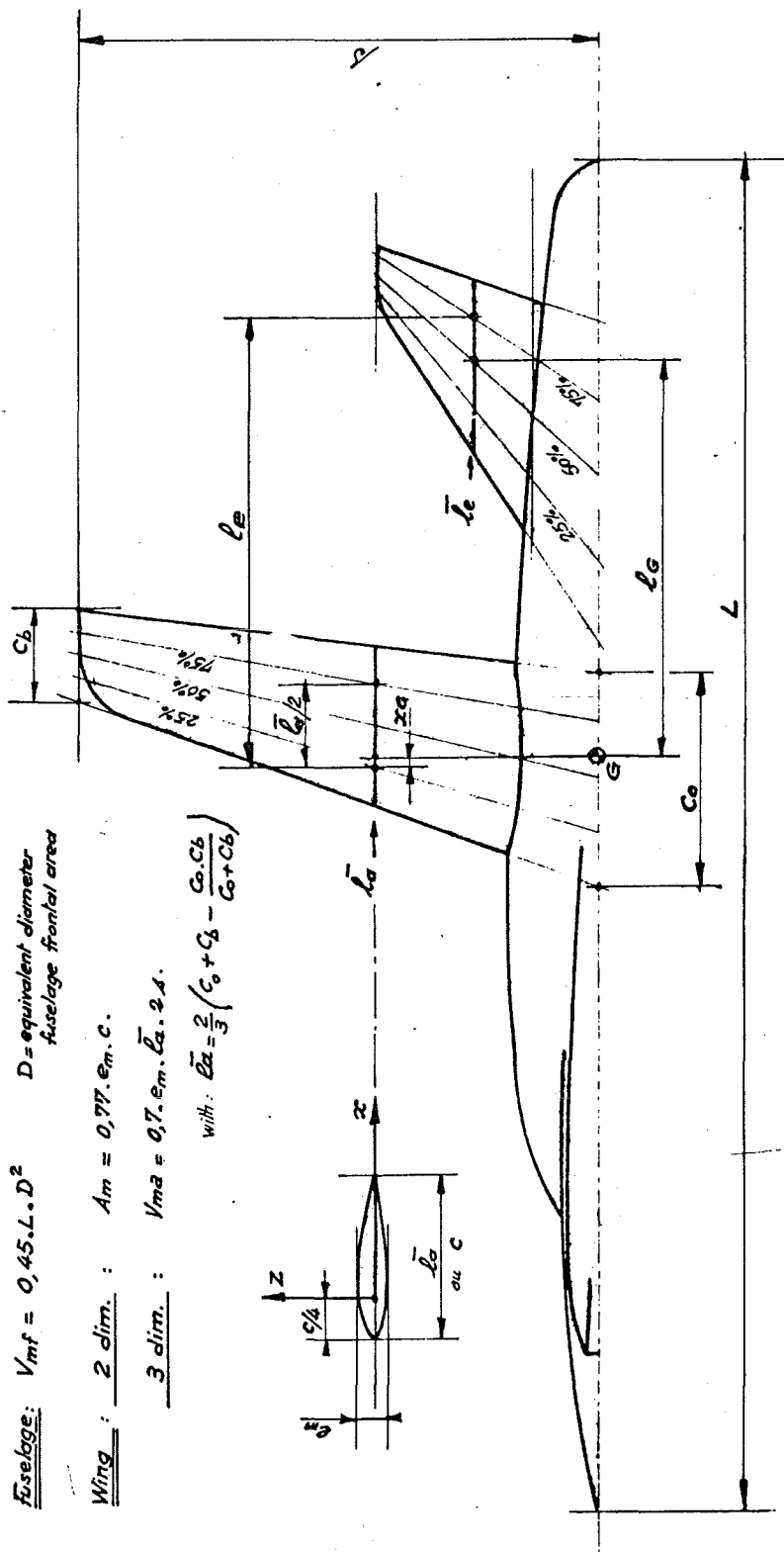
TABLE II . SYMBOLS

Fuselage:  $V_{mf} = 0,45 \cdot L \cdot D^2$   $D = \text{equivalent diameter}$   
 $\text{fuselage frontal area}$

Wing:  $2 \text{ dim.} : A_m = 0,77 \cdot \sigma_m \cdot C$

$3 \text{ dim.} : V_{ma} = 0,7 \cdot \sigma_m \cdot \bar{L}_a \cdot 2 \cdot A$

with:  $\bar{L}_a = \frac{2}{3} (C_0 + C_b - \frac{C_0 \cdot C_b}{C_0 + C_b})$



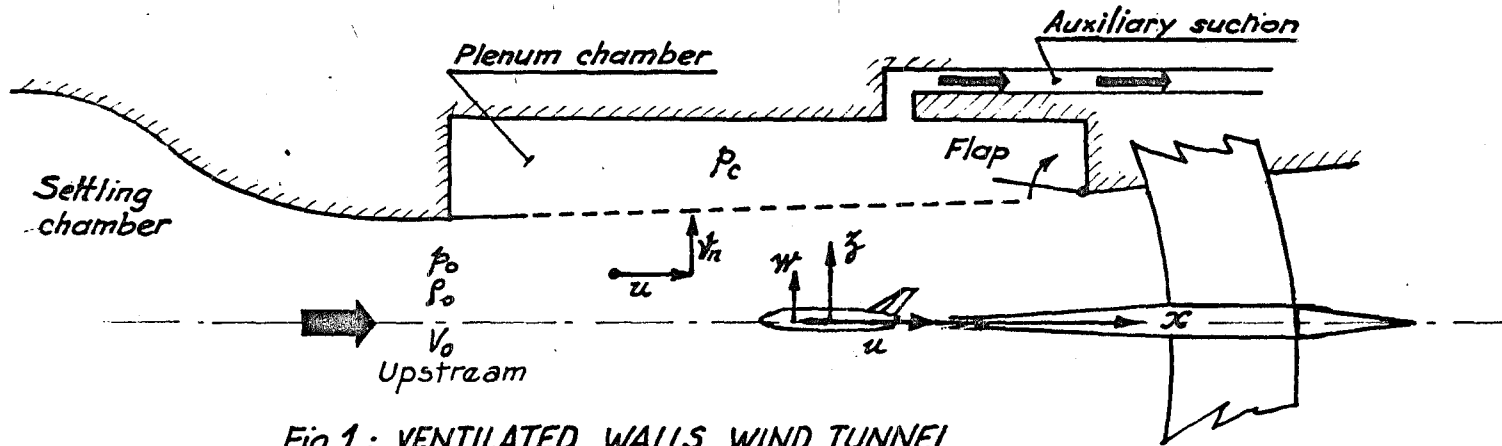


Fig 1: VENTILATED WALLS WIND TUNNEL  
SCHEMATIC

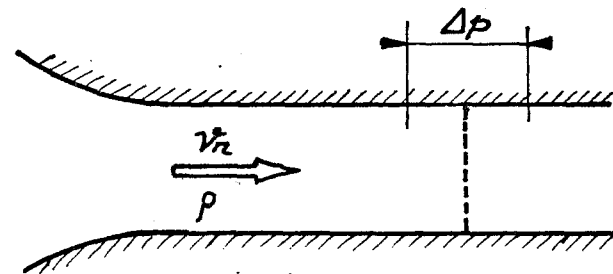
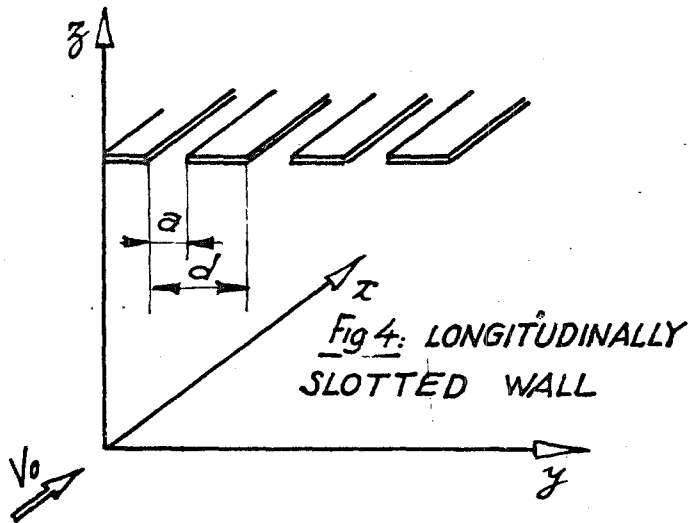
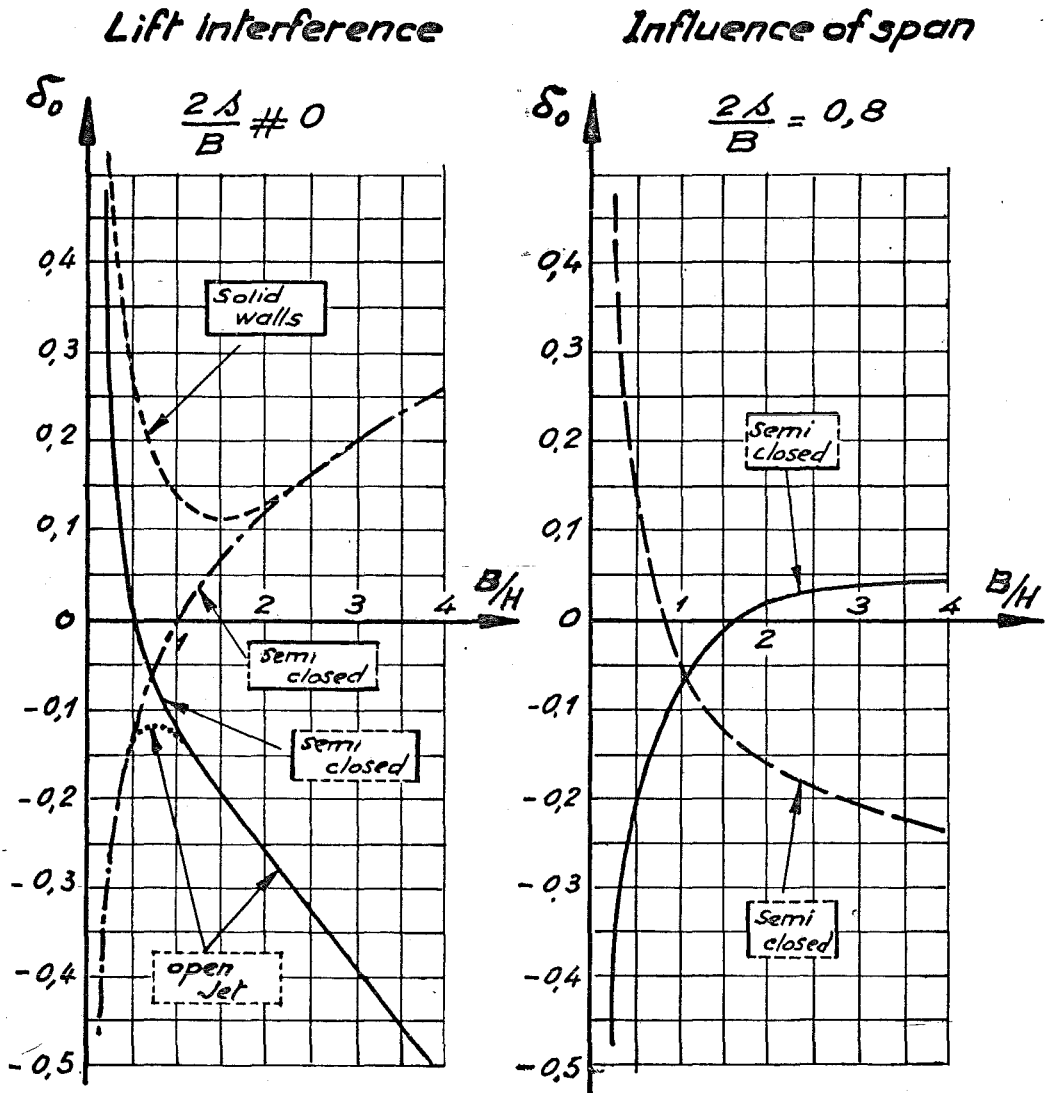


Fig 5: PERFORATED WALL POROSITY CALIBRATION

Fig. 2. RECTANGULAR WORKING SECTION



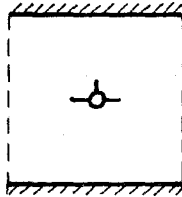
Method of vortex images by TOUSSAINT

# Fig. 3. RECTANGULAR WORKING SECTION

Semi closed walls

$$2s/B \neq 0$$

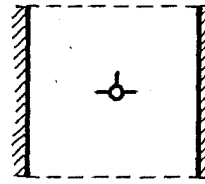
$$B/H = 1$$



Lift interference

$$\delta_0 = 0$$

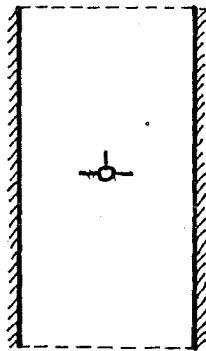
$$B/H = 1$$



Lift interference

$$\delta_0 = -0,125$$

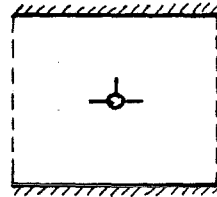
$$B/H = 0,5$$



Lift interference

$$\delta_0 = 0$$

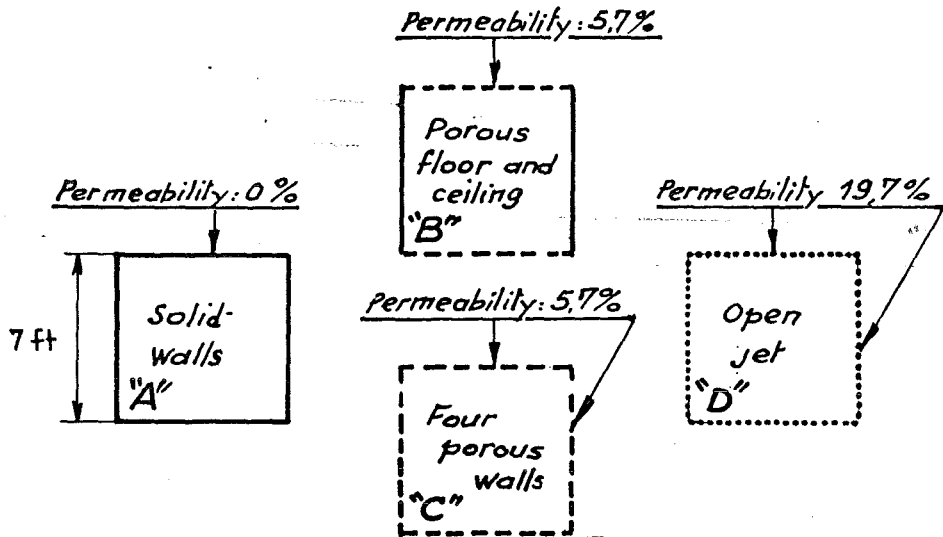
$$B/H = 1,17$$



Solid blockage = 0

(Wieselsberger)

**Fig. 6 . NORTH AMERICAN ROCKWELL CORPORATION  
WALL INTERFERENCE STUDIES**



Model N°	1	2	3	4
$\frac{2\Delta}{B}$	0,71	0,68	0,33	0,81
$\frac{S}{B^2} = \frac{S}{C}$	$\frac{1}{17}$	$\frac{1}{17}$	$\frac{1}{18}$	$\frac{1}{14}$
Blockage% $\alpha=0^\circ$ : $\frac{\Sigma}{C}$	1	0,8	0,5	1,5
Mach number	0,5 - 0,775	0,3 - 0,85	0,7   0,96	0,6   0,8
Facilities	"A" "B" "D"	"A" "B" "D" "D" "B" "C"	"A" "B" "D"	"D" "B" "D" "C"
$C_L$ max	$\geq 0,7$	$\geq 0,64$	$\geq 0,6$	$< 0,2$

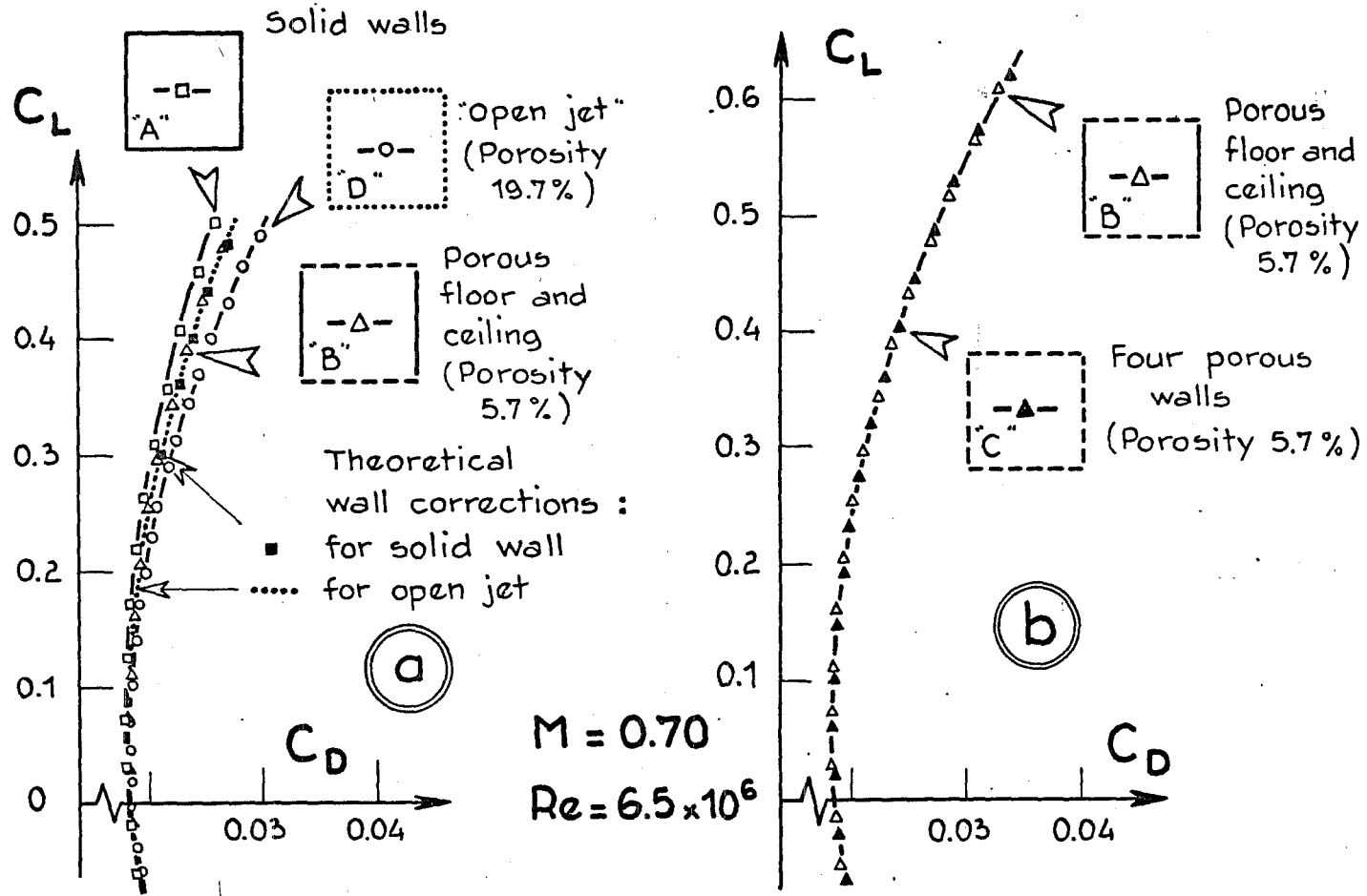


Fig. 7 - NORTH-AMERICAN 3 DIM. TESTS (7'x7' trisonic w-t) on model 2 : blockage 0.8% ;  $s/c = 1/17$  ;  $2\Delta/B = 0.68$  .

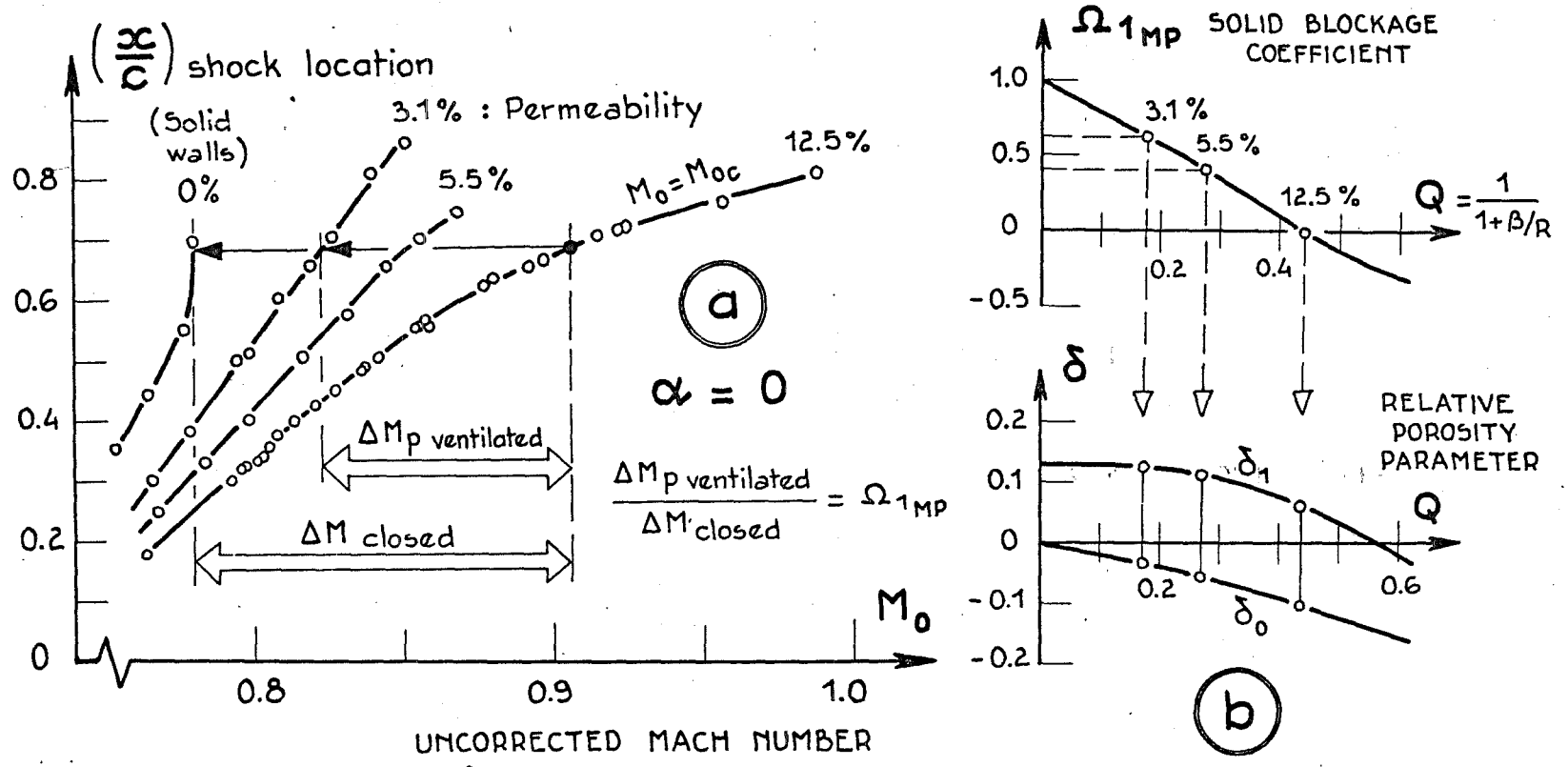


Fig. 8. ONERA TESTS IN R<sub>1</sub> Chalais W-T. NACA 0012 SECTION

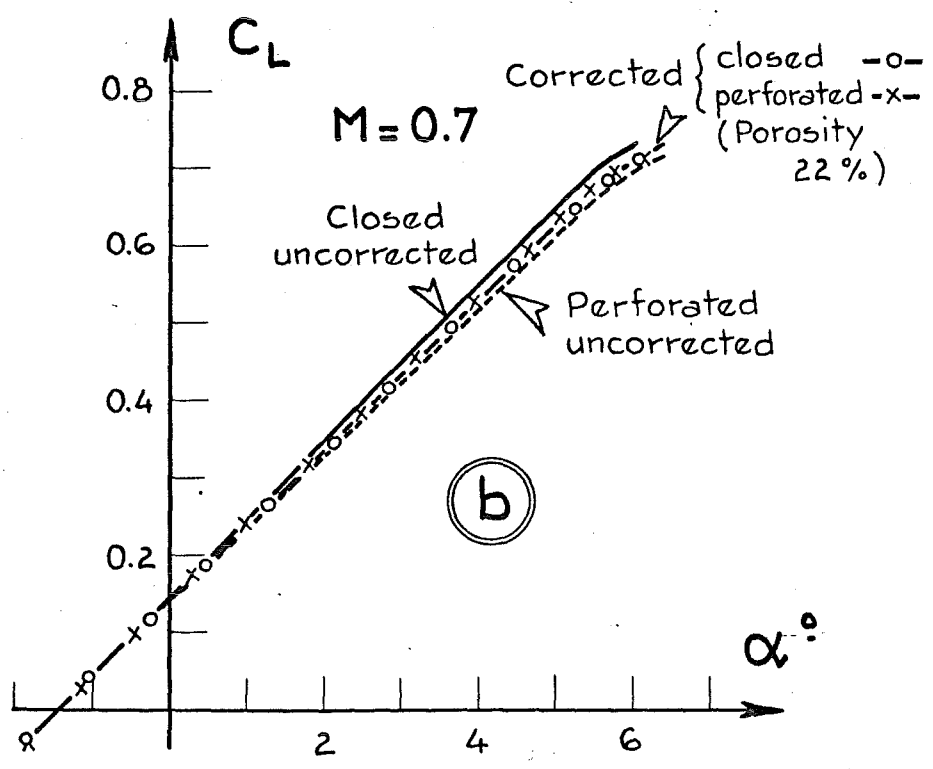
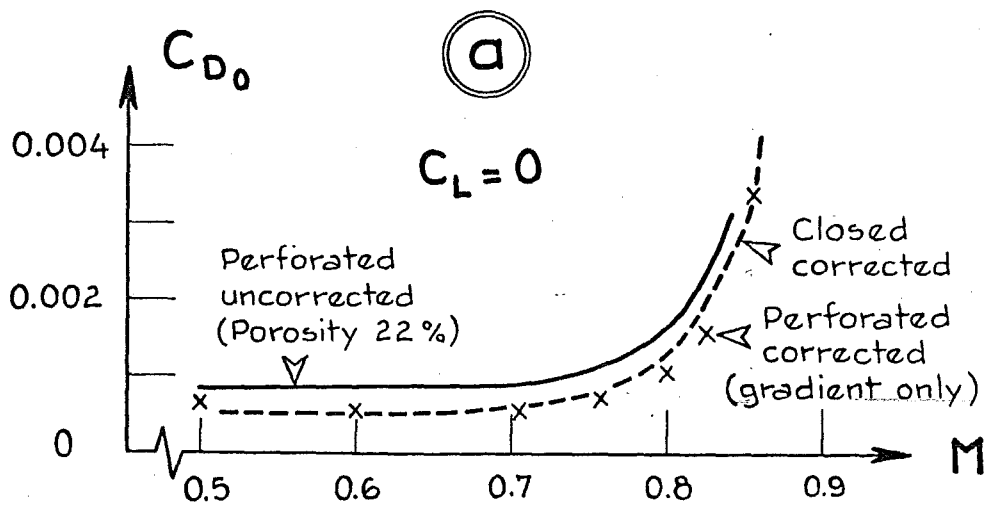


Fig. 9 . A.R.A. 3 DIM. TESTS (8'x9' w.t)  
 model 1 : blockage 0.74% .  $2\Delta/B = 0.57$



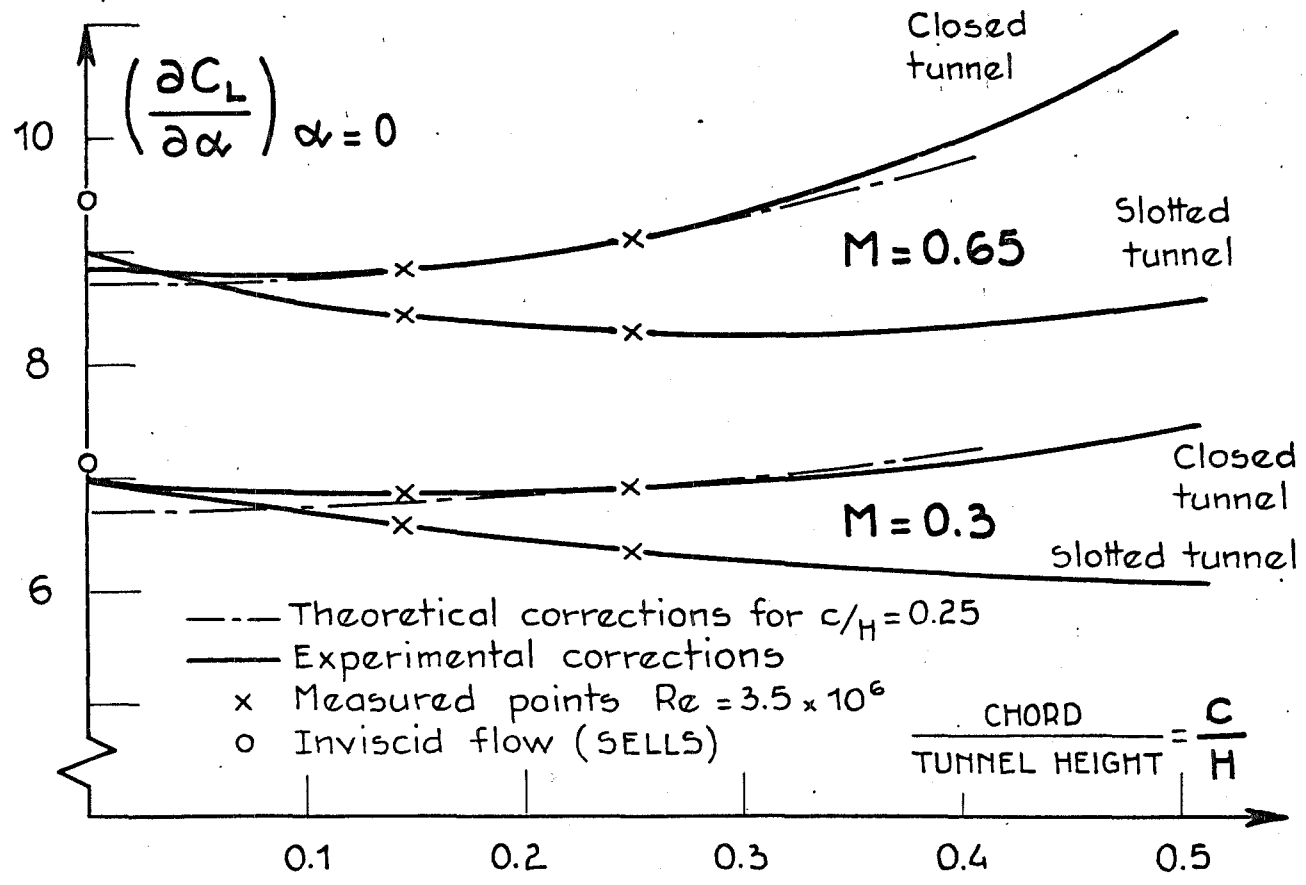


Fig.10. R.A.E. 2 DIM. TESTS ( 8'x6' Farnborough W.T )  
Deduced variation of lift curve slope with  
tunnel size for RAE 101 section ( $e_m/c = 10\%$ )

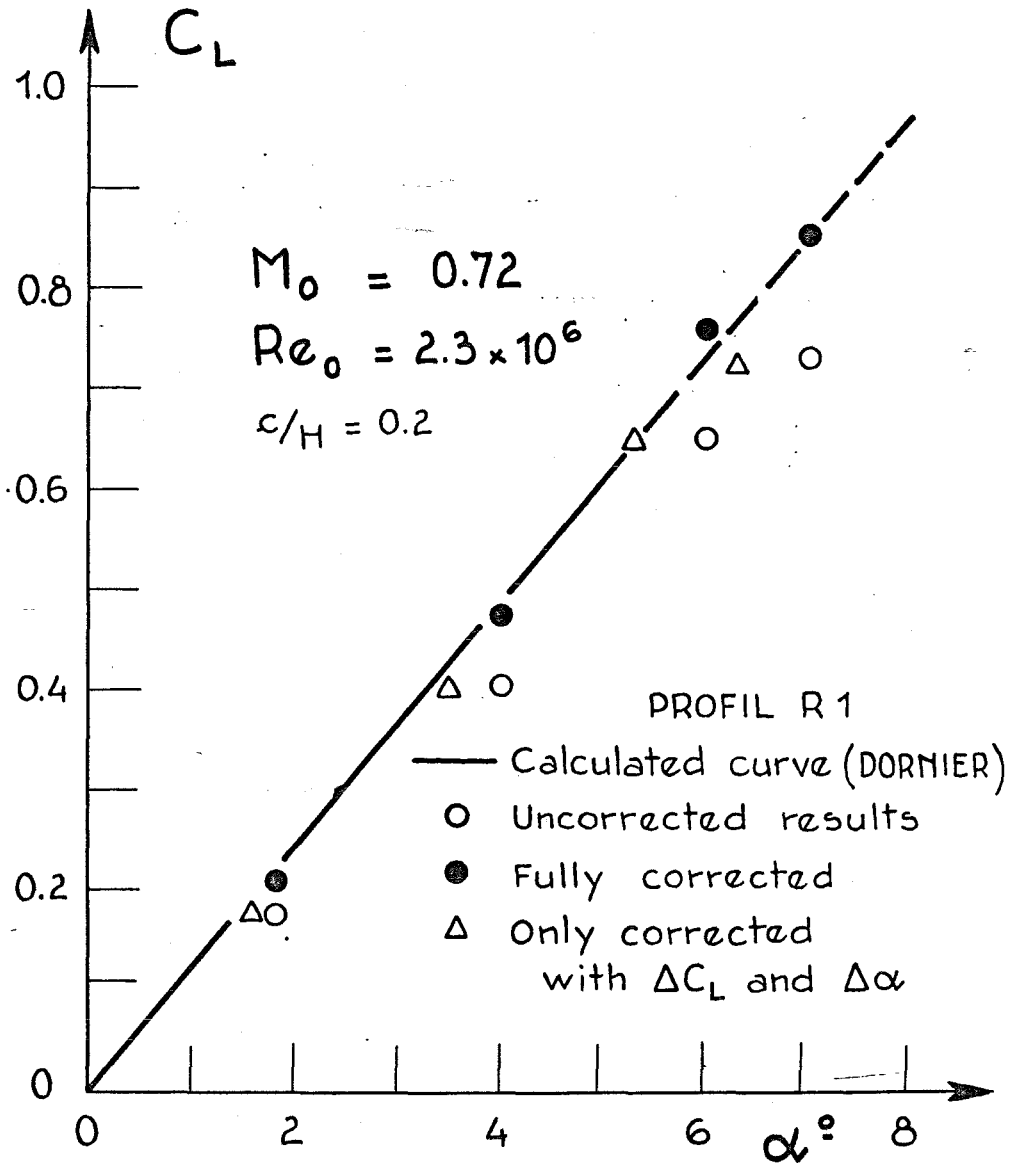
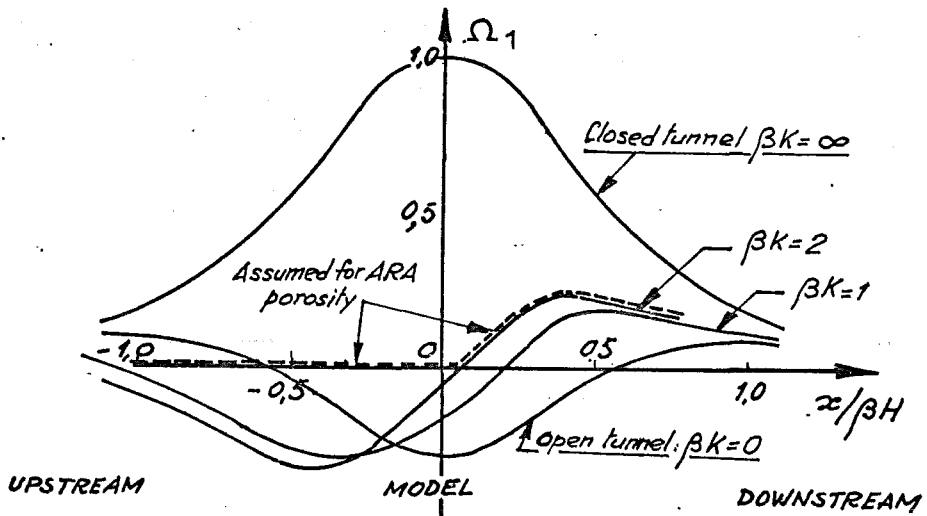


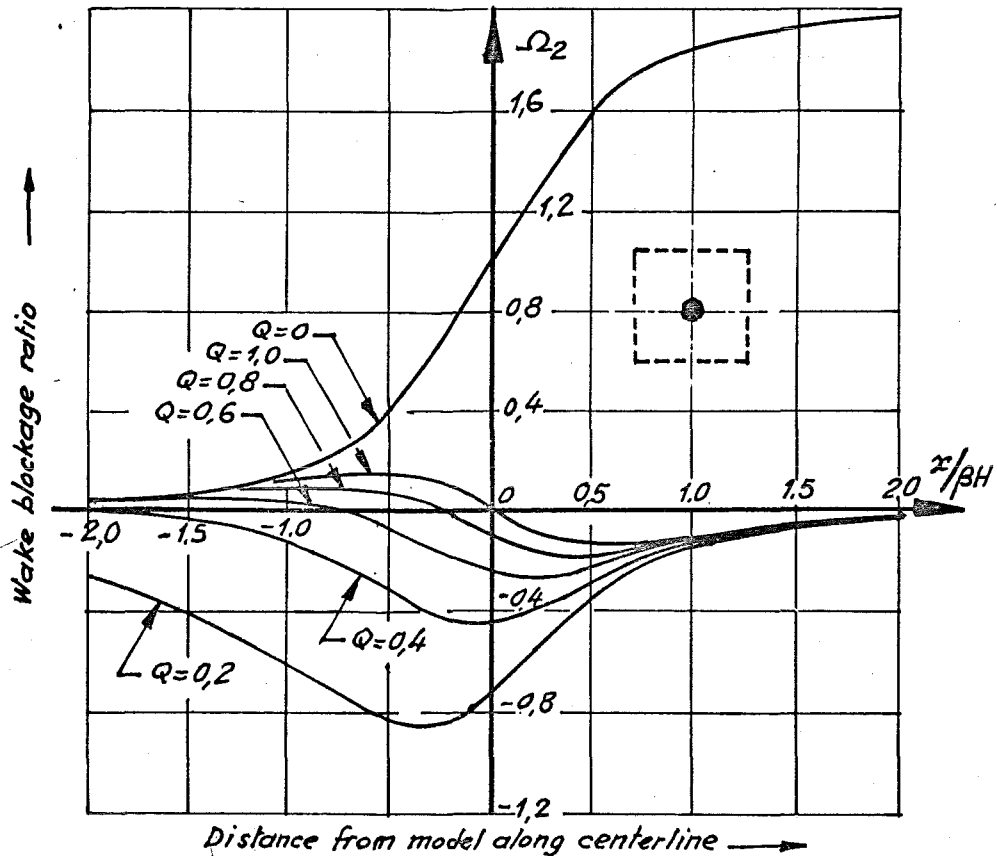
Fig. 11 - A.V.A. Göttingen 2 DIM. TESTS (1x1m W.T)

Fig. 12

SQUARE TUNNEL WITH FOUR PERFORATED WALLS



12 a : DIAGRAMMATIC DISTRIBUTION OF SOLID BLOCKAGE



12 b : DIAGRAMMATIC DISTRIBUTION OF WAKE BLOCKAGE

$\delta^+$  : boundary-layer displacement thickness.

$\Phi$  : diameter of holes in perforated plates

$$\Phi = 1/8 \text{ in.}$$

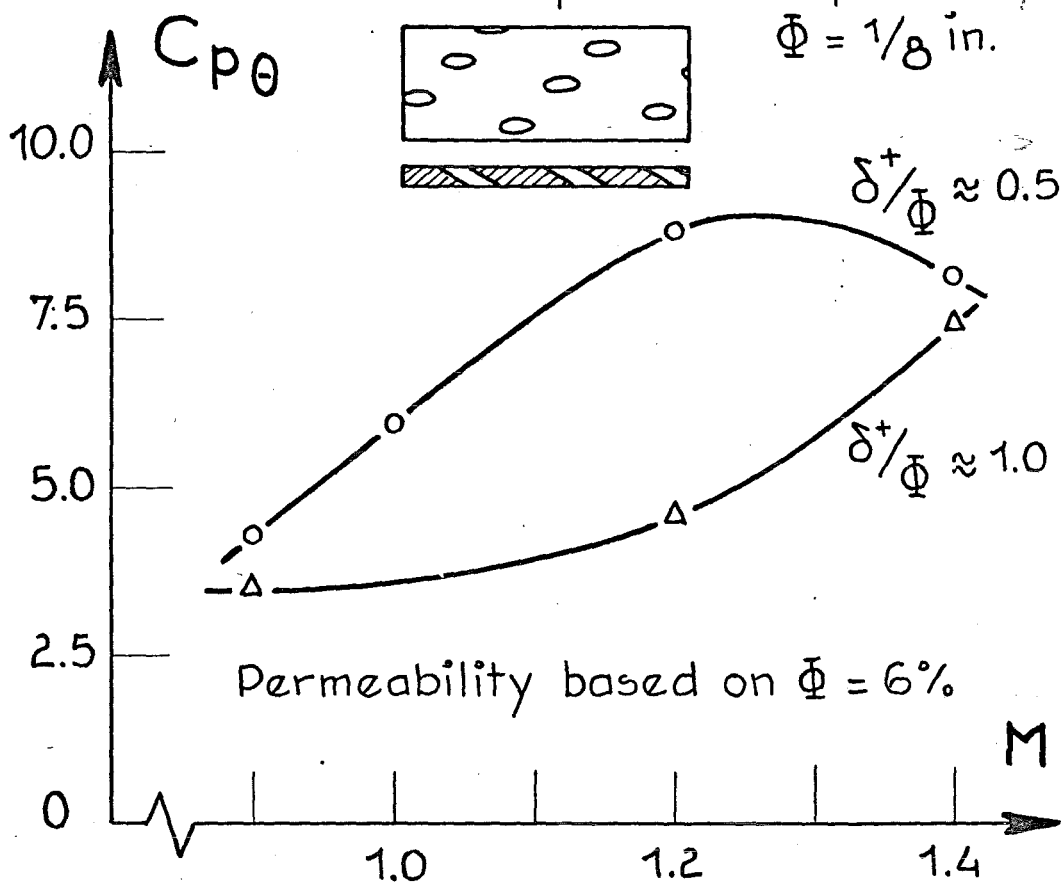


Fig. 13. EFFECT OF MACH NUMBER ON CROSS-FLOW CHARACTERISTICS AND EFFECT OF BOUNDARY-LAYER THICKNESS.

APPENDIX  
THEORETICAL APPROACH

UNCONSTRAINED FLOW

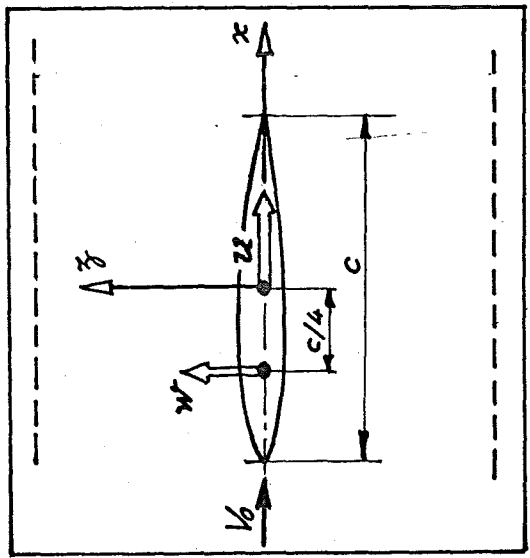
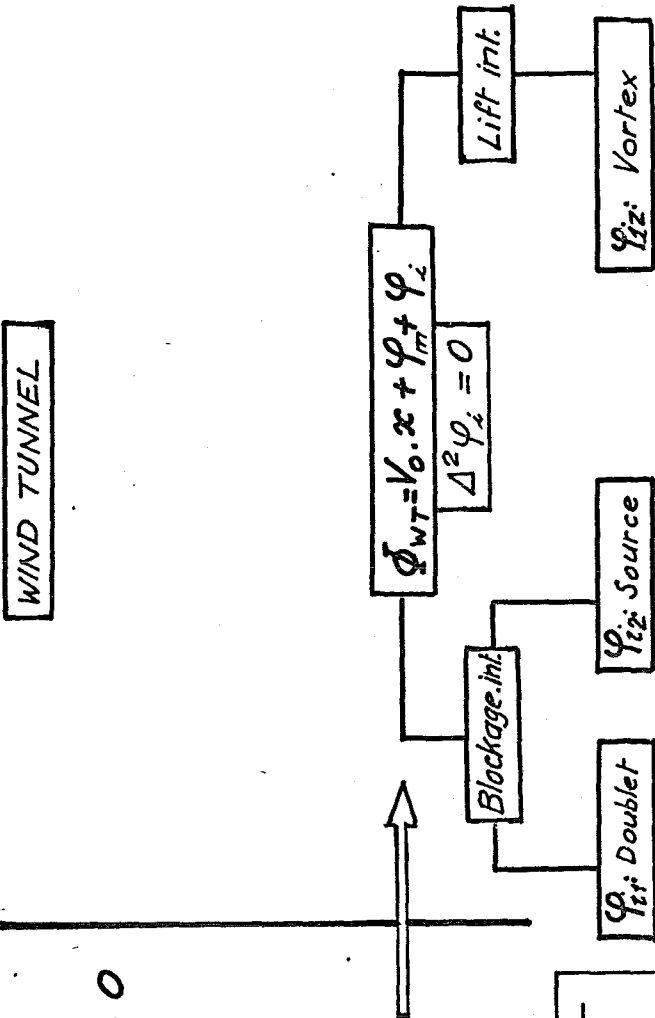
$$\beta^2 \frac{\partial^2 \phi_{\infty}}{\partial x^2} + \frac{\partial^2 \phi_{\infty}}{\partial y^2} + \frac{\partial^2 \phi_{\infty}}{\partial z^2} = 0$$

$$x_0 = x_M, y_0 = \beta y_M, z_0 = \beta z_M$$

$$\beta = \sqrt{1-M^2}$$

$$\Delta^2 \phi_{\infty} = 0$$

$$\phi_{\infty} = V_0 x + \phi_m$$



$$u_{1,2} = \frac{\partial \phi_{1,2}}{\partial x} \quad (x=z=0)$$

$$\epsilon_{1,2} = \frac{u_{1,2}}{V_0}$$

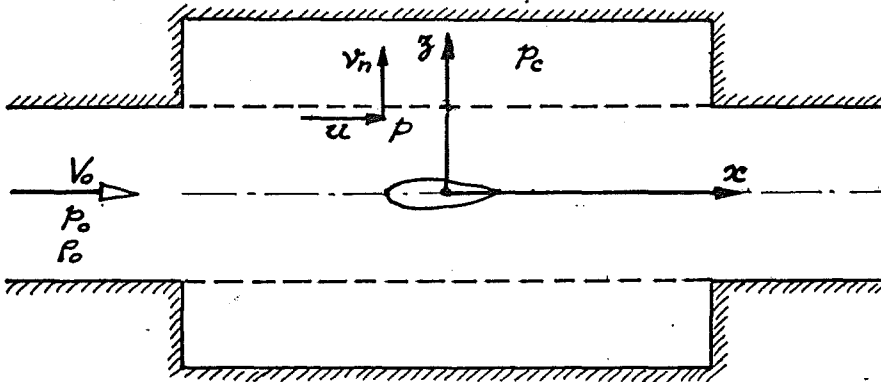
$$\frac{\partial \epsilon_{1,2}}{\partial x} = \text{Gradient due to blockage}$$

$$w = \frac{\partial \phi_{1,2}}{\partial z}$$

$$\Delta z = \frac{w}{V_0}$$

$$\frac{1}{V_0} \frac{\partial w}{\partial x} = \text{Streamline curvature}$$

## BOUNDARY CONDITIONS



$$\boxed{u}$$

Flow with model  
in W.T

$$\Delta p = p - p_0 = \rho_0 V_0 u$$

$$\downarrow$$

$$\left(\frac{\Delta p}{q}\right)_{W.T} = 2 \frac{u}{V_0}$$

$$\boxed{v_n}$$

Flow through ventilated  
walls

$$\Delta p = p - p_c = f(v_n)$$

$$f(v_n) = f\left(\begin{array}{l} \text{geometric permeability} \\ \text{viscosity} \end{array}\right)$$

$$\downarrow$$

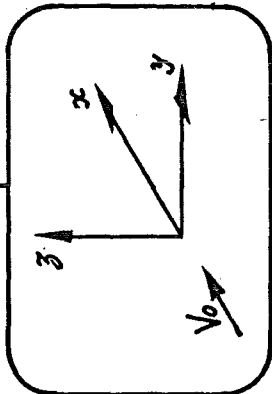
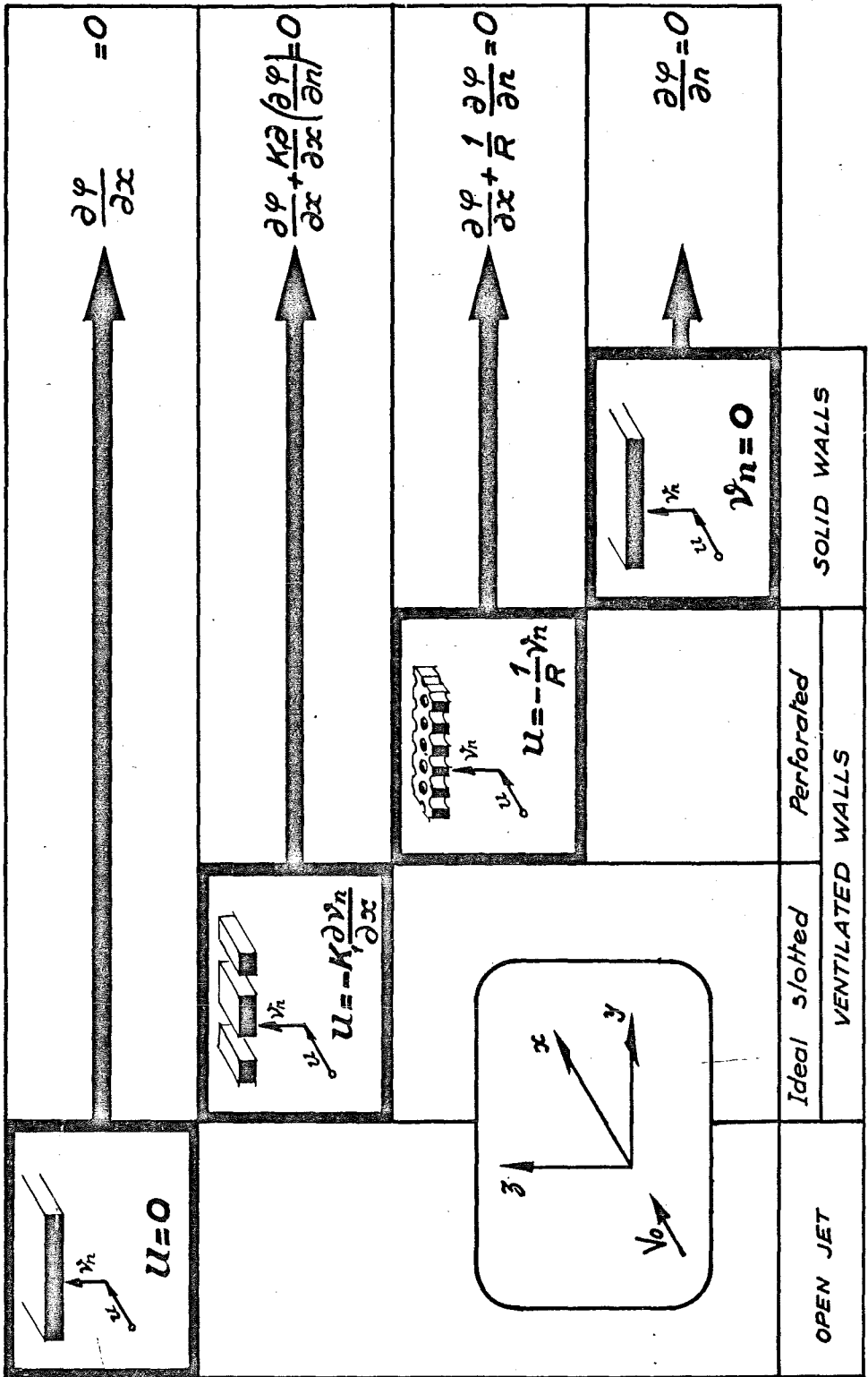
$$\left(\frac{\Delta p}{q}\right)_{\text{walls}} = \frac{2}{V_0} K_1 \frac{\partial v_n}{\partial x} + \frac{2}{R} \frac{v_n}{V_0}$$

$$\text{si } p_c = p_0$$

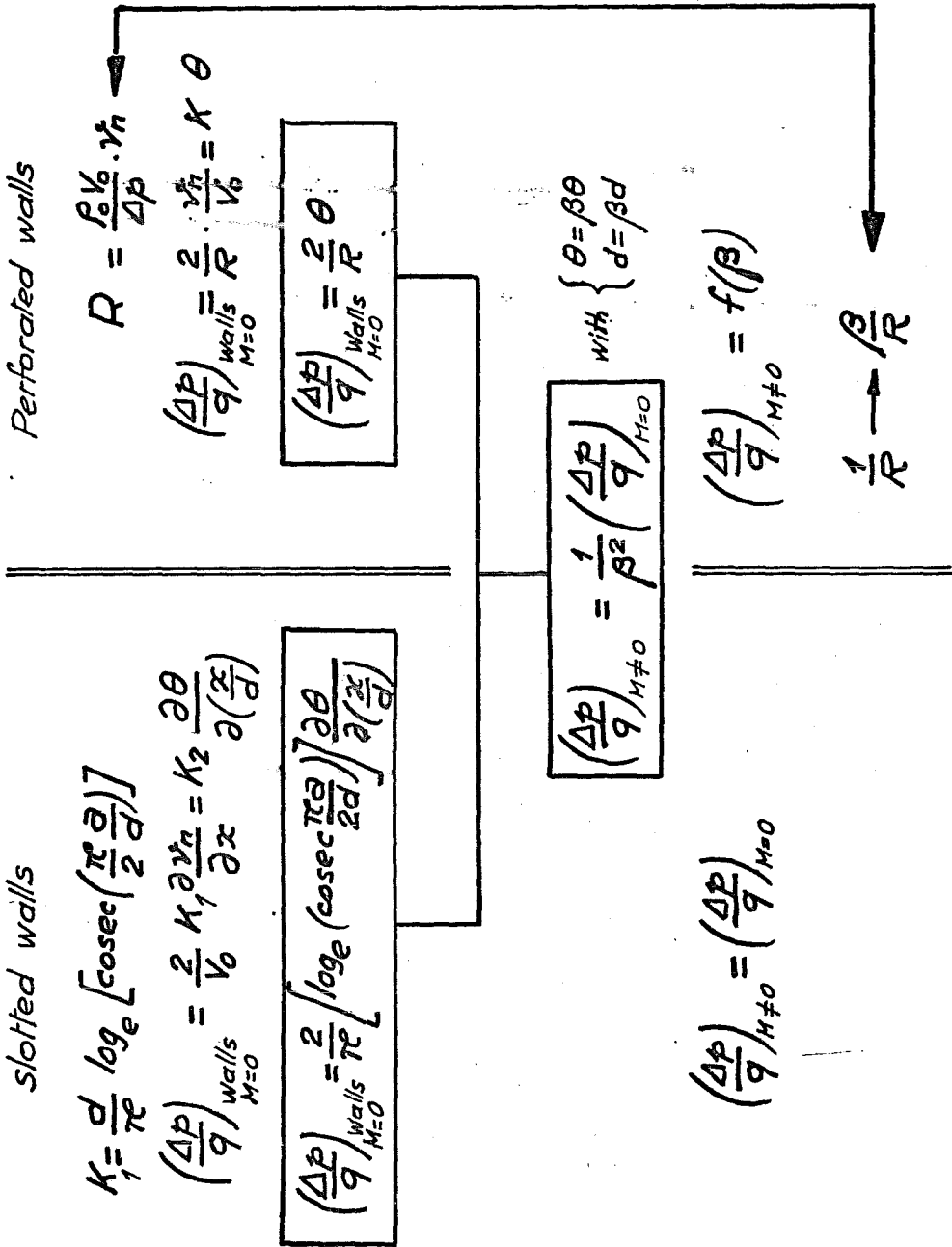
$$\boxed{\left(\frac{\Delta p}{q}\right)_{W.T} + \left(\frac{\Delta p}{q}\right)_{\text{wall}} = 0}$$

$$\frac{\partial \psi}{\partial x} + \kappa \frac{\partial}{\partial x} \left( \frac{\partial \psi}{\partial n} \right) + \frac{1}{R} \frac{\partial \psi}{\partial n} = 0$$

A.M.D.



COMPRESSIBILITY





**THEORETICAL APPROACH**

\_\_\_\_ **HYPOTHESIS SUMMARY** \_\_\_\_

<i>Flow</i>		<i>Linearized potential flow</i> <i>Linearized compressibility rule</i>
<i>Boundary conditions</i>	<i>Walls of infinite length</i>	
	<i>Solid walls</i> <i>Open jet</i> <i>Semi-closed walls</i> <i>Ventilated walls</i> <i>Slotted</i>  <i>Perforated</i>	<i>Exact</i>  <i>Linearized approximate</i> <i>Linearized "semi" approximate</i>  <i>Homogeneous linearized porous walls</i>  <i>Geometry : <math>K_1</math> coefficient</i> <i>Porosity : <math>\beta/R</math> coefficient</i> <i>Porosity : <math>\beta/R</math> coefficient</i>
<i>Upstream conditions</i>	$x = -\infty$	<i>Flow : undisturbed</i>
<i>Downstream conditions</i>	<i>Large positive values of <math>x</math></i>	<i>Flow : independent of <math>x</math></i>

COMMENTS ON WALL CONSTRAINT PROBLEMS  
IN TRANSONIC WIND TUNNELS

1 - THEORETICAL AND PRACTICAL CONSIDERATIONS

1.1 - A gap often lies between theoretical and practical considerations and a balance is required.

With the present stage of knowledge, theoretical approaches for calculating wall constraints, i.e. :

i - blockage and lift interferences in subsonic WT testing,

ii - shock waves reflection in low supersonic WT testing,

use linearized (subsonic or supersonic) compressible flows. These theories do not exactly represent actual flow conditions.

1.2 - First, for subsonic flow, it is necessary to make a choice of mathematical models - such as doublets, sources, vortices in allowing for lifting line or lifting surface theories - in order to establish velocity field induced by aircraft and its wake in free-air.

To allow for walls, consideration shall be given to boundary conditions.

Mathematical treatment uses either image methods or wall perturbation methods as recalled by Carbonaro's paper (1).

Mathematical treatment can be developed in compressible flow or incompressible flow and, then, compressibility effect is introduced in agreement with Göttert's linearized compressibility rule.

Regarding ventilated walls, linearized porous conditions of the equivalent wall, involving mixed potential and viscous flows, are used instead of actually slotted or perforated walls.

1.3 - Boundary conditions always assume working sections boundaries of infinite length and free from disturbance. These hypotheses are exact for solid walls, but approximate for open jets. They are also approximate for ventilated walls which consist of both solid and open walls.

2 - IMMEDIATE REQUIREMENTS

2.1 - In spite of the above-mentioned simplifying hypotheses, essential theoretical corrections for ventilated W.T are known since one two years. They are not yet in operational use and seem limited in Mach number values. These corrections are in experimental use only and for Mach numbers generally less than 0.9.

Regarding the porosity parameter  $R$ , no analytical solution is available to calculate its value related to wall geometry. Only experimental methods for investigating  $R$  are used. Few values are known.

Therefore, it appears more and more necessary to test models and to apply wall interference corrections to prove their validity.

2.2 - Some corrections cannot be achieved, viz pitching moment correction, since  $\delta_1$  streamline curvature factor is not known. This must be calculated at any point in the working section, especially in the region of the tail unit.

2.3 - Finally, effects on off-centre models will be discussed.

3 - ACTUAL FLOW CONDITIONS

3.1 - Theoretical approaches are linearized. Therefore, model size (or scale) shall be considered to define lift coefficient  $C_L$  (or angle of attack  $\alpha$ ) and test Mach number limits beyond which these corrections cannot be applied successfully.

This theoretical work shall be associated with proposals from ONERA for testing various scale calibration models in European and American facilities (2).

3.2 - Walls shall not be considered as having an infinite length as proved with open jets (3, 4, 5).

Test section wall of finite length shall be taken into consideration between collector (or nozzle) and diffuser.

Model position relative to streamwise direction shall also be investigated.

Vortex lattice methods will be useful (6, 7). These methods consider test section of finite length and can be used to satisfy a large range of problems, for example, considering span effect (large - span sweep-back wing), and placing the model anywhere in the test section.

Method of calculating spanwise distribution of interference factor is then possible. Also a method will perhaps be found thus enabling a choice to be made between two or four ventilated walls for a fixed value of B/H in a rectangular test section.

#### 4 - POROSITY

4.1 - With present knowledge, ventilated walls shall be designed to obey Darcy's law (linearized flow across porous wall).

Porosity parameter is determined experimentally. Porosity calibration methods shall be summarized in data sheets against actually porous wall geometric specifications, and corresponding R values. The aim is then to lay down operating selected porosity parameter schedules for true ventilated WT and to substantiate their value relative to several different models.

An appropriate choice of walls will then be possible.

4.2 - Effects of boundary layer in subsonic and supersonic flows on R values shall be well understood. Therefore it is necessary to take into account Lukasiwicz's paper (8)

The subsonic or supersonic wall boundary layer has an effect on the hole characteristics. Parameter R, function of  $C_{pg}$  slope, is dependent on the ratio of boundary layer to hole diameter. The cross flow can also become non linear with a thick boundary layer.

4.3 - Calculated results and experimental data have shown that porosity for zero interference or for no shock waves reflection depends on Mach number, so as

$$\frac{\sqrt{1 - M^2}}{R} = \text{constant} \quad (\text{subsonic flow})$$

$$R = \sqrt{M^2 - 1} \quad (\text{supersonic flow})$$

An ideal wall porosity schedule as a function of Mach number can be achieved. But a WT is to be used for testing of aircraft models over a wide range of Mach numbers. Therefore it is of interest to study the effects of R deviations from design conditions, as already stated by the CAL concerning the low supersonic flow (9).

It is convenient to know if, for practical purposes, R can be taken as a constant upon a wide range of Mach numbers and to see whether the deviations introduced into the corrections have the same magnitude as test measurement accuracy, i.e. sensitivity to R.

#### 5 - TRANSONIC FLOW

5.1 - Consistent results have been obtained in relation to R, first in the incompressible and then compressible flow domain, until shocks have appeared.

The change in parameter porosity values at supercritical Mach numbers shall give rise to additional investigations which will also be subject to the outcome of a current research program as proposed by the NLR (10). Then, it appears that the theoretical approach relative to the problem can be derived from Berndt's work (11). By the way it should be recalled that the first broad survey of experimental results and theoretical work making use of non-linear transonic flow theory and transonic similarity rule was set up by the previously-named author concerning wall constraints in transonic wind tunnels. In this survey, boundary layer effect was not neglected (12).

5.2 - A transonic flow is a mixed flow, since it lies between subsonic and supersonic flows. In the transonic (and supersonic) regimes, the shock-wave/boundary layer interaction along the walls should be understood to make of the proper porosity.

Research fields on wings as suggested by Hartzuiker should be partly applied to ventilated walls (13).

5.3 - Furthermore, stagnation pressure variation effects upon wall boundary layer are still to be investigated. An auxiliary suction will perhaps be useful in order to produce thin boundary layers. How the parameter R reacts in these conditions is not clearly known, assuming that theoretical porous corrections still prove to be applicable. Finally, correction factors and gradients can be modified by auxiliary suction and research work is required for a good understanding (14).

5.4 - In any case, subsonic or supersonic porous flows use linearized approaches as Göthert's compressibility rule.

Corrections for a Mach number range around  $M = 1$  are no longer definite and available.

Some authors tried to overcome these difficulties, such as Oswatitsch, Guderley, Yoshihara, Tirumalesa, Berndt, Spreiter, Page, Drogge, ten or twenty years ago.

5.5 - Indeed, a trend towards a return to the non-linear transonic flow theory and development of unsteady approaches by using computers, can solve new methods for correcting tests results for walls constraints.

Murman's (15, 16) or Cole's (16) calculation methods, or other authors', already mentioned in 5.4 and summarized by Yoshihara (17) can look to the future for extension of planar theories (unsteady flows with viscous effects) to three dimensional flows taking into account a number of boundary conditions (18). So to compute such transonic problems, time dependent methods or small disturbance theory could be used.

## 6 - VARIABLE POROSITY

With present knowledge, use of porous wall theory is only possible for correcting ventilated wall tests results and we return to porosity parameter :

$$R(\sqrt{1-M^2}, \sqrt{M^2-1}, x)$$

Variable geometry wall is then introduced to produce an interference free subsonic or supersonic flow. This can only be used if corrections are already known and their validity proved.

It is not possible to eliminate all types of interference for a given value of porosity.

A given porosity can nullify only one interference (and perhaps minimize other ones interferences).

A wall porosity as a function of Mach number can be achieved.

Two zero interferences - by example, relative to lift and pitching moment - can be obtained with a streamwise distribution of porosity.

Therefore, an appropriate choice of ventilated walls shall be made, taking into account, first, the magnitude of the interferences and their magnitude to one another, then the interference which results in zero correction following the research work envisaged by the engineer or wind tunnel operator.

Of course, it will be necessary to investigate varied ventilated walls.

## 7 - REMARKS

Finally, a number of remarks shall be made about experimental methods used in wind tunnels.

It should be of interest to compare methods for measuring reference upstream velocity as well as upstream kinetic pressures, and so on.

Development of angle of attack  $\alpha_0$  and pitching moment coefficient  $C_{m0}$  for zero lift as a function of struts or stings and Mach number should be taken into consideration, even if theoretical work need be carried out, in agreement with streamline curvature.

## 8 - REFERENCES

- 1 - M. Carbonaro                      Review of some problems related to the design and operation of low speed wind tunnels for V/STOL testing. Von Karman Institute for Fluid Dynamics 1972.
- 2 - Ph. Poisson-Quinton            Facilities and Techniques for aerodynamic testing at transonic speeds and high Reynolds number. Göttingen - AGARD - C. P. 83 1971.
- 3 - A. Toussaint                      Experimental Methods - Wind tunnels. Influence of the dimensions of the Air Stream Aerodynamic Theory (ed. W.F. Durand) Vol III Div. 1 - Chap III - J. Springer - Berlin 1935.
- 4 - F.W. Riegels                      Wind Tunnel Corrections for incompressible flow - A.V.A. Monographs (ed. A. Betz) - Section D3 4.1 - Göttingen 1947.
- 5 - S. Katzoff  
C.S. Gardner  
L. Diesendruck  
B.J. Eisenstadt                      Linear Theory of Boundary Effects in open wind tunnels with finite jet lengths.  
N.A.C.A. Report 976 - 1950.
- 6 - R.G. Joppa                         A method of calculating wind tunnel interference factors for tunnel of arbitrary cross-section. N.A.S.A. C.R. 845 - 1967.
- 7 - J.D. Keller  
R.H. Wright                         A numerical method of calculating the boundary-induced interference in slotted or perforated wind tunnels of rectangular cross-section.  
N.A.S.A. T.R. R. 379 - 1971.
- 8 - J. Lukaszewicz                    Effects of boundary layer and geometry characteristics of perforated walls for transonic wind tunnels. Aerospace Eng. Vol 20 n° 4 1961.
- 9 - A.H. Flax  
I.G. Ross  
R.S. Kelso  
J.G. Wilder                         Development and operation of the C.A.L. perforated-throat transonic wind-tunnel. Transonic Testing Techniques Institute of Aeronautical Sciences S.M.F. Fund Paper n° FF 12 - Los Angeles 1954.

- 10 - M.E.E. Enthoven      2 Dimensional wall-interference investigations at N.L.R. National Aerospace Laboratory NLR. Internal note AC 71-029.
- 11 - S.B. Berndt            Theoretical aspects of calibration of transonic test sections. The Aeronautical Research Institute of Sweden - FFA Report 74 - 1957.
- 12 - S.B. Berndt            Theory of wall interference in transonic wind tunnels - Symposium Transsonicum. Springer - Verlag - Berlin 1964 - pp. 288 - 309.
- 13 - J.P. Hartzuiker        First list for possible future research work on transonic fluid motion problems. N.L.R. Internal Note AC 72-011.
- 14 - L.C. Woods            The theory of subsonic plane flow Cambridge University Press - 1961.
- 15 - E.M. Murman            Computational methods for inviscid transonic flows with embedded shock waves. Numerical Methods in Fluid Dynamics - Lecture series 34 - 1971. AGARD lecture series n° 48 - 1972. Von Karman Institute for Fluid Dynamics.
- 16 - E.M. Murman  
      J.D. Cole                Calculation of plane steady transonic flows - AIAA journal Vol 9 n° 1 Janvier 1971. AIAA Paper n° 70 - 188.
- 17 - H. Yoshihara         Some recent developments in Planar Inviscid Transonic Airfoil Theory. AGARD ograph n° 156 - 1972.
- 18 - G. Moretti  
      et al.                 Numerical Methods in Fluid Dynamics (Ed. J.J. Smolderen)  
AGARD lecture series n° 48 - 1972.

INTERFERENCE EFFECTS OF MODEL SUPPORT SYSTEMS

by

E.C.Carter

Aircraft Research Association Limited  
Manton Lane, Bedford, U.K.

SUMMARY

A brief discussion is given of the forms of interference occurring in subsonic and transonic wind tunnels due to the model support system. Two types of model attachment, rear sting and vertical blade sting are considered and the form and magnitude of interference terms is given for some particular examples. It is seen that apart from drag the major interference is on  $[C_m]_0$  tail on due to the upwash interference at the rear fuselage.

The buoyancy interference in the working section due to a typical sting joint and roll mechanism behind a model is considered and the effect on drag evaluated for two typical bodies. The effect of increase of stagnation pressure is shown to give a significant increase in buoyancy drag interference. The use of improved materials helps to reduce this term but currently known material limits do not contribute significantly.

The buoyancy interference in the working section due to a vertical or horizontal incidence support strut is also considered although in practice, the term should be measured in the working section calibration.

It is unlikely that any of these interferences can be eliminated and their effect will have to be allowed for in the planning of test schedules for future high Reynolds number tunnels.

1. INTRODUCTION

It is generally accepted that a rear model support system is the most suitable for complete model testing at high subsonic and transonic Mach numbers. A main support member situated in a vertical plane at the entrance to the diffuser provides ample stiffness and strength to carry the very large normal and pitch loads. Such support systems are readily adaptable to the housing of roll and incidence mechanisms and read-out equipment. These supports introduce local blockage which must be designed into the wall shaping but more important they introduce an upstream pressure field which at the best will have a buoyancy effect in the working section and at the worst could tip the balance of an incipient separation on a model. Simple estimates may be made of the upstream influence of a support body from potential flow assumptions where the body is replaced by a source system. The size of the support body directly affects the working section buoyancy and so the introduction of very high model loads associated with high Reynolds numbers with a consequent increase in size could lead to changes in the magnitude of the interference. Anything that tends to increase the size of the support system, particularly in the nature of a temporary attachment such as a pitch/yaw mechanism or blowing connection should be seriously considered in relation to the effects on the particular experiment.

Considering a single sting support system in the rear of the model, it is very unlikely that an undistorted rear fuselage can be represented. This is true of even current test situations at transonic speeds at atmospheric stagnation pressure. For stagnation pressures 5 - 10 atmospheres, gross distortions will be necessary. In these conditions the flow approaching the tailplane is aware of the sting and adjusts its angle and curvature accordingly, the curvature being dependent upon the sting inclination. Attempts to allow for these effects have been made with the twin sting or the blade support system. These methods themselves introduce additional interferences and greatly increase the testing time and cost.

The introduction of new materials might have a small influence on the severity of the support interference problem but a very significant increase in both ultimate strength and stiffness is necessary to retain the current level of interference in future high Reynolds number facilities.

2. TUNNEL SUPPORT INTERFERENCE

Reference 1 gives an expression for the forward influence of a sting taper located behind a model. This expression has been verified to a first order by measurements of both force and pressure in the A.R.A. tunnel. It has also been shown that the weak relationship with Mach number is true to a first order. In Fig.1 the layout of the rear sting support system for the A.R.A. tunnel has been taken as representative for 1 atmosphere total pressure operation. The simple assumption of scaling for constant stress shows that tunnel size has no effect on the  $C_p$  interference in the working section. For increased total pressure however, using the same assumption of constant stress, the centreline pressure interference increases significantly. At 10 atmospheres for example the base pressure interference is increased from  $\Delta C_p = 0.015$  to 0.07.

The use of improved materials will reduce this scaling by a significant amount - for example, a 115 Ton/in<sup>2</sup> maraging steel instead of the S99.85T/in<sup>2</sup> material reduces the  $\Delta C_p$  of 0.07 to 0.056.

It can be argued that a compensating increase of sting length behind the model will be used for higher Reynolds numbers but the rate of exchange is very small i.e. the distance of 15" used between start of taper and base of model has to be almost double to reduce the interference of the 10 $\alpha$  curve to that of 5 $\alpha$ , (n.b. the increase of bending moment with increase of sting length causes some of this loss of sting length benefit).

The major effect of this support interference is to cause a positive axial buoyancy force on the model. The magnitude depends upon the body area distribution, typical values being given in Fig.1. It will be noted that for the usual case of the measured base pressure being used to correct the base force to zero, the size of the buoyancy term is significantly reduced (given in the Table headed Forebody). Other effects, which may not be secondary in magnitude, could stem from the superimposed pressure and velocity gradient on the normally developing flow field.

Results of simple calculations of the forward interference due to a representative vertical strut are given in Fig.2. These results are presented to illustrate the possible magnitude of this term, the numbers have not been validated by experiment and it would appear from A.R.A. measurements that the buoyancy term on the model centreline is almost entirely due to the sting support and not the strut support. However the strut interference may become more significant in depth above and below the model. In practice of course the strut interference will normally be incorporated in the tunnel calibration. In the calculations, allowance has been made for a reduced interference due to the lower Mach number field in the region of the strut. It should be noted that the results of the strut interference and the support body interference have not been summed in the curves of Fig.2.

### 3. REAR STING INTERFERENCE

The previous section has dealt with the potential flow field associated with the solid blockage of the rear support bodies. In addition we have the effect of the sting on the base of the model and its constraining effect on the flow over the rear fuselage and tailplane. Evidence on the magnitude of this effect has been obtained from tests with a twin sting support which permitted wing mounting on slender stings and the representation of the correct rear fuselage shape. Force and pressure results from tests with the correct rear fuselage and with a dummy single sting have indicated the magnitude of the effects as shown in Figs. 3 and 4.

The first figure, Fig.3, indicates diagrammatically the zones of interference pressure due to the sting on the tailplane. It will be seen that in this particular instance, where the fuselage was cut-away but not distorted, the interference was largest on the lower surface of the tail. The strength of this interference was very significant at the leading edge giving local positive pressure increments as large as  $\Delta C_p = 0.18$  associated with an effective local upwash interference. The second figure, Fig.4, gives the results of pressure integration for tailplane normal force, pitching moment and hinge moment. These emphasize the strong effect on the lower tail surface for all components and also indicates that for this configuration the twin stings give a significant interference on both upper and lower tail surfaces.

These results are for zero sting inclination and may be reliably determined from the twin sting support method, results for the effect of incidence could however be affected by the presence of the twin stings both directly or indirectly through their interference on the wing lift. Only limited data is available from twin sting tests at incidence and the above reservations should be borne in mind. Figure 5 indicates that the interference on total tailplane normal force remains substantially constant over  $10^\circ$  of incidence at the lower Mach number, being equivalent to an interference upwash of  $3^\circ$ . For the higher Mach number a change in tailplane lift slope is inferred with its consequent effect on aircraft stability.

Results obtained from fuselage pressures indicate similar interference results to those for the tailplane, the consequences of course being less significant.

Tests made with this configuration indicated a difference in total aircraft  $[C_m]_0 (= C_m \text{ at } C_L = 0)$  of the order of 0.05 between tests with and without a rear sting. Figure 6 shows the results of the investigation to determine the sources of this difference, it will be noted that the interference affected: upper and lower tailplane surface, fuselage external pressures, and fuselage cavity pressures.

Measurements made at Langley (Ref.3) stated that "the single sting interference effects obtained in the presence of a support dorsal strut were small in magnitude". The tests reported in this instance were on 3 large transport models in which the models were supported on a large dorsal fin and the effect of a single sting was measured by testing with and without its presence. Despite the comments in the conclusions quoted above, closer study of the results gives tare values very close to those listed in the table in Section 4.

#### EFFECT OF STING

		$C_L = 0 \text{ to } 0.5$			
Model	$C_{Do}$	$[C_m]_0$	$\frac{\partial C_L}{\partial \alpha}$	$\alpha_0$	Mach number range
A	+0.0005	-0.025	0	-0.1	0.75 - 0.82
B	+0.0005 ) +0.0015 )	-0.035 ) -0.025 )	0	-0.2	0.80 - 0.84
C	0.0005	Tail off 0	0	-0.05	0.7 - 0.8

### 4. BLADE SUPPORT INTERFERENCE

Philosophies differ regarding the use of an underfuselage blade support system, arguments centre around the relative benefits of the correct representation of the rear fuselage and tailplane in the presence of the blade wake, compared with the more conventional sting support. There must inevitably be cases where one of the two methods has advantages, so no further addition to the arguments will be added here.

Test results are available at Mach numbers up to 0.78 of the measured effect of a blade support and of a single sting support. Twin sting results are not available for the corresponding correct fuselage representation for this configuration and the effect of the blade support or sting support was obtained by testing on a single sting with and without the blade present, or on a blade with and without sting. The test builds are shown in Fig. 7. The blade support was very slender and representative of an absolute minimum blade, more practical blade thicknesses would probably have larger effects.

Figure 8 shows the effect on  $[C_m]_o$  of the blade interference (in the presence of a single sting support) and the single sting interference (in the presence of the blade support). In this figure the same definition of  $\Delta[C_m]_o$  is used as for the previous Section 3 and Fig. 6. It will be noted that these results are not dissimilar from those of the previous case for the single sting interference i.e.  $\Delta[C_m]_o$  is positive and of similar magnitude when allowing for  $S_{tail}/S_{wing}$ . It will be noted that the blade interference is however almost identical with that of the single sting but of opposite sign. In both cases the effect is small without the tailplane.

A general summary of the interference effects for this particular configuration is given below:

EFFECT OF	ON	$C_{D_o}$	$[C_m]_o$	$\frac{\partial C_L}{\partial \alpha}$	$\frac{\partial C_m}{\partial C_L}$	$\alpha_o^o$
Blade sting		+0.001	TAIL ON +0.02 TAIL OFF 0	+0.5	TAIL ON -0.06 TAIL OFF -0.02	+0.15
Single sting		0	TAIL ON -0.03	-0.1 to -0.3	TAIL ON -0.02	-0.1 to -0.2

Calculations made at N.L.R. by the potential flow 'panel method', Ref. 2, for a similar blade sting configuration show an interference on the tailplane lift of opposite sign to that measured in the A.R.A. experiments. This work did not include any direct experimental check of the effect of the sting so the theory has not been validated in this particular case. If it could be shown to be adequate it would be a very useful tool for assessing sting effects.

## 5. CONCLUSIONS

Some collected results from tunnel tests indicate the existence of significant interference terms associated with a conventional rear support sting and support mechanism, and a blade support sting. It is shown that a rear support housing carrying a sting and a vertical incidence strut will create a gradient of pressure on a forward mounted body giving rise to an axial buoyancy force. The sting, if mounted asymmetrically off-axis in the rear fuselage may give rise to pressure interference on the fuselage and lower tail surface, with a resultant interference in tail load, tail-on  $[C_m]_o$ ,  $\alpha_o$  and stability. In a similar manner the underfuselage blade support system can give rise to aerodynamic interferences which are accentuated in the presence of the tail.

It is unlikely that these interferences can be eliminated and their effect will have to be allowed for in the planning of test schedules for future high Reynolds number tunnels. Increase of tunnel size will maintain interference levels at the present or slightly reduced values, increase of stagnation pressure will significantly increase the centreline pressure gradient with its associated drag interference.

## REFERENCES

1. TUNNELL, P.J. An investigation of sting support interference on base pressure and forebody chord force at Mach numbers from 0 to 1.3.  
NACA RM A54K16A.
2. LOEVE, W.  
SLOOF, J. On the use of 'panel methods' for predicting subsonic flow about aerofoils and aircraft configurations.  
NLR MP 71018 U, October 1971.
3. LOVING, D.  
LUOMA, A. Sting-support interference on longitudinal aerodynamic characteristics of Cargo-type airplane models at Mach 0.7 to 0.84.  
NASA TN D-4021.



$C_D$  INCREMENT DUE TO BUOYANCY

	TOTAL	FOREBODY
<u>BODY I</u>		
1atm.	-0.012	0.0048
10atm.	-0.051	0.0187
<u>BODY II</u>		
1atm.	-0.0077	-0.0048
10atm.	-0.0325	-0.0206

BASED ON BODY FRONTAL AREA

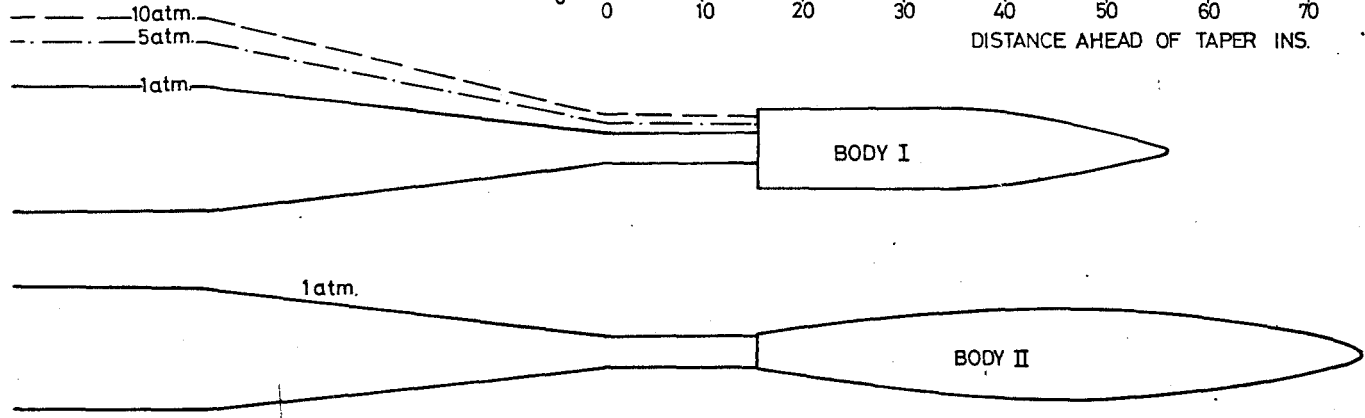
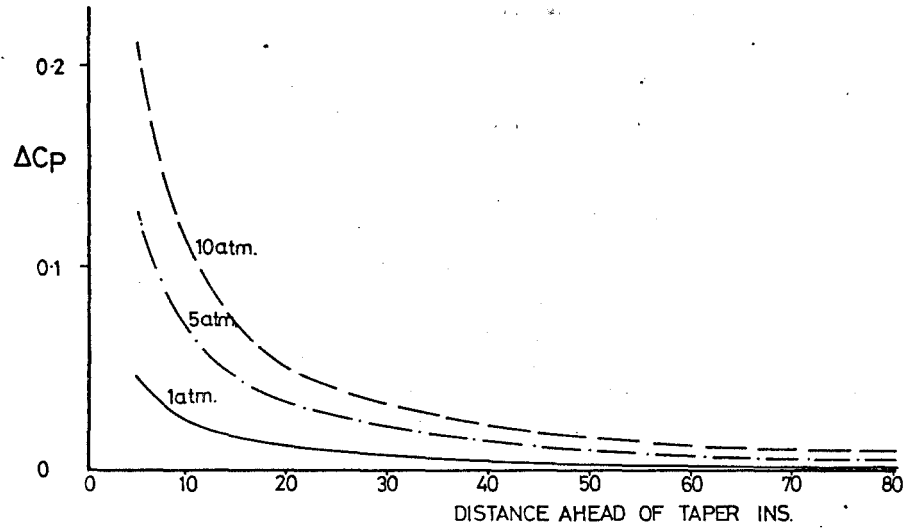


FIG. 1. REAR SUPPORT BODY BUOYANCY INTERFERENCE

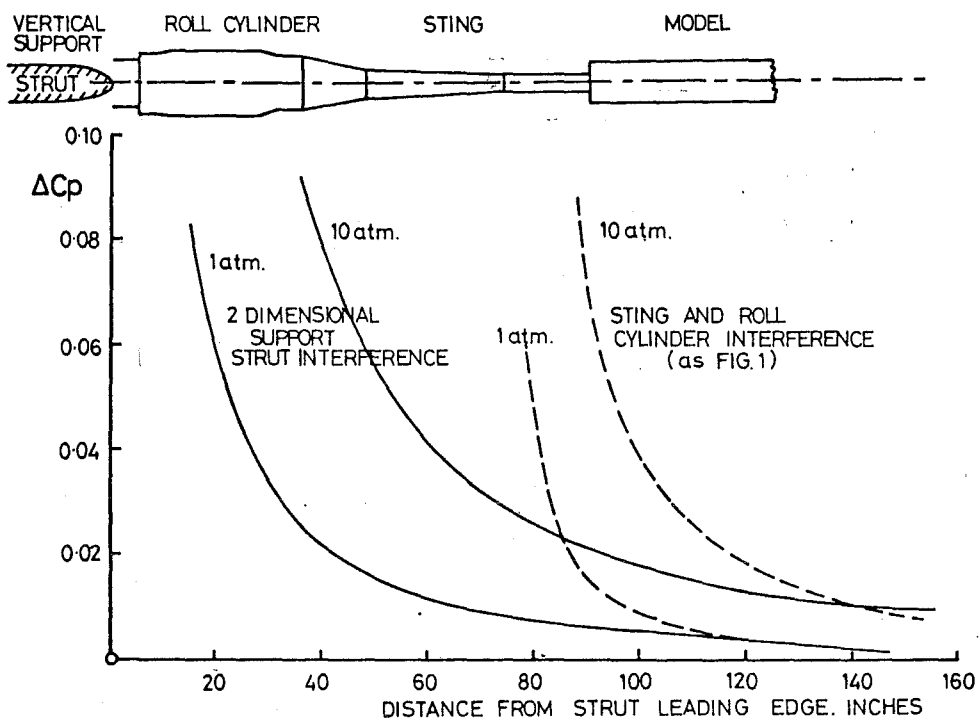


FIG. 2. VERTICAL SUPPORT STRUT BUOYANCY INTERFERENCE.

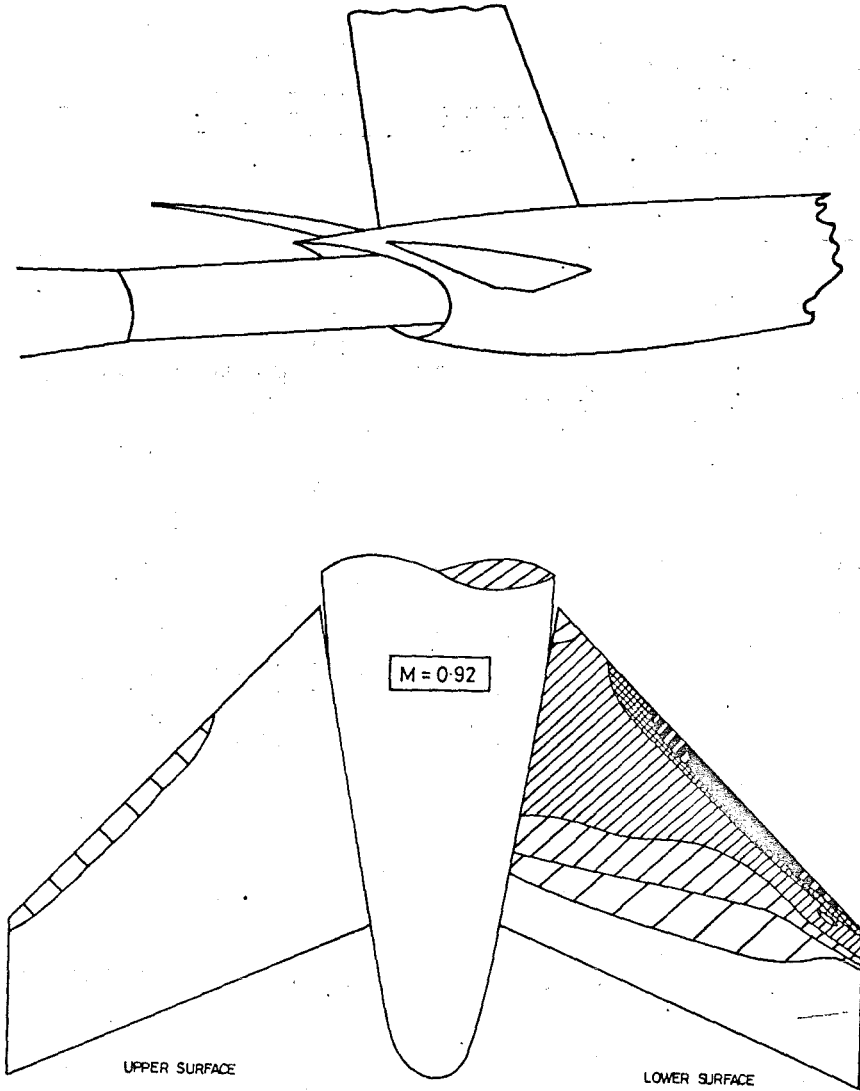


FIG. 3. CONTOURS OF SINGLE STING INTERFERENCE ON TAILPLANE PRESSURE DISTRIBUTION

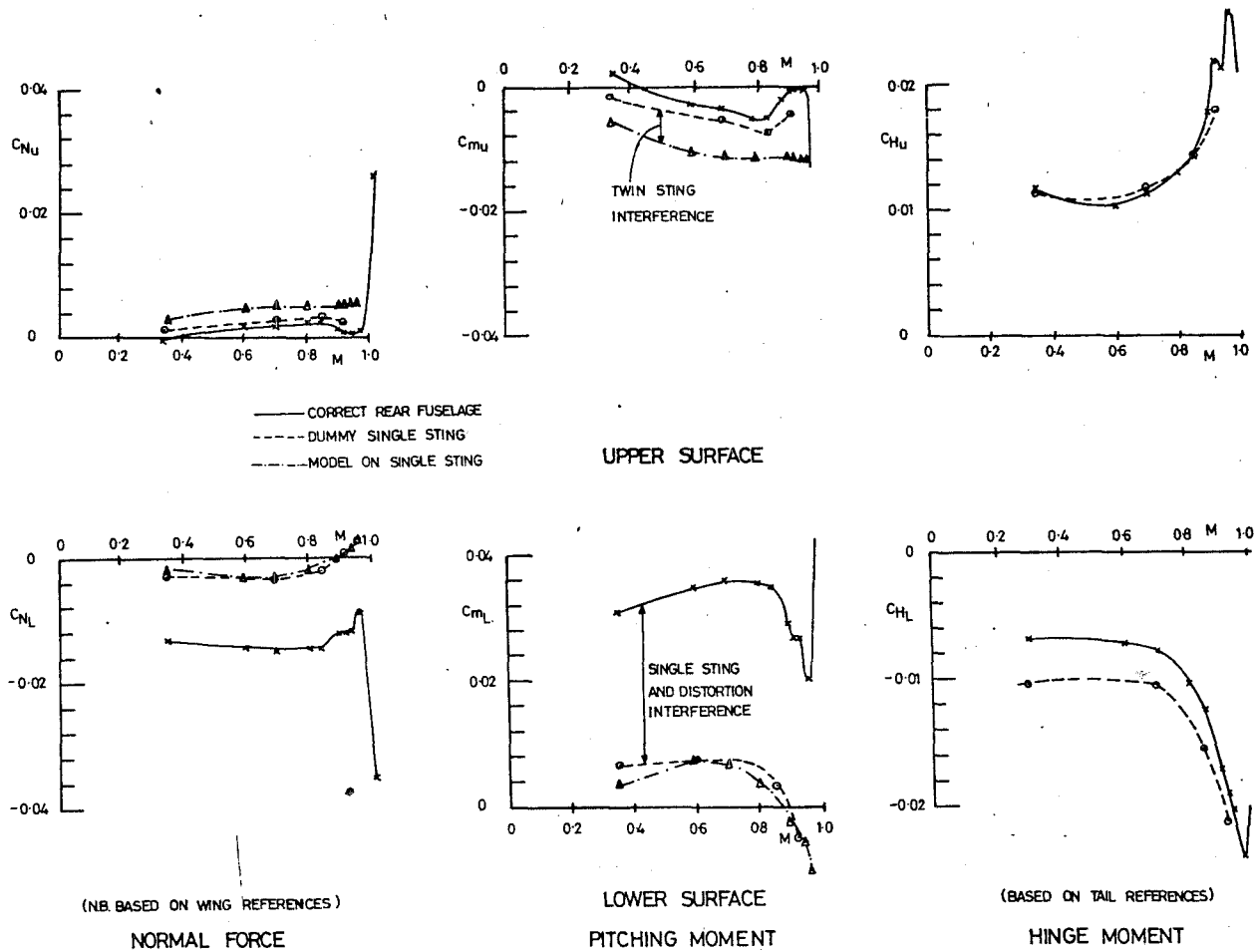


FIG. 4. VARIATION OF TAILPLANE LOADS DUE TO STING INTERFERENCES

$\eta_t = 0, \alpha = 0^\circ$

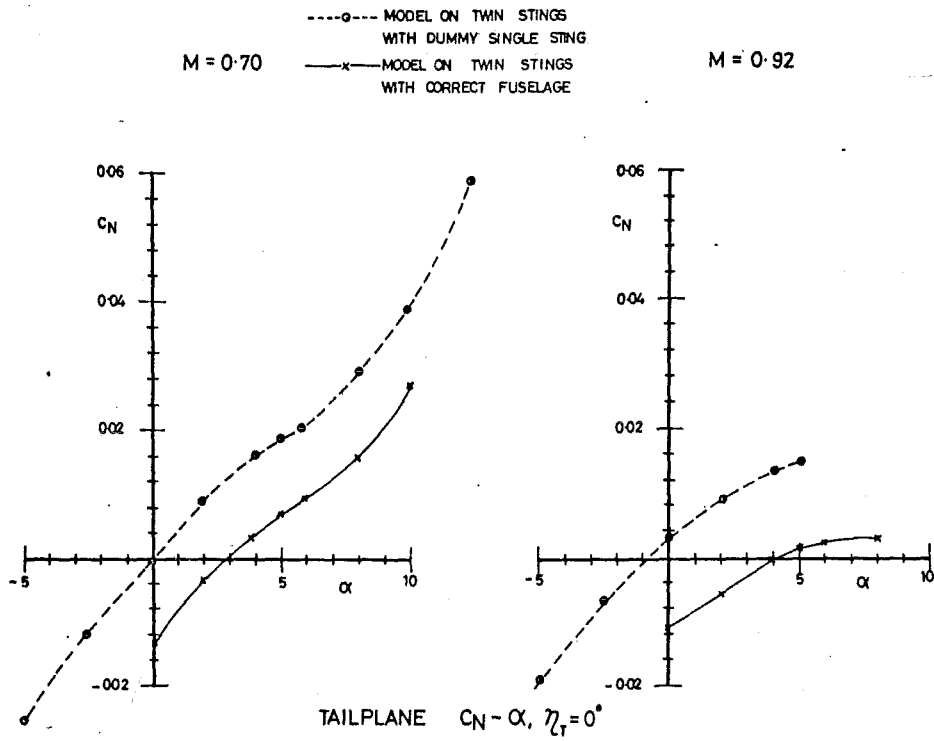


FIG. 5. EFFECT OF INCIDENCE ON SINGLE STING INTERFERENCE

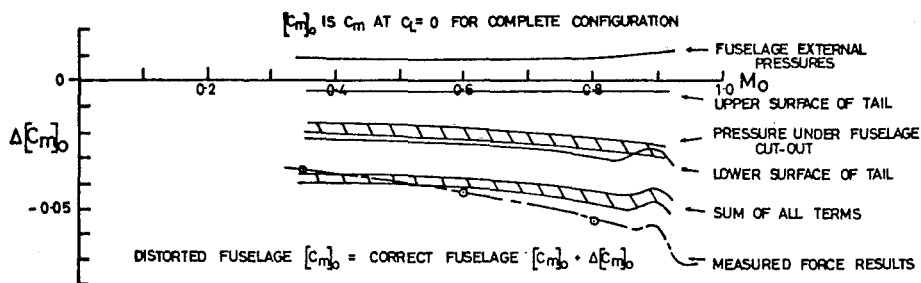
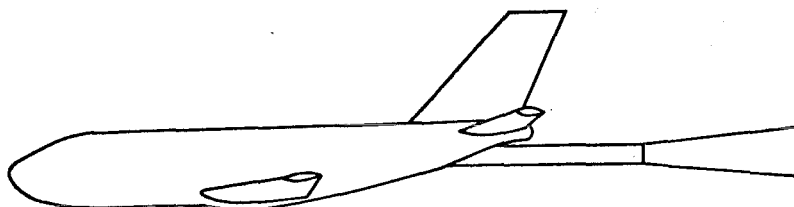
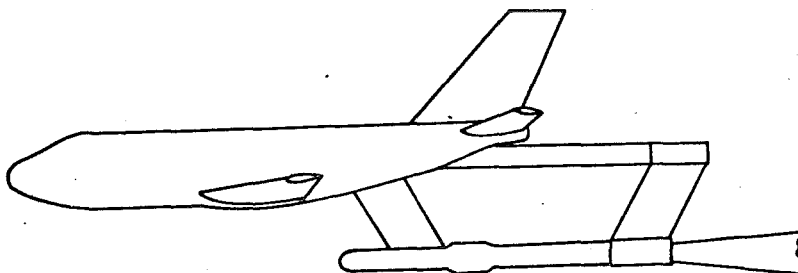


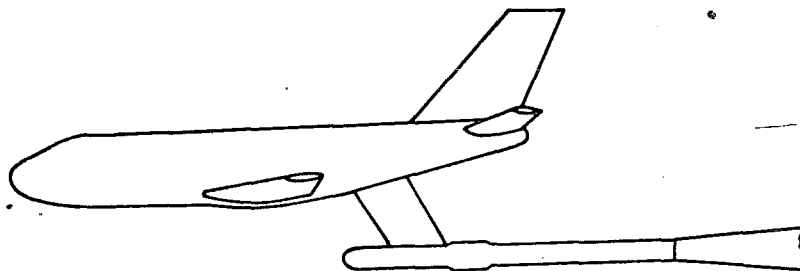
FIG. 6. ITEMS CONTRIBUTING TO THE ERROR IN  $[C_{m_0}]$  DUE TO STING DISTORTION



(a) Normal Sting



(b) Blade Sting + Dummy Sting + Bracket



(c) Blade Sting with Fuselage C.B.E.

FIG. 7. ASSEMBLIES OF MODEL SUPPORT SYSTEMS.

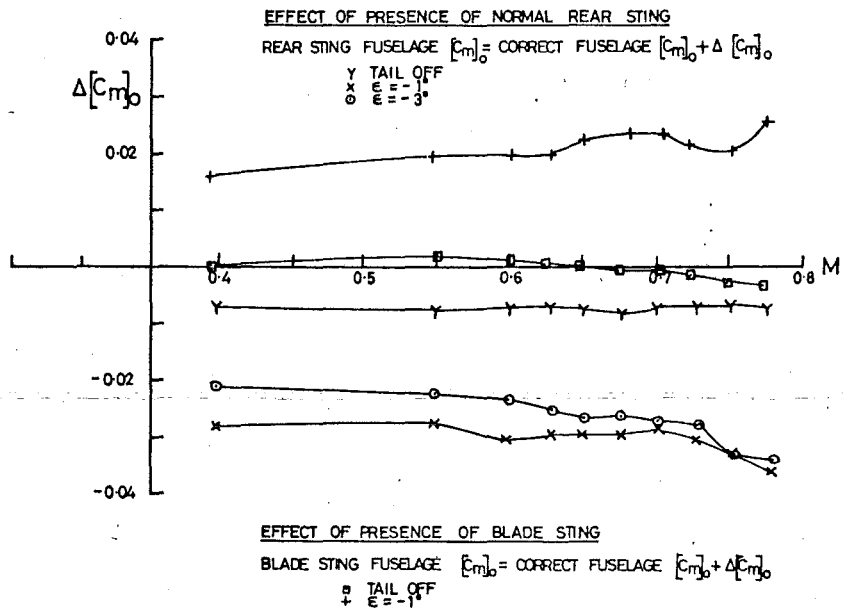


FIG. 8.  $\Delta [C_m]_o - M$  EFFECT OF PRESENCE OF NORMAL STING AND BLADE STING ASSEMBLY

MINIMUM REQUIRED MEASURING TIMES TO PERFORM  
INSTATIONARY MEASUREMENTS IN TRANSONIC  
WIND TUNNELS

by

J.W.G. van Nunen, G. Coupry and H. Försching

respectively  
NLR, Amsterdam  
ONERA, Châtillon-sous-Bagneux  
DFVLR (AVA), Göttingen

## 1. INTRODUCTION

The minimum required run times for instationary measurements at transonic speeds has been the subject of several discussions within the LaWs Group. The discussions were mainly based on LaWs papers no. 45 and no. 95 (refs. 1 and 2).

At the time of these discussions the LaWs Group decided to request the representatives from ONERA, DFVLR and NLR to discuss the matter again between them, and to lay down their findings in a report to the LaWs Group.

As a consequence some consultation has taken place between Messrs. Coupry and Destuynder (ONERA), Dr. Försching (DFVLR-AVA) and Messrs. Bergh, Tijdeman and van Nunen (NLR).

This report lays down the agreement reached on the minimum running time needed for different kind of tests.

## 2. INSTATIONARY PRESSURE MEASUREMENTS

In doing instationary pressure measurements on an oscillating model the minimum time will strongly depend on the frequency of oscillation, e.g. at 5 Hz some 20 sec will be required, but at 10 Hz some 15 sec may be sufficient, while at 50 Hz a measuring time of only 10 sec even will present workable results.

The test frequency to be applied depends strongly on the scale of the model to be used: the smaller the model the higher the frequency rises.

Performing tests in a 5 m-span test section will demand for full models of cargo planes to be of scale of about 1 : 20 and for models of fighter planes of the order of 1 : 5. This means, that the lowest test frequencies will lie in the range of 10 - 20 Hz.

The measuring times mentioned above are all related to methods and possibilities which are available at present. The excitation of the models for instationary pressure measurements for instance are thought to be excited at their resonance frequencies. This method, however, takes quite a long settling time to stabilize the model, thus increasing the measuring time considerably. Excitation out of resonance on the other hand requires large amounts of power to be installed, but may diminish the settling time of the model oscillation.

## 3. FLUTTER TESTS

Performing flutter tests on dynamically scaled models while using the natural turbulence of the wind tunnel as an input (ref. 2), will require for too long measuring times. Decaying oscillations may present fair results and will not require long measuring times (in the order of 2 - 3 seconds). The interpretation of the results, however, may become difficult, when the model is near the flutter point.

At the moment a method is under development at ONERA, which requires fairly short measuring times by making use of certain cross-correlations between an input force and the response of the model. The time consumed by this method is in the order of 10 seconds.

## 4. BUFFET MEASUREMENTS

The time to be used for doing buffet measurements strongly depends on the method applied.

When only a wing-root-bending moment is to be determined as to its RMS-value, a measuring time of about 3 - 5 sec is expected to be sufficient. When the buffet load is to be measured via determining unsteady pressures at various points the time required to get reasonable results will go up to about 10 - 15 sec.

It should be pointed out, that these measuring times are related to one data point and that several data points are to be measured to have a fair idea about the buffet behaviour of a model at a certain Mach-number.



## 5. CONCLUSIONS

It is concluded that, according to present-day standard test techniques, some types of testing (instationary pressure measurements, flutter tests) require running times of more than 10 secs. Prospects for diminishing the required time by the application of new techniques appear to be bright however. It may be expected that, by the time a large wind tunnel comes in operation, running times of less than 10 sec can be realised. As far as buffet measurements are concerned running times of 10 secs appears to be sufficient.

Finally, for all unsteady aerodynamic measurements and investigations, it must be postulated that the wind tunnel is absolutely free from oscillating shock waves or other unsteady aerodynamic flow disturbances within the actual measuring time. From an unsteady aerodynamicist's point of view this is an important aspect which must be well kept in mind.

## REFERENCES

1. van Nunen, J.W.G. Some considerations concerning unsteady measurements in transonic wind tunnels of relatively short running time. NLR-AA-72-002, LaWs paper 45.
2. Coupry, G.  
Destuynder, R. Part I - Perspectives d'utilisation des souffleries transsoniques pour les problèmes de Structures Aeronautique  
Part II - Considerations sur les mesures instationnaires en soufflerie transsonique à rafales courtes. LaWs paper 95.

## SOME CONSIDERATIONS OF TESTS UNDER DYNAMIC CONDITIONS IN LOW-SPEED WINDTUNNELS

by

D. N. Foster

Aerodynamics Department

Royal Aircraft Establishment, Bedford

## SUMMARY

Tests under dynamic conditions require special equipment and test techniques. This paper considers a range of dynamic tests with different objectives, and outlines the developments which will be necessary in order to achieve effective tests, under these conditions, in the proposed European low-speed windtunnels.

## 1 INTRODUCTION

It is now well recognised that aerodynamic research will be increasingly concerned with dynamic aspects and with problems of transient motions. In its Report, the LaWs Working Group attaches great importance to the provision of adequate testing facilities for dealing with problems of flight dynamics. For a large number of these problems the main need will be for detailed measurements of the static aerodynamic characteristics of the aircraft, combined with some basic dynamic measurements such as can be obtained from oscillatory or steady rolling rigs. This aerodynamic data will then be integrated by means of a mathematical model to give the overall representation of the dynamic behaviour.

The range of variables for which measurements of the static aerodynamics are required will probably exceed the range required for performance estimations, but the basic characteristics required of the windtunnel in which these tests are to be made will be the same. Fig 1, from ref. 1, shows that, at low speeds and high-lift, both Reynolds number and Mach number have a profound influence on the aerodynamic characteristics at limiting angles of incidence, and this has an important effect on the estimation of aircraft dynamic behaviour under these conditions, as well as on the estimation of aircraft performance. It is therefore considered essential that it should be possible to separate the effects of Reynolds number and Mach number for tests at low speed and high-lift, regardless of whether the measurements are intended for performance estimations or dynamic calculations. Thus whilst it is not the intention of this paper to enter into a discussion of the various forms of a new windtunnel, it would appear that consideration of tests for both performance estimations and dynamic calculations support the case for a pressurised windtunnel.

As the techniques required for measurements under static conditions intended to support dynamic calculations are the same as those for measurements to support performance estimations, they will not be discussed here, but the paper will be concerned with the development work necessary to ensure that the required oscillatory measurements can be made in the new large low-speed windtunnels which the LaWs Group proposes.

For a number of specific problems involving transient motions it is possible that special techniques and rigs will need to be developed. Within the timescale envisaged for the new windtunnels it is possible to consider how useful such rigs could be, and, perhaps, to use existing facilities to demonstrate the basic features of such rigs. Two such problems, that of the effect of gusts and that of the effect of the rate of descent into ground effect, are considered in this paper.

## 2 MEASUREMENT OF OSCILLATORY DERIVATIVES

Methods of measuring the oscillatory derivatives for unpowered models are now well-established<sup>2</sup>. One such technique, developed at RAE, consists of measuring the response of the model to forced vibrations at a fixed frequency, usually in the range 0 to 10 Hz. However, techniques for obtaining similar measurements on powered-lift models are not so well-established.

The magnitude of the extension required to the established technique depends on the nature of the contribution of the power. If the model incorporates propellers or rotors driven by electric motors, then the standard test arrangement may be used with the simple addition of wires to conduct power to the motors. However, if compressed air is required to provide the power for the motors, or to power models of turbofan engines for the external-flow jet-flap concept, by using air turbines, then difficulties may be experienced. However, some NASA dynamic stability tests<sup>3, 4</sup>, where a flow of compressed air was required, did suggest that, by careful arrangement of the supply pipes, the constraints imposed by the pressurised pipes may be minimised, and the existing test techniques may again be used.

More extensive revisions of the test arrangement will be needed when large mass-flows of compressed air are necessary for the simulation of the efflux of propulsion or lift engines, or of the flow of air for internal plain- and augmented-jet flaps. It is then almost inevitable that the rigs will be limited to a single degree of freedom in order to provide a pivot through which to pass the air. If only one derivative is required, the decaying-oscillation principle may be utilised, although such a rig developed at RAE<sup>5, 6</sup> for an internal-flow jet-flap suffered from some lack of repeatability of results. If cross-derivatives are also required, the rig must take the form of an inexorably forced rig, measuring the forces and moments on the model in a forced oscillation.

The development of such a rig, to carry models of the size which will be tested in the low-speed windtunnels proposed by the LaWs Group, will inevitably be time-consuming and expensive. Nevertheless there does not appear at this stage to be any outstandingly difficult engineering problems. The main criterion must be to ensure that the increase of size, compared with existing rigs, does not result in the separation of the frequency of the model oscillations from the resonant frequency of the rig being reduced to an unworkably small margin; that the balance measuring the forces and moments on the model is made

sufficiently stiff so that it is insensitive to windtunnel noise, and that the mechanical stiffness of the rig is not affected by air loads. These loads may arise from external air flows and, for pressurised wind-tunnels, from the effect of pressure differences across the working section boundary to which the rig is attached, and also from internal flows if a flow of pressurised air is required. It is possible to conceive of aircraft layouts in which measurements are required of the dynamic derivatives in the presence of jet efflux, but without the contribution of the efflux being included. Such a rig would not need a constraint-free air connector, as the air feed system could be regarded as part of the earthed side of the rig. However for the majority of configurations it will be necessary to measure the contribution from the efflux, and to pass air into the model itself. For these configurations it will be necessary to develop an air connector whose mechanical stiffness is not affected by the passage of compressed air.

The techniques of measurement of forces and moments and of the analysis to yield the derivatives will be similar to those currently employed. No special problems should therefore arise in their extension to larger rigs.

It is, perhaps, worthwhile mentioning that a pressurised windtunnel can, in some specific areas, enable more accurate measurements to be made of the damping derivatives. Assuming that the aerodynamic stiffness terms and the windtunnel noise vary with the dynamic pressure (i.e. proportional to  $\rho V^2$ ) and that the damping terms vary with  $\rho V$ , tests in which the density  $\rho$  is increased and the velocity  $V$  decreased to maintain constant dynamic pressure will result in the stiffness and noise contributions remaining constant, but the damping terms increasing as the square root of the density. Windtunnel tests show that as a result the scatter of the measurements of the damping terms falls almost linearly with the increase of the square root of the density.

### 3 MEASUREMENTS OF OTHER TRANSIENT MOTIONS

In this section two possible dynamic motions - that occurring when an aircraft encounters a gust, and that occurring in a rapid descent into ground effect - will be considered, and possible ways of simulating them in a windtunnel will be discussed.

#### 3.1 Measurement of the effects of gusts

The margin between the maximum lift coefficient of an aircraft and the lift coefficient specified for the approach must be such as to ensure safe flight in gusty conditions. It has been suggested<sup>7</sup> that the sensitivity of STOL aircraft to longitudinal and vertical gusts is different from that of conventional aircraft. It may be, therefore, that each of the different categories of aircraft to be tested in the windtunnels requires different lift margins from the stall in order to achieve comparable levels of safety.

It is thus necessary to consider how the dynamic motion of an aircraft encountering a gust might be simulated in a windtunnel, bearing in mind that a dynamic manoeuvre is to be simulated with a fixed model. Considering first the response to symmetrical gusts, there exists a particular length of gust, the tuned-gust length  $\bar{H}$ , for which the response of an aircraft is a maximum. The magnitude of the tuned-gust length depends on the aircraft speed, and on whether the response to longitudinal or vertical gusts is being considered. The form of the gust considered is shown on Fig. 2, and a typical response of the angle of incidence, for a rigid aircraft for which the damping of the short-period oscillation is fairly high, is shown on Fig. 3. It is this variation in angle of incidence, rather than the perturbation velocity of the gust itself, which must be simulated in the windtunnel. Curves such as Fig. 3 could be calculated theoretically; however the relevance of simulating such curves, before values of the derivatives required in the calculation have been measured for the flow conditions and perturbation amplitudes corresponding to excursions to the stall, is questionable.

It is, therefore, suggested that a more general approach is required, and that this might be gained by simulating the variation of angle of incidence illustrated on Fig. 4. As it is possible that the non-linearities present near the stall will affect the magnitude of the tuned-gust length, the response of the model to the triangular profile at or near the tuned-gust length  $\bar{H}$ , (suitably scaled by the mean chord  $c$ ) should be studied for a range of amplitudes. Assuming that the model is initially in a trimmed condition, it will be possible to determine the minimum amplitude of the disturbance which will result in a stall, and the theory presented by Jones<sup>8, 9</sup> can then predict the probability of meeting a gust in the atmosphere which will produce this disturbance. By testing over a range of initial trimmed lift coefficients, the initial condition which yields a probability, acceptable from the viewpoint of safety, of encountering a gust of sufficient magnitude to stall the aircraft can be determined. At the same time, these tests will yield the values of the derivatives necessary to derive the more representative variation of angle of incidence, Fig. 3, and this profile should be simulated to check that the triangular profile, with its lack of rounding at the peak of the perturbation, has not resulted in an unrepresentative response.

During the period before the new windtunnels become operational it is possible that flight test evidence will become available to show whether there are aircraft configurations whose sensitivity to gusts is sufficiently different to that of conventional aircraft to warrant the development of a rig to simulate these effects. If this is so, it may be possible to design a rig for the new windtunnels based on one being tested by ONERA for use in the S1 windtunnel at Modane, and which utilises the jet-flap principle to change the direction of the flow.

One further problem concerned with symmetrical gusts is their uniformity across the span of an aircraft. As flight speeds are reduced into the STOL regime, the tuned-gust length  $\bar{H}$  tends to decrease and, equally, such short gusts become more frequent as the aircraft penetrates the lower parts of the atmosphere. If it is assumed that the velocity gradients in a gust are of a similar magnitude in the direction of the flight and normal to it, then for the short gust, there may be an appreciable velocity gradient across the span of the aircraft. It should be possible to confirm if such lateral velocity gradients do exist in the atmosphere by measurements on ground based towers, and it is recommended that such measurements be made before consideration is given to including the capability of generating spanwise variations of angle of incidence into the rig referred to above.

The magnitude of the most intense lateral gust which can safely be encountered is determined by the available lateral control power whilst, for some configurations, such as the external-flow jet-flap, a lateral gust may, when combined with the failure of an engine, result in the occurrence of the stall. The philosophy outlined above for the determination of the critical longitudinal gust could be applied to the determination of the critical lateral gust, starting from a trimmed condition corresponding to an approach in cross-wind. It is possible that the technique described in a recent paper by Azuma et al, in which the model support system always retains the model in a trimmed state, could find application here, and its development should be studied.

### 3.2 Measurement of the effects due to the approach to the ground

Whereas flight experience with conventional transport aircraft<sup>11</sup> indicated that the influence of ground proximity is favourable, in that the lift at a constant angle of incidence was increased, windtunnel tests on a STOL configuration<sup>12</sup> suggested that the effect of ground proximity was unfavourable. These results were obtained under conditions equivalent to flight at a constant height. However, STOL aircraft are likely to use an approach path having an angle at least twice that for conventional aircraft, and so will enter the region of ground influence at least twice as rapidly. The STOL approach will terminate in a full or partial flare performed in a very short time scale. Similarly, the final phase of the descent of a VTOL aircraft or a rotorcraft will result in large changes of the aerodynamic forces and moments which arise from the influence of ground proximity.

It is possible therefore that the flight of a V/STOL aircraft or a rotorcraft in regions of ground influence may result in dynamic changes in the forces and moments on the aircraft. The extent to which these dynamic changes may affect the control of the aircraft and its margin from the stall is currently not clear, and it will be necessary again to establish the need to simulate this motion before embarking upon a design of a rig for the new windtunnels. A rig designed to simulate this motion is currently being developed by ONERA for the S1 windtunnel at Modane, and it should be possible to use information gained from this rig in conjunction with a mathematical model to establish if there are likely to be significant dynamic effects resulting from this motion.

## 4 CONCLUSIONS

It is concluded that the main requirements for data relevant to dynamic effects can be met by accurate measurements under static conditions over a wide range of variables, and by the development of a rig to measure oscillatory derivatives in forced oscillations. This rig should be capable of passing large quantities of compressed air to the model without affecting the accuracy of the measurements. Consideration should be given to the need to develop specialised rigs to simulate particular transient motions, and indications have been given of the ways in which such needs might be established.

## REFERENCES

- |   |  |    |   |
|---|--|----|---|
| 1 | D.M. McRae. The aerodynamic development of the wing of the A300B. To be published in J R Ae S.   | 7  | W.J.G. Pinsker. Theoretical assessment of the general stability and gust response characteristics of STOL aircraft. RAE TR 71028 (1971).  |
| 2 | J.S. Thompson, R.A. Fall. Oscillatory derivative measurements on sting-mounted windtunnel models at RAE Bedford. RAE TR 66197 (1966).  | 8  | J.G. Jones. Turbulence models for the assessment of handling qualities during take-off and landing. Unpublished Ministry of Defence Report.   |
| 3 | J.R. Chambers, S.B. Grafton. Static and dynamic longitudinal stability derivatives of a powered 1/9 scale model of a tilt-wing V/STOL transport. NASA TN D-3591 (1966).                | 9  | J.G. Jones. Trends in aircraft gust response associated with reducing approach speeds to the low values typical for STOL. RAE TR (In preparation).  |
| 4 | D.C. Freeman, S.B. Grafton, R. D'Amato. Static and dynamic stability derivatives of a model of a jet transport equipped with external-flow jet-augmented flaps. NASA TN D-5408 (1969). | 10 | A. Azuma et al. A free-flight support system. Institute of Space and Aeronautical Science, University of Tokyo. Report No. 477 (1972).  |
| 5 | A.P. Cox. The design and development of an air-bearing for the measurement of damping in yaw of a jet-blowing model. ARC CP No. 796 (1964).  | 11 | C.O. O'Leary. Flight measurements of ground effect on the lift and pitching moment of a large transport aircraft (Comet 3B) and comparison with windtunnel and other data. RAE TR 68158 (1968). |
| 6 | A.P. Cox, S.F.J. Butler. Low-speed windtunnel measurements of damping in yaw ( $n\psi$ ) on an AR 9 jet-flap complete model. ARC CP No. 869 (1967).                                    | 12 | R.D. Vogler. Windtunnel investigation of a four-engine externally blowing jet-flap STOL airplane model. NASA TN D-7034 (1970).  |

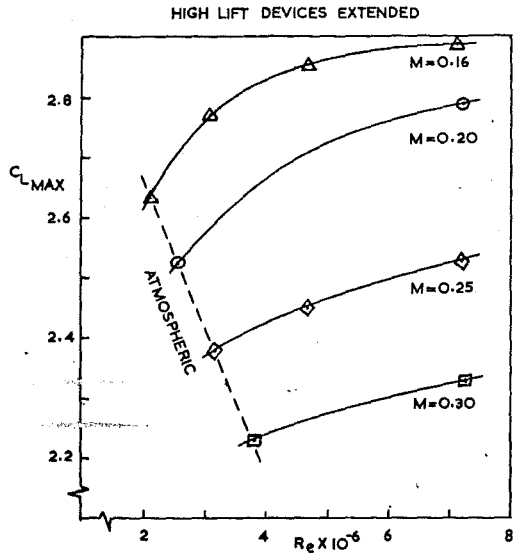


FIG.1 EFFECT OF REYNOLDS NUMBER AND MACH NUMBER ON  $C_{L\text{MAX}}$  - CONSTANT CHORD WING WITH ADVANCED WING SECTION

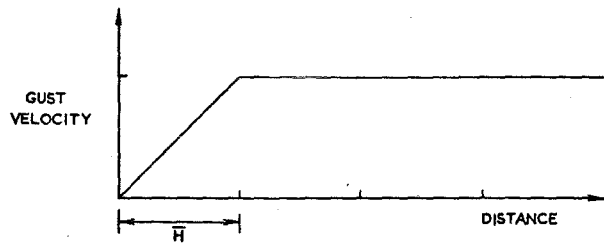


FIG.2 ASSUMED GUST SHAPE

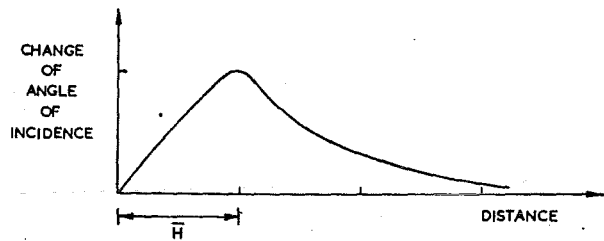


FIG.3 RESPONSE OF ANGLE OF INCIDENCE TO GUST

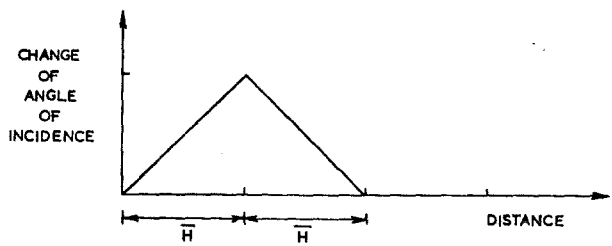


FIG.4 SUGGESTED INCIDENCE VARIATION

USE OF MODEL ENGINES  
(V/S/CTOL)

by

E. Melzer and R. Wulf

Deutsche Forschungs- und Versuchsanstalt für Luft- und Raumfahrt E. V.  
Aerodynamische Versuchsanstalt Göttingen  
D 34 Göttingen, Bunsenstr. 10  
Germany

SUMMARY

Propulsion matters are of importance in airplane development. There is a need of more effort in future large wind tunnel testing. The most important aerodynamic viewpoints for modern jet simulation by means of model engines which are to realize are given. The insert of the present known systems for simulation in atmospheric tunnels are discussed. It is looked into the problems of realizing these methods in pressurized tunnels. An estimation of the energy, the plants and the test equipments needed for engine simulation are listed. Some important jobs for a future programme of work in this subject are set out and an abstract of other LaWs papers concerning this job is added.

For the preparation of the report, some aeronautical research establishment in Europe were visited. These establishments are listed in fig. 10 together with the names of the people visited and the subjects discussed with them.

LIST OF SYMBOLS

$l$	[m]	length
$A$	[m <sup>2</sup> ]	area
$V_{\infty}$	[m/s]	free stream velocity
$v$	[m/s]	velocity
$u$	[m/s]	tip speed
$n$	[1/min]	revolutions per minute
$T$	[°K]	temperature
$p$	[N/m <sup>2</sup> ]	pressure
$\rho$	[kg/m <sup>3</sup> ]	density
$\dot{m}$	[kg/s]	mass flow
$F$	[N]	thrust
$P$	[W]	power
$H_{ad}$	[ $\frac{W}{kg/s}$ ]	specific power
$R$	[ $\frac{N \cdot m}{kg \cdot ^\circ K}$ ]	gasconstant
$\alpha$	[1]	ratio of specific heats
$Re$	[1]	Reynolds number
$Ma$	[1]	Mach number
$M$	[1]	model-scale, $M = l_f/l_m$

Subscripts

$o$	static, stagnation
$j$	jet
$m$	model
$f$	full scale

## 1. General Considerations

Engine simulation has become of great importance in the past. For future development of modern airplanes there will be increasing demand for more detailed simulation of all parts of the engine in order to predict the final performance of the aircraft.

Drag prediction without proper engine simulation has turned out to be unsatisfactory. Due to the increase of the cross section area and the mass flow of modern engines, the influence of the engine flow on the flow field can no longer be neglected. For STOL-systems with BLC, jet flaps, or externally blown flaps the jet parameters are of superior significance. In the case of VTOL especially when freestream velocities are very small the engine air flow is predominant.

Fig. 1 shows which parts of the engine cause aerodynamic and thermodynamic variations of the flow field around the airplane. The various parts have different influences on fuselage, wing and tailplane and

engine part	reason for influence	main parameter
inlet	geometry sink-effect upstream flow field losses	model-scale suction coefficient stream tube Re-number, Ma-number
interior	principle of jet generation	pressure- and flow coefficient sound frequency spectrum sensitivity to outer flow field
jet	physics of the jet  chemics of the jet	pressure profile velocity profile temperature profile turbulence profile noise generation ratio of specific heats gas constant
cowl	geometry flow around the cowl; losses	model-scale Re-number, Ma-number

Fig. 1 Parameter list

on noise generation. If accurate simulation is desired all scaling laws for model and full scale should be realized at the same time. Due to development schedule and budget these conditions are met in a few cases only.

Therefore experienced aerodynamicists have to determine the priority of the various similarity parameters. Depending on the state of the project more or less detailed information about the effect of the engine flow field is required.

## 2. Classification of Engines

The development of airplane engine has begun with piston motor driven air-screws and was continued over turboprop, turbojets to turbofans. At present airplanes with advanced fan propulsion are under development. Fan propulsion is characterized by high bypass ratios, low exit velocities, low noise production and high theoretical efficiency. The hot jet will become less important.

Turbofans are used mainly for modern transport and passenger airplanes. Turbojets are still dominant for fighter aircraft. Advanced fans are most promising for V/STOL systems. Therefore wind tunnel simulation has to be carried out for turbojets, turbofans and advanced fans. Main characteristics of these engines are shown in fig. 2.

Other complex propulsion units which are somehow integrated in the airframe can be reduced mostly to engines as described above.

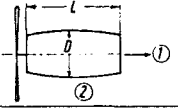
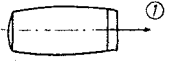
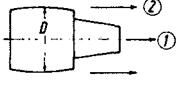
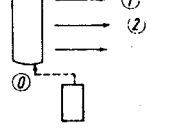
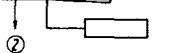
Types of engines		$L/D$	$T$ [ $^{\circ}K$ ] turbine inlet	$T_1$ [ $^{\circ}K$ ]	$T_2$ [ $^{\circ}K$ ]	$V_1$ [ $\frac{m}{s}$ ]	$V_2$ [ $\frac{m}{s}$ ]	$m_2/m_1$
1	Turboprop 	2,5	1200	800	300	500	200	15
2	Turbojet 	5	1400	900	—	500	—	—
3	Turbofan 	2	1200 -1600	800	300	300-500	200-300	5-15
4	Advanced Fan 	0,2-0,3	1200 -1600 -(1700)	500	300	200-300	150-250	20
5	Rotor 				300		200	

Fig. 2 Types of engines

At present state systems are tested with separate gas generators, the high pressure air of which is used for driving fans. The gas generator can also be used for jet flaps, BLC devices and similar techniques.

With these complex and integrated schemes no major additional technical problems arise. But the aerodynamic problems and the testing programme increase very much.

### 3. Power Requirement of Engines

#### 3.1 Total Power Requirements

The maximum engine power is needed during take-off and landing phase. The estimation of the power requirement for model engines is based on the maximum jet power.

Generally the following equations are valid:

$$\text{thrust} \quad F = \dot{m} (v_j - v_o) \quad (1)$$

$$\text{with } v_o = 0 \quad v_j = \frac{F}{\dot{m}} \quad (2)$$

$$\text{and the power of the jet } (v_o = 0) \quad P_o = \frac{\dot{m}}{2} v_j^2$$

$$P_o = \frac{F^2}{2\dot{m}} \quad (3)$$

The value  $P_o$  indicates the effective energy per unit time that is leaving the engine. Formula (3) calculated for some airplanes using the known static thrust and mass flow. Fig. 3 indicates the power versus wing span for some large planes, fighters and VTOL planes.

If the engine is scaled down by factor  $M$  for model testing the effective energy is reduced to

$$P_{om} = P_{of} \cdot \frac{1}{M^2} \quad (4)$$

( $m$  - model,  $f$  - full scale).

This is valid for the case when

$$v_{jm} = v_{jf} ; T_{jm} = T_{jf} ; \rho_{jm} = \rho_{jf} \quad (5)$$



The required power for models with different wing span is to be seen in fig. 3. It is obvious that the installed energy per unit wing span is much higher for fighters and VTOL planes than for conventional airplanes.

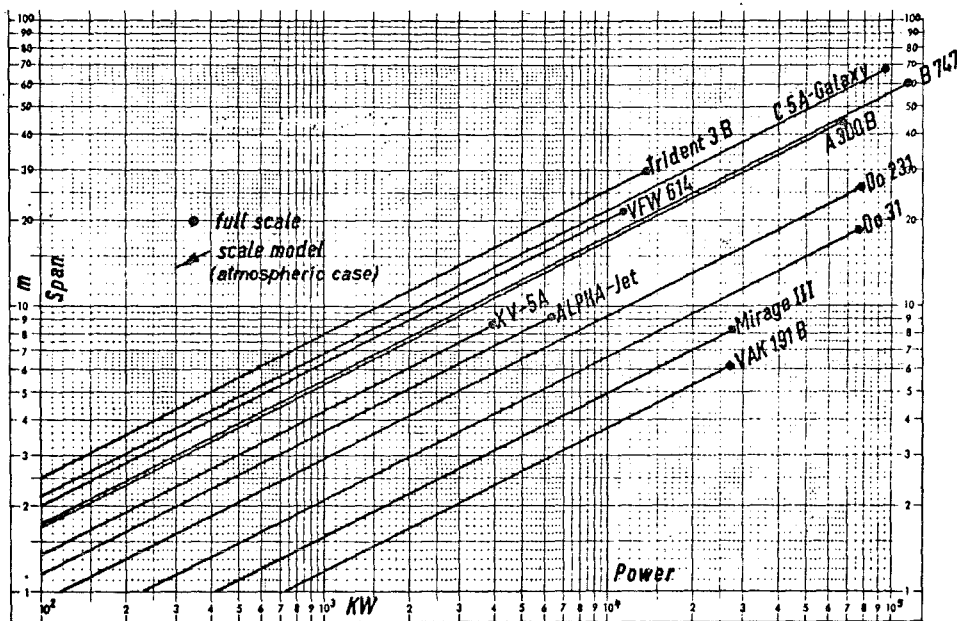


Fig. 3 Power of engines

For 4 typical airplanes and for the proposed types of wind tunnels power and mass flow requirements are listed in fig. 4.

In this table model wing span for CTOL aircraft is defined in such a manner that maximum Reynolds number can be tested. A maximum model span of 0.7 tunnel width is used for this calculation.

In the case of VTOL planes the power requirement per unit span is very large. Flow break down is an important parameter for definition of model scale. Only little work has been done to define the exact values when flow break down will occur. The main parameters are the effective jet diameter, velocity ratio  $v_j/v_{\infty}$  and tunnel size. For VTOL planes a maximum model span of 0.3 tunnel width is assumed to be valid.

The calculated mass flow and the effective power are depending on model scale and tunnel pressure as it is given by eq. (6) and (8).

By feeding the effective power from outside to the model large losses have to be expected. No efficiencies better than 30 % will be obtainable either by using compressed air - or electric power - or chemical energy supply. Good total efficiency of about 30 % will be reached for power installation in a few cases only.

The span of fighters (CTOL, VTOL) is so small that these planes could be tested full scale in all proposed atmospheric tunnels so that original real engines can be used.

For the smallest proposed atmospheric tunnel (type G) model scales of about 1:3 are necessary as well for CTOL as for VTOL transports. Whether for these models small real engines can be used depends on the value of the front area thrust. This front area thrust for all existing engines decreases very much below 40 000 N thrust, as it is shown in fig. 5 separately for turbojets and turbofans. If small real engines are not available and power supply from outside is used, the installed power plant for tunnel type G should have about 35 ÷ 43 MW (fig. 4).

In tunnel type B full scale tests without jet simulation can be performed under atmospheric conditions for CTOL and VTOL fighters. At least for CTOL fighters original engines can be used. For VTOL fighters with original jets a larger tunnel would be preferable. Under high pressurized conditions jet simulation with original engines is impossible.

Present CTOL and VTOL transport models with a scale factor of about 1:5 are typical for tunnel type B. With this scale factor the thrust of the model engine is much below 40 000 N and therefore small real engines with correct front area thrust are not obtainable (for atmospheric tests).

For this reason and due to the need of other techniques for jet simulation in pressurized

type		A	B	C	D	E	F	G	remarks
low speed windtunnel	max. pressure [bar]	4	3	2,5	2	1	1	1	LaW's paper 46 B (revised)
	width [m]	11,25	15	18	22,5	45	60	25	
	height [m]	8,5	11,25	13,5	17	34	45	18,75	
	power for max demand [MW]	59	99	137	203	567	1.007	209	
for CTOL-max. model span	~ 0,7 tunnel width [m]	7,9	10,5	12,6	15,7	31,5	42,0	17,5	
CTOL-Transport i.e. A 300 B	model scale	1 : 5,7	1 : 4,3	1 : 3,57	1 : 2,87	(1 : 1,43)	~ 1 : 1	1 : 2,57	full scale span ~ 45 m see eq. (6) see fig. 3 and eq. (8) total efficiency ≈ 30 % assumed
	mass flow [kg/s]	191	254	305	381	(763)	1.562	237	
	effective power [MW]	8,8	11,4	13,75	17,2	(34,0)	60,0	10,5	
	~ installed power [MW]	30	38	46	57	(113)	200	35	
CTOL-Fighter i.e. Mirage III	model scale	~ 1 : 1	1 : 1	1 : 1	1 : 1	not necessary	real engine real airframe	1 : 1	full scale span ~ 3,3 m
	mass flow [kg/s]	probably no testing for original full scale airframe with real engines under pressurized conditions and jet-simulation							
	effective power [MW]								
	~ installed power [MW]								
for VTOL-max. model span	~ 0,3 tunnel width [m]	3,4	4,5	5,4	6,75	13,5	18	7,5	
VTOL-Transport i.e. Do 31	model scale	1 : 5,44	1 : 4,12	1 : 3,43	1 : 2,74	(1 : 1,37)	~ 1 : 1	1 : 2,47	full scale span ~ 18,5 m see eq. (6) see fig. 3. and eq. (8) total efficiency ≈ 30 % assumed
	mass flow [kg/s]	82	109	131	164	(328)	816	101	
	effective power [MW]	10,4	13,8	16,5	20	(40)	real airframe	13	
	installed power [MW]	35	46	55	67	(133)	real engines	43	
VTOL-Fighter i.e. VAK 191 B	model scale	1 : 1,82	(1 : 1,38)	(1 : 1,15)	1 : 1	not necessary	real engine	1 : 1	full scale span ~ 6,2 m see eq. (6) see fig. 3 and eq. (8) total efficiency ≈ 30 % assumed
	mass flow [kg/s]	205	(268)	(320)	340				
	effective power [MW]	34	(43,5)	(52,5)	no testing for original full scale airframe with real engines				
	~ installed power [MW]	113	(145)	(175)					

( ) Unrealistic test configuration

Fig. 4 Power requirements

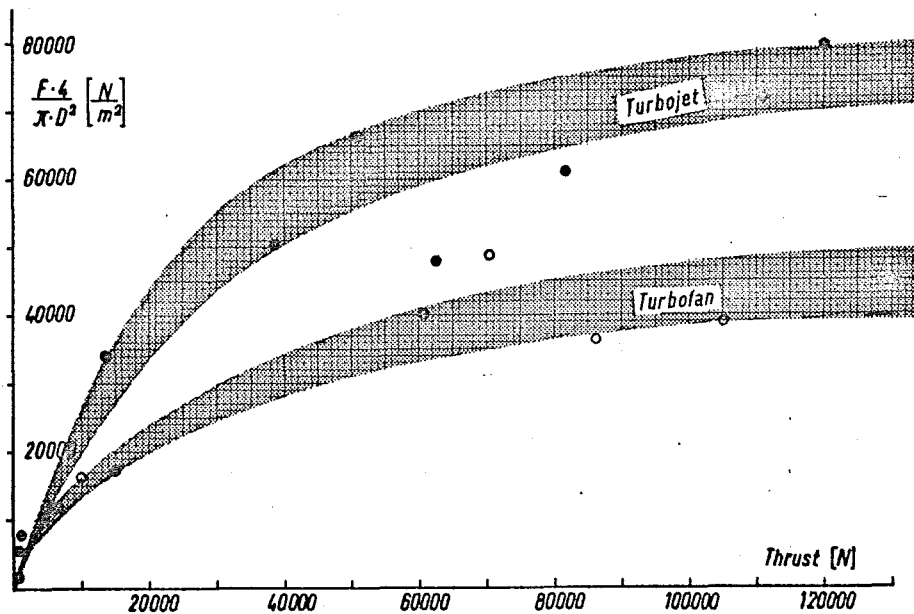


Fig. 5 Front area thrust of engines

wind tunnels (type B) an installed power plant of about  $38 \pm 46$  MW (fig. 4) is necessary.

### 3.2 Compressor and Air Storage Plants

In most cases compressed air supply is used for various simulation techniques. Air supply can be realized by systems of continuously working compressors and/or high pressure air storage.

Continuously working compressors increase the total power demand, i. e. for tunnel B or G max. 46 MW. This leads to higher electrical energy costs per kWh. Compressed air storage on the other hand needs more energy for the higher pressures (more than 60 bar) related to the same daily air mass. The total capacity of the storage depends as well on total air mass which is needed from storage as on the maximum pressure of storage and from the fact, if the storage can be filled up between the tests.

By using ejectors or powered nacelles only a part of the maximum engine mass flow is supplied from compressors or air storage. Assuming that 50 % of the air will be taken from storages and that 1/3 of engine mass flow is drive air, then the daily-mass-demand is:

$$\text{daily-mass} = \text{blowing time} \times \frac{\text{max. engine mass flow}}{2 \times 3}$$

The daily-mass-demand for engine simulation is listed in fig. 6 for various time schedules and compared with the mass which is needed to fill pressurized tunnels. The air mass for one tunnel fill is much higher than the mass even for 5 hours blowing time from storage. But comparing maximum pumping power with maximum installed power for jet simulation both values are of the same order of magnitude. So a compressor-plant (with i. e. 4 simple stages each of which having a compression ratio of about 4) could be used for different tasks:

1. All stages working in parallel (max. mass flow) to fill the tunnel or supply continuously low pressure air for jet simulation
2. All stages working in series (max. pressure) to fill the high pressure storage
3. Two or three stages working in series to supply continuously medium pressures for jet simulation

This compressor-plant would be able to fill the air storage during the pauses between the tests.

Proposed tunnel type	A			B			C			D			E			F			G			
Max. pumping power [MW] for tunnel	19			30			41			56			37			67			11			
Max. installed power for jet simulation; no air storage [MW]	35 (113)			46			55			67			(113)			(200)			43			
Max. mass flow for jet simulation [kg/s]	205			268			320			381			(763)			(1562)			237			
Daily use of high pressure storage [hours]	1	3	5	1	3	5	1	3	5	1	3	5	1	3	5	1	3	5	1	3	5	
Daily mass from storage (50% from total mass) [Mkg]	0,12	0,37	0,62	0,16	0,48	0,81	0,19	0,58	0,96	0,23	0,69	1,15	0,46	1,37	2,29	0,94	2,81	4,7	0,14	0,43	0,71	
Air mass to fill wind tunnel [Mkg]	0,84			1,32			1,73			2,23			-			-			-			
Proposed air-mass to be stored [Mkg]	0,4			0,6			0,8			1,0			0,6			1,0			0,2			
High pressure volume [m <sup>3</sup> ]	200 bar	2150			3220			4290			5370			3220			5370			1070		
	300 bar	1320			1980			2640			3300			1980			3300			660		
	500 bar	745			1120			1490			1870			1120			1870			370		

( ) unrealistic test configuration

Fig. 6 Compressor and air storage plants

For the proposed pressurized tunnels it is assumed to install pumps which fill the tunnel to maximum pressure in 6 hours. By combining air supplies from compressors and storage this time could be reduced to 3 hours. For this case the air mass to be stored is about one half of the air mass to fill the tunnel which is the "proposed air-mass to be stored" in fig. 6. This quantity fits quite good to the daily mass to be taken from storage for jet simulation. If jet simulation tests are to be performed air storage has to be enlarged. The final capacity of the storage is a matter of the organisation of tunnel schedule. The volume to store the "proposed air-mass" is listed in fig. 6.

Fig. 7 shows how the energy costs are influenced by using air storages at different pressures. This figure gives only an idea and it is calculated for tunnel G with 209 MW tunnel power for max. demand and 43 MW for air supply. It is assumed that the pumps to fill the air storage are working only outside the tunnel time (fig. 7a). The total energy demand of 209 MW x 5 h + 43 MW x 5 h

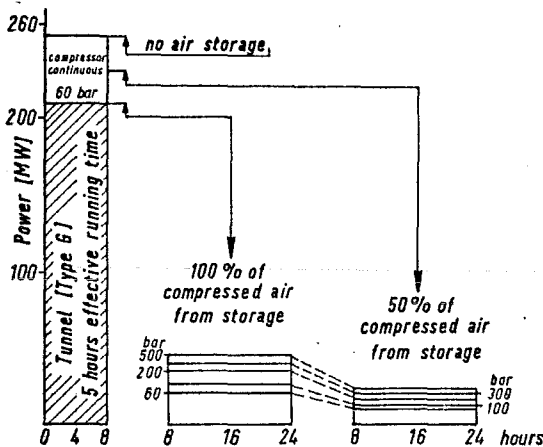
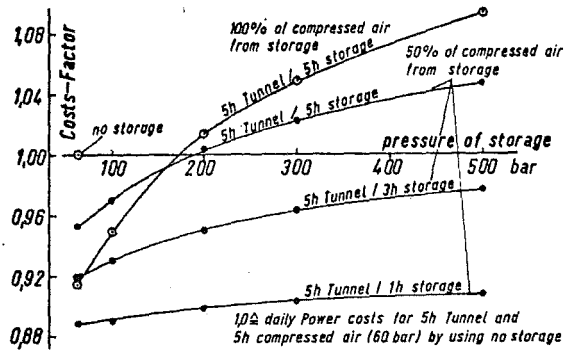


Fig. 7 Use of high pressure storage  
a) Power installation

(5 hour tunnel and 5 h simulation time) correspond to a costs factor of 1 (fig. 7b). If the total power demand is reduced by 17 % the cost per KWh is reduced by 8.5 % (which is the "100 % storage" case). But this relation depends on the location of the tunnel and can differ very much from the values which are given here.

Fig. 7b shows that for pressures higher than 180 bar air storage causes a costs factor higher than 1.0 if the 100 % storage case is considered as well as the 50 % storage case, both for 5 h tunnel



b) Costs factor (running costs)

and simulation running time. If simulation time is reduced to only three or one hour in the 50 % storage case costs factors are obtained which are always lower than 1 and are at least in the one hour case nearly independent from the pressure level.

A low pressure (40 ± 60 bar) buffer storage and a turbine between the high pressure storage and the buffer storage probably could recover a part of the high pressure energy and hence reduce the costs factor.

#### 4. Simulation Parameters

For the power requirements described in chap. 3 it is assumed that the jet velocities of model and full scale engines are equal. Until now it was discussed whether it is better to simulate velocity ratio, momentum ratio, pressure ratio or other parameters, since it was very difficult to obtain full scale velocities and temperatures for model engines. Turbofans and advanced fans have lower exit velocities and the main part of the jet is of ambient temperature. This makes it easier to simulate full scale velocities.

It is obvious that model engines for a large wind tunnel will be installed which at least will be able to simulate full scale velocities for the cold jet of turbofans and advanced fans. If this is fulfilled, momentum ratio, velocity ratio, pressure ratio and Mach number of the fan jet will be correct too.

With model scale  $M$  and  $K$  for pressurization the main parameters will reduce as follows  
 $(v_{jm} = v_{jf}; T_{jm} = T_{jf}; \rho_{jm} = K\rho_{jf})$

$$\text{mass flow} \quad \dot{m}_m = \dot{m}_f \cdot \frac{1}{M^2} \cdot K \quad (6)$$

$$\text{thrust} \quad F_{om} = F_{of} \cdot \frac{1}{M^2} \cdot K \quad (7)$$

$$\text{power} \quad P_{om} = P_{of} \cdot \frac{1}{M^2} \cdot K \quad (8)$$

The values discussed above are mean values. Nothing is said about the distribution of velocity, turbulence and temperature. These distributions affect the jet mixing with the ambient flow and the noise generation. Measurements for such investigations require higher qualities of the jet. The best way to obtain adequate jet qualities is to use similar principles for jet generation in the model engine as in the full scale engine. The influence of model scale, Reynolds number and Mach number is not yet investigated. Simulators which use equivalent principles for jet generation will have similar sensitivity to the ambient flow field. This behaviour will be of higher importance for advanced fans.

At the present state it is possible to produce good cold jets (fan-jet) but there are no adequate methods available for the hot turbine jet. For pure turbojet simulation hydrogen peroxyde ( $H_2O_2$ ) is used to produce the hot jet. This method has not yet been practiced for the hot jet of turbofans and advanced fans. Air heating outside the wind tunnel is used for pure jet testing only and not for engine simulation.

By using cold compressed air for driving a turbine, as it is done already for some powered nacelles, it is only possible to simulate either momentum ratios, mass flow ratios or velocity ratios.

The power requirement of the turbine in order to drive the fan is (assumed efficiency is 100%)

$$P = \dot{m} H_{ad} \quad (9)$$

The specific power per unit mass flow has the value

$$H_{ad} = \frac{\kappa}{\kappa - 1} R T_0 \left[ 1 - \left( \frac{p}{p_0} \right)^{\frac{\kappa - 1}{\kappa}} \right] \quad (10)$$

and is plotted in fig. 8 versus temperature for different pressure ratios.

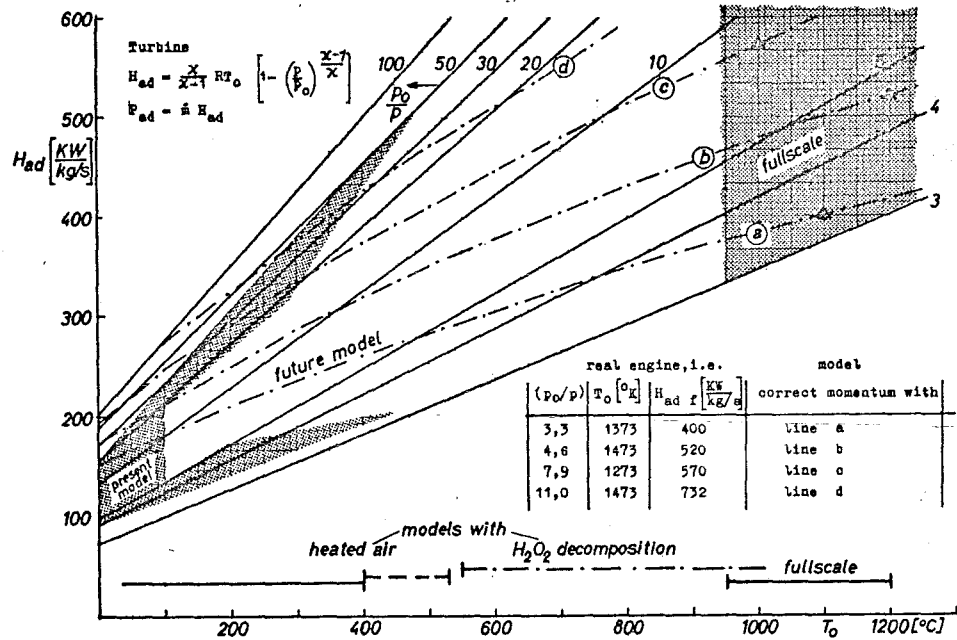


Fig. 8 Specific power per unit mass flow of an ideal turbine

The temperatures in full scale engines are higher than 1 000 °C. With pressure ratios of about  $p_0/p \approx 4$  the specific power per unit mass flow becomes  $H_{ad} \approx 400$  kW/kg/s. With cold air compressed to 100 bar ( $p_0/p \approx 100$ ) a specific power of only  $H_{ad} = 200$  kW/kg/s can be reached. In order to get the necessary power for driving the fan, the mass flow has to be increased for this example by a factor of 2. A correct simulation for all parameters is only possible when temperatures are also simulated. Heated and compressed air (200 ÷ 500 °C; 50 bar) enables specific powers which are similar to full scale engines. With heated air it is possible within certain limits for a turbine of given power to vary mass flow-, momentum-, temperature- and Mach number ratios. In addition, heating avoids icing problems and reduces diameter of air supply-pipes (smaller mass flow).

If for model and full scale engine constant specific power is used, then momentum ratio of fan jet to turbine jet is incorrect. But in most cases jet momentum (thrust) simulation is the primary requirement. For a correct momentum simulation mass flow, velocity and specific power of turbine jet become:

$$\dot{m}_m = \dot{m}_f \cdot \frac{1}{M^2} \cdot \sqrt{\frac{T_{jf}}{T_{jm}} \cdot \frac{R_{jf}}{R_{jm}}} \quad (11)$$

$$v_{jm} = v_{jf} \cdot \sqrt{\frac{T_{jm}}{T_{jf}} \cdot \frac{R_{jm}}{R_{jf}}} \quad (12)$$

$$H_{adm} = H_{adf} \sqrt{\frac{T_{jm}}{T_{jf}} \cdot \frac{R_{jm}}{R_{jf}}} \quad (13)$$

Lines of constant  $H_{adm}$  for correct momentum are drawn in fig. 8.

The ratio of hot jet mass flow to total mass flow is small so that an exact simulation of a hot inner part may be of minor importance. For advanced fans where the cold jet is covered by the hot jet, the influence of the hot part cannot be neglected for reasons of jet mixing with the ambient flow and noise generation.

In order to come to a full understanding to which extend temperature is of influence, methods for air heating in simulators must be developed.

## 5. Methods for Simulation in Atmospheric Tunnels

For engines which are listed in fig. 2 and types which are similar to these, suitable methods of simulation have to be found and put into action. The choice of any kind of simulator is affected by development schedule and budget considerations. Characteristics of these engine types are

turbojet	-	cold influx of small mass flow
	-	hot jet with high velocity
turbofan	-	cold influx of medium mass flow
	-	cold outer jet
	-	hot inner jet
advanced fan	-	cold influx of high mass flow
	-	cold inner jet
	-	hot outer jet

For basic studies and development of fundamental new airplanes mostly the final engine is still under construction. Therefore the final characteristics and definitions of geometry of the engine is not known during the current tests. Due to this fact some uncertainties arise with early simulation and a very exact simulation can be done only in the end phase of the airplane development.

The development of a simulator for exact simulation of several of the parameters listed in fig. 1 presuppose the accurate knowledge of these parameters.

The production requires very high expenses, is difficult and time consuming. Pure constructive development does not settle all problems. In wind tunnel tests the simulator has to run continuously over a long time and without much maintenance.

Therefore it is useful to start with simple model engines until better simulators are available. Tests with different types of simulators (free flow nacelle, extended cowl nacelle, blown nacelle and powered nacelle) have shown that the jet is not correctly simulated either by a free flow or by an extended cowl nacelle. It is desirable to obtain better simulators in an early state of development. Generally the question arises whether it is of advantage to transfer optimal jet characteristics which are found from model tests to full scale engine. This means that the engine manufacturer would have to build engines with predestined characteristics. This procedure is done for inlet configurations.

Tunnel tests for airplanes which are equipped with already existing engines can be performed with good earlier simulators from the beginning.

### 5.1 Simulation of the Inlet

For pure inlet investigations it is sufficient to suck in the exact mass flow (see (6)). With additionally simulated exact free stream velocity similar stream tubes and pressure distributions are obtained. Large suction pipes for high mass flows may influence the whole flow field.

Possible distortions have to be simulated too for engines with a small distance between the fan disk and engine inlet plane, especially if cross flow occurs. The simulation of such inlets seems to be possible only by using real fans.

### 5.2 Simulation of the Jet

#### a) Cold Jets

The compressed air system will be the best solution for pure jet investigations i. e. turbojet. High pressure level permits small supply pipes. The required power depends on model scale and engine type as discussed in chap. 3. Turbofans will need higher mass flows. The simulation of advanced fans with very small axial extension by compressed air is very difficult. The problem is to find a system which deflects high mass flow within small space.

## b) Hot Jets

Hot jets for turbojets and hot turbine exhaust of turbofans and advanced fans can be produced by the decomposition products of  $H_2O_2$ . Temperature of the jet is a function of the liquid  $H_2O_2$  concentration (max. temperature  $1\ 000\ ^\circ C$ ). In addition this hot jet could be mixed with compressed air. No principle scale limitations and/or pressure level limitations in the test section arise for this jet simulation device.

Heating of compressed air outside the model will raise difficulties by decreasing the material strength and by temperature effects on the measuring systems, i. e. strain-gage balances. The resulting large time constants due to heat losses delay fast procedures.

Other than the conventional used combustion chambers which can be installed inside the model or the model engine are not known. It would be useful to develop new small heaters for hot jet simulation and for increasing the enthalpy in turbine flow (fig. 8).

## 5.3 Simulation of Inlet and Jet

### a) Ejectors

Many types of ejectors are already used for the simulation of inlet and outlet flux. The disadvantage is that the mass flow ratio of inlet to outlet flux never reaches the value of the full scale model. This ejector technique enables quick and cheap simulation which has no limitations in terms of scale and pressure level. Therefore mass flow ratios should be improved by better utilization of the primary air flow. It might be possible to use a supersonic primary air flow, the energy of which could be increased by heating. Heating reduces the necessary primary mass flow.

In order to simulate characteristics of turbojets the ejector may be suitable. For turbofans this is valid only for the inner jet. Characteristic behaviour of the cold fan of turbofans and advanced fans cannot be simulated by ejectors. Therefore real fans are possible only.

### b) Powered Nacelles for Turbofan and Advanced Fan Simulation

Good characteristics for turbofans and advanced fans could be obtained with hub- or tip turbine driven fans. Momentum-, velocity- and mass flow ratios meet the values of full scale engines. Simulators of 145 mm overall diameter with hub turbine worked satisfactory. Design problems decrease if these nacelles can be built larger for larger wind tunnels.

In case of simulating jets for turbulence and noise measurements more details of the turbomachinery have to be transferred but the similarity laws are still unknown to a certain extent.

Advanced fan simulators of less than 150 mm in diameter are too small for examining overall aircraft characteristics with a complete model without scale and Reynolds number effects. Up to 300 mm diameter detailed flow studies on partial models are possible. Fans of about 600 mm diameter seem to be free of scale and Re-number effects.

Exact dependencies are not yet known. For a 1/6 scale model with fans of 265 mm in diameter discrepancies to full scale plane are measured. There are not enough results available to give exact values for minimum fan size. Because advanced fans scaled down to 150 mm in diameter have worked already, it is obvious that for larger wind tunnels the design problems will decrease.

In order to improve the momentum shares of the turbine jet which either can be a centered or covered jet one has to use higher pressures and higher temperatures according to fig. 8. It is proposed to install plants for pressures up to 50 bars and temperatures up to  $400\ ^\circ C$ .

Fans which are driven by electric or hydraulic motors are not adequate, because the power per unit volume is too small.

It must be pointed out that the time to develop, manufacture and calibrate these units is a multiple of that for simple types of compressed air jets or ejectors. The same is true for prices.

### c) Small Real Engines

Models with small real engines have not yet been tested in European wind tunnels. As far as model scale is large enough existing full scale engines can be used if type and front area thrust are suitable. At present time for medium wind tunnels front area thrust of small engines is not high enough. The reason for this may be the fact that for engines of this size there are no special requirements with regard to the front area thrust. The aim to model simulation would be small real engines in the order of magnitude of 500 N to 20 000 N, both the turbojet and the turbofan type.

In any case these engines should be developed by engine manufacturers, especially to perform free flight model tests in hovering and transition phase.

## 5.4 Test Facilities for Development and Calibration

For all above described methods for partial or total simulation of engines adequate test



rigs with universal connections to the power plant have to be installed. The power plant systems have to be large enough to supply wind tunnel and these test rigs as well.

The main tasks for these test rigs are to improve the simulators so that they are safe in operation for many tests, to get characteristics for static and flight conditions with parallel flow and cross flow.

For these tests a calibration wind tunnel is necessary with similar conditions as in the large tunnel.

It is irresponsible to produce results in a large expensive tunnel which are not based on exact knowledge of simulators.

## 6. Engine Simulation in Pressurized Tunnels

In fig. 9 those parameters are shown which are influenced by scale and pressure variations. Compared are values of full scale engines with models in atmospheric and K-times pressurized tunnels. Both tunnels have the same Re-number and velocities.

Full scale		large atmospheric tunnel ①	small pressurized tunnel ②	remarks
Pressure	$p = 1 \text{ bar}$	$p_1 = p$	$p_2 = K \cdot p$	tunnel conditions
Length	$l$	$l_1 = l \cdot \frac{1}{M}$	$l_2 = l_1 \cdot \frac{1}{K} = l \cdot \frac{1}{K} \cdot \frac{1}{M}$	
free stream velocity	$V_\infty$	$V_\infty 1 = V_\infty$	$V_\infty 2 = V_\infty 1 = V_\infty$	
Re - number	$Re$	$Re_1 = Re \cdot \frac{1}{M}$	$Re_2 = Re_1 = Re \cdot \frac{1}{M}$	
Jet velocity	$V$	$V_1 = V$	$V_2 = V_1 = V$	assumptions for perfect jet simulation
Jet temperature	$T$	$T_1 = T$	$T_2 = T_1 = T$	
tip speed	$u$	$u_1 = u$	$u_2 = u_1 = u$	
specific power	$H_{ad}$	$H_{ad1} = H_{ad}$	$H_{ad2} = H_{ad1} = H_{ad}$	
pressure ratio	$\frac{p_0}{p}$	$\frac{p_{01}}{p_1} = \frac{p_0}{p}$	$\frac{p_{02}}{p_2} = \frac{p_{01}}{p_1} = \frac{p_0}{p}$	
Ma - number	$Ma$	$Ma_1 = Ma$	$Ma_2 = Ma_1 = Ma$	characteristic engine data
rev p min	$n$	$n_1 = M \cdot n$	$n_2 = K \cdot n_1 = KM \cdot n$	
area	$A$	$A_1 = A \cdot \frac{1}{M^2}$	$A_2 = A_1 \cdot \frac{1}{K^2} = A \cdot \frac{1}{K^2} \cdot \frac{1}{M^2}$	
mass flow	$\dot{m}$	$\dot{m}_1 = \dot{m} \cdot \frac{1}{M^2}$	$\dot{m}_2 = \dot{m}_1 \cdot \frac{1}{K} = \dot{m} \cdot \frac{1}{K} \cdot \frac{1}{M^2}$	
thrust	$F$	$F_1 = F \cdot \frac{1}{M^2}$	$F_2 = F_1 \cdot \frac{1}{K} = F \cdot \frac{1}{K} \cdot \frac{1}{M^2}$	
power	$P$	$P_1 = P \cdot \frac{1}{M^3}$	$P_2 = P_1 \cdot \frac{1}{K} = P \cdot \frac{1}{K} \cdot \frac{1}{M^3}$	
power per unite volume	$\frac{P}{l^3}$	$\frac{P_1}{l_1^3} = M \cdot \frac{P}{l^3}$	$\frac{P_2}{l_2^3} = K^2 \cdot \frac{P_1}{l_1^3} = M \cdot K^2 \cdot \frac{P}{l^3}$	
total pressure	$p_0$	$p_{01} = p_0$ $p_{01} = X \cdot p_0$	$p_{02} = K \cdot p_{01} = K \cdot p_0$ $p_{02} = K \cdot X \cdot p_{01} = K \cdot X \cdot p_0$	fan turbine ( $T_{2,1} \neq T$ )

Fig. 9 Influence of model scale and tunnel pressure

In order to see the effects on engine simulation a complete jet simulation is assumed, i. e.  $v$ ,  $T$ ,  $u$ ,  $H_{ad}$ ,  $p_0/p$ ,  $Ma$  for engines are equal in both tunnels.

### 6.1 Simulation of the Inlet

Reasons mentioned in chap. 5.1 are valid for a pressurized tunnel too. In case of pure inlet measurements with "suction" a pump system is not necessary if the tunnel pressure is sufficiently high. Tunnel pressures of about 3 ÷ 5 bars are high enough to give high Ma-numbers in the inlet if the inlet is connected to the atmosphere. For reduced Re-numbers i. e. low tunnel pressure, additional suction is needed.

## 6.2 Simulation of the Jet

### a) Cold Jets

In atmospheric tunnels with compressed air jet, high pressures are used to keep supply pipes small. Only a portion of this pressure energy is necessary for jet generation. Comparing a pressurized and an atmospheric tunnel it can be seen from fig. 9 that mass flows are reduced by factor  $K$  and areas by factor  $K^2$ . If duct areas are scaled down by the same factor as the model the pressure in the duct has to be increased by factor  $K$ .

With this primary pressure increased by a factor  $K$  it is possible to generate the desired velocities.

A  $K$ -times loaded tunnel requires a  $K$ -times loaded compressed air system. The necessary mass flow is smaller by a factor  $K$ .

### b) Hot Jets

There are no principle difficulties to produce hot jets by the decomposition products of  $H_2O_2$ . For the pressurized tunnel a  $1/K$ -times quantity of  $H_2O_2$  is needed only. If heating occurs outside the tunnel difficulties increase very much. In addition to strength diminution due to temperature increase, higher loads are induced by higher primary pressures.

Combustion chambers inside the engines would be of benefit. These systems have to be developed for both atmospheric and pressurized testing.

## 6.3 Simulation of Inlet and Jet

### a) Ejectors

There are not additional principle problems for ejectors in pressurized tunnels. Only the pressure level of the ejector is higher so that again  $K$ -times larger primary pressures are required. To get exact information about the characteristics in a loaded wind tunnel, calibration measurements have to be performed at the same pressure level. If these tests are not carried out in the large expensive pressurized tunnel an adequate small pressurized calibration tunnel is necessary. Even static tests have to be performed at pressurized levels.

### b) Powered Nacelles for Trubofan and Advanced Fan Simulation

For the desirable complete simulation the above outlined values have to be simulated. In this case similar aerodynamic behaviour is present. Under these assumptions in a pressurized tunnel  $K$ -times smaller dimensions and  $K$ -times higher pressures as in atmospheric tunnel the variations which are listed in fig. 9 appear.

The  $M \cdot K$ -times dependency of the speed of rotation and the  $M \cdot K^2$ -times dependency of power per unit volume should be mentioned especially. The value  $M \cdot K$  is the total scale factor.

Limits for the speed of rotation seem to be reached in powered nacelles for models in tunnels with  $3 \div 5$  m width. For this reason a pressurized tunnel should not be smaller.

The power per unit volume increases in a pressurized tunnel by the factor  $K$  in addition to the total scale factor  $M \cdot K$ . For atmospheric tunnels in the order of magnitude  $3 \div 5$  m width, the maximum power per unit volume, which is obtainable today, is already used. It seems to be questionable if this increase of load is possible especially when tunnel pressures of 5 bar are required.

From an aerodynamic point of view the power could be raised if the primary pressure of model turbines would be enlarged by  $K$ . The result would be that pressures of  $K \cdot (20 \div 50)$  bar =  $100 \div 250$  bar have to be realized. Important for mechanical strain of engine components and sealing problems is the pressure difference. Operation pressures in such order of magnitude for complicated engines are unrealistic at present time.

### c) Small Real Engines

With the application of small real engines it was thought to make use of existing engines. They are not designed for  $K$ -times higher pressures. In other respect here it is valid too that all pressures inside the engine increase by  $K$ . In this case all aerodynamic characteristics remain constant.

## 6.4 Test Facilities

Here again chap. 5.4 is suitable. A corresponding calibration tunnel has to be pressurized too.

## 7. Resumé

The main results for the use of model engines in VTOL tunnels can be summarized as follows:

### 7.1 Aerodynamic Viewpoints

- The main parts of the engine should be simulated completely; i. e. geometry, free stream velocity (parallel- and cross flow), jet velocities, tip speed, pressure ratio, Ma-number, jet temperatures.
- Depending on time schedule and budget incomplete simulation is necessary also, i. e.
  - compressed air jets
  - inlet suction
  - ejectors
- Development is necessary for complete simulators, i. e.
  - powered nacelles (turbine driven fans)
  - small real engines (for thrust 500 - 20 000 N)
  - small air heaters
- Technical problems decrease in larger atmospheric wind tunnels. Power plants have to be designed according to the power requirement of chap. 3.
- In a pressurized tunnel the pressure level of the model engine increases proportional. The primary pressures for ejectors and powered nacelles increase in the same manner (see chap. 6).
- Pressure level of power plants for pressurized tunnels are a multiple of that for atmospheric tunnels. Successful development of small real engines for the considered tunnel pressures seems to be questionable.
- Small real engines use demands tunnel air exchange.

### 7.2 Power Plants and Test Equipment

Requirements for engine simulation are

- Compressed air supply systems
  - continuous compressor system
  - system to dry air (dew point - 100 °C)
  - high pressure air storage
- Heating system
  - H<sub>2</sub>O<sub>2</sub> system
  - heat exchangers (electric power, liquid or gaseous fuels)
- Vacuum systems
  - pump system
  - vacuum vessels
- Calibration test facilities
  - static test rigs
  - calibration tunnel
  - data acquisition system

### 7.3 Further Remarks

Only an experienced staff of scientists and engineers can solve the aerodynamic and technology problems which arise with development, design and application of such different techniques for model engine simulation.

## 8. Programme of Work

Work on engine simulation which has been done till now has shown that most of the methods could be improved. For a new large wind tunnel this leads to some important jobs which have to be tackled. Some of these jobs are touched in catch-words.

### 8.1 Further Development of Simulators

- Standardized units should be practiced.
- Burners ( $H_2O_2$ , liquid or gaseous fuels) to be built inside the models or inside the ducts, especially for increasing specific power and reducing drive-mass flow; avoiding icing; step forward to small real engines.
- Improvement of existing units for pressurized tunnels; investigations how far those models could be used under pressurized conditions.
- Development of test methods to get quick and characteristic engine/jet data; high precision balance with ducts for drive medium.

### 8.2 Examples for New Simulators

- Development of small real engines with front area thrust similar to full scale engines and thrust lower 40 000 N; similar inner aerodynamics for noise and turbulence measurements.
- Simulators, i. e. ejectors and powered nacelles driven by decomposition products of liquid  $H_2O_2$ .
- Small real highly loaded compressors and turbines for separately integrated propulsion schemes.
- Further and new development of advanced fans with similar aerodynamic characteristics; determination of scale factor limits and extrapolation laws.
- Engine and control systems for free flight models.
- Systems for thrust vectoring and thrust reversing.

### 8.3 Activities

- Extension of LaWs work for the installation of a development and calibration center as an additional facility to the large wind tunnel.
- In future more man power, time and costs for this subject have to be considered; international collaboration.
- More use of engine manufacturers know-how for the solution of aerodynamic and technology problems in the field of engine simulation.

## 9. LaWs Paper Concerning the Job "Use of Model Engines"

Crabtree, L. F.

Engine simulation for wind-tunnel models  
unpublished paper

The paper is giving a review of the present state of the art for various model engines. Some modern powered nacelles which are fans with driving hub turbine and some papers concerning the necessary test work are explained. The possibility of using ejector units is shown and some new types are published. For the field of lift-engine simulation some activities, techniques and datas are described. (12 ref.)

Wood, M. N.

The use of injector units for engine simulation on wind tunnel models at high speeds  
RAE/TR 71215

A simple onedimensional analysis of injector performance is presented in a form suited to the examination of the potential of injectors for simulating engine flow effects in wind tunnel tests at high speeds. The analysis reveals an interesting feature of the internal flow perhaps not previously appreciated, which could explain the unsatisfactory performance of earlier designs of injector unit for engine flow simulation at high speeds. It is concluded that the potential of injectors justifies a programme of experimental work to check the performance given by the theoretical analysis and to provide empirical factors that are required before a design procedure is possible. (5 ref.)

Jaarsma, F.  
Munniksmma, B.

NLR viewpoints on engine simulation in wind tunnels  
NLR/AH-72-04; unpublished paper

The most important questions concerning the inlet and exhaust flow field of VTOL system are given which have to be answered before a model with engine simulation can be defined. Principal techniques for representing the engines are stated i. e. direct suction and/or blowing, miniature turbine driven fan simulators, injector units and fan units driven by motors. A table gives a survey of four simulator configurations for the same engine showing certain specific data, advantages and disadvantages. For CTOL systems the report AGARD AR-36-71 (Feri, Jaarsma, Monti), part II on engine-airplane interference in transonic tests contents experience and viewpoints. Conclusions of this report are repeated. Further some remarks, assumptions for correct simulation and calculations on injector units are given. The conditions which cannot be matched are treated. (2 ref.)

Holmes-Walker, J. M.  
Kemp, E. D. G.  
Tipper, D. H.

An engine manufacturer's view of the low speed test facility requirements for future high by-pass ratio lift and propulsion engines  
HSA/Hatfield/Projects 1745/EDGK; unpublished paper

This note considers the facilities required for low speed tests (i. e. 0 to 100 m/sec) to determine the installed engine performance and the associated interference forces on the aircraft. The type of aircraft considered are subsonic civil aircraft for which the achievement of a low noise level is a major requirement, including conventional, RTOL, STOL and VTOL types. The chapters are "Reasons for changing the approach to engine testing" and "Test facility requirement" for propulsion and lift engine installation. (2 ref.)

Pike, M. R.

V/STOL aircraft propulsion aerodynamic test requirements  
RR (Derby engine division)/Installation research/MRP 1 PL; unpublished paper

This note considers potential future test requirements, from an engine manufacturers viewpoint, to provide design data for the propulsion engines of RTOL aircraft using conventional engines and V/STOL aircraft using vectored thrust engines and propulsion engines.

The purpose of this note is to give some indication of how nearly the foreseen requirements are likely to be met by existing test facilities and what need exists for new facilities.

Especially treated is the work for aero acoustics, intake-engine aerodynamic compatibility and airframe-engine aerodynamic compatibility.

Hurd, R

STOL transport aerodynamic test facilities - A powerplant viewpoint  
RR (Bristol engine division)/Powerplant aerodynamic department/  
GN 14958; unpublished paper

Main systems of powerplants for STOL transport and the different methods used for conventional aircraft with high lift devices, powered circulation wings, jet lift aircraft and rotating wing aircraft are listed. Tasks for testing ground effects, free air high lift performance, low speed internal/external powerplant aerodynamics, stability effects and cruise powerplant performance are given as well as the types of aerodynamic test emerging. Test requirements and the capability are pointed out. A time scale for the development of the first and second generation of STOL transport is given.

Pauley, G.

The effectiveness of alternative methods of simulation pylon mounted fan engines in use of high speed wind tunnel models  
ARA/Memo 130; unpublished paper

A variety of fan engine simulators have been used in tests at A. R. A. ranging from simple free flow nacelles, topowered nacelles in which a small high speed fan is driven by a high pressure air turbine. The effectiveness of the differing types is investigated. It is shown that properly designed free flow nacelles are in general better simulators than extended cowl nacelles, but that neither can represent model fan jetstream effects completely. (1 ref.)

Munniksmma, B.

Simulation of a fan engine in wind tunnel models  
NLR/AH-72-010-Provisional; unpublished paper

In this note the NLR viewpoint with respect to engine exhaust and inlet flow simulation are shortly given. From this viewpoint the design requirements of a turbine driving a fan are calculated, especially if  $H_2O_2$  is used to drive the turbine.

Institution visited	Persons met	Subjects discussed
NLR, Nordostpolder	Jaarsma, F.	Jet simulation by means of compressed cold and hot air or by the decomposition products of hydrogen peroxide ( $H_2O_2$ ). Facilities for hot jet simulation. Size of new low speed tunnels.
RAE, Farnborough	Küchemann, D. Bagley, J. A. Owen, T. B. Forster, D. N.	Work for job "Use of model engines"; Influence of tunnel pressurization on engine simulation. Air mass flow and pressure requirements for STOL models. Ejector simulation.
RAE, Bedford	Spence, A. Wood, W. Taylor, C. R. Hall, J. R.	Possibilities of engine simulation with ejector arrangements. Experience with powered nacelles.
ARA, Bedford	Pauley, G. Harris, T. Holmes-Walker, J. M. (HSA)	Methods of fan engine simulation used at ARA. Powered nacelles for jet simulation and calibration problems.
HSA, Hatfield	Kemp, E. D. G. Stephensen, A. Holmes-Walker, J. M. Böielle, P. L. Farley, H. C. Tipper, D.	Simulation methods of lift engines used at HSA with types of ejectors, fans and sucked/blown units. Problems of engine simulation in pressurized tunnels. Engine representation in tunnel testing.
BAC, Preston	Knott, P. G. Matthews, A. W. Wade, J. M.	Ejectors for lift engine simulation. Model and balance design. Simulation in pressurized tunnels.

Fig. 10 Visited Institutions

## WIND TUNNEL REQUIREMENTS FOR HELICOPTERS

I A. Simons  
Westland Helicopters Limited  
Yeovil, Somerset, England.

and

H. Derschmidt  
Helicopter Division, MBB  
Otto-Brunn/Munich.

## SUMMARY

An attempt is made to define those sizes of model which are most suited to various aspects of wind tunnel investigation of helicopters. The scaling laws and associated constructional problems of small-scale rotor systems are discussed. Tunnel sizes, taking into account interference effects, are suggested for various ranges of model size.

## NOTATION

a	(m/s)	speed of sound
b	(m)	wind tunnel test section breadth
c	(m)	rotor blade chord
D	(m)	rotor diameter
E	(N/m <sup>2</sup> )	structural elasticity
g	(m/s <sup>2</sup> )	gravitational acceleration
h	(m)	wind tunnel test section height
L	(m)	length
R	(m)	rotor radius
Re	(-)	Reynold's number
T	(N)	rotor thrust
V	(m/s)	velocity
W	(Kg)	aircraft mass
x	(-)	non-dimensional radius
$\mu$	(N.s/m <sup>2</sup> )	air viscosity
$\mu_x$	(-)	rotor tip-speed ratio
$\rho$	(Kg/m <sup>3</sup> )	air density
$\sigma$	(Kg/m <sup>3</sup> )	structural density
$\psi$	(rads.)	blade azimuth position, $\psi = 0$ downstream
$\Omega$	(rads/s)	rotor angular velocity

ISA International Standard Atmosphere.  
SL Sea Level

$$\text{Span Loading} = \frac{T}{D^2} \quad (\text{N/m}^2)$$

$$\text{Disc Loading} = \frac{T}{\pi R^2} = \frac{4}{\pi} \cdot \text{Span Loading} \quad (\text{N/m}^2)$$

## 1. INTRODUCTION

The details of the continuously varying flow environment encountered by a rotor blade as it rotates - which includes varying Mach and Reynold's numbers, incidence and sweep angles, reverse flow and dynamic stalling - and the associated blade flexural and torsional motions define to a very great extent the performance, vibration, noise and stability characteristics of a rotor system. There is however a virtual lack of fundamental knowledge of many aspects of the aerodynamic/dynamic behaviour of the helicopter rotor and consequently our ability to predict and improve rotor system characteristics is severely limited.

Any significant advances in our knowledge can only come from a proper programme of experimental work which, because of the inseparable nature of the various aspects of the rotor environment, must consist in the main of either full-scale or suitably detailed model rotor testing.

As rotorcraft capabilities improve and speeds increase the development costs escalate, especially if novel rotor systems are being considered. Possible configuration changes of the future include the use of very stiff, gyro-controlled, circulation controlled, stoppable, stowable and tilting rotors; the use of the new composite materials; utilization of various aeroelastic phenomena and 'fly-by-wire' concepts.

It appears necessary, more now than ever before, that proper and sufficient testing is undertaken. Future generations of rotorcraft must be more-or-less completely tested in the wind-tunnel before a commitment to full-scale manufacture and flight development is made - in much the same way as happens in the fixed-wing aircraft industry.

A number of recent papers (refs 1 - 7) have pointed out that, in order to promote any substantial advance in our knowledge of helicopter rotor behaviour, much more wind tunnel testing is required. Of course full scale flight testing has been, and continues to be, extremely useful but for a number of reasons (ref. 2) it is desirable to test rotary-wing systems in tunnels. Emphasis has been placed on two main areas:-

- (i) that small-scale models should be more accurately designed and manufactured and that more and better instrumentation is needed.
- (ii) that there is a European requirement for a large low-speed wind-tunnel capable of taking full-sized helicopter rotors.

## 2. MODEL SCALING LAWS

Any decision as to the suitability, or otherwise, of a certain size of model rotor for a particular investigation cannot normally be made without first considering the scaling laws and any difficulties in model design and construction arising from an application of these laws.

In order to achieve the same non-viscous incompressible aerodynamic characteristics on a model rotor as exist on the full-scale rotor which is to be simulated it is necessary for the aerodynamically important portions of the rotor (i.e. the blades) to be geometrically scaled.

Dimensional analysis, taking into account the viscous aerodynamic and dynamic effects, shows that, as well as geometric scaling, the following five parameters must be correct for complete simulation (refs. 2,7)

i)	Mach number	$V/a$
ii)	Reynold's number	$\rho VL/\mu$
iii)	Froude number	$V^2/gL$
iv)	density ratio	$\sigma/\rho$
v)	elasticity ratio	$E/\rho V^2$

Before discussing the relevance of these parameters it must be noted that only wind tunnels utilising air at atmospheric pressure are being considered here. Other tunnel fluids and pressures will be briefly mentioned later.

### 2.1 Mach number

Compressibility effects on aerofoil section characteristics are very extensive, the lift-curve slope, maximum lift coefficient, stalling behaviour, profile drag and pitching moment all being susceptible to Mach number variation especially at the high subsonic - even transonic - Mach numbers encountered over the very important outboard regions of rotor blades. Thus correct simulation of Mach number is a prerequisite for aerodynamic accuracy and hence for the great majority of rotor tests. "Mach scaling" naturally implies a model tip-speed the same as full-scale (180 - 240 m/s) and a wind tunnel capable of covering the whole full-scale flight speed range (up to 130 m/s).

### 2.2 Reynold's number

The use of a "Mach scaled" model rotor however prohibits the correct simulation of Reynold's number (refs. 2,4,5,8). The importance of this parameter to rotors is not completely understood although its significance to two-dimensional aerofoil characteristics is well known.

The Reynold's numbers of full-scale helicopter rotor blades may be expressed

$$Re = \frac{\rho}{\mu} \Omega R c (x + \mu_x \sin \psi)$$

where, to a fair degree of accuracy, the parameter  $\Omega R c$  may be related to helicopter size thus

$$\Omega R c \approx 1.24 \cdot W^{\frac{1}{2}}$$

Hence  $Re(ISA, SL) \approx 8.5 \times 10^4 \times W^{\frac{1}{2}} \times (x + \mu_x \sin \psi)$

The range of Reynold's numbers encountered in practice is illustrated in Figure 1.

A small 'Mach scaled' model rotor of about three metres diameter will have blade tip Reynold's numbers of the order of 1-2 million, which is certainly a region where considerable changes in aerofoil characteristics (notably  $C_{Lmax}$ ) with Reynold's number variation can be expected. The use of transition strips to ensure turbulent flow has been well proven in fixed wing aerodynamic testing and the same techniques can be used of course in rotary-wing studies although their efficacy in this field has not been verified to any great extent.

In using small models it must be accepted therefore that the Reynold's number is incorrect and that the consequences of this are to a large extent simply unknown but, at the same time, it must be noted that there is little information that suggests that Reynold's number plays an important part in defining helicopter rotor characteristics; at least in the normal regime of operation.

### 2.3 Froude number

The Froude number expresses the ratio of body inertia forces to gravitational forces acting on the body. This parameter cannot be simulated correctly with a "Mach scaled" model rotor and the gravitational terms are effectively reduced in magnitude.

For rotors with the disc plane substantially horizontal the weight forces act in the blade flapping plane with a constant value and, as the flapwise aerodynamic and centrifugal loadings on a rotor blade are usually far in excess of the blade weight, these gravitational forces can usually be ignored. In fact for conventional rotors a 50% error in Froude number leads to only about 0.1 degree discrepancy in blade coning angle. However it must be borne in mind that Froude number may become an important parameter when considering 'off-loaded' rotors at high tip-speed ratios or 'stoppable' rotors.



Froude number is much more significant to rotors which operate with their disc plane vertical. In this case the gravitational forces act as a once-per-revolution exciting force in the blade lag sense. The phenomena of air and ground resonance and whirl flutter - all potentially disastrous instabilities - are very dependent on the lagwise behaviour of rotor blades, and thus in any investigation connected with these phenomena it would be unwise to ignore Froude number effects.

#### 2.4 Mass and elasticity ratios

It is apparent from the previous definitions of the five nondimensional scaling parameters that for a "Mach scaled" model rotor, the structural density and modulus of elasticity of the model system should be identical to the full-scale values in order to ensure similar dynamic characteristics.

These structural parameters define the rotor blade normal mode shapes, associated natural frequencies and modal inertias which in turn define to a greater or lesser extent rotor performance, stability, loading and vibration characteristics. An obvious method of ensuring correct mass and elasticity values is to scale down exactly the full-scale manufacturing techniques, using of course the same materials. It is worthy of note here that, if this procedure is followed, then the stresses in the rotor system are the same as at full-scale.

Naturally this method of model fabrication could be very difficult and expensive and it is fortunate that such exactitude is not always necessary and in many instances it is sufficient if only a few (or even one) blade modes are correctly simulated.

#### 2.5 Pressurised wind tunnels

Pressurised wind tunnels and those using a gas other than air as a working fluid have not been mentioned hitherto, and will now only be briefly covered since it appears to be generally accepted that the consequential problems of model rotor design and construction are substantially increased (refs. 5,9,13).

Pressurisation of an air tunnel enables considerably higher Reynolds's numbers to be achieved with small scale models. However wind tunnels are generally limited to pressures of 2 or 3 bars which, although allowing a most desirable increase of Reynold's number, is not enough to ensure correct simulation of Reynold's number on 1/4 or 1/5 scale models (3 or 4 metres rotor diameter).

But there is an additional advantage in using pressurised tunnels for rotor investigations - outside Reynold's number considerations - and this is the ability to examine altitude effects. As the (full-scale) blade density and elasticity ratios change with altitude different rotor models are required if behaviour at various altitudes is to be investigated in an atmospheric tunnel. The design of a model rotor such that its use in tunnel at high pressure simulates full-scale sea-level conditions, allows altitude effects to be studied simply by decreasing tunnel pressure. Of course there is also a Mach number variation with altitude due to the change in sonic velocity with temperature but this effect is small, in comparison with the density and elasticity ratio variations, and can be taken into account by slight adjustments to the rotor rotational and tunnel speeds or by a change in tunnel temperature (ref. 13).

The use of a refrigerant gas as a tunnel working fluid (refs. 9,13) provides added advantages in that the correct Mach and Reynold's numbers could be achieved on 1/4 or 1/5 scale models with tunnel pressures of less than three bars. In fact the possibility also exists of arranging model scale and tunnel pressure such that the Froude number is also correctly simulated. However, as only air tunnels are under consideration by the Law's groups, this topic will not be discussed further except to state that there are a number of practical problems associated with the use of refrigerant gases.

It may be concluded that, although pressurised tunnels with air or refrigerant gases offer the possibility of improved or exact simulation with small scale models, any rotor modelling problems would still exist and most probably be quite exaggerated. Certainly a considerable programme of work in the modelling field would have to be initiated if the full advantages of such pressurised tunnels for rotor testing were to be realised.

### 3. REDUCED VERSUS FULL-SCALE TESTING

The following discussion attempts to clarify the applicability, and possible merits or drawbacks, of various sizes of wind tunnel models to the investigation and simulation of full-scale rotary-wing systems.

There are two obvious categories of model:- the full-scale, which would probably be the actual 'flight hardware' rotor system, and the reduced-size model, which must be specially designed and built.

#### 3.1 Reduced scale models

It is assumed here that all reduced size models have geometrically scaled blades, some form of control system for varying the collective and cyclic blade pitch angles, and are 'Mach scaled'.

Now reduced scale models cannot simulate full-scale Reynold's numbers, although the use of a large model (approaching full-size) or transition strips on the blades may reduce any discrepancy to negligible proportions. Fortunately incorrect Reynold's number is not too much of a limitation as there is no great evidence to suggest that the effects are important in the normal operating regimes of helicopter rotors. On the other hand it is perhaps to be expected that the maximum stall limited thrust (and corresponding power requirements) of a small scale model may not correlate too well with the full scale rotor values. In such cases recourse to the sophisticated computational procedures commonly available today, along with rotor blade aerofoil section characteristics for the appropriate Reynold's numbers, would most probably predict the order of magnitude of the effects attributable to Reynold's number.

Certainly it would be unwise to insist on full-scale rotor tests merely for the purpose of having the correct Reynold's number. It is suggested that, if more information in this area is required, a series of specially designed experiments with non-representative rotor models would be more appropriate. For instance a rotor with extremely stiff blades (as a propeller), such that dynamic effects are drastically reduced, could be tested in a pressurised wind tunnel at various pressures.

Gravitational forces will be considerably underestimated in all small Mach scaled models but, fortunately, they can probably be ignored in most cases. In those investigations specifically concerned with gravitational effects, such as the lag plane behaviour of rotors with their disc vertical, either full-scale models or 'Froude scaled' models will probably be required.

It is possible to identify within the category of reduced-scale models two types:- the 'generalised' and the 'detailed' model. The former type of model is not normally a correct simulation of the full-scale system in all its details but only in respect of a selected number of primary features, whilst the latter is as correct a model in any many aspects as possible. The generalised model is used to gain information on the overall characteristics of the rotor system, and to study various aspects of its working state and behaviour in some detail, although specific items of information are not necessarily directly applicable to the full-scale rotor. In the case of 'detailed' models though it is intended that the majority of model results should be directly transferable to full-scale.

Of course there is no hard and fast demarcation line between the two types of model but nevertheless such a division is of help when considering the problems of reduced scale model design and fabrication.

### 3.1.1 'Generalized' reduced scale models

For many generalised investigations - in the sense described above - it is not essential for the model structure to be exactly similar to the full-scale rotor system. In such cases it is often sufficient if the model blade structural characteristics are correct only to the extent that the integrated effect in the fundamental flapping (and lagging) modes is adequately represented; that is the blade Lock's number and natural frequency is correct. In fact, for conventional articulated rotor systems the blade elasticity may often be ignored to a large extent, although in the case of hingeless rotors where the elasticity of the hub/blade root regions plays a primary role in defining the fundamental flapping mode the elastic effects must be scaled. However it is not essential to geometrically scale the hub/root areas, as they are not of particular aerodynamic importance, and this may ease the scaling of the elastic effects to some degree.

Generalised models, although perhaps reproducing full-scale behaviour quite satisfactorily under most testing conditions, could well behave in a misleading manner under certain extreme conditions when, for example, the higher elastic blade flexural and torsional modes may become very important.

It should also be remembered though that some rotor systems possess blade and/or control system flexural and torsional properties which affect the overall, as well as the detailed, aspects of rotor system performance. Obviously for this type of rotor simply scaling the fundamental modes is not sufficient and the model design and construction may well become very complex and difficult.

The relatively simple generalised model can be successfully built at very small sizes but feasibility of model construction is not the only criterion to be considered. Instrumentation of wind-tunnel models is also very important. In rotor work it is desirable to measure not only the overall mean forces and moments but also the oscillatory components, the blade deflections and stresses and the pressure distribution over the blade. This latter requirement in particular imposes certain limitations on the size of model blades because of the difficulties involved in inserting sufficient pressure transducers into small blades, without unduly compromising the blade structure or aerofoil section. A popular model rotor size is about 3 metres diameter which, besides allowing considerable instrumentation, results in a quite robust and manageable structure.

### 3.1.2 'Detailed' reduced scale models

Detailed models are those which, as far as possible, have the correct mass and elasticity characteristics throughout the structure so that the rotor system dynamic behaviour is accurately portrayed. A true scaling down of the full scale constructional techniques is undoubtedly difficult and expensive especially for blades with extruded spars although it may be somewhat easier for fabricated blades, such as those of the Westland Lynx, or for fibre-glass blades as used on the Boelkow Bo105. It is thought that the Lynx blade could be manufactured in this way at 1/2 scale and perhaps, after some development of techniques, even at 1/3 scale but this would seem to be the limit. One-quarter scale models of plastic, glass or carbon blades may be possible but, again, some development work would be necessary.

A more promising approach appears to be to temper the technique of exact reproduction with the use of other materials and methods in certain areas of difficulty e.g. the trailing edge of blades. (refs. 10,18). Extremely good dynamic similarity has been achieved in this way with model rotors of some 3 or 4 metres diameter.

Materials and techniques other than those used at full-scale are often used in an attempt to reproduce the correct dynamic properties (refs. 11,12) but in general it does not appear that such methods are as accurate as those based on the full-scale principles of construction.

Successful though such techniques are it must be noted that, in the main, they have been aimed at achieving dynamically similar blades for articulated rotors. The design and manufacture of control systems and hingeless rotors at small scale have not received enough attention in the past.

Special care must be taken in the modelling of the control system, particularly as regards its stiffness characteristics, as most of any blade torsional displacements occur in the control system. Torsional behaviour is of very considerable consequence to overall rotor performance and stability and control as well as to the details of blade loadings and motion. The elastic properties in the area of the hub, blade root, feathering hinge and control system can have pronounced effects on hingeless rotors in particular (refs. 14,15,16) and, in order that these effects may be studied confidently with a model, it is essential that the details of the full-scale rotor system are reproduced very precisely. Furthermore there is a growing interest in utilising blade elastic torsional deflections as a beneficial influence and it is to be expected that a correct representation of control systems will be increasingly demanded of model rotors. Recent work at Boeing-Vertol (refs. 17,18) indicates that it is possible to simulate control system stiffness on small scale models, at least to a first order of accuracy, although there is still considerable scope for improvement.

Instrumentation requirements for 'detailed' reduced scale models are much the same as for 'generalised' models, although it is most likely that a greater number of measurements would be desirable. Now however considerably more care must be taken to ensure that the inclusion of instrumentation into the rotor system does not alter its dynamic characteristics.

It may be concluded that very reasonable dynamically scaled model rotors as small as 3 or 4 metres diameter, even including to a first approximation the control system, are certainly within our present capabilities-although it must be noted that good models are a product of good staff having sufficient resources (ref. 17). However if a high level of confidence is required, especially in the area of hingeless rotors with 'active' elastic torsional behaviour of the blades/control system, it would appear beneficial to have larger models of perhaps 1/3 or 1/2 full size - i.e. 5 to 8 metres diameter. Even at this relatively large scale modelling problems may still exist and the Reynold's number will be incorrect. It seems unlikely that European helicopter companies will embark on the construction of such sophisticated models of existing or projected rotor systems due to the sheer design and development effort involved. The costs of building up such a capability is obviously high and the number of qualified design staff available may not be enough to allow a company to devote the requisite manpower to such a venture.

There is a body of opinion (refs. 1,3,4,5,7) which suggests that facilities for the testing of full-scale rotors are required if really detailed investigations of rotor systems are to be undertaken at all; although it must be noted that there is also some qualified opposition to these views (ref. 6).

### 3.2 Full-scale models

There are a number of advantages that full-scale rotor system, or complete aircraft, testing has over reduced scale testing. The Mach, Reynold's and Froude numbers are always correct as are the structural properties. Development and installation of the necessary instrumentation may well be easier at full-scale than with small scale models, whilst at the same it may serve as a development phase for some flight test instrumentation.

Tests at full-scale are especially attractive if there is some doubt as to the ability to model at small scale which is of particular significance in the area of control systems, especially if the elastic properties of the rotor system are being used in an active manner. In the case of novel rotor systems it may well be desirable to test at full-scale because the details of the system may not be well enough defined before the actual full-scale manufacturing techniques have been sorted out.

Full-scale tests can be compared with small scale model tests thus allowing the accuracy of model constructional techniques and Reynold's number effects to be assessed. Comparison with flight test results would also be very valuable especially if the full scale rotor system and associated instrumentation used in the tunnel investigations was used in the flight tests.

In connection with the development of a particular aircraft investigations of vibration levels, engine levels, engine intake airflow, drag reduction, ad-hoc modifications etc. could be undertaken in closely controlled manner and probably more cheaply than by flight test.

## 4. WIND TUNNEL INTERFERENCE

Prior to a decision on the wind-tunnel required to test a particular size of rotor or on those sizes of rotors which may be tested in a particular tunnel, some knowledge of the interference to be expected is desirable.

Heyson has made available to the LaW's group a considerable amount of information on tunnel/rotor interference (ref. 20) and this is shown in Figures 2 and 3, where the span loading ( $T/D^2$ ) is plotted against rotor diameter/tunnel breadth ratio ( $D/b$ ) for the two tunnel height/breadth ratios of 1/2 and 2/3. The interference criterion adopted is a flow angle error of  $5^\circ$  at the centre of the rotor.

A particular value of span loading of  $240N/m^2$  has been chosen as fairly typical of medium helicopters in level flight, and the corresponding variation of permissible diameter/breadth ratio with tunnel speed, using the results of the previous figures, is shown in Figure 4. Also plotted in this diagram are the curves pertaining to a span loading of  $360N/m^2$  which applies to large helicopters or to high thrust (manoeuvring) conditions on smaller helicopters. Extrapolation from these results allows similar curves to be drawn for a tunnel height/breadth ratio of 3/4 (Figure 5) which is the value chosen by the LaW's group (ref. 21).

It is apparent from these figures that the permissible diameter/breadth ratio is primarily determined by the velocity at which it is desired to test the rotor rather than its span loading, provided this is greater than about  $200N/m^2$ . Thus in the following only two specific span loadings will be considered - 240 and  $360N/m^2$  - even though tests at high thrusts (perhaps two or three times the normal loading) is a most important part of rotor experimental programmes.

Referring to Figures 4,5 it is seen that at high speeds fairly large diameter/breadth ratios (up to 0.8) are possible, although with such ratios the minimum speeds at which accurate testing can be done is then also quite considerable. Thus it is the minimum speed at which tests are desired that defines the maximum diameter/breadth ratio.

It is suggested that a minimum test velocity of about 30 m/s may be often acceptable, in which case a diameter/breadth ratio of the order of 0.55 - 0.6 is suitable. However, by making use of the settling chambers that most conventional wind tunnels have, it is possible to test at the lower speeds without compromising the diameter/breadth ratio. Of course it must be remembered that the flow quality in the settling chamber is unlikely to be as good as that in the main test section.

A settling chamber of the same height/breadth ratio as the test section and with a cross-sectional area four times as great is assumed for illustrative purposes. Taking a maximum test section velocity of 130 m/s (as suggested in refs. 3,4,5,6,21) and thus a maximum settling chamber velocity of  $32\frac{1}{2}$  m/s it is seen that a diameter/breadth ratio of 0.6 (i.e. 0.3 in the settling chamber) allows the rotor to be tested from about 10 -  $32\frac{1}{2}$  m/s in the settling chamber and from  $32\frac{1}{2}$  - 130 m/s in the normal test section without in either case contravening the interference limits. Figure 5 illustrates the use of the two tunnel working sections.

It must be noted however that these interference limits do not take account of any flow separation phenomena which may well impose an additional limit at very low velocities (ref. 20).

The effect on diameter/breadth ratio of varying tunnel maximum velocity and settling chamber area/test section area is easily determined from the curves of fig. 5. These results are shown in figure 6. As before the assumption is made that there is no "velocity gap" between the settling chamber maximum velocity and minimum velocity suitable in the test section. It is seen that in order to preserve a particular diameter/breadth ratio with a larger settling chamber the maximum tunnel velocity must be considerably increased. If however the maximum velocity is fixed then a larger settling chamber is accompanied by a reduction in the diameter/breadth ratio.

A rotor diameter/tunnel breadth ratio of 0.6 is taken as a basis for the following discussion, but it must be remembered that values for the span loading, minimum test speed required, tunnel maximum velocity and settling chamber area/test section area ratio other than those assumed above may affect to some extent the value of diameter/breadth ratio which is desirable.

#### 5. WIND TUNNEL REQUIREMENTS FOR HELICOPTERS

The tunnels considered in this section are assumed to have a test section of height/breadth ratio of 0.75 and, from the previous chapter, a rotor diameter/tunnel breadth ratio of 0.6. It is to be remembered that this diameter/breadth ratio implies a lower speed suitable for testing in the main tunnel test section of about 30 m/s. The maximum test section velocity must also be at least 130 m/s if the complete speed range of helicopters is to be covered (refs. 4,5,6,21).

Three ranges of rotor size have been identified in chapter 3:- 3-4 metres diameter for many small scale models, 5-8 metres diameter for certain detailed models, and full-scale. The wind tunnels required to accommodate rotors of 3-4 metres diameter will have tunnel breadths in the range of 5-7 metres, whilst those suitable for testing the larger models of 5-8 metres diameter will be 8-13 m in size.

Sizes of wind-tunnels capable of taking full scale rotor systems or aircraft cannot be defined without some reference to the sizes and roles of rotary-wing aircraft now in existence and expected in the future. Some insight may be gained from the relationship between helicopter weight and rotor diameter which, to a fair degree of accuracy, may be expressed.

$$D \approx 0.84 \times W^{\frac{1}{3}}$$

Fast manoeuvrable helicopters of the present appear to be limited to below about 10000-11000Kg all-up-weight - i.e. their rotors are of 19m diameter or less. The heavier helicopters with larger rotors tend to be transport or crane machines which are not designed for particularly high speeds, although there is evidence to suggest that high performance helicopters of the future will be somewhat larger than 10000Kg.

In order to be able to test the majority of full-scale rotors, the need is for a large wind tunnel with a test section width not less than 25m (Refs. 3,4,5,6). Such a tunnel would allow testing of 15 m diameter rotors from about 30 m/s upwards, whilst rotors of 18 or 19 metre diameter could also be tested at the higher velocities. However it is considered (Ref. 3) that such a large facility is not warranted for the European helicopter industry alone as they are unlikely to make use of it for more than about one-third of the time. Without a lot of support from the fixed-wing aircraft industry such a tunnel facility is just not possible.

If a large wind tunnel of 25 m or thereabouts were available then this tunnel, along with the tunnels of 5-7 metres for testing 3-4 metre diameter model rotors, would satisfy most of the needs of the European helicopter industry.

However, if the large 25m tunnel were not built then, besides the 5-7 metre tunnels of the order of 8-13 metres would be required for the larger model rotor necessary for detailed testing. At the same time it would be necessary for more emphasis to be put on, and resources into, the establishment of sophisticated modelling facilities.

The range of large low speed tunnels under consideration by the LaWs Group include 15 and 18 metre tunnels (ref. 21). A choice of tunnel in the size range would allow rotors of up to 9-11 metres diameter to be tested. This diameter spectrum encompasses full scale rotors of small helicopters (up to about 2500 Kg) and the larger detailed model rotors considered previously. Again the fixed-wing aircraft industry's support for such a tunnel would be necessary, as would the helicopter industry's

support of increased modelling facilities. Nevertheless a European tunnel in the 15-18m category would provide a sorely needed full-scale testing capability - albeit somewhat limited. In fact it is to be expected that novel rotor systems which make use of new materials, control systems or changes in aerodynamic operation will appear over the next few years; and in such instances it will probably be deemed prudent to build a "demonstrator" vehicle before proceeding further even if wind-tunnel tests etc. prove satisfactory. A small helicopter suitable for use as a demonstrator would probably be of the order of 2000-2500 Kg all-up-weight with a rotor diameter of some ten metres. It would of course be most desirable if the actual flight rotor system of any demonstrator aircraft could be thoroughly tested in a wind tunnel prior to flight and this would certainly be feasible if a tunnel of the order of 18m were available.

Before finishing this discussion of wind tunnel requirements for helicopters there are a couple of fundamental points peculiar to helicopter rotors that are worthy of mention. Changes in the operating altitude, and hence air density (see Chapter 2), or the execution of manoeuvres involving pitching or rolling rates, which bring gyroscopic forces into play (ref. 19), can give rise to significant variations in the aerodynamic and/or dynamic behaviour of rotors. Pressurised tunnels and/or specially designed rotor models would allow study of the influence of altitude, but the use of full-scale flight hardware rotor systems in tunnel tests would of course preclude such a study unless the tunnel working pressure could be reduced below atmospheric. The simulation of pitching or rolling angular velocities with a wind tunnel model is obviously almost impossible and these manoeuvre conditions will remain a province of flight testing.

## 6. CONCLUSIONS

Much valuable experimental work can be done with rotor models of 3-4 metres diameter for which wind-tunnels of 5-7 metres breadth with maximum velocities of the order of 130 m/s are required. The majority of generalized rotary-wing investigations will be done with such models. The improvement of modelling techniques to allow detailed simulation of rotary-wing structures and control systems would require a considerable expansion of resources in the area of modelling facilities and, with the present size and organisation of the European helicopter industry, this appears somewhat unlikely.

It is recommended that a large wind-tunnel of some 25m test section breadth with a maximum velocity of at least 130 m/s should be provided to enable the majority of helicopter rotors to be tested full-scale.

If so large a tunnel cannot be provided then a tunnel of 18m breadth would be of considerable use to the helicopter industry. Such a tunnel would enable rotors suitable for helicopters up to about 2000-2500Kg all-up-weight to be tested full-scale; and so provide a means of testing novel rotor systems of sufficient size to be used on a "demonstrator" flight vehicle.

Either facility however must be supported in the main by the fixed-wing aircraft industry.

## REFERENCES

1. J.P. Jones "The Wind Tunnel Needed for Rotorcraft Research" A.R.C. 31949, P.L.574, March 1970.
2. I.A. Simons "Some Objectives and Problems Associated with Model Testing", The Aeronautical Journal, Vol.74, No.715, p539, July 1970.
3. J.P. Jones "Factors Affecting Choice of Wind Tunnels for Rotorcraft", Appendix to "Views of the U.K. Aerospace Industry of Future Wind Tunnel Facilities", Aerotest Paper, May 1972.
4. I.A. Simons "Wind Tunnel Requirements for Helicopters", LaWs Paper 69, May 1972.
5. H. Derschmidt "The Use of Rotor Models of Rotary Wings", LaWs Paper 76, April 1972.
6. J. Sculez-LaRiviere "The Requirement for a Large Wind Tunnel for the Future Development of Helicopters" A Contribution to the LaWs Group, September 1972.
7. I.A. Simons "Wind Tunnel Requirements for Helicopters" LaWs Paper 107 (and appendices 107a, 107b), September 1972.
8. M. Philippe "Note Provisoire sur les Regles de Similitude pour Maquette de Rotors en Soufflerie". LaWs Paper 75, April 1972.
9. C. Lee "Weight Considerations in Dynamically Similar Model Rotor Design" Proceedings of the 27. Annual Conference of the Society of Aeronautical Weight Engineers, Paper 659, May 1968.
10. E.A. Fradenburgh "Development of Dynamic Model Rotor Blades for High Speed Helicopter Research" Journal of the American Helicopter Society, Vol.9, No.1, January 1964.
11. A. Anscombe "Experience at R.A.E. in the Construction of Dynamically Scaled Model Rotor Blades" LaWs Paper 51, February 1972.

12. J. Higgs  
M.C. Jones "Semi-Rigid Rotor Model Helicopter Study - Preliminary Rotor Construction Research"  
British Hovercraft Corporation Ltd., Experimental and Electronic Laboratories, Report X/O/1377, July 1970.
13. D.G. Long  
I.A. Simons "Some Thoughts on the Use of Pressurised Wind-Tunnels and Refrigerant Gases to Achieve Similarity Between Full-Scale and Model Rotors".  
Westland Helicopters Limited, Research Memo.61, April 1970.
14. G. Reichert  
H. Huber "Influence of Elastic Coupling Effects on the Handling Qualities of a Hingeless Rotor Helicopter"  
Paper presented to the 39. AGARD Flight Mechanics Panel Meeting on 'Advanced Rotorcraft', September, 1971.
15. J. Gallot "Effects Aeroelastiques sur les Qualites de Vol d'un Rotor Rigide"  
AGARD CP46, 1969.
16. R.E. Hansford  
I.A. Simons "Torsion-Flap-Lag Coupling on Helicopter Rotor Blades"  
Westland Helicopters Ltd., Research Paper 405, September 1971.
17. F. Harris "Private Communication", August 1972.
18. C.O. Albrecht "Factors in the Design and Fabrication of Powered Dynamically Similar V/STOL Wind Tunnel Models"  
Paper presented at the American Helicopter Society Mid-East Region Symposium 'Status of Testing and Modelling Techniques for V/STOL Aircraft', October 1972.
19. C.L. Livingston "Prediction of Stability and Control Characteristics of Rotorcraft"  
Paper presented at the American Helicopter Society Mid-East Region Symposium 'Status of Testing and Modelling Techniques for V/STOL Aircraft', October 1972.
20. M. Carbonaro "Review of Some Problems Related to the Design and Operation of Low Speed Wind Tunnels for V/STOL Testing"  
LaWS Paper 113, September 1972.
21. A. Spence  
B.M. Spee "European Needs for Low Speed Tunnels"  
LaWS Paper 46B, 1972.

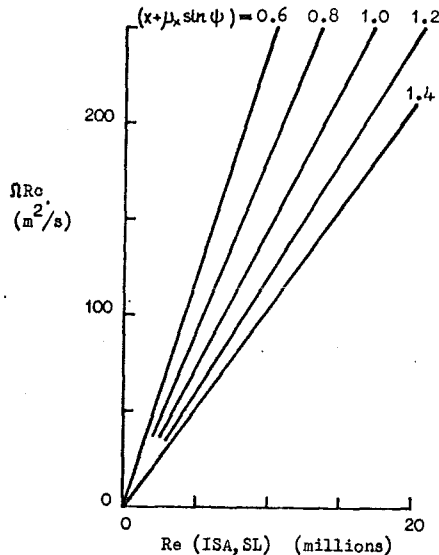


FIG. 1 THE REYNOLDS NUMBERS OF ROTOR BLADES

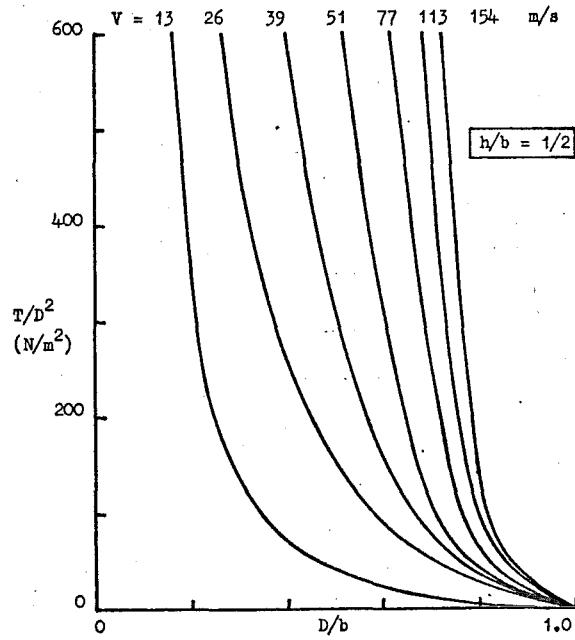


FIG. 2 WIND TUNNEL INTERFERENCE LIMITS

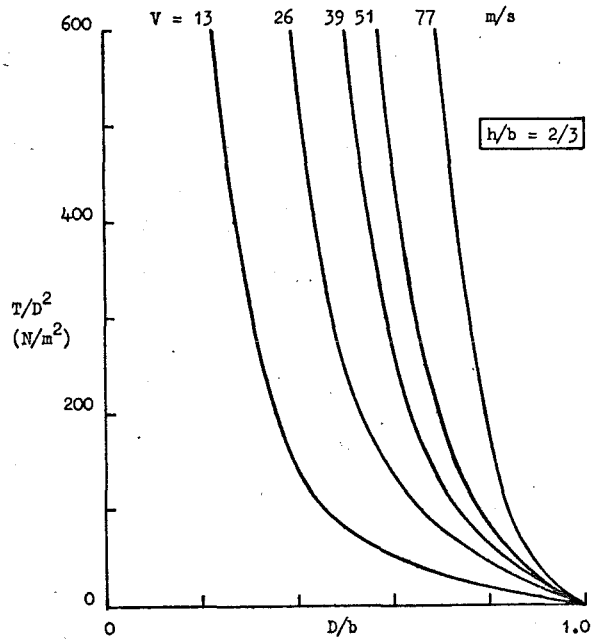


FIG. 3 WIND TUNNEL INTERFERENCE LIMITS

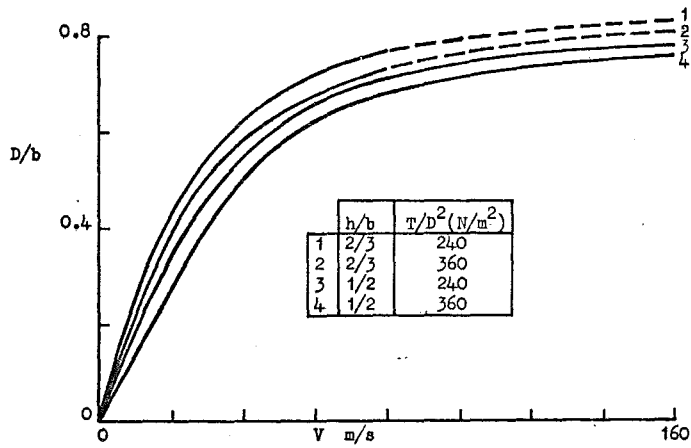


FIG. 4 TUNNEL INTERFERENCE LIMITS AT PARTICULAR SPAN LOADINGS

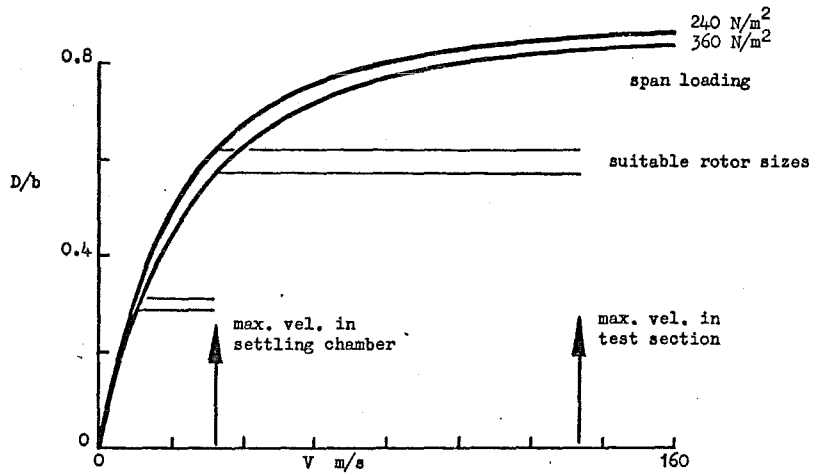


FIG. 5 ROTOR SIZES SUITABLE FOR WIND TUNNEL USE

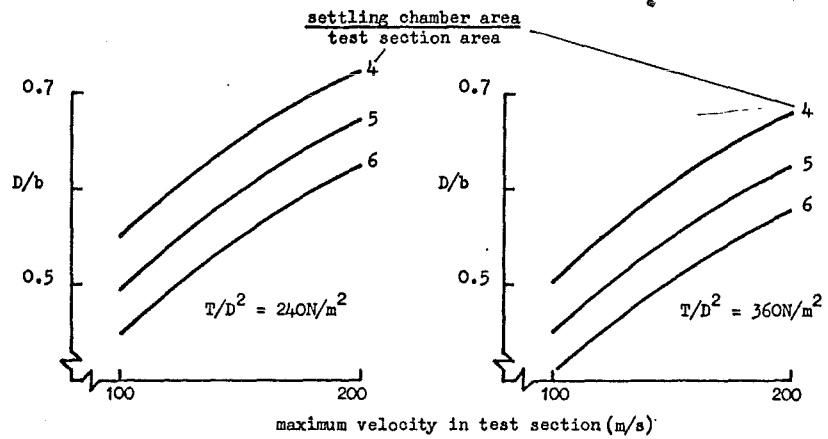


FIG. 6 EFFECT OF SETTLING CHAMBER SIZE AND MAXIMUM VELOCITY ON ROTOR SIZE



ACOUSTIC CONSIDERATIONS FOR NOISE EXPERIMENTS AT  
MODEL SCALE IN SUBSONIC WIND-TUNNELS\*

by

T. A. HOLBECHE

J. WILLIAMS

Aerodynamics Department, Royal Aircraft Establishment,  
Farnborough, Hampshire, England.

SUMMARY

The need for wind-tunnel model experiments on aircraft noise is first briefly reviewed, the advantages and problems relative to flight testing being summarised. The basic requirements for model noise investigations in tunnels are then analysed with particular attention to similarity conditions, noise measurement constraints on model and tunnel sizes, the parasitic effects of background noise, and the various factors contributing to the generation of background noise. The specific contributions to tunnel noise from the tunnel drive fan, the tunnel circuit, the test-section mainstream flow and the particular test-section boundary conditions are each discussed, along with possible noise alleviation techniques and tunnel correction-factor difficulties.

The features of some existing tunnels which are known to have been employed already for model noise experiments are outlined in Appendix A. A bibliography of about 120 published papers specially relevant to acoustic considerations for model noise testing in subsonic tunnels is provided by Appendix B.

---

\* RAE Technical Report 72155 (July, 1972) with minor corrections.

CONTENTS

	<u>Page</u>
1 INTRODUCTION	3
2 NEED FOR WIND-TUNNEL MODEL EXPERIMENTS ON AIRCRAFT NOISE	3
3 BASIC REQUIREMENTS FOR MODEL NOISE EXPERIMENTS IN TUNNELS	4
3.1 Model similarity considerations	4
3.2 Noise measurement constraints	5
3.3 Background noise effects	6
3.4 Background noise generation	7
4 INTRINSIC TUNNEL NOISE AND ATTENUATION METHODS	7
4.1 Tunnel drive fan	8
4.2 Tunnel circuit	9
4.3 Test-section mainstream flow and boundary conditions	10
5 CONCLUDING REMARKS	12
5.1 General background	12
5.2 Tunnel design	13
5.3 Model testing techniques	13
5.4 Further analysis	13
Acknowledgment	14
Appendix A Some existing tunnels used for model noise experiments	15
Appendix B Bibliography of published papers specially relevant to model noise testing in subsonic wind tunnels	19
Illustrations	Figures 1-9

## 1 INTRODUCTION

The prediction and minimisation of aircraft noise, particularly during subsonic flight conditions appropriate to airfield operations and associated climb-out/approach-descent paths, have now assumed equal importance to those of aircraft performance and handling aspects, for civil and military transport projects at least. Currently, most experimental noise research for practical aircraft applications can be carried out thoroughly only under static conditions, provided by outdoor test stands or anechoic chambers, being then complemented by qualitative corrections from some crude or specialised flight checks. Although there do exist a few small-scale 'near-anechoic' wind tunnels, while a large one has recently been constructed at NSRDC Carderock, MD, USA (1-15), most sizable tunnels were designed with little concern about noise model testing as distinct from aerodynamic model testing (including unsteady pressure measurements). These latter tunnels, if left acoustically untreated, tend to act as reverberant chambers and ducts which amplify significantly aircraft-model generated noise, while at the same time generating embarrassing background noise themselves.

Thus, any examination of possible new subsonic-tunnel test facilities or of possible improvements to existing tunnels, must be influenced not only by projected aerodynamic test considerations, but also by the increasingly important demands to determine the distribution of noise around future airframe/engine designs under relevant flight conditions, particularly in relation to studies of airfield performance capabilities (GTOL, RTOL, STOL, VTOL). Furthermore, while many of the desirable tunnel-design features to ensure good noise testing are similar to those for good aerodynamic testing (e.g. minimisation of airflow separations), others could be strongly conflicting. Thus, as the respective needs and design features become better appreciated, the inherent compromises or penalties necessary to achieve an acceptable dual-purpose tunnel will have to be properly assessed; possibly even leading into a comparative appraisal of the cost-productivity of such a combined facility as against two complementary tunnels biased individually towards aerodynamic and noise testing.

The present study was especially stimulated by a demand to explore quickly the test conditions and techniques necessary for making reliable acoustic measurements on aircraft models with powered noise sources in subsonic wind tunnels. Apart from considerations of tunnel-design features, this raises a variety of interacting problem areas simultaneously from acoustic and aerodynamic viewpoints - which themselves can be interdependent (Fig.2). In particular, the essential features of the airframe and power sources have to be carefully selected and the appropriate model/rig design techniques critically applied, taking into account tunnel testing constraints and measurement limitations, to ensure adequate simulation for research purposes and for prediction of practical full-scale effects.

Firstly, the need for wind-tunnel model experiments is briefly reviewed, the advantages and problems relative to flight testing being summarised (section 2). The basic requirements for model noise investigations in tunnels are then analysed (section 3), with particular attention to similarity conditions, noise measurement constraints on model and tunnel sizes, the parasitic effects of background noise and the various factors contributing to the generation of background noise. The specific contributions to tunnel noise from the tunnel-drive fan, the tunnel circuit, the test-section mainstream flow and the particular boundary conditions are then discussed in turn (section 4), along with possible noise alleviation techniques and tunnel correction-factor difficulties. The concluding remarks (section 5) serve to summarise the major problem areas as regards tunnel-design and models for the investigation of mainstream flow effects on aircraft noise, and to refer to some further studies proposed on relevant techniques including consideration of possible 'mobile' rigs as complementary or alternative facilities to wind tunnels.

Appendix A outlines the features of some existing tunnels which are known to have been employed already for model noise experiments. Appendix B provides a bibliography of about 120 published papers specially relevant to acoustic considerations for model noise testing in subsonic tunnels. It should be noted that the allied problems of the influence of tunnel noise on model aerodynamics are not considered explicitly here.

## 2 NEED FOR WIND-TUNNEL MODEL EXPERIMENTS ON AIRCRAFT NOISE

The aircraft designer is now faced with the problem of predicting, assessing and guaranteeing the noise field from future aircraft projects to a much greater accuracy than hitherto, while at the same time achieving much lower noise levels and improved airfield performance, as well as employing novel airframe/engine schemes.

During the next decade, predictions to within  $\pm 1$  or  $\pm 2$  dB may have to be attained, along with about 20 dB reduction in noise levels at airport boundaries (e.g. 110 PNdB to 90 PNdB) and in the surrounding populated areas. Similar reductions are also desirable for some military operations; not merely for transports but also for low-level search, reconnaissance, and rescue aircraft. Moreover, such improvements are required with minimum penalties on aerodynamic, structural and propulsive efficiency. Many of these demands tend to make the resultant noise field much more sensitive to aircraft configuration, powerplant installation, and flight conditions.

The complexity of the noise estimation process can be appreciated from the simplified breakdown illustrated in Fig. 1, where also the noise factors affected directly by the presence of relative mainstream flow are indicated. Thus, apart from conventional static and meteorological effects, uncertainty in predictions of far-field sound pressure levels and spectra arise from poor knowledge of flow-field effects on engine noise and its diffraction by the airframe, together with noise arising directly from airframe aerodynamics - including the wing-lift augmentation devices. In turn, such effects influence some of the radiation factors (directivity and atmospheric attenuation), and ultimately some subjective factors (e.g. through broadband spectrum and pure tones), required in the calculation of far-field noise annoyance. For the clarification of such effects, and for guidance towards the formulation of reliable theoretical frameworks and prediction methods, experimental research and development studies are essential at model scale in suitable anechoic wind tunnels, as well as at full-scale.

Wind-tunnel testing of an appropriate model noise generator can provide in principle most of the necessary features of flyover noise generation and, in complementing or superseding much of the relevant flight testing, offers a variety of advantages similar to those often argued aerodynamically. For example:-

- (i) The test environment can be more precisely controlled and repeated.
- (ii) The aircraft model condition and configuration can be varied systematically without unwanted restraints from flying-quality and flight-safety requirements.
- (iii) Special research tests can be undertaken on partial models and unconventional models, to clarify particular noise features, to check directly possible theoretical treatments or prediction methods, and to explore novel concepts quickly.
- (iv) Usually, measurements can be made more precisely and extensively.
- (v) Usually, the tests can be carried out more economically, flexibly and quickly.
- (vi) The elimination or control of ground reflection effects and of relative motion between the noise source and the measuring point (Doppler effect) can facilitate analysis greatly.

Likewise, with wind-tunnel testing, there arise certain disadvantages or problems which must not be ignored, for example:-

- (i) For adequate simulation at model scale, certain geometrical features have to be selected for representation and some noise/aerodynamic similarity parameters have to be reasonably satisfied or properly interpreted. The special difficulty of adequately simulating the powerplant noise source and radiation characteristics, other than perhaps pure jet noise, represents an area in which much progress is needed soon.
- (ii) Parasitic unacceptable noise fields can be produced automatically by the tunnel testing environment, unless special precautions are taken. These include reverberation or standing waves caused by reflection from the tunnel walls and around the tunnel circuit, the intrinsic noise of the tunnel in operation, and the noise associated with flow over the measuring microphones and over the model rig.

These will be discussed later in relation to open-return tunnels (straight through) and closed-return tunnels (complete-circuit), with special reference also to open test-sections (free-boundaries) and closed test-sections (wall boundaries).

### 3 BASIC REQUIREMENTS FOR MODEL NOISE EXPERIMENTS IN TUNNELS

#### 3.1 Model similarity considerations

For wind-tunnel tests on model noise, with particular reference to the influence of mainstream speed,

the selection of a simplified partial model to represent adequately the primary features of the practical full-scale problem to be explored presents as usual a major difficulty. Furthermore, apart from questions relating to geometrical similarity, appropriate values of certain major similarity parameters ought to be reproduced to achieve similarity for both airflow and acoustic fields, at least within a limited test range. Since the experiments of necessity incorporate aerodynamic effects, the classical parameters of mainstream Mach number ( $V_\infty/a_\infty$ ) and airframe Reynolds number ( $V_\infty \ell / \nu_\infty$ ) remain significant. Other aerodynamic parameters also need to be introduced for particular tests; such as effective dynamic pressure-ratio of jet-efflux to mainstream-air [ $(\rho V^2)/(\rho_\infty V_\infty^2)$ ] if powered-lift systems are to be incorporated, or blade tip-speed to mainstream-speed ratio ( $V/V_\infty$ ) and Froude number ( $V_\infty^2/g\ell$ ) in the case of lifting rotor tests.

Since acoustic effects are of primary interest, some of the aerodynamic-representation demands may possibly be relaxed, provided the deficiencies involved are well appreciated and allowed for. As regards acoustic similarity, mainstream Mach number ( $V_\infty/a_\infty$ ) assumes special significance along with other particular parameters, such as jet-speed and density ratios in relation to jet-mixing noise aspects; or blade tip Mach number and aerodynamic loading for rotating blade noise. Further scaling laws for appropriate noise frequencies  $f$  (or wavelengths  $\lambda$ ) also need to be introduced; e.g. identity of the noise frequency-parameter ( $f\ell/V$ ) in the case of a simple jet of diameter  $\ell$  and velocity  $V$ , or in the case of a rotating blade of linear dimension  $\ell$  and velocity  $V$  at its reference section.

In attempting to ensure realistic tunnel testing conditions, correct representation of relative air-speed  $V_\infty$  thus becomes of high priority, because of Mach number effects both acoustically and aerodynamically - under high-lift conditions at low  $V_\infty$  as well as at high  $V_\infty$ . In principle, the use of a working fluid with speed of sound lower than air (e.g.  $\text{CO}_2$  or Arcton) could offer some advantages. Provision of high Reynolds number, though desirable at least from aerodynamic aspects, as usual becomes difficult because of various restrictions on model size. Again, in principle, the use of a working fluid of lower viscosity than air (e.g. Freon 12) could offer some advantages.

The achievable model size, apart from manufacturing/cost/handling problems, is influenced as usual aerodynamically by the relative size of the available test-section and the boundary conditions, in order to minimise tunnel constraint effects on model aerodynamic behaviour and to ensure adequate account can be taken of such effects. Simple acoustic requirements can of course be formulated as regards the acceptable absorption/refraction properties of the test-section boundaries in terms of the character and extent of the model noise source. However, some novel tunnel testing constraint factors have also come to light from our deliberations on noise measurement requirements in tunnels, as argued in the next sub-section.

### 3.2 Noise measurement constraints

Usually, to facilitate analysis of model noise measurements and extrapolation to full-scale far-field conditions, the noise measurement locations must be situated in the 'free-field' portion of the model-source far-field. Here, the particle velocity is primarily in the direction of the sound propagation and the sound pressure level varies almost inversely as the square of the distance (apart from atmospheric attenuation), i.e. decreases 6 dB for each doubling of distance. Fig.3 illustrates how this free-field region is bounded by the near-field region of the source and the reverberation field of the enclosure, in both of which noise-field measurements will be difficult to interpret. Even if the test-section boundaries are acoustically fully absorbing, allowance must be made for the fact that free-field measurements should not be attempted closer than about one-quarter wavelength from the absorber. Moreover, when the boundaries are not fully absorbing, the interference region may extend several wavelengths from the absorber - depending on its reflection coefficient/frequency characteristics, so that the extent of the source free-field can be considerably reduced (4-3).

For tunnel tests, the extent of the source near-field region can have an important bearing not only on the measurement region available, but also directly on the size of test-section required. In general, this extent depends on the source type (monopole, dipole, quadrupole), wavelength and intensity. But it is roughly of the order of one or two wavelengths, which therefore makes the lowest test-frequency required the important criterion. For example, on the basis of some current model research (about 1/10 full-scale) on external jet-flap noise, test measurements down to 250 Hz (or lower) can be required. Thus an appropriate tunnel must have a test-section radius of at least 3 m (or more) to ensure that proper far-field conditions can be reached (within the test-section) down to the required low frequency limit -  $f_{\min}$  of

interest. If, as the model scale dimension  $d$  is increased, similarity may be retained on the basis of frequency parameter (say  $fd/V$ ), then  $f_{\min} \propto 1/d$  so that the maximum wavelength of interest  $\lambda_{\max} \propto d$ , and the required tunnel radius increases proportionally also.

Correspondingly, the high-frequency limit of interest tends to increase with reduced model scale, depending on the assumed scaling law. Thus restriction of the smallest model scale can occur since practical problems are likely to arise in attempting noise measurements much above 20 kHz, on account of the more rapid attenuation of noise by the tunnel air as the frequency is increased.

This will cause an asymmetric distortion of the noise field, in particular greater loss occurring upstream than downstream, for which corrections could become extremely difficult. Moreover, as discussed further below, measurements at very high frequencies bring in problems of reduced microphone sensitivity and lower signal/noise ratio. Also, for natural reasons, there are experimental advantages in restricting the frequencies of interest to within the aural range when possible. Thus, from acoustic measurement considerations, the minimum acceptable size of model can be constrained by such practical difficulties with very high frequency measurements; while, as previously discussed, the maximum size of model (or minimum size of tunnel) is restricted by the need to achieve far-field conditions within the tunnel test-section.

In order to ensure adequate frequency response and spatial resolution, measurements at high frequencies (short wavelengths) require microphones of small diameter - to maintain a sufficiently small ratio of diameter/wavelength. Unfortunately this leads to a loss in sensitivity which becomes particularly acute at very high frequencies associated with small model scale. For example, the upper frequency limit of measurement may typically be raised from about 18 kHz to about 140 kHz by changing from a microphone capsule of 25mm (1in) diameter to one of 3mm ( $\frac{1}{8}$ in) diameter, but then a sensitivity loss of some 35 dB is incurred. Thus, to maintain the original signal/noise ratio with a given source SPL, the electronic background noise of the measuring system must be correspondingly reduced by restricting its effective bandwidth with filters or equivalent techniques. Hence, a simple broadband measurement technique can no longer be applied.

It is also worth noting that the dynamic range (signal/noise ratio) of most measurement and analysis systems is far less than that of the microphone alone; rarely exceeding 60 dB and typically not more than 45 to 55 dB when a tape recorder is included. Because of this restriction in dynamic range, microphone transducers of sufficiently large intrinsic sensitivity must be selected so that the dynamic range of the system is fully utilised whenever possible. This may sometimes require some sacrifice of upper frequency limit and spatial resolution.

### 3.3 Background noise effects

The noise field of primary interest is naturally that from the representative 'model' (airframe with power source), as modified by the influence of the tunnel mainstream flow on the model's acoustic characteristics and airflow field (Fig.2). All other noise sources, which either directly or indirectly contribute to the unwanted background, need to be minimised by careful design of the tunnel and experimental rig. Obviously, to permit reliable experimental analysis, the acoustic power from model noise sources must be sufficiently large in comparison with background noise.

In this connection, it is important to realise that the model-source noise level available for measurement may prove almost independent of model scale, assuming acoustic/aerodynamic similarity is being attempted. A simple illustration of this follows from a basic experiment involving a model jet-noise-source (diameter  $d$ ) where the sound pressure level (SPL) at the measuring point (distance  $R$ ) is roughly proportional to  $d^2/R^2$  as the experimental scale is varied. However to satisfy the far-field measurement conditions (acoustic and aerodynamic),  $R$  must exceed  $nd$ , a prescribed number of diameters (typically of the order 10). Thus the maximum measurable SPL becomes independent of  $d$ , i.e. of the experimental scale, which itself is limited by the scale of the tunnel (diameter  $> 2nd$ ).

Where measurements at discrete frequencies only are required by the experimental investigation, narrow-band analysis or correlation techniques may be employed with advantage to increase the effective discrimination of the periodic signal against the background noise. Even so, care is still necessary to ensure that the measurement system is not overloaded by the background noise at other frequencies (normally lower). Furthermore, the application of such correlation techniques implies the provision of adequate spatial separation in relation to the wavelength of the acoustic disturbance being measured, thus introducing another constraint on acceptable tunnel size. Provided a directional response is acceptable, successful

measurements giving improved discrimination against background noise can also be obtained with a probe microphone. This operates across a relatively narrow frequency-band where the resonances in the probe duct are sufficiently well damped to ensure reliable performance. Although its use requires considerable care, including a full appreciation of its frequency characteristics, the probe microphone may in certain circumstances be the only practical alternative to the more commonly used wide-band linear-response omnidirectional microphones.

More generally, where broadband measurements are essential such as for the determination of overall SPL with a view to definition of say a 'noise footprint' at full-scale, then the background noise level must clearly be reduced to well below the model noise-source levels. A useful working datum is that, provided the difference between the total noise measured and the background level exceeds about 10 dB, the correction to the overall measured noise level in order to derive the model-source contribution is below about  $\frac{1}{2}$  dB, i.e. probably negligible.

### 3.4 Background noise generation

The principal factors contributing to the background noise level are also included in Fig.2, and these can conveniently be discussed in turn.

#### (i) External ambient noise

This warrants particular consideration in the design of 'straight-through' type tunnels, and for 'open-jet' test-sections where the test-section volume should be surrounded by a large anechoic chamber. One existing straight-through open-jet 'anechoic' tunnel required extensive muffling at the tunnel inlet, with attendant pressure-drop problems, to reduce the noise convected into it from outside. Although structural transmission of mechanical vibration and motor noise from the tunnel-drive system may require special precautions, external noise should not present a problem in closed-circuit tunnels of reasonably rigid and solid construction.

#### (ii) Model rig noise

Air supplies to model jets and fans, or to resonance-tube type generators, may lead to extraneous valve or pipework noise together with vortex shedding noise from unfaired model supports, wires, etc; for example, see Figs.7 and 8. Additionally, the complementary aerodynamic interference by the rig on the model aerodynamics can lead to parasitic changes in the model-generated noise field.

#### (iii) Noise from measurement devices

The broadband self-generated noise from microphones in airstreams is well appreciated and can be minimised by careful design and intelligent use; for example, see Ref.5-4. Another fundamental problem arises at high frequencies when the sound wavelength is of the same order as (or less than) the microphone diameter. Under these conditions, the diffracted field due to the microphone is superimposed on the incident field and leads to a very directional response characteristic. Thus corrections to free-field conditions then become increasingly significant and more difficult.

#### (iv) Residual background noise

The remaining noise elements may be considered to make up the 'intrinsic' tunnel noise background. The relevant origins and effective attenuation methods are discussed under appropriate sub-headings in the next section.

## 4 INTRINSIC TUNNEL NOISE AND ATTENUATION METHODS

In general, because aerodynamic noise is associated with unsteady flow conditions, those qualities needed for a tunnel of good aerodynamic design ensuring uniform low-turbulence flow in the test-section also help towards providing a quiet tunnel. Such features include the minimisation of separated flows round the whole circuit, good fan efficiency, and careful choice of diffuser, contraction, resistance screens and cooler. The achievement of low turbulence may be particularly important both as regards reduction of tunnel fan noise and avoidance of unrepresentative intake conditions during noise tests on say model lift-fans, which may result in spurious noise radiation. The corner or turning vanes in a return circuit must also be designed to avoid 'singing', i.e. noise from vortex shedding.

To be specific, attention has been restricted here to the continuously-running atmospheric facility

employing a fan drive (e.g. Fig.4), though many of the points raised can have relevance to other types. The following sub-sections deal in turn with noise-generation aspects of the tunnel-drive fan, the tunnel circuit, the test-section mainstream flow and boundary conditions.

#### 4.1 Tunnel-drive fan

The results of some careful and detailed investigations into the sources of background or intrinsic noise in the 3m diameter subsonic open-jet closed-return tunnel of the DFVLR (Porz-Wahn, Germany) have been given by Schulz (1-1, 1-2), including an informative microphone traverse around the entire tunnel circuit (Fig.5). The principal noise was found to come from the tunnel-drive fan, the sound pressure level increasing as the fifth power of the rotational speed and generally increasing with any rise of the fan 'modulus' or advance ratio (the ratio of axial-flow speed to tip-speed) from change of pitch setting. The position of minimum noise was found to be at the collector mouth (downstream of the test-section), the level rising some 10 dB towards the jet-exit (upstream of the test-section). In-duct sound-absorption techniques, including the fitting of wall liners and a splitter on the upstream side of the fan, effected a 10 to 15 dB improvement at the collector mouth, though only a minor improvement at the jet exit. However, the fan itself was apparently not modified, nor were in-duct sound absorption techniques applied downstream of the fan.

There is now a comprehensive literature on fan noise in ducts and some relevant references are collected in Appendix B (sections 2 and 3). For the purpose of the present discussion, some qualitative points can usefully be summarised:-

- (i) The noise is usually of broadband dipole type arising from lift fluctuations on the blades, associated with vortex shedding at the trailing edges. Superimposed on this spectrum are discrete tones at the blade passing frequency (BPF) whose intensities are a function of tip speed as well as inlet turbulence.
- (ii) Quadrupole noise may also arise due to inflow turbulence. Together with item (i), this implies that steps must be taken to ensure the smoothest possible intake flow.
- (iii) The fan should run at the lowest possible rotational speed, preferably with a tip-speed not exceeding half the local speed of sound. Moreover, as far as possible, the fan should operate near to its position of maximum pressure rise (on-design) since this tends to coincide with minimum noise generation and with the blades well clear of the stall. This in turn implies low or moderate blade incidence. Blade design (section, camber, incidence, twist, aspect-ratio, etc.) is therefore all important along with the character of the inflow distribution. Qualitatively, minimum noise occurs for a fan having small blade chord (1-10), slender blade profile, and blade spacings of the order of one-half to one chord length (2-1).
- (iv) If the length-scale (L) of inflow turbulence is small compared to the transverse spacing (D) between the fan blades (e.g.  $L/D < 0.5$ ), then the BPF noise contribution usually disappears though the level of broadband noise tends to rise (2-2); a honeycomb fixed upstream of the fan can also be beneficial.
- (v) Any stators or fan hub supports must be located well away from the fan disk and preferably be round-nosed to avoid flow separation.
- (vi) With straight-through type tunnels, BPF noise is reduced considerably if the intake duct is bell-mouthed rather than sharp-edged.
- (vii) The number of in-duct straightening vanes should not be an integral multiple of the number of fan blades. This is important in closed-return tunnels.
- (viii) Schemes for fluctuating-flow attenuation at the fan tips, or for acoustic absorption over nearby surfaces, could be usefully considered.

For example, some recently published work (2-34) on a model ventilating fan shows considerable noise reduction when the blade tip region is made of porous metal or of porous plastic material, with quite small increase in driving power for a given mass flow.

More generally, in view of the close relationship between fan efficiency and the fan noise radiation, optimisation of fan performance should form an integral part of the tunnel operation routine, including the incorporation of variable blade-pitch and possibly even the facility to alter the blade-camber or twist.



## 4.2 Tunnel circuit

### (i) Cross-section

For a prescribed circuit length, designing for minimum wind-swept area of the duct can assist in restricting the amount of noise arising from wall-pressure fluctuations. Thus, on this count, a circular cross-section may offer an advantage over non-circular, although possibly at the expense of additional engineering complexity. Also, the area of duct wall in contact with relatively high-speed flow should be kept as small as possible, commensurate with other considerations; a point nominally in favour of the open working section, though the free-boundary mixing effects are objectionable.

### (ii) Basic circuit design

In designing a new facility, special attention must be paid to the avoidance of flow separations of the ducted airflow, in view of their significance as sources of noise as well as of aerodynamic inefficiency or unsteadiness. Particularly important regions include those in immediate proximity to the test-section e.g. in the first diffuser particularly at the entry (or collector cowl), and at the ends of the contraction (or nozzle), together with those adjacent to the driving fan. Prevention of possible wake oscillations from corner vanes and the like is also vital, to preclude tone generation or 'singing'. There might also be a case for providing adequate distance of the model upstream of the tunnel corner vanes to allow the total wake from the model (and rig) to be effectively dissipated before passing through them, subject of course to maintaining acceptably low aerodynamic interference.

### (iii) Noise suppression

For a large cylindrical wind-tunnel duct, the sound cut-off frequency may be so low as not to offer in itself an effective practical means of noise suppression; e.g. perhaps as low as 20 Hz for a 10m diameter duct. Fortunately, for existing tunnels where radical modifications are not practicable to provide low noise design features along the lines already mentioned, direct sound absorption techniques can be applied to achieve some reduction of broadband noise levels by means of duct linings, splitters, mufflers, etc. (Fig.4). However, a particular problem arises in applying such techniques to wind tunnels because the efficiency of the absorber is progressively reduced as the duct airspeed increases. At least two fundamental factors have to be considered:-

(a) At frequencies above the duct cut-off frequency, the broadband sound energy will not propagate uniformly along the duct, but rather in various modal patterns determined by the ratio of duct diameter to wavelength. At some frequencies sound will be concentrated along the duct axis, or away from the absorber surface in other frequency zones, thus reducing the absorber effectiveness in these cases.

(b) Because of the convective effect of the duct airflow, absorption of sound travelling downstream becomes less than that upstream. This implies that, for a given attenuation, duct absorbers would have to be lengthened in the streamwise direction compared to the static condition; by a factor of about  $(1 + M)$  from simple arguments. The acoustic resistance of the absorber is also affected by the local airspeed in the duct, while the amount of sound absorption can vary with the angle of incidence to the surface. All this naturally suggests that the most reliable region for the application of in-duct absorption techniques is where the airflow speed is a minimum, i.e. in the tunnel settling chamber before the contraction or well downstream of the diffuser.

### (iv) Absorber design

The design of absorption features for wall treatments, in-duct splitters and mufflers has progressed considerably for ventilation systems where flow speeds are low, but it is not certain that there exists adequate capability for designing a system which combines good broadband absorption with minimum pressure loss and little self-generated aerodynamic noise. Some possible schemes for application of these techniques to wind tunnels are sketched in Fig.4 though they are not all intended to be applied simultaneously. The modifications to the existing DFVLR tunnel (1-2) (Porz-Wahn, Germany) and the design of the new NSRDC 'anechoic' tunnel (1-15) (Carderock, MD, USA) provide useful overall examples.

As regards in-duct splitters, commercial versions are usually designed to work on flow velocities below 15 m/s (50 ft/s), so there is naturally no flow-noise data above this velocity. The flow losses resulting from the insertion of such splitters into the tunnel represent an important design consideration.

The absorption of high-frequency noise will require closely-spaced splitters, whereas low frequency absorption will require large absorber lengths, both leading to increased losses of flow total head. In the NSRDC anechoic tunnel (Fig.9), acoustic mufflers are located upstream and downstream of the driving fan to alleviate fan noise, particularly in the low frequency range at test-section windspeeds up to 60 m/s (200 ft/s). Each muffler consists of two sinuous absorbing splitters in the middle of the tunnel and one along each wall. The large-radius sinuous bends are used to avoid flow separation, and also to provide additional high-frequency noise reduction by eliminating an unobstructed linear sound-path through the muffler. This sinusoidally-curved type of passage also increases the effective acoustic length of the passage for a given length of muffler. The total head losses estimated for each muffler, at a test-section velocity of 60 m/s (200 ft/s), were roughly 15% of the overall loss round the tunnel circuit, and about the same as the loss through the cooler or through the 'antiturbulence screen' section.

Some tunnel designs may have to utilise 90° corner splitters for space reasons, in combination with or instead of 'straight-duct' splitters (Fig.4). But, at present, basic information is lacking for comparative purposes; for example to ascertain the length of straight splitter which would give the same absorption per bandwidth as a 90° corner splitter.

The usefulness of simple absorber techniques applied to the surfaces bounding a tunnel test-section, as a means of providing a 'semi-anechoic' enclosure, can be illustrated by experiments with the 24ft open-jet closed-return tunnel at RAE Farnborough (Fig.6a). The floor, the ceiling and the outside of the internal wall of the return-circuit have all been lined with porous polyether foam sheet of 7½cm (3in) thickness, along with a matching 'wall' comprising an absorption curtain which is retractable to permit ready access to the test-section. The results of some preliminary tone-burst tests, in which a simple electroacoustic noise source was used radiating at right-angles to the tunnel axis and with the omnidirectional microphone some 2½ m (8 ft) below the tunnel centre-line, are shown in Fig.6b. Whereas there was quite negligible reflection at 12.5 kHz and 6.3 kHz, some reflected sound is evident at 3.15 kHz though the relative levels of -20 dB (and greater for subsequent reflections) are seen to be insufficient to modify the direct field to any appreciable extent. In fact the present treatment allows noise tests down to frequencies of about 2 kHz before reflections become troublesome.

More detailed noise calibration of the RAE 24ft tunnel is now being carried out, and further sound absorber treatment is to be applied around the test-section in an attempt to preclude troublesome reflections down to usable test frequencies of 250 Hz. No in-duct treatment has been provided as yet.

#### (v) Significance of source type on sound convection

The variation in the transmitted source power with airspeed along the duct (at frequencies well above cut-off) can depend appreciably on the type of source which is radiating. It has been argued (3-4) that a simple convective correction factor is  $(1 \pm M)^2$  for monopole radiation, unity for dipole sources - i.e. no convective effect, and  $1/(1 \pm M)^2$  for quadrupoles; where + and - refers to downstream and upstream conditions respectively. One design consequence of this is that, if the fan noise can be regarded mainly of dipole type, then it need not be positioned with convective effects in mind, but located more or less equidistant from the test-section boundaries; a practical choice of fan position depends of course on aerodynamic and engineering considerations as well as noise.

### 4.3 Test-section mainstream flow and boundary conditions

#### (i) Open and closed test-sections

At first sight, an open test-section with a free-boundary would appear to be far more attractive for model noise experiments than a closed test-section, particularly if the large chamber housing the open-jet is itself acoustically treated. The background noise emanating from the contraction nozzle and collector can radiate freely (at least hemispherically) along with that from the model, with negligible reflections from external boundaries. Thus, in principle, the achievable lower limit to background noise may be expected to be set by the broadband noise produced by turbulence in the mixing region at the free-jet boundary.

However the apparent need for 'spoilers' located at intervals round the jet nozzle exit, to suppress the formation of vortex rings, introduces an important additional feature as regards the design of large open test-section tunnels where low self-noise is required. Any spoiler-generated noise is presumably offset by the improved flow mixing and essential flow steadiness which they are intended to promote in the

main jet; the principle of some current types of jet-engine noise suppressors is similar. But little evidence seems to be available as to how this would limit the background noise-floor attainable in such tunnels and as to whether better schemes than 'spoilers' are feasible. At any rate, without such form of vortex control, the formation frequency of the vortex rings may coincide with an 'organ-pipe' resonance frequency for the tunnel duct, thus possibly setting up a longitudinal standing wave with disastrous effects on tunnel performance or even on tunnel structure. Cases are known where this has happened in both 'closed-return' and 'straight-through' types of circuit construction.

The extent of the region available for satisfactory measurements of far-field noise generated by the model is also of significance. Allowance must be made for the presence of the jet boundary mixing region, particularly since microphone self-noise increases considerably due to the interaction of the turbulent eddies with the microphone housing; relevant evidence is available from some RAE tests. Figs.7 and 8 give some preliminary information on acoustic noise background levels as indicated by a microphone of 2.5cm diameter traversed through the open-jet of the RAE 24ft tunnel at a test-section windspeed of about 36 m/s (120 ft/s).

Within the tunnel mainstream, the measured background sound-pressure levels are less than in the boundary mixing region or just external to it. Some tests currently being analysed indicate that the background sound intensity in a 1/3-octave band varies as the seventh power of mainstream-speed over a wide frequency range, which suggests that a major component of the noise originates from the jet-mixing process and is therefore of fundamental significance to tests with an open test-section.

It will also be noted from Fig.7 that the wake from a vertical support tube of 15cm diameter located upstream of the microphone is associated with a very large increase in background noise at all measurement frequency bands. The largest increases (of order 20 dB) are found to occur at low frequencies, and a similar effect occurs when the microphone is allowed to traverse the wake from the jet-stabilising 'spoilers' mounted around the periphery of the nozzle. This effect has particular relevance to the necessity for careful design of model rig supports if generation of spurious noise is to be minimised in either open or closed test-sections. Additionally, in Fig.8, the pronounced peak in the noise spectrum at 1.25 kHz is almost certainly due to tones from vortex shedding by the tube bracing wires in the airstream.

Admittedly, for open test-sections surrounded by a relatively-large acoustically-treated chamber, it could be argued that reliable measurements may be taken with the microphones located in nominally still air well outside the jet boundary (not merely inside). However, this would imply that the test frequencies must be sufficiently low for the sound wavelengths of interest to be large compared with the thickness of the jet-boundary mixing region. Typically, this would appear to restrict measurable frequencies to below about 1 kHz with an 8m diameter jet. Moreover, quite apart from such a restriction, there remains the considerable risk that such measurements taken outside the jet boundary will be falsified and also rendered unsteady due to scattering and refraction by the turbulent eddies within the mixing region. Thus, tentatively at least, an important recommendation as regards techniques is that noise measurements should usually be taken within the uniform flow of the tunnel mainstream and well inside the jet boundary.

The major deficiency of closed test-sections (with wall boundaries) for model noise measurements would seem to arise from the 'containment' of the noise emanating from the contraction/first-diffuser, and from the possibility that transverse standing waves may be set up, between the parallel reflecting walls (or semi-reflecting) with the model noise source in operation. However, it can be argued that, with good tunnel design and acoustic treatment, the relevant tunnel background noise and wall-reflection interference effects on model noise could be reduced to an acceptable level. Comparable standards to those for an open test-section should certainly be achievable, at least as far as background noise is concerned, particularly since the expected advantages from freedom for noise radiation with an open test-section is counterbalanced by the disadvantages from jet-boundary mixing.

More generally, from both acoustic and aerodynamic viewpoints, the open test-section has the obvious attractions of ease of access for model-rigging and testing, along with better visibility since transparent panels may not be acceptable with acoustic treatment of closed test-sections. Again, however, this is counterbalanced by the greater difficulty of achieving reliable testing of half-models and ground-effects in completely open test-sections.

Overall, for model noise testing, no clear preference can be firmly recommended between open and closed test-sections without more quantitative analysis, possibly accompanied by some comparative experimental studies.

(ii) Possible tunnel corrections for reverberation effects on acoustic test results

Because of the superposition of the reverberant field, noise measurements in an unmodified tunnel will be larger in general than the required free-field values, especially at positions far from the model noise source - as may be necessary to satisfy source far-field conditions. Thus, corrections become essential though there is little experience available as yet.

One first-order correction technique employs comparative 'control' measurements, of the noise from a point source under ambient conditions outdoors and then in the tunnel test-section wind-off, to evaluate the amount of reverberation amplification for the simplest 'static model' over appropriate ranges of sound frequency and measurement locations. The resulting corrections across selected frequency bands and for the same relative positions of source and microphone, are then applied directly to the wind-on tunnel tests of the practical model. It should be stressed that the amount of the correction depends on both the particular frequency band and the direction of measurement, and possibly on the source-strength.

This technique has already been applied to some measurements of helicopter rotor noise, by Hickey (1-6) in the NASA Ames 40ft x 80ft tunnel and more recently by Broll (1-5) in the ONERA Modane 8 metre tunnel (S1MA). Typically, the ONERA results imply that the correction decreases as the centre-band frequency increases, i.e. being about 8 to 9 dB for the octave 180 Hz to 350 Hz but having practically disappeared over the octave 2.8 kHz to 5.6 kHz. A similar trend is apparent in the Ames data though with a somewhat larger residue at the high frequency end of the measurement bands. This decrease with increasing frequency may reasonably be a characteristic of large tunnels. Nevertheless, the magnitude and spatial variation of the correction can pose severe difficulties of interpretation when attempting proper application to measurements of noise from a distributed rather than a local source.

At the present time, gross corrections of this nature are undoubtedly expedient and useful for qualitative noise estimates, and are certainly of interest towards evaluating the applicability of noise measurements in particular wind tunnels. However, the reverberant field may not invariably be diffuse (e.g. can include standing waves), while the corrections can be comparable in magnitude to the changes in noise level being investigated in the tests (i.e. demand accurate corrections). Then, more refined correction methods are essential, providing an area which clearly needs special investigation before the viability of existing 'aerodynamic' tunnels (untreated or simply treated acoustically) can be accepted for reliable quantitative measurements of mainstream effects on the model noise field, particularly broadband.

## 5 CONCLUDING REMARKS

### 5.1 General background

Aircraft design demands to ensure low noise in low-level flight have now become of comparable importance to those for good aerodynamic characteristics, at least as far as the success of transport projects is concerned. However, the available experience on powered-model noise testing in wind tunnels and on associated techniques is currently very little, comprising quite small efforts over the past few years, as compared with extensive aerodynamic testing on high-lift and VSTOL models over the last two decades.

Fortunately, as regards the investigation of relative mainstream effects on model noise, mainly basic experiments on simplified models in appropriate tunnels could be especially productive by providing adequate corrections (favourable or unfavourable) to results obtained from static experiments on much more complex models, in a way not normally applicable to investigation of aerodynamic characteristics. Thus, while development of better tunnel facilities for adequate noise testing is vital, the foregoing aspect should be borne in mind when examining any compromises or additions to the design features of any new very-large V/STOL tunnel in order to permit adequate noise testing as well as the primary aerodynamic purpose. Moreover, if significant deficiencies or penalties would thereby be incurred in relation to the aerodynamic performance or cost productivity of this tunnel, the possible adequacy of particular model noise testing in a complementary large facility (different but specialised) would seem worth exploration.

However, it must be stressed that we cannot yet assess properly the degree of practical aerodynamic representation necessary to cover aircraft noise aspects, nor the degree to which any powered noise source itself will need to be represented at model scale. Moreover, the careful determination of forward-speed effects on noise may become increasingly significant because of demands for even lower noise levels, greater accuracy of prediction and the introduction of novel airframe/engine arrangements.

## 5.2 Tunnel design

Although specific recommendations on a particular wind-tunnel design for model noise testing have not been attempted here, we have examined and to some extent clarified some of the major factors involved. Primary tunnel design features on which further analysis and debate will be necessary, before outline specifications can be properly prescribed and useful cost-productivity assessments made, include the following:-

- (i) Test-section speed range; particularly with respect to desired maximum Mach number (say up to 100 m/s) and tunnel background noise levels then achievable.
- (ii) Test-section size; particularly with respect to far-field extent for measurements of model noise, and acoustic/aerodynamic interference from test-section boundaries (sections 3.2 and 4.3(ii)).
- (iii) Test-section type; especially the choice needed between free and walled boundaries from noise aspects (section 4.3(i)).
- (iv) Tunnel-circuit type; especially the choice needed between straight-through and closed-circuit from noise aspects (section 4.2).
- (v) Tunnel drive; especially fan design and position in duct, which we regard as particularly critical features for any noise-testing tunnel (section 4.1); also consideration of other drive schemes.

Of course, all these items are likewise important as regards model aerodynamic testing, but the optimum choices or preferences are not necessarily the same or immediately compatible.

## 5.3 Model testing techniques

Primary aspects of model testing techniques which also demand further consideration, because of their immediate bearing on tunnel utilisation and usefulness, include:-

- (i) Model design problems; especially model power-source simulation as regards noise generation and associated airflow characteristics (section 3.1).
- (ii) Model rig problems; especially provision of adequate supports and 'feeds' to models without unacceptable interference (section 3.4(ii)).
- (iii) Measurement problems; especially 'separation' of model-generated noise from parasitic noise, and achievement of reliable noise measurements inside (or outside) mainstream flow (sections 3.3 and 3.4(iii)).

## 5.4 Further analysis

Vital relevant background on some of the items listed under sections 5.2 and 5.3 should become available soon from proving experience with the NSRDC specially-designed noise tunnel and other smaller facilities, as well as from model-noise testing attempted in existing 'aerodynamic' tunnels with simple acoustic modifications - e.g. the RAE 24ft. Additional analysis based on this and our own further experience should then permit more specific recommendations to be made, at least on experimental work essential to establish quantitatively the necessity for and the technical equipment required for reliable noise measurements with aircraft models in wind tunnels. This is vital not only in respect of providing detailed guidance towards the design of any new large low-speed tunnel specially suitable for model-noise testing, but also helping to ensure that existing facilities can be usefully adapted and employed in the interim period before such a new tunnel could be constructed and fully commissioned (say 8-10 years hence).

Apart from free-flight vehicles, there are of course other earth-bound alternatives to wind tunnels for model experiments under forward-speed conditions, which directly involve motion of the model in nominally still air. Such 'mobile' facilities include for example the 'track' with rectilinear motion of the model on a 'rail-supported' carriage, the 'whirling-arm' with rotary motion of the model mounted towards the extremity of the arm, and the specially-modified 'road-vehicle' running on a specially-prepared

surface. Some of the demerits and merits of their use for aerodynamic testing apply equally well for noise-testing but, as with wind tunnels, some radical new problems are then introduced. It is intended next to examine such mobile facilities similarly from a noise-testing viewpoint, and ultimately to attempt to assess the extent to which wind tunnels, mobile rigs, and flight investigations could best be utilised as alternative or complementary facilities for noise research at forward speeds.

Acknowledgement

The authors have appreciated helpful comments particularly from Southampton University, HSA Hatfield, BAC Weybridge, NSRDC Carderock and NASA Ames.

Appendix A

SOME EXISTING TUNNELS USED FOR MODEL NOISE EXPERIMENTS

This Appendix summarises the principal features of a few existing wind tunnels in which measurements of acoustic noise are known to have been made at model or full-scale in a mainstream. The brief particulars given are based on some information immediately available at this time and which is specially relevant to acoustic testing. Naturally, additional information not already contained in the references listed would be welcomed by the authors, along with any up-to-date amendments.

1 RAE 24ft low-speed wind tunnel (Fig.6); Farnborough, UK

Tunnel operational since 1934 on aerodynamic experiments, and only small aerodynamic improvements since. Substantial aerodynamic and noise improvements now under consideration.

Open-jet test-section, with circular nozzle of 7.2m (24ft) diameter which has spoilers fitted around its periphery.

Closed return-circuit, with fan between collector and first corner.

Maximum test-section windspeed 50 m/s (165 ft/s).

Tunnel drive: 6-bladed fixed-pitch wooden fan of 9m (30ft) diameter.

Max. rev/min 250. Installed power 1500 kW (2000 hp).

Duct material:- prefabricated concrete; not lined.

Chamber enclosing open test-section about 13.5 m x 13.5 m x 9 m (45 ft x 45 ft x 30 ft).

Test-section turbulence level high ( $u'/V \approx 0.3\%$ ) and some low frequency unsteadiness.

Background noise intensity inside empty test-section mainstream flow:-

- (a) varies approximately as  $V^7$  at high frequency,
- (b)  $\propto V^6$  at low frequencies (of order BPF and low harmonics),
- (c)  $\propto V^6$  overall in range 25 Hz to 20 kHz.

Overall sound pressure levels at 37 m/s (120 ft/s):-

- $\approx 113$  dB (re  $2 \times 10^{-5}$  N/m<sup>2</sup>) for range 25 Hz to 20 kHz
- $\approx 103$  dB ( " ) " " 100 Hz to 20 kHz
- $\approx 95$  dB ( " ) " " 250 Hz to 20 kHz
- $\approx 86$  dB ( " ) " " 2 kHz to 20 kHz

(see Fig.8 for corresponding 1/3-octave band SPL).

Acceptable test frequency range:-

From about 2 kHz upwards with present test-section enclosure lining using 7.5cm (3in) thick polyether porous foam sheet.

Extension down to about 250 Hz planned by addition of absorber wedges to enclosure lining.

2 DFVLR subsonic wind tunnel (1-1,1-2), Porz-Wahn, Germany

Tunnel operational from about 1960 on aerodynamic experiments, but some aerodynamic and noise improvements since.

Open-jet test-section with rectangular nozzle of area 7 m<sup>2</sup> (75 ft<sup>2</sup>).

Closed-return circuit with fan between first and second corners.

Maximum test-section windspeed 80 m/s (260 ft/s).

Tunnel drive:- variable-pitch fan of 5m (16 ft) diameter. Max rev/min 380.

Installed power 1000 kW (1350 hp).

Duct material:- concrete;

First diffuser and corner (upstream of fan) lined with sound-absorbing material and also fitted with sound-absorbing splitter.

Test-section turbulence level low ( $u^*/V \approx 0.05\%$  to  $0.1\%$  inside jet).

Background noise level inside empty test-section:-

SPL at 80 m/s = 100 dB (A) re  $2 \times 10^{-5}$  N/m<sup>2</sup>

cf. 110 dB (A) without sound-absorbing treatment.

Background noise intensity variation (see Refs. 1-1 and 1-2):-

Fan noise found to vary as (tip speed)<sup>5</sup>.

Free-jet noise  $\propto V^5$  and is considered to set lower limit on background noise level.

### 3 ONERA large subsonic/sonic wind-tunnel S1MA (1-5); Modane, France

Tunnel operational from about 1959 on aerodynamic experiments.

Closed test-section, of circular cross-section 8m (26ft) diameter and 14m (46ft) length.

Closed return-circuit with twin fans between first and second corners.

Settling chamber 24m (80ft) diameter.

Maximum test-section wind-speed  $M \approx 1.02$ .

Tunnel drives:- twin contra-rotating coaxial fans of 15m (49ft) diameter.

Installed power 88000 kW. (Pelton water turbines).

Duct mostly of metal sheet and unlined.

Test-section turbulence level moderate ( $u^*/V \approx 0.12\%$ ).

Tunnel noise found to be broadband with a few tones at low frequencies which are attributed to the tunnel drive fans.

Background noise inside settling-chamber:-

SPL at test-section speed =  $\begin{cases} 100 \text{ dB at low frequencies} \\ \text{falling to } 80 \text{ dB at } 2 \text{ kHz.} \end{cases}$   
of about 100 m/s (330 ft/s)

Background noise resonances centred around about 1 kHz removed by placing screens across air exits from settling chamber.

Helicopter rotor noise measurements attempted (1-5) but subject to reverberation effects up to frequencies of 3 kHz (see section 4.3 (ii)).

### 4 NSRDC Carderock anechoic test-facility (Fig.9, Ref.1-15); Maryland, USA

Test-facility completed in 1971 specifically for wind-tunnel experiments on noise.

Open-jet test-section with near-hexagonal nozzle of effective diameter 2.5 m (8.3 ft). Enclosed in anechoic chamber 7.2m height x 7.2m width x 6.3m length (23.5 ft x 23.5 ft x 21.1 ft).

Also, closed test-section with near-hexagonal cross-section of 2.4m height x 2.4m width x 2.7m length (8 ft x 8 ft x 8.9 ft). Walls acoustically treated.

Closed return-circuit with fan between second and third corners and with closed test-section directly upstream of open test-section.

Maximum test-section windspeed 60 m/s (200 ft/s).

Tunnel drive: 24-bladed aluminium fan of 3.5m (11.5ft) diameter.

Max. rev/min 500. Installed power 1600 kW (2140 hp).

Duct material: reinforced concrete with acoustic liner on diffuser sections. Special acoustic mufflers incorporated upstream and downstream of fan to attenuate fan noise.

Test-section turbulence level low ( $< 0.1\%$  specified).

Specified background noise level in empty test-section:-

SPL 1 Hz bandwidth at 60 m/s not to exceed about 62 dB below about 400 Hz, and not to exceed about 35 dB at 10 kHz.

Test frequency range:- about 145 Hz upwards, this lower limiting frequency being set by the wedges used in the anechoic chamber.



5 NASA Ames 40ft x 80ft subsonic wind-tunnel (1-6); California, USA

Tunnel operational from about 1944 on aerodynamic experiments.

Closed test-section of near-elliptic cross-section with 12m height x 24m width x 24m length (40 ft x 80 ft x 80 ft).

Closed return-circuit with fans between second and third corners.

Maximum test-section wind-speed about 103 m/s (200 kn).

Tunnel drive:- six 6-bladed fans of 12m (40ft) diameter. Max. rev/min 290, with 195m/s (630ft/s) tip-speed. Installed power = 27000 kW (36000 hp).

Duct material:- contraction cone, test-section and first diffuser constructed of  $\frac{1}{2}$ -inch thick steel plate; with rectangular portions of rest of circuit made from fibre-coated corrugated metal.

Test-section turbulence level -- .

Background noise level inside empty test-section:-

OASPL at 36 m/s (70 kn)  $\approx 105$  dB re  $2 \times 10^{-5}$  N/m<sup>2</sup>

SPL at 51 m/s (100 kn) < about 95 to 100 dB at frequencies above 300 Hz.

Background noise intensity variation estimated as  $V^4$ , from published data (see Ref.1-6).

Test-frequency range (see section 4.3 (ii) of main text):-

Reported noise measurements, covering range 37.5 Hz to 4800 Hz in acoustically untreated working section, required correction for reverberation effects.

Helicopter rotor noise measurements attempted (1-6,1-8) but subject to significant reverberation effects over whole frequency range of interest (see section 4.3 (ii)).

6 United Aircraft acoustic research tunnel; Connecticut, USA

Tunnel operational from 1971.

Open-jet test-section with circular nozzle-exit of area 0.93 m<sup>2</sup> (10 ft<sup>2</sup>) and 9 to 1 contraction-ratio, or square nozzle-exit of area 0.41 m<sup>2</sup> (4.5 ft<sup>2</sup>) and 17 to 1 contraction ratio.

Open return-circuit with bell-mouth intake direct from atmosphere, followed by honeycomb section and anti-turbulence screens, feeding via contraction to nozzle, which has vortex generators fitted around its periphery.

Fan located at end of long diffuser from collector.

Anechoic chamber (around open-jet test-section) roughly a cube of 6 m (20 ft) side.

Maximum test-section wind-speed  $\approx 195$  m/s (650 ft/s) being limited by implosive stresses on anechoic chamber round open-jet.

Tunnel-drive:- suction by centrifugal fan (backward-curved vanes).

Duct mufflers included upstream of fan.

Screen fitted on tunnel intake to prevent external noise from entering test chamber.

Test-section turbulence level probably low.

Background noise intensity variation principally from jet mixing noise at high speeds.

For measurements external to the tunnel jet flow, noise intensity  $\propto V^6$  over band 300 Hz to 10 kHz;  $\propto V^8$  at frequencies over 10 kHz.

Test-frequency range:- about 250 Hz upwards;

(for anechoic chamber lined with fibre-glass wedges 20cm (8in) long having greater than 99% absorption above 250 Hz).

7 MIT Cambridge low-noise low-turbulence wind tunnel (1-3), Massachusetts, USA

Tunnel completed about 1968 for the Acoustics and Vibration Laboratory.

Open jet test-section with nozzle-exit 38cm (15in) square and 20:1 contraction. Enclosed in 'anechoic' chamber 4.1m length x 2.7m width x 2.1m height (13.5 ft x 9 ft x 7 ft). Test chamber can

also offer reverberant mode by change of wall treatment.

Also closed test-section 38cm (15in) square can be used.

Open return-circuit, with inlet direct from atmosphere, followed by honeycomb and settling chamber containing several fine-mesh anti-turbulence screens.

Maximum test-section windspeed about 55 m/s (180 ft/s).

Tunnel drive:- suction by centrifugal-type blower fan located downstream of the diffuser.

Fan has 12 blades of backward-slanted aerofoil shape (to reduce noise).

Max. rev/min 960. Installed power 15 kW (20 hp).

Special muffler installed in diffuser to absorb blower-generated noise.

Test-section turbulence level low;  $u'/V \approx 0.05\%$ .

Background noise level from open jet in anechoic chamber: SPL at about 45 m/s (150 ft/s) < 85 dB at frequencies above 200 Hz.

Test-frequency range: about 500 Hz upwards; (absorption at low frequencies to be improved by replacing fibreglass blankets on walls on 'anechoic' chamber).

## 8 Transonic tunnel noise experience

Although the performance of transonic tunnels is outside the scope of the present paper, some reference is of interest to illustrate the severe noise problems to be faced in facilities of this type.

For example (2-17) in the 16ft x 16ft Propulsion Tunnel and 4ft x 4ft Aerodynamic Tunnel at AEDC (Tennessee, USA), high-energy noise of discrete frequency was found to be generated at the perforations in the test-section walls. Among the techniques proposed for noise alleviation in these transonic continuous flow facilities were:-

- (i) Modifications to the profiles of the hole edges.
- (ii) Use of a test-section enclosure of high acoustic-absorption characteristics.

Furthermore (2-22), in the 14in x 14in transonic/supersonic blowdown tunnel at Marshall Space Flight Center (Alabama, USA) noise was also found to be produced by turbulence from the upstream control-valve of the tunnel and the unsteady diffuser shock. In Ref.2-22, it is considered practical to optimise test-section porosity to achieve minimum noise. A short review of the sources of acoustic perturbations in various facilities elsewhere is also given.

Appendix BBIBLIOGRAPHY OF PUBLISHED PAPERS SPECIALLY RELEVANT TO  
MODEL NOISE TESTING IN SUBSONIC WIND TUNNELSList of Topics

- 1 - Wind-tunnel calibration and use for model noise measurements.
- 2 - Inherent sources of noise in wind tunnels.
- 3 - Sound propagation in ducts.
- 4 - Absorber characteristics.
- 5 - Noise measurement techniques.
- 6 - Simulation of noise field at model scale.
- 7 - Other topics.

1 Wind-tunnel calibration and use for model noise measurements

<u>No.</u>	<u>Author</u>	<u>Title</u>
1-1	Schulz, G.	Noise measurements on bodies in the flow in subsonic wind-tunnels. Part 1. German DLR 68-43, July 1968. RAE Library Translation 1352.
1-2	Schulz, G.	On the measurement of the noise in the neighbourhood of bodies in subsonic wind-tunnels. Part 2. German DLR-FB-69-86 (1969). RAE Library Translation 1465.
1-3	Hanson, C.E.	The design and construction of a low-noise, low turbulence wind-tunnel. Massachusetts Inst. of Tech Rep DSR 79611-1, Jan. 1969.
1-4	Bies, D.A.	Investigation of the feasibility of making model acoustic measurements in the NASA Ames 40 x 80ft wind-tunnel. NASA-CR-114352 (1971) (Bolt Beranek.)
1-5	Broll, C.	Mesures de bruit dans la grande soufflerie de Modane. (Noise measurements in the large Modane wind-tunnel.) La Recherche Aerospatiale, No.1972-1, pp.47-51, Jan.-Feb. 1972. RAE Library Translation 1683 (1972).
1-6	Hickey, D.H. Soderman, P.T. Kelly, M.W.	Noise measurements in wind-tunnels. NASA SP-207. Basic aerodynamic noise research, Session III, pp.399-408 (1969).
1-7	Ver, I.L. Malme, C.L. Meyer, E.B.	Acoustical evaluation of the NASA Langley full-scale wind-tunnel. NASA-CR-111868, Jan.1971.
1-8	Cox, C.R.	Rotor noise measurements in wind-tunnels. Vol.1, Proc 3rd USAAVLABS Symposium on aerodynamics of rotary wing and V/STOL aircraft. Buffalo, June 1969.
1-9	Shaw, W.J. Cole, R.M.	Acoustical calibration of the Douglas 4-foot transonic wind tunnel. Supersonic Tunnel Assoc, 20th Semi-annual meeting (1963).
1-10	Batchelor, G.K.	Sound in wind tunnels. Australian Council for Aeronautics. Rep ACA-18, June 1945
1-11		Anechoic wind tunnel. J. Acoust. Soc. Amer., Vol.49 (1), p.35, Jan. 1971
1-12	Baratono, J.R. Smith, F.A.	Scale-model wind-tunnel acoustic data. USN Res Lab Shock and Vibr Bull, Vol.37, pp.221-252, Jan. 1968
1-13	Evans, J.Y.G.	A scheme for a quiet transonic flow suitable for model testing at high Reynolds number. RAE Technical Report 71112 (1971)

No.	Author	Title
1-14	Cockshutt, E.P. Chappell, M.S. Mair, G.E.	Proposal for an engineering acoustic research laboratory. NAE Quart. Bull. pp.15-36, Oct. - Dec. 1971
1-15	Brownell, W.F.	An anechoic test facility design for the Naval Ship Research and Development Center, Carderock. NSRDC Rep.2924, Sept. 1968
2	<u>Inherent sources of noise in wind tunnels</u>	
2-1	Sharland, I.J.	Sources of noise in axial flow fans. J. Sound Vib., Vol.1, (3), pp.302-322 (1964)
2-2	Mani, R.	Noise due to interaction of inlet turbulence with isolated stators and rotors. J. Sound Vib., Vol.17 (2), pp.251-260 (1971)
2-3	Barry, B. Moore, C.J.	Subsonic fan noise. J. Sound Vib., Vol.17 (2), pp.207-220 (1971)
2-4	Wills, J.A.B.	Spurious pressure fluctuation in wind tunnels. J. Acoust. Soc. Amer. Vol.43 (5), pp.1049-1054 (1968)
2-5		Basic aerodynamic noise research. Session II. Fan noise. NASA SP-207 (1969)
2-6	Irani, P.A. Iya, K.S.	Aerodynamic noise in aircraft and wind tunnels. Indian National Aeronautical Lab. Sci. Rev.AE-2-63, Aug. 1963
2-7	Murphy, J.S.	Wind tunnel investigation of turbulent boundary layer noise as related to design criteria for high performance vehicles. NASA TN D-2247, April 1964
2-8	Stallabrass, J.R.	Aerodynamic noise in heat exchangers. NAE. Quart. Bull. No.1, pp.53-86 (1966)
2-9	Gaillet, D.	Noise created by obstacles in an initially noise-free flow. (Some experimental results.) (In French.) Revue d'Acoustique, Vol.1 (2), pp.101-113 (1968)
2-10	Ross, D.H.	Aerodynamic noise investigation in a short-duration shock tunnel. USN Res Lab. Shock and Vib.Bull, Vol.37 (3) (1968)
2-11	Pate, S.R. Schueler, C.J.	An investigation of radiated aerodynamic noise effects on boundary-layer transition in supersonic and hypersonic wind tunnels. AIAA Paper 68-375, April 1968
2-12	Gaster, M.	Some observations on vortex shedding and acoustic resonances. NPL Aero 1311. ARC-CP-1141 (1971)
2-13	Boone, J.R. McCanless, G.F.	Evaluation of the acoustic sources of background noise in wind-tunnels. Chrysler Corp Aero Mech Branch. NASA-CR-98155, June 1968
2-14	Credle, O.P.	Evaluation of the acoustic silencer in the AEDC-PWT 4 foot transonic tunnel. AEDC-TR-68-234, Oct.1968
2-15	McCanless, G.F.	Additional correction of 4 per cent Saturn 5 protuberance test data. NASA-CR-103064, Jan.1971
2-16	Robertson, J.E.	Final report, June 1969-June 1970. Model study of the exhaust flow noise of the proposed AEDC high Reynolds number tunnel. AEDC-TR-71-146, July 1971
2-17	Credle, O.P.	Perforated wall noise in the AEDC PWT 16 ft and 4ft transonic tunnels. USA AEDC-TR-71-216, Oct. 1971

<u>No.</u>	<u>Author</u>	<u>Title</u>
2-18	Morfev, C.L. Sharland, I.J. Yeow, K.W.	Fan noise. Chap.10 of 'Noise and acoustic fatigue in aeronautics'. Ed. by E.J. Richards and D.J. Mead, Wiley 1968
2-19	Eckelmann, N.	Measurement of the wind tunnel turbulence by the hot wire method and reduction of wind tunnel oscillations. DLR-FB-70-39, AVA-FB-70-21, Sept. 1970
2-20	Hubbard, H.H. Lansing, D.L. Runyan, H.L.	A review of rotating blade noise technology. J. Sound Vib., Vol.19, (3), pp.227-249 (1971)
2-21	Van Niekerk, C.G.	Noise generation in axial flow fans. J. Sound Vib., Vol.3, pp.46-56 (1966)
2-22	Boone, J.R. McCanless Jr., G.F.	Application of the techniques for evaluating the acoustic sources of background noise in wind tunnel facilities. NASA CR 102623 (Chrysler Corp) (1969)
2-23	Uberoi, M.S.	Effects of wind tunnel contraction on free stream turbulence. J. Aero. Sc., Vol.23 (8), pp.754-764, Aug. 1956
2-24	Roshko, A.	On the drag and shedding frequency of two-dimensional bluff bodies. NACA TN 3169, July 1954
2-25	Roshko, A.	On the wake and drag of bluff bodies. J. Aero. Sci., Vol.22, pp.124-132, Jan. 1955
2-26	Gumpsty, N.A. Whitehead, D.S.	The excitation of acoustic resonances by vortex shedding. J. Sound Vib., Vol.18 (3), pp.353-369 (1971)
2-27	Brown, D. Ollerhead, J.B.	Propeller noise at low tip speeds. Rep. No. WR-71-9, AFAPL-TR 71-55. Wyle Labs., Hampton, Va, Sept. 1971
2-28	Burdsall, E.A. Urban, H.H.	Fan-compressor noise: prediction, research and reduction studies. PWA Rep. No. 4154, FAA-RD-71-73, Feb. 1971
2-29	Wenzell, A.R. Keller, J.B.	Propagation of acoustic waves in a turbulent medium. J. Acoust. Soc. Amer., Vol.50 (3), pp.911-920 Jan. 1971
2-30	Brown, F.T. Knebel, G. Margolis, D.	Unsteady flow in tubes and tunnels. MIT Eng. Proj. Lab., DSR-76107-4, FRA-RTL-72-22, Aug. 1971
2-31	Lordi, J.A.	Noise generation by a rotating blade row in an infinite annulus. AIAA Paper 71-617, 1971
2-32	Fry, A.T.	Noise in high-velocity ventilation systems. Rev. de Acustica, Vol.2 (1-2), pp.78-86 (1971)
2-33	Channaud, R.C.	Aerodynamic sound from a rotating disk. J. Acoust. Soc. Amer., Vol.45, pp.392-397 (1971)
2-34	Channaud, R.C.	Noise reduction in propeller fans using porous blades at free-flow conditions. J. Acoust. Soc. Amer., Vol.51 (1), pp.15-18, Jan. 1972
2-35	Mugridge, B.M.	Acoustic radiation from aerofoils with turbulent boundary layers. J. Sound Vib., Vol.16 (4), pp.593-614 (1971)
2-36	Hosier, R.N. Mayes, W.H.	A procedure for predicting internal and external noise fields of blowdown wind tunnels. NASA TM X-2556. May 1972
3	<u>Sound propagation in ducts</u>	
3-1	Eversman, W.	Signal velocity in a duct with flow. J. Acoust. Soc. Amer., Vol.50 (2), pp.421-425, Aug. 1971

<u>No.</u>	<u>Author</u>	<u>Title</u>
3-2	Fry, A.T.	Acoustic measurements in ducts, standing wave tubes and air moving systems. British Acoust. Soc. Proc. Vol.1. paper 71/47, Summer 1971
3-3	Mason, V.	Some experiments on the propagation of sound along a cylindrical duct containing flowing air. J. Sound. Vib., Vol.10 (2), pp.208-226 (1969)
3-4	Morfey, C.L.	Sound transmission and generation in ducts with flow. J. Sound Vib., Vol.14 (1), pp.37-55 (1971)
3-5	Christie, D.R.A.	Theoretical attenuation of sound in a lined duct. Some computer calculations. J. Sound Vib., Vol.17 (2), pp.283-286 (1971)
3-6	Mariano, S.	Effect of wall shear layers on the sound attenuation in acoustically lined rectangular ducts. J. Sound Vib., Vol.19 (3), pp.261-275 (1971)
3-7		Basic aerodynamic noise research. Session III. Inlet duct noise, boundary layer noise diagnostic techniques. NASA SP-207 (1969)
3-8	Mechel, F. et al	Research on sound propagation in sound-absorbent ducts with superimposed air streams. Vols.1-4. Gottingen Univ. Physics Inst. USA AMRL-TDR-62-140 (1)-(4) (1962-3)
3-9	Mertens, P.A.	Interaction between air flow and airborne sound in a duct. Vol.1 Propagation of shock fronts and nonlinearity of porous absorbers. Gottingen Univ. Physics. Inst. AMRL-TR-67-120-1 Nov. 1967
3-10	Mechel, F.P. Mertens, P.A.	Interaction between air flow and airborne sound in a duct. Vol.2 Acoustic excitation of boundary layer and radiation impedance of orifices. Gottingen Univ. Physics Inst. AMRL-TR-67-120-2, Nov. 1967
3-11	Morse, P.M. Ingard, K.U.	Theoretical Acoustics. pp.701-704. McGraw-Hill Book Co., New York (1968)
3-12	Doak, P.E.	A report on the Southampton 'Flow Duct Acoustic Symposium', 11-14 Jan 1972. ISVR (Southampton) Tech Rep.55, Feb. 1972
3-13	Egorov, N.F.	Investigation of the sound field in ducts with sound-absorbing walls. Soviet Physics-Acoustics, Vol.17 (3), pp.395-396 Jan.-Mar. 1972
4	<u>Absorber characteristics</u>	
4-1	Powell, J.G. Van Houten, J.J.	A tone-burst technique of sound absorption measurement. J. Acoust. Soc. Amer, Vol. 48 (6), pp.1299-1303, Dec. 1970
4-2	Delany, M.E. Bazley, E.N.	Acoustical properties of fibrous absorbent materials. Applied Acoustics, Vol.3, pp.105-116 (1970) NPL Aero Report Ae 37 (1969)
4-3	Delany, M.E. Bazley, E.N.	A note on the sound field due to a point source inside an absorbent-lined enclosure. J. Sound Vib., Vol.14 (27), pp.151-157 (1971)
4-4	Delany, M.E. Bazley, E.N.	Monopole radiation in the presence of an absorbing plane. J. Sound Vib., Vol.13 (3), pp.269-279 (1970)
4-5	Velizhanina, K.A. Vorantina, N.N. Kodymskaya, E.S.	Impedance investigation of sound-absorbing systems in oblique sound incidence. Soviet Physics - Acoustics, Vol.17 (2), pp.193-197, Oct.-Dec. 1971
4-6	Zwikker, C. Kosten, C.W.	Sound absorbing materials. Elsevier, New York (1949)

<u>No.</u>	<u>Author</u>	<u>Title</u>
4-7	Pyett, J.S.	The acoustic impedance of a porous layer at oblique incidence. Acustica, Vol.3 (3), pp.375-382 (1953)
4-8	Powell, J.G. Van Houten, J.J.	Techniques for evaluating the sound absorption of materials at high intensities. NASA CR-1698, Jan. 1971
4-9	Sidey, D.J. Mulholland, K.A.	The variation of normal layer impedance with angle of incidence. J. Sound Vib., Vol.14 (1), pp.139-142 (1971)
4-10	Attenborough, K.	The prediction of oblique incidence behaviour of fibrous absorbents. J. Sound Vib., Vol.14 (2), pp.183-191 (1971)
4-11	Davern, W.A. Hutchinson, J.A.E.	Polyurethane ether foam wedges for anechoic chamber. Applied Acoustics, Vol.4 (4), pp.287-302, Oct. 1971
4-12	Husztly, D. Illenyi, A. Vass, G.	Equipment for measuring the flow-resistance of porous and fibrous materials. Applied Acoustics, Vol.5 (1), pp.1-14, Jan. 1972
4-13	Davern, W.A.	A design criterion for sound-absorbent lining of an anechoic chamber. Technical Note in Applied Acoustics, Vol.5, No.1, pp.69-71, Jan 1972
4-14	Attenborough, K.	The influence of microstructure on propagation in porous fibrous absorbents. J. Sound Vib., Vol.16 (3), pp.419-442 (1971)
4-15	Ffowcs Williams, J.E.	The acoustics of turbulence near sound-absorbent liners. J. Fluid Mech., Vol.51 (4), pp.737-749 (1972)
5	<u>Noise measurement techniques</u>	
5-1	Fiala, W.T. Van Houten, J.J.	The condenser microphone for boundary layer noise measurement. Shock, Vibr. and Assoc. Environ. Bull. 33, Part 3, March 1964
5-2	Carlson, H.W. Morris, O.A.	Wind-tunnel sonic-boom testing techniques. AIAA Paper 66-765 (1966) J. of Aircraft, Vol.4, pp.245-249, May-June 1967
5-3	Gorton, R.E.	Facilities and instrumentation for aircraft engine noise studies. ASME Prep 66-GT/N-41 (1966)
5-4	Waldschütz, S.	A survey of literature concerning self-noise reduction in acoustical transducers used for measurements in flowing air. German DVL DVL-775 DLR-Mitt-68-31, Dec. 1968 RAE Library Translation 1660 (1972)
5-5	Hoch, R.	Equipment and facilities used at SNECMA for noise-testing. (in French) L'Aero et L'Astron, Vol.15 (8), pp.15-21 (1969)
5-6	Johnson, R.I. Macourek, M.N. Saunders, H.	Boundary layer acoustic measurements in transitional and turbulent flow at $M = 4.0$ . AIAA Paper 69-344, April 1969
5-7	Ferri, A. Wang, H-Ch	Observations on problems related to experimental determination of sonic boom. NASA 3rd Conf on sonic boom. NASA SP-255, pp.277-284 (1970)
5-8	Nakamura, A. Matsumoto, R. Sugiyama, A. Tanaka, T.	Some investigations on output level of microphones in air streams. J. Acoust. Soc. Amer., Vol.46 (6), pp.1391-1396, December 1969
5-9	Smith, M.W. Lambert, R.F.	Acoustical signal detection in turbulent airflow. J. Acoust. Soc. Amer., Vol.32, pp.858-866 (1960)
5-10	Channaud, R.C.	Aerodynamic sound from a rotating disk. J. Acoust. Soc. Amer., Vol.42, pp.392-397 (1969)

<u>No.</u>	<u>Author</u>	<u>Title</u>
5-11	Bergstrom, E.R. Raghunathan, S.	Flat plate boundary layer transition in the LUT gun tunnel: a transition-radiated aerodynamic noise correlation for gun tunnel and conventional wind tunnel data at supersonic and hypersonic Mach numbers. Loughborough Univ. of Tech. Dept of Transport Tech TT 7107, August 1971
5-12	Lyon, R.H.	On the diffusion of sound waves in a turbulent atmosphere. J. Acoust. Soc. Amer., Vol. 31, pp.1176-1182 (1959)
5-13	Beranek, L.L. (Edit)	Noise and vibration control. McGraw Hill (1971)
5-14	Corcos, G.M.	Resolution of pressure in turbulence. J. Acoust. Soc. Amer., Vol. 35 (2), pp.192-199, February 1963
5-15	Magrab, E.B. Blomquist, D.S.	The measurement of time-varying phenomena: fundamentals and applications: Wiley-Interscience (1971)
5-16	Thoma, G. von Meier, A.	An apparatus for measuring low acoustical background noise. IEEE Trans. on Broadcasting, Vol. BC-17, No.4, pp.106-109, Dec. 1971
5-17	Thomas, W.G. Prellar, M.J. Farmer, J.C.	Calibration of condenser microphones under increased atmospheric pressures. J. Acoust. Soc. Amer., Vol. 51 (1), pp.6-14, Jan. 1972
5-18	Bendat, J.S. Piersol, A.G.	Random data: Analysis and measurement procedures. Wiley-Interscience (1971)
5-19	Fuchs, H.V.	Measurements of pressure fluctuations with microphones in an airstream. ISVR (Southampton) Memo-281, May-1969
5-20	Schomer, P.D.	Measurement of sound transmission loss by combining correlation and Fourier techniques. J. Acoust. Soc. Amer., Vol. 51 (4), pp.1127-1141, April 1972
5-21	Nakamura, A. Sugiyama, A. Tanaka, T. Matsumoto, R.	Experimental investigation for detection of sound-pressure level by a microphone in an airstream. J. Acoust. Soc. Amer., Vol. 50 (1), pp.40-46 (1971)
6	<u>Simulation of noise field at model scale</u>	
6-1	Wilhold, G.A.	Aerospace noise. Astronautics and Aeronautics, Vol. 5, pp.64-69, May 1967
6-2	Hinterkeuser, E.G.	Synthesis of aircraft noise. NASA-SP-189, pp.537-545 (1968)
6-3	Gordon, C.G.	Spoiler-generated flow noise. J. Amer. Acoust. Soc, Vol. 43, pp.1041-1048 May 1968
6-4	Eaton, D.C.G.	Development and testing of Concorde structure from noise aspects. Environmental Engineering, pp.7-11. Sept. 1969
6-5	Ancell, J.E. Shapiro, N.	Model study of high bypass jet noise. Amer. Acoust. Soc., 79th Meeting, April 1970
6-6	Casalegno, L. Martini, G. Ruspa, G.	Use of models to estimate fuselage pressure in VTOL aircraft. J. Sound Vib., Vol. 17, pp.309-321, Aug. 1971
6-7	Hargest, T.J.	Some experimental aircraft engine noise facilities in the United Kingdom. J. Sound Vib., Vol. 20 (3), pp.359-380 (1972)
6-8	Bushell, K.W.	A survey of low velocity and coaxial jet noise with application to prediction. J. Sound Vib., Vol. 17 (2), pp.271-282 (1971)

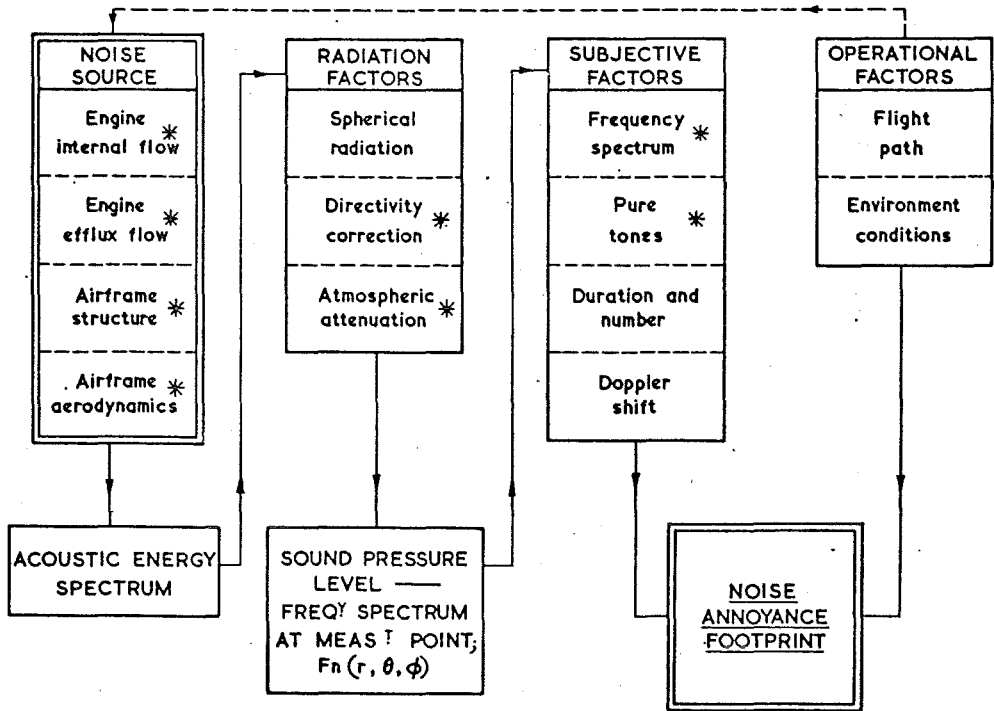


<u>No.</u>	<u>Author</u>	<u>Title</u>
6-9	Dorsch, R.G. Krejsa, E.A. Olsen, W.A.	Blown flap noise research. NASA-TM-X-67850 (1971)
6-10	Dorsch, R.G. Kreim, W.J. Olsen, W.A.	Externally-blown-flap noise. AIAA Paper No. 72-129, Jan. 1972
6-11	Gruschka, H.D. Schrecka, G.O.	Aeroacoustic characteristics of jet flap type exhausts. AIAA Paper No. 72-130, Jan 1972
6-12	Olsen, W.A.	Noise produced by a small-scale externally blown flap. NASA TN D-6636, March 1972
6-13	Groeneweg, J.F. Minner, G.L.	Measured noise of model fan-under-wing and fan-on-flap jet flap configurations. NASA TN D-6781, May 1972

NOTE A bibliography of the large number of available papers on basic jet noise is not attempted here. Useful lists of relevant papers may be found in Refs.7-6 to 7-10, for example.

#### 7 Other topics

7-1		SAE Conference on Aircraft and the Environment (Washington, DC), Pts.1 and 2, Feb.8-10 1971
7-2	Glough, N. Diedrich, J.H. Yuska, J.A.	NASA Lewis 9- by 15-foot V/STOL wind tunnel. NASA-TM-X-2305, July 1971
7-3	Everett, C. Luckinbill, D.L.	Automated environmental control of an acoustic test facility, Part A Final Project Report. Tennessee Technological Univ. NASA-CR-115072, Jan. 1971
7-4	Miller, R.L. Onoley, P.B.	The experimental determination of atmospheric absorption from aircraft acoustic flight tests. NASA CR-1891, Nov. 1971
7-5	Van Houten, J.J.	The development of sonic environmental testing. Sound and Vibration, Vol.3, pp.16-24, April 1969
7-6		Progress of NASA research relating to noise alleviation of large subsonic jet aircraft. NASA SP-189 (1968)
7-7		Basic aerodynamic noise research NASA SP-207 (1969)
7-8	Richards, E.J. Mead, D.J. (Editors)	Noise and acoustic fatigue in aeronautics. John Wiley (1968)
7-9		Aerodynamic noise. Proc. AFOSR-UTIAS symposium (Toronto 1968) Univ. of Toronto Press.
7-10		Aircraft engine noise and sonic boom. AGARD Conf. Proc.42, May 1969
7-11	Beranek, L.L. (Edit.)	Noise and vibration control. McGraw Hill (1971)



\* Noise factors affected directly by mainstream flow

Figure 1

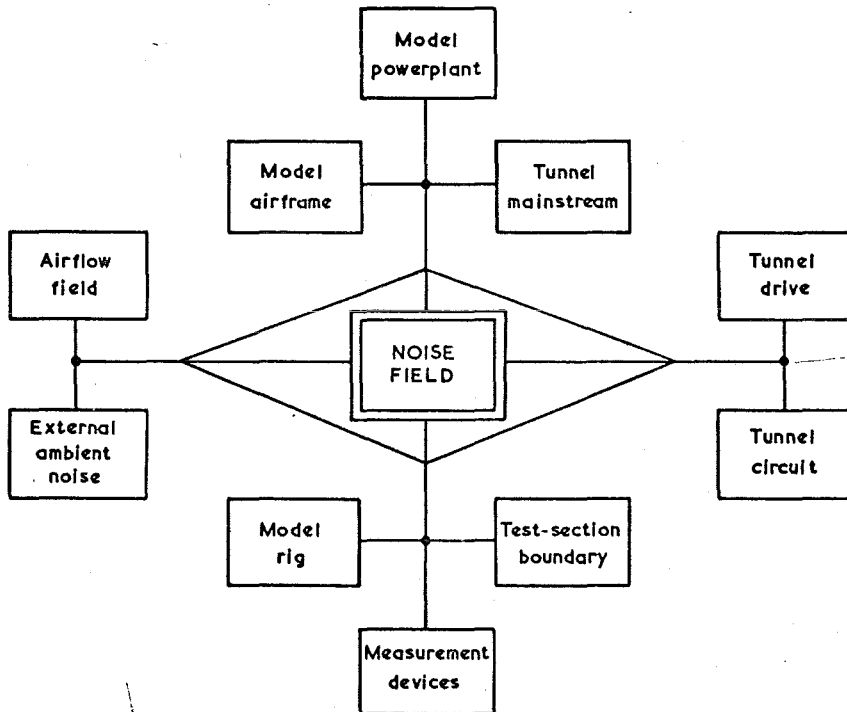
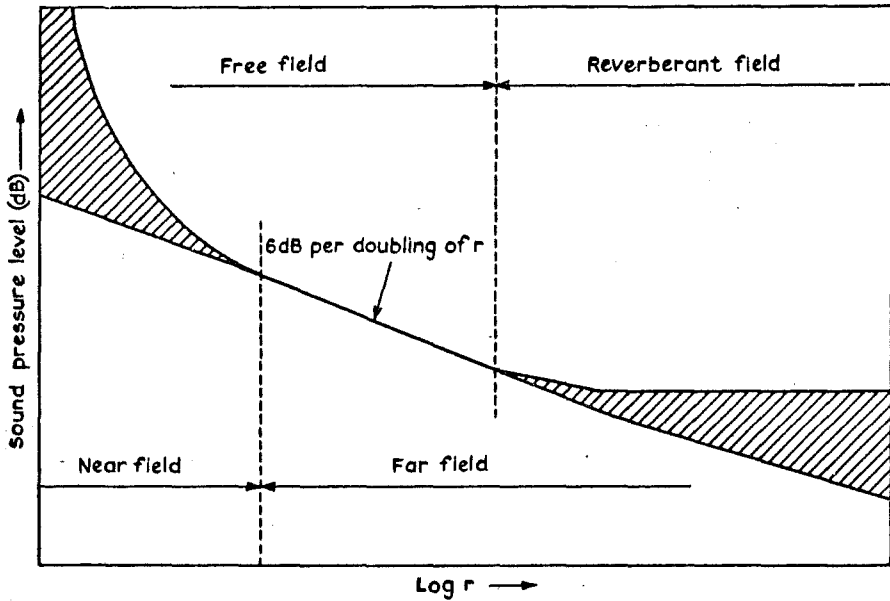


Fig.2 Simplified interaction element diagram



Large fluctuations of SPL with distance occur within shaded areas

Fig.3 Domains of measurement at distance r from a noise source in a reverberant enclosure

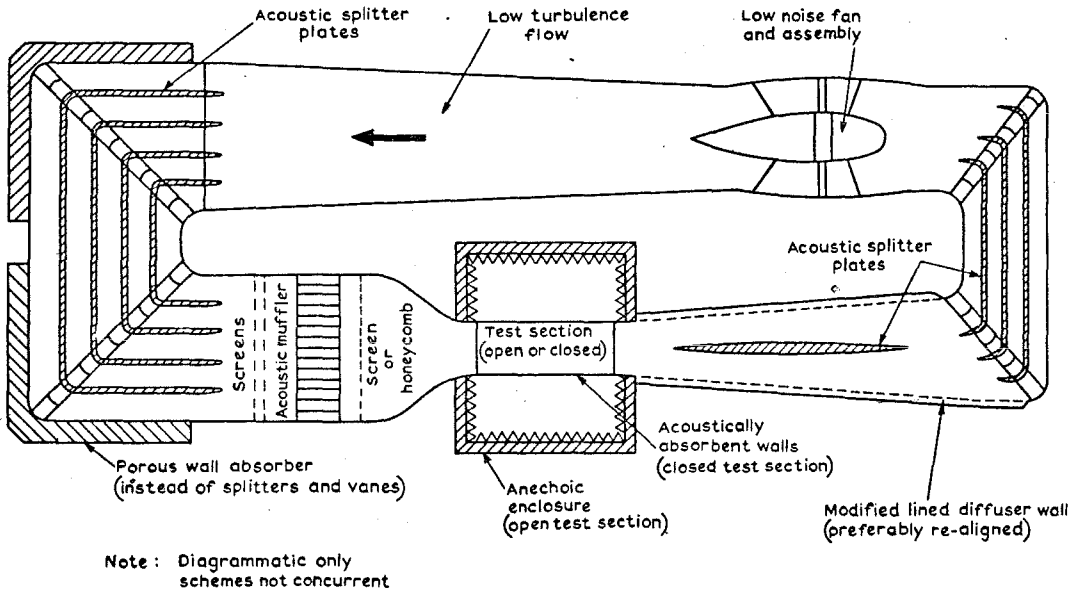


Fig.4 Typical subsonic wind-tunnel circuit with possible noise-suppression schemes

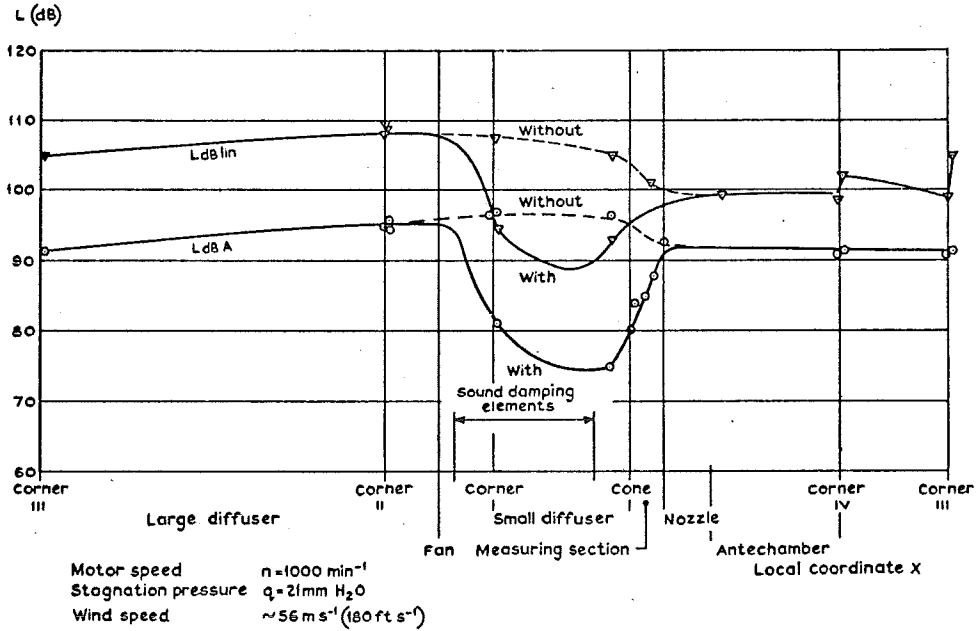


Fig. 5 Sound level in the duct before and after the installation of sound damping material 3-m DFVLR (Porz-Wahn) subsonic open-jet closed-return tunnel

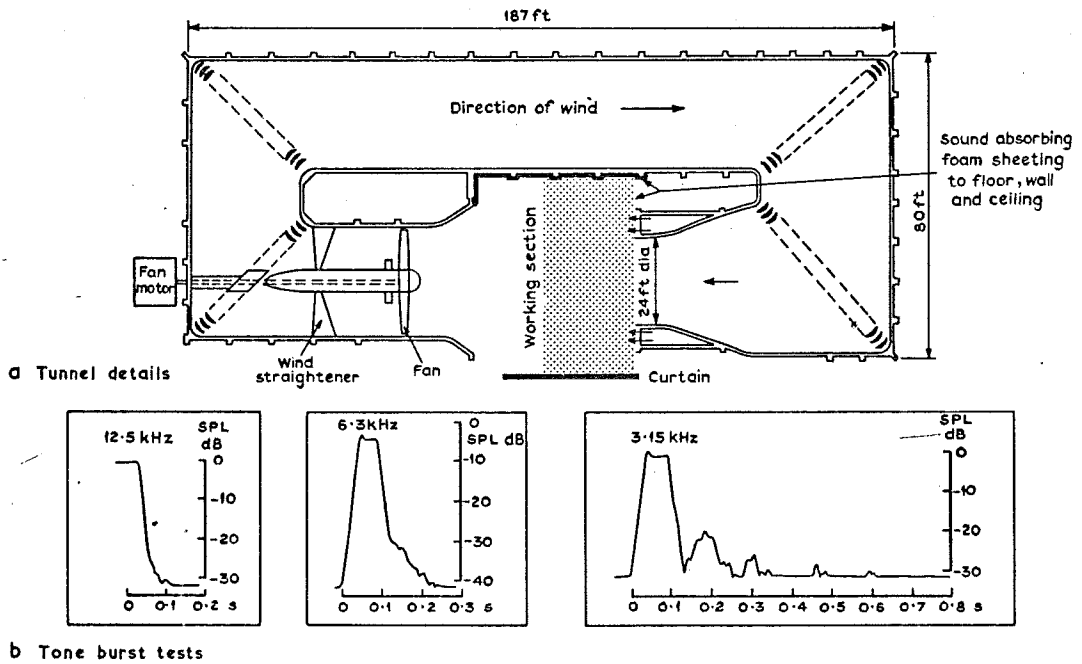


Fig. 6 a & b Details of 24ft wind tunnel at RAE Farnborough showing partial sound treatment and performance with tone bursts

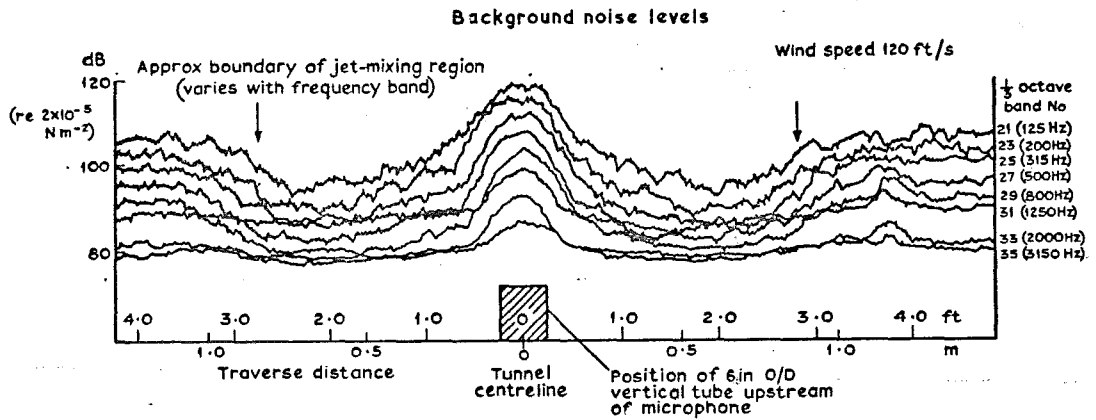


Diagram showing microphone traverse position

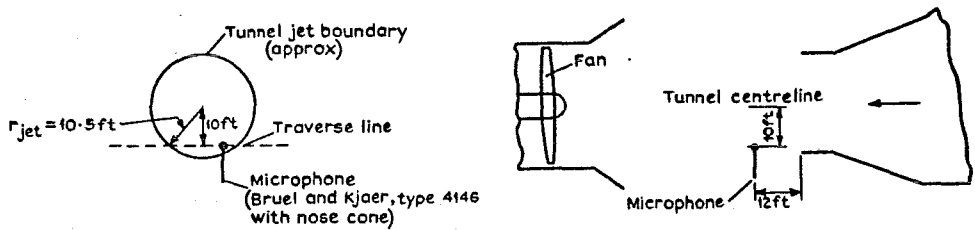


Fig.7 Background noise level in RAE 24ft open-jet wind tunnel measured inside the jet for various  $\frac{1}{3}$ -octave bands

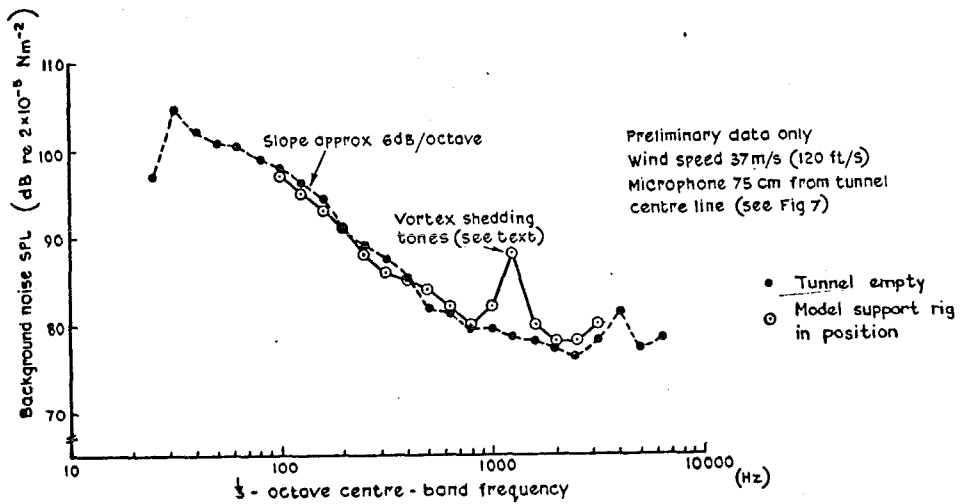


Fig.8 RAE 24-foot open-jet wind tunnel, background noise v frequency

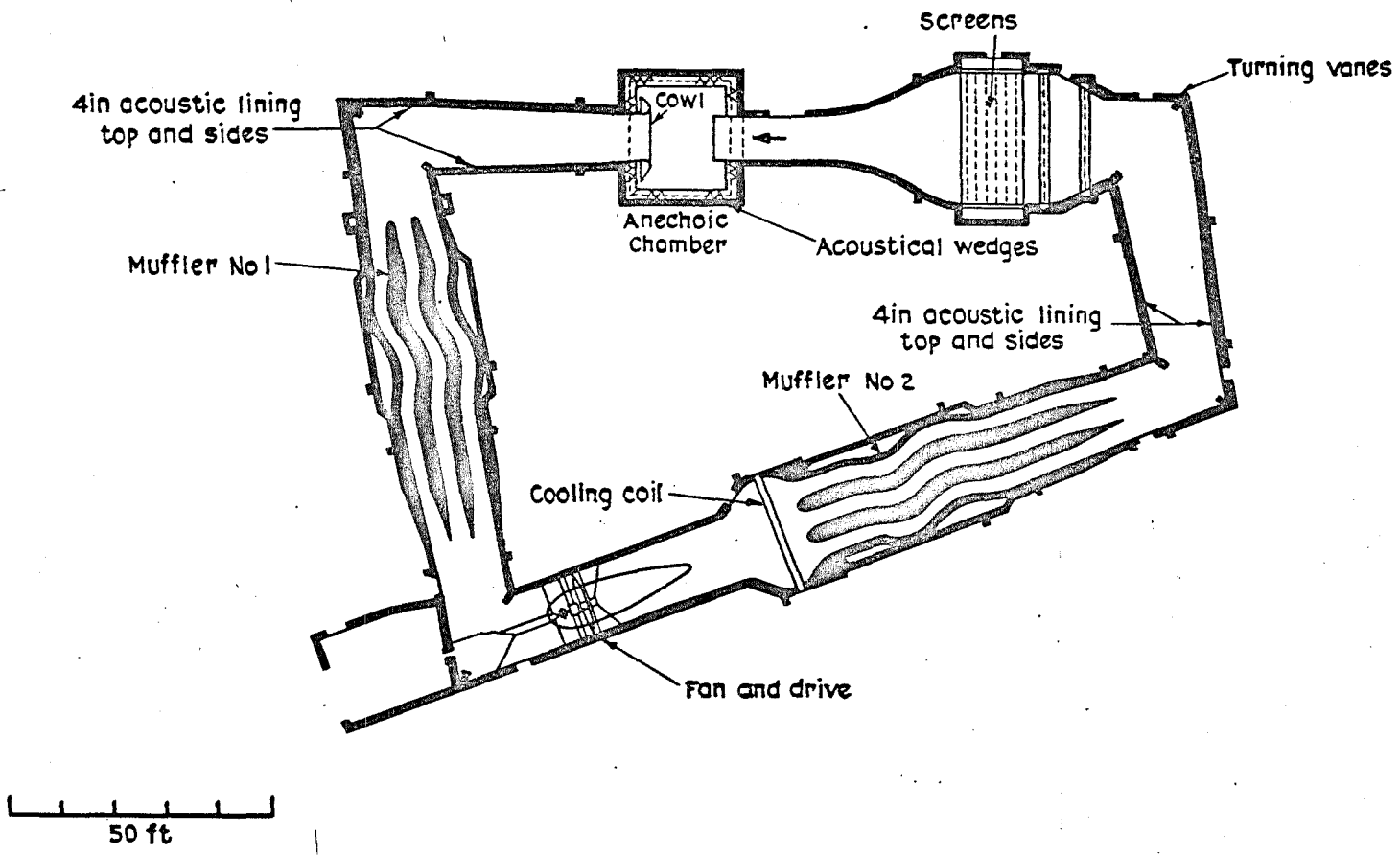


Fig.9 NSRDC anechoic test facility

## APPENDIX I

This Report is one of four issued as documents complementary to Advisory Report 60 of the Large Wind Tunnels Working Group of the AGARD Fluid Dynamics Panel. The other reports in the series are as follows:

### AGARD REPORT No.598

EXPERIMENTS ON MANAGEMENT OF FREE-STREAM TURBULENCE: by R.I.Loerke and H.N.Nagib

### AGARD REPORT No.600

#### PROBLEMS OF WIND TUNNEL DESIGN AND TESTING

Some considerations of future low-speed tunnels for Europe: by A.Spence and B.M.Spee.

Project study of a large European transonic Ludwig Tube wind tunnel: by H.Ludwig, H.Grauer-Carstensen, and W.Lorenz-Meyer.

The development of an efficient and economical system for the generation of a quiet transonic flow suitable for model testing at high Reynolds numbers: by P.G.Pugh.

Induction transonic wind tunnel: by P.Carrière

Soufflerie à compresseur hydraulique: by M.Ménard

Testing at supersonic speeds: by Ph. Poisson-Quinton

Facilities for aerodynamic testing at hypersonic speeds: by F.Jaarsma and W.B. de Wolf.

### AGARD REPORT No.602

#### FLUID MOTION PROBLEMS IN WIND TUNNEL DESIGN

The influence of the free-stream Reynolds Number on transition in the boundary layer on an infinite swept wing: by E.H.Hirschel

Some examples of the application of methods for the prediction of boundary-layer transition on sheared wings: by D.A.Treadgold and J.A.Beasley.

The need for High-Reynolds-Number Transonic Tunnels: by C.R.Taylor.

The influence of free-stream turbulence on a turbulent boundary layer, as it relates to wind tunnel testing at subsonic speeds: by J.E.Green.

Effects of turbulence and noise on wind tunnel measurements at transonic speeds: by A.Timme.

Design of ventilated walls, with special emphasis on the aspect of noise generation: by R.N.Cox and M.M.Freestone.

# NATIONAL DISTRIBUTION CENTRES FOR UNCLASSIFIED AGARD PUBLICATIONS

Unclassified AGARD publications are distributed to NATO Member Nations through the unclassified National Distribution Centres listed below

## BELGIUM

Coordonnateur AGARD – VSL  
Etat-Major de la Force Aérienne  
Casernes Prince Baudouin  
Place Dailly, 1030 Bruxelles

## CANADA

Director of Scientific Information Services  
Defence Research Board  
Department of National Defence – ‘A’ Building  
Ottawa, Ontario

## DENMARK

Danish Defence Research Board  
Østerbrogades Kaserne  
Copenhagen Ø

## FRANCE

O.N.E.R.A. (Direction)  
29, Avenue de la Division Leclerc  
92, Châtillon-sous-Bagneux

## GERMANY

Zentralstelle für Luftfahrtokumentation  
und Information  
Maria-Theresia Str. 21  
8 München 27

## GREECE

Hellenic Armed Forces Command  
D Branch, Athens

## ICELAND

Director of Aviation  
c/o Flugrad  
Reykjavik

## ITALY

Aeronautica Militare  
Ufficio del Delegato Nazionale all'AGARD  
3, Piazzale Adenauer  
Roma/EUR

## LUXEMBOURG

Obtainable through BELGIUM

## NETHERLANDS

Netherlands Delegation to AGARD  
National Aerospace Laboratory, NLR  
P.O. Box 126  
Delft

## NORWAY

Norwegian Defense Research Establishment  
Main Library,  
P.O. Box 25  
N-2007 Kjeller

## PORTUGAL

Direccao do Servico de Material  
da Forca Aerea  
Rua de Escola Politecnica 42  
Lisboa  
Attn of AGARD National Delegate

## TURKEY

Turkish General Staff (ARGE)  
Ankara

## UNITED KINGDOM

Defence Research Information Centre  
Station Square House  
St. Mary Cray  
Orpington, Kent BR5 3RE

## UNITED STATES

National Aeronautics and Space Administration (NASA)  
Langley Field, Virginia 23365  
Attn: Report Distribution and Storage Unit

\* \* \*

If copies of the original publication are not available at these centres, the following may be purchased from:

<i>Microfiche or Photocopy</i>	<i>Microfiche</i>	<i>Microfiche</i>
National Technical Information Service (NTIS) 5285 Port Royal Road Springfield Virginia 22151, USA	ESRO/ELDO Space Documentation Service European Space Research Organization 114, Avenue Charles de Gaulle 92200, Neuilly sur Seine, France	Technology Reports Centre (DTI) Station Square House St. Mary Cray Orpington, Kent BR5 3RE England

The request for microfiche or photocopy of an AGARD document should include the AGARD serial number, title, author or editor, and publication date. Requests to NTIS should include the NASA accession report number.

Full bibliographical references and abstracts of the newly issued AGARD publications are given in the following bi-monthly abstract journals with indexes:

Scientific and Technical Aerospace Reports (STAR)  
published by NASA,  
Scientific and Technical Information Facility,  
P.O. Box 33, College Park,  
Maryland 20740, USA

United States Government Research and Development Report Index (USGDRI), published by the Clearinghouse for Federal Scientific and Technical Information, Springfield, Virginia 22151, USA

